

**Metabolomic analysis on anti-HIV activity of selected
Helichrysum species**

by

Simin Emamzadeh Yazdi

Submitted in partial fulfilment of the requirements for the degree of

PHILOSOPHIAE DOCTOR (Medicinal Plant Sciences)

in the

Department of Plant & Soil Sciences

of the

Faculty of Natural and Agricultural Sciences

University of Pretoria

Pretoria



Supervisor: Prof. J.J.M. Meyer

Co-supervisors: Prof. G. Prinsloo & Dr. H.M. Heyman

2019

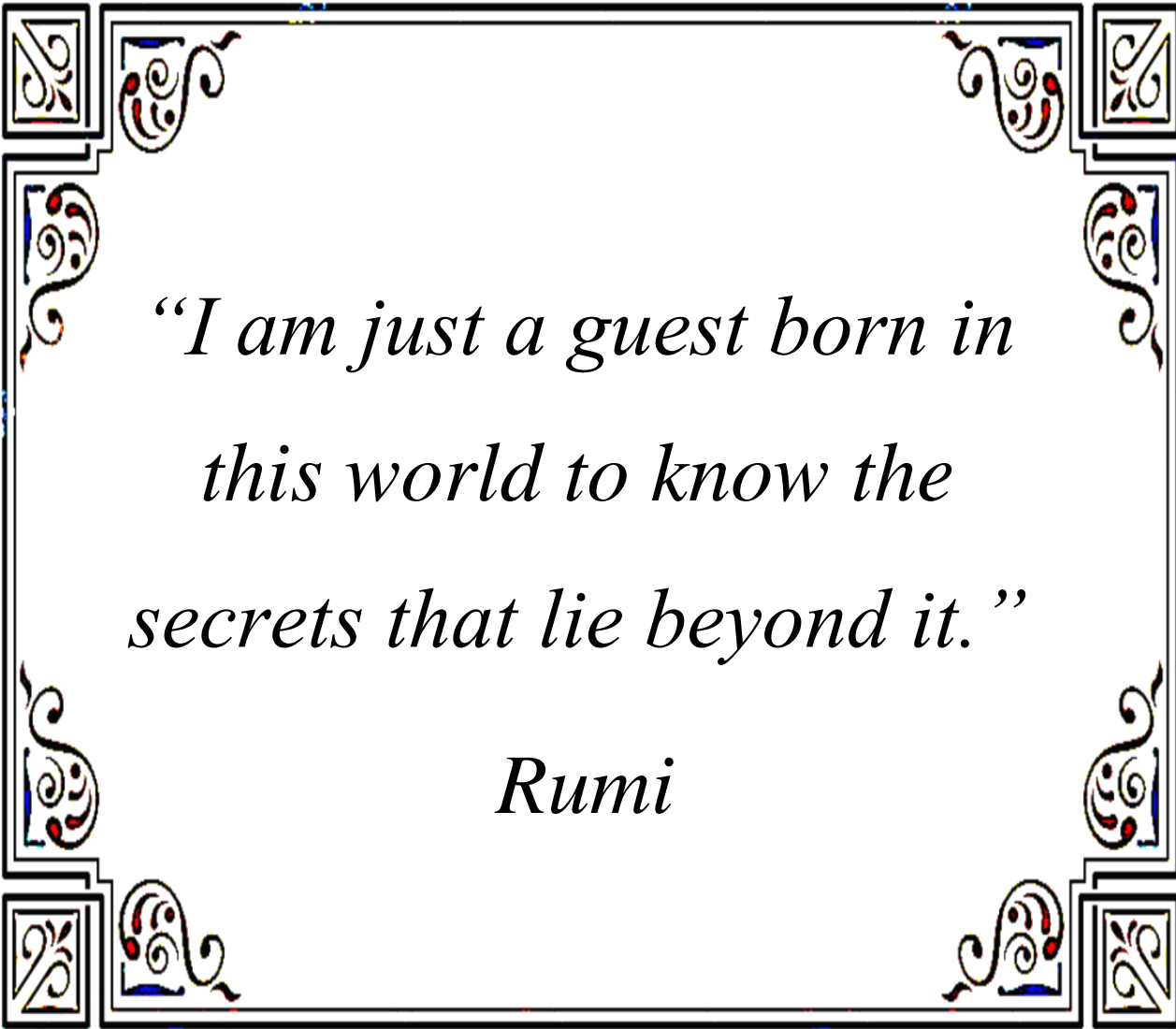
Declaration of Originality

I, **Simin Emamzadeh Yazdi** declare that this thesis, which I hereby submit for the degree, Doctor of Philosophy in Medicinal Plant Sciences at the University of Pretoria, is my own work and has not previously been submitted by me for a degree at this or any other tertiary institution.

SIGNATURE:

UP STUDENT NUMBER: 28459149

DATE: 23 October 2019



*“I am just a guest born in
this world to know the
secrets that lie beyond it.”*

Rumi

Metabolomic analysis on anti-HIV activity of selected *Helichrysum* species

by

Simin Emamzadeh Yazdi

Supervisor: Prof. J.J.M. Meyer

Co-supervisors: Prof. G. Prinsloo & Dr. H.M. Heyman

Department of Plant and Soil Sciences

Degree: Philosophiae Doctor Medicinal Plant Sciences

Abstract

Since the beginning of human civilization, medicinal plants have been used to treat a variety of infectious and non-infectious diseases. The therapeutic properties of phytochemicals have been recognized since ancient human history. The genus *Helichrysum* Mill. with its attractive flowers consist of an estimated 500–600 species in the Asteraceae family. In South Africa and Namibia there are about 244–250 species with tremendous morphological diversity. Several *Helichrysum* species are widely used by the indigenous population to treat various disorders such as wounds, infections, respiratory conditions, headaches, coughs, colds and fevers. Several of the *Helichrysum* species exhibit antiviral activity with the most relevant to this study being the discovery of anti-human immunodeficiency virus (anti-HIV) and anti-reverse transcriptase (anti-RT) activity of some species.

Drug discovery and development, from the early stages of a promising compound to the final medication, is an intensive, expensive and incremental process. The ultimate goal is to identify a molecule with the desired effect in the human body and to establish its quality, safety and efficacy for treating patients.

The ability to combine high-throughput analytical techniques like metabolomic and other experimental approaches with drug discovery will speed up the development of safer, more

effective and better-targeted therapeutic agents. The rapidly emerging field of metabolomics and molecular docking analysis provides valuable information on drug activity, toxicity, customized drug treatments and can predict therapeutic outcomes.

Extraction of the aerial parts of 32 *Helichrysum* species was done using polar [methanol (MeOH) 50%: distilled water (dH₂O) 50%] and non-polar [hexane (Hex), dichloromethane (DCM) and acetone (Ace)] solvent systems. Anti-human immunodeficiency virus bioassays on the live HI virus revealed that polar extracts of *H. mimetes* and *H. chrysargyrum* at 2.5 µg/mL and 25 µg/mL, polar and non-polar extracts of *H. infusum* at 25 µg/mL and polar and non-polar extracts of *H. zeyheri*, *H. setosum*, *H. platypterum* and *H. kraussii* at 2.5 and 25 µg/mL, had higher than 90% inhibitory activity. The polar extract of *H. mimetes* also exhibited reverse transcriptase (RT) inhibition as a possible indication of the mechanism of action. Proton nuclear magnetic resonance (¹H NMR) spectra of the polar extracts exhibited the presence of aromatic compounds and carbohydrate moieties. Principal component analysis (PCA) of the polar extracts showed clustering related to the activity of the extracts with good predictability scores ($Q^2 > 0.5$). However, orthogonal projections to latent structures discriminant analysis (OPLS-DA) predictability of the model was low based on the Q^2 at approximately 0.25. Quinic acid (QA), isolated from *H. mimetes* showed promising anti-RT activity [50% inhibition concentration (IC₅₀) = 53.82 µg/mL] which was comparable to the positive drug control, doxorubicin (IC₅₀ = 40.31 µg/mL). The molecular docking study revealed the probable binding site and conformation of QA within cavity 4, with a docking score of -8.03. The docking score of doxorubicin within cavity 4 was -7.87. With this study, it was shown that metabolomic analysis as a tool to predict anti-HIV activity in *Helichrysum* species can be valuable to shorten the process. Moreover, the study of molecular docking revealed the mechanism action of quinic acid and doxorubicin against RT.

Keywords: Asteraceae, Anti-RT, Anti-viral, HIV-1, Metabolomics, Molecular docking, Nuclear magnetic resonance, Quinic acid.

Dedication

This dissertation is lovingly dedicated to the treasures of my life, my parents *Mohammad* and *Mahin*, my beloved husband *Alireza*, my adorable daughter *Aynaz*, and my lovely sister *Soudabeh* and her dear family, for their never-ending love, encouragement and moral support. This journey would not have been possible without your help.

Acknowledgements

- Above all, I would like to thank God for giving me the strength, knowledge, ability and opportunity to undertake this research study.
- I would like to express my sincere gratitude to my advisor Prof Marion Meyer for the continuous support of my Ph.D. study and related research, for his patience, motivation, and immense knowledge. His guidance helped me in all the time of research. Besides my advisor, I would like to thank my co-supervisors: Prof Gerhard Prinsloo, and Dr Heino Heyman, for their insightful comments and encouragement. I appreciate their support and comments during the write up of this dissertation.
- I am so grateful of Prof Thomas Klimkait from Department of Biomedicine, University of Basel for his help, willingness and support for conducting HIV tests.
- I am grateful to the Buffelskloof Nature Reserve research manager, Mr John Burrows, and Mr Alexander Heunis of the Voortrekker Monument Nature Reserve in Pretoria for giving permission to collect plants and providing me with the plant material.
- I would like to acknowledge the SWISS-SA collaboration (SA-JRP14) and the financial contributions made by the University of Basel and the CSIR and to the University of Pretoria for their continued support.
- I would like to thank the National Research Foundation of South Africa (NRF) for financial assistance.
- I would like to thank Dr Mamoalosi Selepe at Department of Chemistry, University of Pretoria for her help and expertise with UPLC-MS/MS analysis.
- I would like to thank to Mr Sewes Alberts for his assistance with the NMR analysis.
- I am so grateful of Dr Carel Oosthuizen for his expertise and assistance with molecular docking analysis.
- I cherish the friendship I had and take this opportunity to thank Dr Danielle Twilley and Dr Marco de Canha for their great friendship and support through the complicated times.
- I am very thankful of my colleagues in the Department of Plant and Soil Sciences for their encouragement and support.

- My acknowledgement would be incomplete without thanking the biggest source of my strength, my beloved family. Thank you for encouraging me in all of my pursuits and inspiring me to follow my dreams.
- As a final word, I would like to thank each and every individual who have been a source of support and encouragement and helped me to achieve my goal and complete my dissertation work successfully.

Table of Contents

| | |
|--|-----------|
| Chapter 1 | 1 |
| General introduction | 2 |
| 1.1 Background and motivation..... | 2 |
| 1.2 Hypothesis..... | 4 |
| 1.3 Aim and Objectives of the study..... | 4 |
| 1.4 Chapter layout..... | 5 |
| 1.5 References..... | 7 |
| | |
| Chapter 2 | 9 |
| Literature review | 10 |
| 2.1 Introduction..... | 10 |
| 2.2 Primary metabolites | 11 |
| 2.3 Secondary metabolites | 11 |
| 2.4 Natural product chemistry and metabolomic analyses | 12 |
| 2.5 A summary of HIV-1 infection..... | 12 |
| 2.5.1 The HIV life cycle | 13 |
| 2.6 Role of reverse transcriptase in viral replication | 15 |
| 2.7 Antiviral potential of medicinal plants | 16 |
| 2.7.1 Anti-HIV activity of medicinal plants..... | 18 |
| 2.7.2 <i>Helichrysum</i> species and their therapeutic potential | 19 |
| 2.8 Selected <i>Helichrysum</i> species for the current study | 20 |
| 2.8.1 <i>Helichrysum acutatum</i> DC. | 21 |
| 2.8.2 <i>Helichrysum adenocarpum</i> DC. | 22 |
| 2.8.3 <i>Helichrysum albilanatum</i> Hilliard..... | 23 |
| 2.8.4 <i>Helichrysum argyrophyllum</i> DC. | 23 |
| 2.8.5 <i>Helichrysum athrxiifolium</i> (Kuntze) Moeser..... | 24 |
| 2.8.6 <i>Helichrysum aureum</i> (Houtt.) Merr. var. <i>aureum</i> | 25 |
| 2.8.7 <i>Helichrysum aureum</i> (Houtt) Merr. var. <i>monocephalum</i> (DC.) Hilliard..... | 26 |
| 2.8.8 <i>Helichrysum caespititium</i> (DC.) Harv. | 27 |
| 2.8.9 <i>Helichrysum callicomum</i> Harv. | 28 |

| | |
|--|-----------|
| 2.8.10 <i>Helichrysum cephaloideum</i> DC..... | 29 |
| 2.8.11 <i>Helichrysum chrysargyrum</i> Moeser | 30 |
| 2.8.12 <i>Helichrysum dasyanthum</i> (Willd.) Sweet..... | 31 |
| 2.8.13 <i>Helichrysum gerberifolium</i> A.Rich. | 32 |
| 2.8.14 <i>Helichrysum harveyanum</i> Wild | 32 |
| 2.8.15 <i>Helichrysum kraussii</i> Sch.Bip. | 33 |
| 2.8.16 <i>Helichrysum lepidissimum</i> S.Moore..... | 34 |
| 2.8.17 <i>Helichrysum mariepsopicum</i> Hilliard | 35 |
| 2.8.18 <i>Helichrysum milleri</i> Hilliard..... | 36 |
| 2.8.19 <i>Helichrysum mimetes</i> S.Moore..... | 37 |
| 2.8.20 <i>Helichrysum mundtii</i> Harv..... | 38 |
| 2.8.21 <i>Helichrysum mutabile</i> Hilliard | 39 |
| 2.8.22 <i>Helichrysum nudifolium</i> (L.) Less. var. <i>nudifolium</i> | 39 |
| 2.8.23 <i>Helichrysum opacum</i> Klatt | 41 |
| 2.8.24 <i>Helichrysum patulum</i> (L.) D.Don..... | 41 |
| 2.8.25 <i>Helichrysum petiolare</i> Hilliard & B.L.Burt | 43 |
| 2.8.26 <i>Helichrysum platypterum</i> DC..... | 44 |
| 2.8.27 <i>Helichrysum polycladum</i> Klatt | 45 |
| 2.8.28 <i>Helichrysum reflexum</i> N.E.Br. | 46 |
| 2.8.29 <i>Helichrysum setosum</i> Harv..... | 47 |
| 2.8.30 <i>Helichrysum truncatum</i> Burt Davy | 48 |
| 2.8.31 <i>Helichrysum wilmsii</i> Moeser | 49 |
| 2.8.32 <i>Helichrysum zeyheri</i> Less..... | 49 |
| 2.9 Metabolomic analysis as a diagnostic aid | 50 |
| 2.10 NMR-based metabolomics..... | 54 |
| 2.10.1 Data mining and data processing..... | 55 |
| 2.10.2 Multivariate data analysis | 56 |
| 2.11 Molecular docking study..... | 57 |
| 2.12 Conclusion | 62 |
| 2.13 References..... | 64 |
| Chapter 3 | 75 |

NMR-based metabolomic analysis and anti-HIV activity of selected *Helichrysum* species. 76

| | |
|--|----|
| 3.1 Introduction..... | 76 |
| 3.2 Materials and methods | 77 |
| 3.2.1 Plant collection and extraction | 77 |
| 3.3 Antiviral bioassays..... | 81 |
| 3.3.1 Anti-HIV screening bioassay and cytotoxicity..... | 81 |
| 3.3.2 Anti-HIV deCIPhR assay | 81 |
| 3.3.3 HIV-1 reverse transcriptase colorimetric assay..... | 82 |
| 3.3.4 ¹ H NMR analysis | 83 |
| 3.3.5 Multivariate data analysis | 84 |
| 3.4 Results and discussion | 84 |
| 3.4.1 Anti-HIV screening bioassay and cytotoxicity..... | 84 |
| 3.4.2 Anti-RT activity..... | 88 |
| 3.4.3 ¹ H NMR analysis and metabolomic investigation..... | 89 |
| 3.5 Conclusion | 93 |
| 3.6 References..... | 95 |

Chapter 4 99

Isolation and identification of compound(s) from *Helichrysum mimetes* polar extract 100

| | |
|--|-----|
| 4.1 Introduction..... | 100 |
| 4.2 Material and methods..... | 101 |
| 4.2.1 Collection and extraction of <i>H. mimetes</i> | 101 |
| 4.2.2 Isolation and fractionation of <i>H. mimetes</i> | 103 |
| 4.2.3 Anti-HIV screening and HIV-1 reverse transcriptase colorimetric assay of isolated fractions from <i>H. mimetes</i> | 105 |
| 4.2.4 NMR-based metabolomics analysis of polar extracts | 105 |
| 4.2.5 Ultra performance liquid chromatography-tandem mass spectrometry (UPLC-MS/MS) analysis | 105 |
| 4.2.6 Statistical analysis..... | 106 |
| 4.3 Results and discussion | 106 |
| 4.3.1 Anti-HIV screening bioassay and cytotoxicity..... | 106 |
| 4.3.2 HIV-1 reverse transcriptase colorimetric assay..... | 107 |

| | |
|---|------------|
| 4.3.3 NMR-based metabolomic analysis and identification of most active fractions | 108 |
| 4.4 Conclusion | 117 |
| 4.5 References | 119 |
| Chapter 5 | 122 |
| Molecular docking study of quinic acid isolated from <i>Helichrysum mimetes</i>..... | 123 |
| 5.1 Introduction..... | 123 |
| 5.2 Material and methods..... | 125 |
| 5.2.1 Receptor and ligand preparation..... | 125 |
| 5.2.2 Active site prediction..... | 126 |
| 5.2.3 Molecular docking using Glide XP | 127 |
| 5.3 Results and discussion | 127 |
| 5.4 Conclusion | 133 |
| 5.5 References..... | 134 |
| Chapter 6 | 136 |
| General discussion | 137 |
| 6.1. Overview..... | 137 |
| 6.2 Recommendation for future research..... | 140 |
| 6.3 References..... | 142 |
| Chapter 7 | 144 |
| Appendix..... | 145 |
| 7.1 NMR spectra of the polar extracts of <i>Helichrysum</i> species using nuclear magnetic resonance Bruker 600 MHz spectrometer (Council for Scientific and Industrial Research, CSIR). Solvent: CD3OD and KH2PO4-D2O solution. | 145 |

List of tables

| | |
|---|-----|
| Table 2.1. Some plant-derived products possessing inhibitory effects on various viruses (Babar <i>et al.</i> , 2013)..... | 17 |
| Table 3.1. Collected <i>Helichrysum</i> species, morphological groups and the percentage yield after extraction. | 78 |
| Table 3.2. Extraction parameters on Buchi SpeedExtractor for samples..... | 80 |
| Table 3.3. Anti-HIV screening result (% inhibition) of <i>Helichrysum</i> species. No activity against HIV was observed for any of the non-polar extracts at 2.5 µg/mL. | 85 |
| Table 3.4. Anti-HIV-RT inhibition of selected <i>Helichrysum</i> species at 100 µg/mL. | 88 |
| Table 4.1. Extraction parameters for <i>H. mimetes</i> extraction..... | 102 |
| Table 4.2. Screening assay result showing the IC ₅₀ and % RT inhibition of the fractions and positive control doxorubicin..... | 108 |
| Table 5.1. Possible binding site and cavity prediction of HIV-RT (PDB: 1RTH) | 128 |
| Table 5.2. Molecular docking results of quinic acid (QA), doxorubicin (Dox) and reference ligand U05 (Ref) within the five binding sites identified..... | 129 |

List of figures

| | |
|---|----|
| Figure 2.1. HIV life cycle and potential antiviral targets (Hosseini & Mac Gabhann, 2013). | 15 |
| Figure 2.2. <i>Helichrysum acutatum</i> collected from Buffelskloof Nature Reserve, Mpumalanga, South Africa..... | 21 |
| Figure 2.3. <i>Helichrysum adenocarpum</i> collected from Amsterdam in Mpumalanga, South Africa. | 22 |
| Figure 2.4. <i>Helichrysum albilanatum</i> collected from Buffelskloof Nature Reserve, Mpumalanga, South Africa..... | 23 |
| Figure 2.5. <i>Helichrysum argyrophyllum</i> collected from Kirstenbosch Botanical Garden, Cape Town, Western Cape, South Africa..... | 24 |
| Figure 2.6. <i>Helichrysum athrxiifolium</i> collected from Voortrekker Monument Nature Reserve, Gauteng, South Africa. | 25 |
| Figure 2.7. <i>Helichrysum aureum</i> collected from Buffelskloof Nature Reserve, Mpumalanga, South Africa..... | 26 |
| Figure 2.8. <i>Helichrysum aureum</i> var. <i>monocephalum</i> collected from Buffelskloof Nature Reserve, Mpumalanga, South Africa..... | 27 |
| Figure 2.9. <i>Helichrysum caespititium</i> collected from Voortrekker Monument Nature Reserve, Gauteng, South Africa. | 28 |
| Figure 2.10. <i>Helichrysum callicomum</i> collected from Buffelskloof Nature Reserve, Mpumalanga, South Africa..... | 29 |
| Figure 2.11. <i>Helichrysum cephaloideum</i> collected from Buffelskloof Nature Reserve, Mpumalanga, South Africa..... | 29 |
| Figure 2.12. <i>Helichrysum chrysargyrum</i> collected from Buffelskloof Nature Reserve, Mpumalanga, South Africa..... | 30 |
| Figure 2.13. <i>Helichrysum dasyanthum</i> collected from Kirstenbosch National Botanical Gardens, Western Cape, South Africa. | 31 |
| Figure 2.14. <i>Helichrysum gerberifolium</i> collected from Buffelskloof Nature Reserve, Mpumalanga, South Africa..... | 32 |
| Figure 2.15. <i>Helichrysum harveyanum</i> collected from Buffelskloof Nature Reserve, Mpumalanga, South Africa..... | 33 |

| | |
|--|----|
| Figure 2.16. <i>Helichrysum kraussii</i> collected from Pretoria Botanical Garden, Gauteng, South Africa. | 34 |
| Figure 2.17. <i>Helichrysum lepidissimum</i> collected from Buffelskloof Nature Reserve, Mpumalanga, South Africa..... | 35 |
| Figure 2.18. <i>Helichrysum mariepsopicum</i> collected from Buffelskloof Nature Reserve, Mpumalanga, South Africa..... | 36 |
| Figure 2.19. <i>Helichrysum milleri</i> collected from Buffelskloof Nature Reserve, Mpumalanga, South Africa..... | 36 |
| Figure 2.20. <i>Helichrysum mimetes</i> collected from Buffelskloof Nature Reserve, Mpumalanga, South Africa..... | 37 |
| Figure 2.21. <i>Helichrysum mundtii</i> collected from Buffelskloof Nature Reserve, Mpumalanga, South Africa..... | 38 |
| Figure 2.22. <i>Helichrysum mutabile</i> collected from Buffelskloof Nature Reserve, Mpumalanga, South Africa..... | 39 |
| Figure 2.23. <i>Helichrysum nudifolium</i> var. <i>nudifolium</i> collected from Buffelskloof Nature Reserve, Mpumalanga, South Africa..... | 40 |
| Figure 2.24. <i>Helichrysum opacum</i> collected from Buffelskloof Nature Reserve, Mpumalanga, South Africa..... | 41 |
| Figure 2.25. <i>Helichrysum patulum</i> collected from Stellenbosch University Botanical Garden, Western Cape, South Africa. | 42 |
| Figure 2.26. <i>Helichrysum petiolare</i> collected from Stellenbosch University Botanical Garden, Western Cape, South Africa. | 43 |
| Figure 2.27. <i>Helichrysum platypterum</i> collected from Buffelskloof Nature Reserve, Mpumalanga, South Africa..... | 44 |
| Figure 2.28. <i>Helichrysum polycladum</i> collected from Buffelskloof Nature Reserve, Mpumalanga, South Africa..... | 46 |
| Figure 2.29. <i>Helichrysum reflexum</i> collected from Buffelskloof Nature Reserve, Mpumalanga, South Africa..... | 46 |
| Figure 2.30. <i>Helichrysum setosum</i> collected from Buffelskloof Nature Reserve, Mpumalanga, South Africa..... | 47 |

| | |
|--|----|
| Figure 2.31. <i>Helichrysum truncatum</i> collected from Buffelskloof Nature Reserve, Mpumalanga, South Africa..... | 48 |
| Figure 2.32. <i>Helichrysum wilmsii</i> collected from Buffelskloof Nature Reserve, Mpumalanga, South Africa..... | 49 |
| Figure 2.33. <i>Helichrysum zeyheri</i> collected from Kalahari Thornveld, North West, South Africa. | 50 |
| Figure 2.34. Flowchart for plant metabolomic studies (Tugizimana <i>et al.</i> , 2013). (MS: mass spectroscopy, NMR: nuclear magnetic resonance, GC: gas chromatography, LC: liquid chromatography)..... | 52 |
| Figure 2.35. Flow chart of the docking procedure (Chen, 2015)..... | 59 |
| Figure 2.36. Schematic design of docking: a small molecule ligand (green) to a protein target (black) producing a stable complex..... | 60 |
| Figure 2.37. The docking mode divided into four types of docking mode (Chen, 2015)..... | 61 |
| | |
| Figure 3.1. Examples of the five extracts of different <i>Helichrysum</i> (H) species using increasing polarities. | 80 |
| Figure 3.2. HIV-1 reverse transcriptase colorimetric assay principle. (www.sigmaaldrich.com/catalog/product/roche/11468120910?lang=en&region=ZA) | 83 |
| Figure 3.3. Nuclear magnetic resonance Bruker 600 MHz spectrometer (Council for Scientific and Industrial Research, CSIR). | 83 |
| Figure 3.4. ¹ H NMR stacked spectra of the most active polar <i>Helichrysum</i> species extracts. | 89 |
| Figure 3.5. PCA score plot did not exhibit significant correlation between active and non-active <i>Helichrysum</i> polar extracts. R ² X: 0.80 and Q ² (cum): 0.61. ● Active extracts, ● Extracts with no activity. The anti-HIV active extracts of <i>H. mimetes</i> and <i>H. lepidissimum</i> clustered closely together in all PC`s..... | 90 |
| Figure 3.6. The OPLS-DA score plot exhibits separation of the active vs non-active <i>Helichrysum</i> polar extracts with some overlap in the center. ■ Active extracts, ● Non-active extracts. <i>H. mimetes</i> and <i>H. lepidissimum</i> polar extracts clustered closely together..... | 91 |
| Figure 3.7. The contribution plot generated by comparing the active and non-active <i>Helichrysum</i> extracts. Bars above the line indicated the NMR regions that are positively associated with the activity of the active extracts. | 92 |

| | |
|--|-----|
| Figure 4.1. <i>H. mimetes</i> collected from Buffelskloof Private Nature Reserve..... | 101 |
| Figure 4.2. A) Polar <i>H. mimetes</i> extract, B) Non-polar <i>H. mimetes</i> extract. | 102 |
| Figure 4.3. Silica gel column for separation of the concentrated <i>H. mimetes</i> polar extract into fractions. | 103 |
| Figure 4.4. Sephadex LH-20 column chromatography to purify fraction 15. | 104 |
| Figure 4.5. Activity and toxicity of 16 isolated fractions tested and <i>H. mimetes</i> crude extract against HI live virus at two concentrations (2.5µg/mL and 25µg/mL). | 106 |
| Figure 4.6. RT enzyme activity of fractions 14 and 15 to calculate the IC ₅₀ values. | 107 |
| Figure 4.7. Inhibition of HIV-RT by F14 (green) & F15 (yellow) at different concentrations compared to the positive control doxorubicin (red). | 108 |
| Figure 4.8. Comparison of the stacked NMR spectra of fractions (1-13) (right graph) with that of a study conducted by Heyman <i>et al.</i> (2015) (left graph). The chemical shifts linked to the caffeoylquinic acid type compounds were present in the isolated fractions (7-13 samples). | 109 |
| Figure 4.9. PCA (R ² = 0.953/ Q ² = 0.778) & OPLS-DA (R ² = 0.892/ Q ² = 0.784) score plots of isolated fractions. The active fraction 15 (red arrow) is separated from the rest of the fractions showing a phytochemical difference. | 110 |
| Figure 4.10. NP/PEG reagent showing the presence of caffeoylquinic acids in fractions 6–13 and the absence of chlorogenic acids in fractions 14–16 with the light blue/green fluorescent region in UV light at λ = 365 nm..... | 111 |
| Figure 4.11. Comparison of the ¹ H NMR spectrum of sub-fraction C (of fraction 15) with the ¹ H NMR spectrum of standard quinic acid (QA) (Sigma-Aldrich). Coloured boxes indicate the relative chemical shifts of standard quinic acid and sub-fraction C peaks..... | 111 |
| Figure 4.12. The ¹³ C NMR spectrum of sub-fraction C. Green boxes indicate the chemical shifts of quinic acid carbons..... | 112 |
| Figure 4.13. Diagram of quinic acid isolation from <i>H. mimetes</i> . First chromatography column: silica gel, eluent: hexane: ethyl acetate mixtures of increasing polarity (0% to 100%) and ethyl acetate: MeOH mixtures also of increasing polarity to 100% MeOH. Second chromatography column Sephadex LH-20, eluent: MeOH. | 113 |

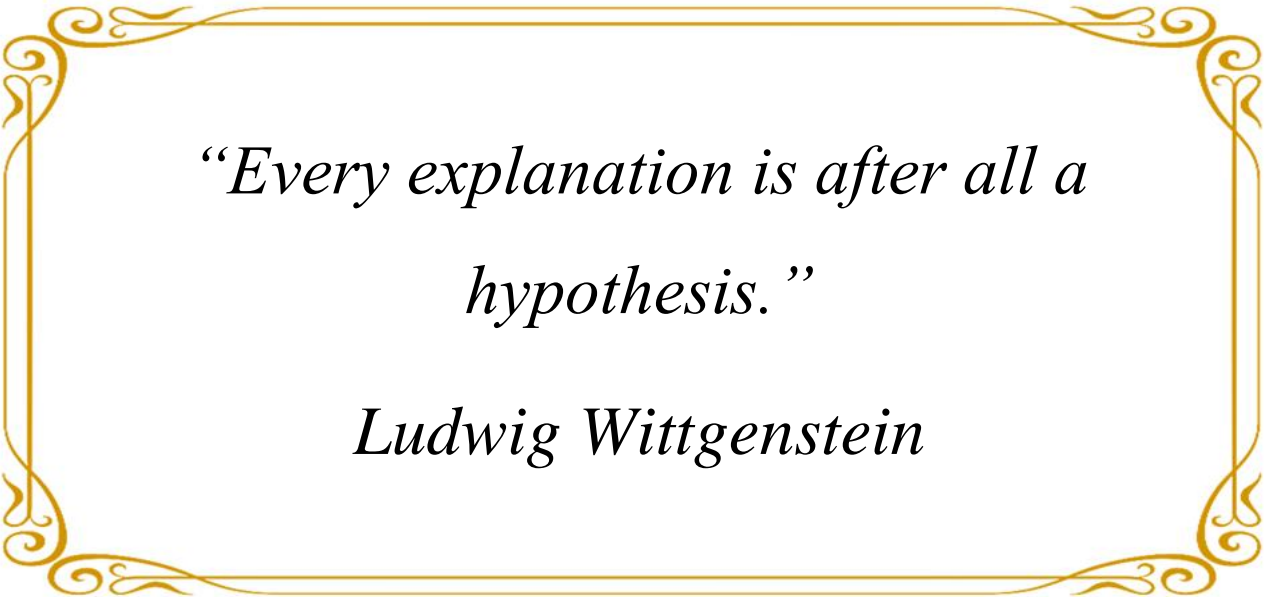
| | |
|---|-----|
| Figure 4.14. Chromatogram in negative mode of sub-fraction C and standard quinic acid (molecular weight: 192.167 g/mol). (a) 0.69; 191.0562, (b) 0.75; 112.9852, (c) 0.60; 112.9852/ 1.17; 96.9596 (d) 0.56; 112.9852/ 0.75; 191.0565 | 114 |
| Figure 4.15. Elemental composition report of isolated quinic acid. | 114 |
| Figure 4.16. MS spectra in negative mode of sub-fraction C and standard quinic acid. The extra peak at 405.1006 is because two quinic acid molecules linked with a sodium molecule. .. | 115 |
| Figure 4.17. Screening isolated sub-fraction C and standards for HIV-1 (pNL-NF) inhibition in deCIPhR method. sf C: sub-fraction C, QA/FA: mixture of QA and FA, QA: quinic acid, FA: formic acid, EFV ctr.: Efavirens. Positive control: Efavirens (5% DMSO) 9.3 - 93 Nm 100% inhibition..... | 116 |
| Figure 5.1. Three-dimensional structures of minimized ligands used in the docking study. From left to right quinic acid, doxorubicin and reference compound U05. | 126 |
| Figure 5.2. Structure of HIV reverse transcriptase (PDB: 1RTH) indicating the identified binding sites; cavity 1 (yellow), cavity 2 (purple), cavity 3 (green), cavity 4 (blue), cavity 5 (red). | 126 |
| Figure 5.3. Quinic acid docked in cavity 4 with a docking score -8.03 (left), interaction diagram of QA indicating the hydrogen bonds between the ligand and binding site residues A: Tyr 188 and A: Lys 101 (right). | 131 |
| Figure 5.4. Reference compound U05 docked in cavity 4 with a docking score of -9.55 (left), interaction diagram of the Reference ligand indicating the salt bridges between ligand and residue A: Tyr 181 and pi-pi stacking with residues A: Trp 229 and A: Tyr 318..... | 132 |
| Figure 5.5. Doxorubicin docked in cavity 1 with a docking score of -7.87 (left), the interaction diagram of doxorubicin ligand indicating the salt bridges between ligand and residue as Thr 409. | 132 |
| Figure 7.1. ¹ H NMR spectrum of <i>H. acutatum</i> DC. [synonym <i>H. schlechteri</i>]..... | 145 |
| Figure 7.2. ¹ H NMR spectrum of <i>H. adenocarpum</i> DC. | 146 |
| Figure 7.3. ¹ H NMR spectrum of <i>H. albilanatum</i> Hilliard. | 146 |
| Figure 7.4. ¹ H NMR spectrum of <i>H. argyrophyllum</i> DC..... | 147 |

| | |
|---|-----|
| Figure 7.5. ^1H NMR spectrum of <i>H. athrixiifolium</i> (Kuntze) Moeser..... | 147 |
| Figure 7.6. ^1H NMR spectrum of <i>H. aureum</i> (Houtt.) Merr. | 148 |
| Figure 7.7. ^1H NMR spectrum of <i>H. aureum</i> (Houtt.) Merr. var. <i>monocephalum</i> (DC.) Hilliard. | 148 |
| Figure 7.8. ^1H NMR spectrum of <i>H. caespititium</i> (DC.) Harv. | 149 |
| Figure 7.9. ^1H NMR spectrum of <i>H. callicomum</i> Harv. | 149 |
| Figure 7.10. ^1H NMR spectrum of <i>H. cephaloideum</i> DC. | 150 |
| Figure 7.11. ^1H NMR spectrum of <i>H. chrysargyrum</i> Moeser..... | 150 |
| Figure 7.12. ^1H NMR spectrum of <i>H. dasyanthum</i> (Willd.) Sweet. | 151 |
| Figure 7.13. ^1H NMR spectrum of <i>H. harveyanum</i> Wild. | 151 |
| Figure 7.14. ^1H NMR spectrum of <i>H. kraussii</i> Sch.Bip. | 152 |
| Figure 7.15. ^1H NMR spectrum of <i>H. lepidissimum</i> S.Moore. | 152 |
| Figure 7.16. ^1H NMR spectrum of <i>H. mariepsopicum</i> Hilliard. | 153 |
| Figure 7.17. ^1H NMR spectrum of <i>H. milleri</i> Hilliard. | 153 |
| Figure 7.18. ^1H NMR spectrum of <i>H. mimetes</i> S.Moore. | 154 |
| Figure 7.19. ^1H NMR spectrum of <i>H. mundti</i> Harv. | 154 |
| Figure 7.20. ^1H NMR spectrum of <i>H. mutabile</i> Hilliard. | 155 |
| Figure 7.21. ^1H NMR spectrum of <i>H. gerberifolium</i> A.Rich..... | 155 |
| Figure 7.22. ^1H NMR spectrum of <i>H. opacum</i> Klatt. | 156 |
| Figure 7.23. ^1H NMR spectrum of <i>H. patulum</i> (L.) D.Don. | 156 |
| Figure 7.24. ^1H NMR spectrum of <i>H. petiolare</i> Hilliard & B.L.Burt. | 157 |
| Figure 7.25. ^1H NMR spectrum of <i>H. platypterum</i> DC. | 157 |
| Figure 7.26. ^1H NMR spectrum of <i>H. polycladum</i> Klatt. | 158 |
| Figure 7.27. ^1H NMR spectrum of <i>H. nudifolium</i> (L.) Less. var. <i>nudifolium</i> | 158 |
| Figure 7.28. ^1H NMR spectrum of <i>H. reflexum</i> N.E.Br..... | 159 |
| Figure 7.29. ^1H NMR spectrum of <i>H. setosum</i> Harv. | 159 |
| Figure 7.30. ^1H NMR spectrum of <i>H. truncatum</i> Burt. Davy..... | 160 |
| Figure 7.31. ^1H NMR spectrum of <i>H. wilmsii</i> Moeser. | 160 |
| Figure 7.32. ^1H NMR spectrum of <i>H. zeyheri</i> Less. | 161 |

List of abbreviations

| | | | |
|--------------------------|--------------------------------------|----------------|---|
| IC₅₀ | 50% Inhibition concentration | QA | Quinic acid |
| ¹H NMR | Proton nuclear magnetic resonance | FA | Formic acid |
| Ace | Acetone | NaOD | Sodium deuterioxide |
| AIDS | Acquired immunodeficiency syndrome | EtOAc | Ethyl acetate |
| C | Carbon | PR | Protease |
| CD₃OD | Deuterated methanol | NCE | Natural chemical entities |
| CDCL₃ | Deuterated chloroform | NMR | Nuclear magnetic resonance |
| DCM | Dichloromethane | OPLS-DA | Orthogonal Projections to Latent Structures-Discriminant Analysis |
| DMSO | Dimethyl sulphoxide | PCA | Principal Component Analysis |
| DNA | Deoxyribonucleic acid | RNA | Ribonucleic acid |
| H | Proton | RT | Reverse transcriptase |
| HAART | Highly active antiretroviral therapy | SARS | Severe acute respiratory syndrome |
| HBV | Hepatitis B virus | TB | Tuberculosis |
| Hex | Hexane | WHO | World Health Organisation |
| HIV-1 | Human immunodeficiency virus type 1 | MS | Mass spectrometry |
| HSV-2 | Herpes simplex virus type 2 | MVDA | Multivariate data analysis |
| HVB | Hepatitis B virus | N | Nitrogen |
| MeOH | Methanol | DeCIPhR | Dual-Enhancement of Cell-Infection to Phenotype Resistance |
| mRNA | Messenger RNA | | |

Chapter 1



*“Every explanation is after all a
hypothesis.”*

Ludwig Wittgenstein

General introduction

1.1 Background and motivation

Natural products or secondary metabolites are present in all higher plants and produce a wide range of organic compounds. They have an essential role for survival and reproduction of plants but they do not participate directly in the growth and development of the plants (Anulika *et al.*, 2016; Wink, 2003). Secondary metabolites of medicinal plants are a major source of drugs for the treatment of various health disorders. The therapeutic properties of natural products have been recognized since ancient human civilizations. About 25% of the drugs prescribed worldwide come from plants (Pan *et al.*, 2013). More than 11% of the 252 drugs considered as basic and essential by the World Health Organization (WHO) are exclusively of plant origin and a significant number are synthetic drugs obtained from natural precursors (Akinyemi *et al.*, 2018). According to the WHO, 75% of people globally still rely on traditional plant medicines for primary health care (Veeresham, 2012; Dar & Mir, 2017). The potential of natural products as antiviral agents is a valuable source for future development of new drugs. Thus, future research is necessary to continue the search for a large number of potential lead compounds (Mundinger & Efferth, 2008; Lin *et al.*, 2014).

Among the contagious elements, diseases caused by viruses are one of the major causes of death, disability, and social and economic disruption for millions of people. The search for novel therapeutic agents for viral diseases is a challenging pursuit. Human immunodeficiency virus/acquired immunodeficiency syndrome (HIV/AIDS) is one of the major public health problems and is still a threatening disease worldwide. Africa has witnessed the full devastation of the HIV/AIDS pandemic more than elsewhere in the world. HIV/AIDS threaten more than 30 million people worldwide and most of them in Africa and sub-Saharan Africa (Cohen *et al.*, 2008). Globally, 37.9 million people were living with HIV at the end of 2018 (WHO, 2018). Unfortunately, despite all recent progress in HIV treatment and prevention, the total number of persons living with HIV in South Africa increased from an estimated 4.72 million in 2002 to 7.03 million by 2016 (Africa, 2017). Important sociological consequences of HIV/AIDS include family disruption, socioeconomic damage, a decrease in life expectancy, a secondary epidemic of

tuberculosis (TB), hepatitis B virus (HBV) infection and a dramatic increase in the number of orphans (Cohen *et al.*, 2008).

Many research approaches are currently aimed at the development of novel agents to inhibit the replication of HIV through various targets. Secondary metabolites in recent years have become popular for the treatment of HIV symptoms. However, the rapid appearance of HIV strain resistance to currently available drugs and the rapid spread of the AIDS epidemic, suggests that effective and durable chemotherapy of the HIV disease will require the use of innovative combinations of drugs having different mechanisms of anti-HIV activity (Richman *et al.*, 2009; Salehi *et al.*, 2018). Alongside the development of resistance, the acceptable levels of toxicity, high cost, unavailability and lastly the lack of curative effect are the main shortcomings and concerns of the current HIV/AIDS drugs (Cihlar & Fordyce, 2016). This has thus created a great and urgent need to search for and develop new and different anti-HIV treatment candidates. Therefore, new research to identify these candidates from plants and natural products is essential.

Some chemical classes such as acylphloroglucinols, diterpenes and flavonoids from the South African *Helichrysum* species have shown promising antimicrobial activity, which should lead to further studies of these specific plants (Lourens *et al.*, 2008). The very promising reported medicinal value of *Helichrysum* species, as well as limited research on anti-HIV activity of these species has inspired this PhD research to further investigate selected *Helichrysum* species and their bioactivity on HIV. The aim was to discover novel constituents and possible novel drug(s) in the fight against this important pathogen. It is also very important in the search of novel drugs to discover and make use of high-throughput techniques such as metabolomics that will enable many possible candidates to be scanned for possible use as new drug leads.

The development of metabolomic technologies holds the potential to significantly improve diagnosis, unravel more appropriate therapeutic targets, and enable a more precise prognosis of disease development. In recent years, the development of instrumental systems, such as high-resolution nuclear magnetic resonance spectroscopy (NMR) and mass spectrometry (MS), ultra-performance liquid chromatography, and more sophisticated bioinformatics and analytical techniques, has enabled more comprehensive coverage of the metabolome (Zhang *et al.*, 2015).

Applying metabolomic analysis provides a unique opportunity to investigate the metabolomic patterns based on NMR spectroscopy techniques to identify and isolate the active constituents against the HI virus.

The molecular docking approach employed in this study can be used to model the interaction between a small molecule and a protein at the atomic level, which allows us to characterize the behavior of an isolated molecule(s) in the binding site of target points, as well as to elucidate fundamental biochemical processes. The docking process involves two basic steps: prediction of the ligand conformation, as well as its position and orientation within these sites which is usually referred to as pose and assessment of the binding affinity (Meng *et al.*, 2011).

1.2 Hypothesis

A metabolomic investigation of bioactivity and chemical variation in plant extracts can be statistically quantified and be used as a tool to predict anti-HIV activity in *Helichrysum* species.

1.3 Aim and Objectives of the study

The discovery of natural-based antiviral agents has increased globally in the past decades. Many investigations confirmed the potential of plant extracts and their isolated substances to inhibit viruses. There is much concern about the lack of effective antiviral agents, the drug resistance problem and the health and economic damage caused by viruses in humans. These are the essential reasons for the development of novel anti-HIV agents, which are urgently needed.

The specific objectives of this study were:

- To investigate the anti-HIV activity and cytotoxicity of selected *Helichrysum* species;
- To determine the chemical classes of these *Helichrysum* species with the use of different organic solvents covering the polarity range;
- To investigate the anti-RT activity of the most promising *Helichrysum* species and determine the mode of action;

- To use the bioactivity and NMR results of the plants to select one species to identify the most active extract;
- To use metabolomic patterns based on NMR spectroscopy to identify and isolate the active constituents against the HI virus;
- To determine the value of statistical analysis of both bioactivity and metabolomic analysis for a better understanding of the most active extract/compound;
- To perform molecular docking studies to determine the possible mechanism of action of the isolated compound against the RT-enzyme to describe the structure-activity relationship.

1.4 Chapter layout

| | |
|-----------|---|
| Chapter 1 | The introductory chapter consists of the general background of natural products, HIV-1 and metabolomic analyses. The specific objectives of the study are explained. |
| Chapter 2 | An introduction to plant primary and secondary metabolites, as well as chemometric approaches is discussed. Furthermore, the chapter gives a brief overview of HIV-1 infection. It describes antiviral potential of medicinal plants with emphasis on anti-HIV activity. Selected <i>Helichrysum</i> species and their therapeutic potential are also described in this chapter. Metabolomic analysis as a diagnostic aid and NMR-based metabolomics are discussed. |
| Chapter 3 | The extraction procedure of the selected <i>Helichrysum</i> species is described in this chapter. The antiviral, cytotoxicity and anti-RT activity of the plant extracts are investigated against the HI virus, as well as NMR-based metabolomic analysis on anti-HIV activity. |
| Chapter 4 | The isolation and identification of the compounds from the <i>H. mimetes</i> extract using various isolation and identification procedures such as column chromatography, thin layer chromatography and nuclear magnetic resonance |

(NMR) are described. The antiviral, cytotoxicity and anti-RT activity of the isolated fractions are also evaluated.

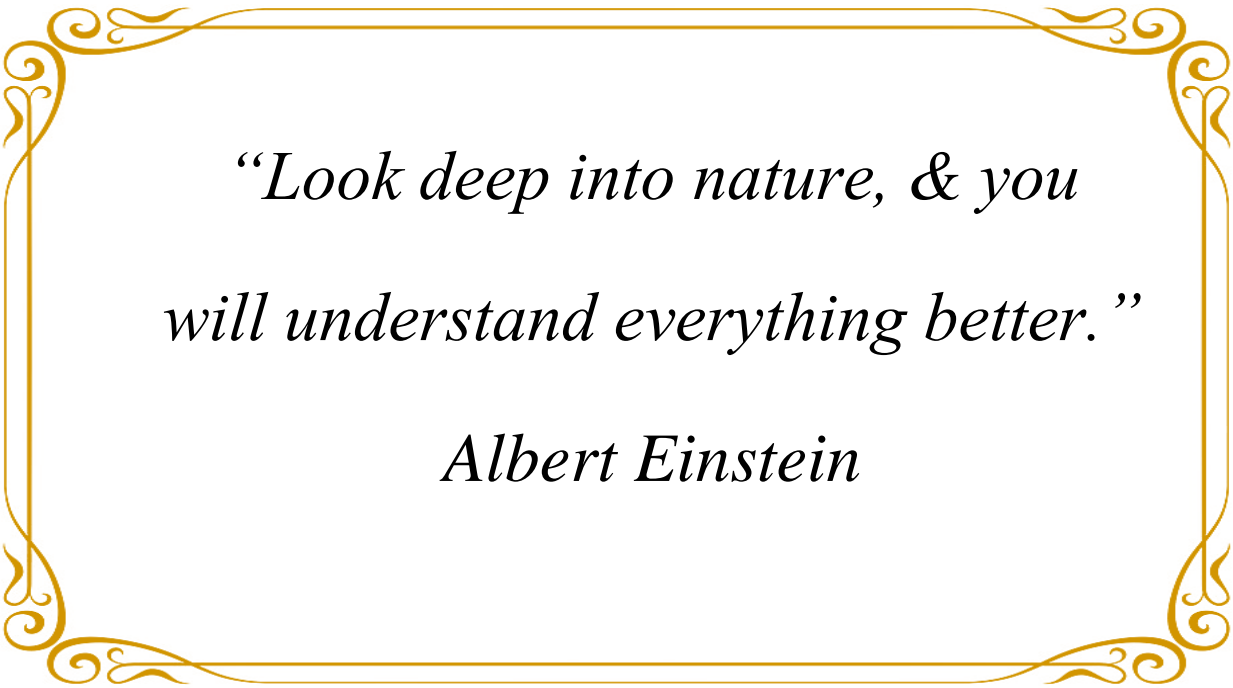
- Chapter 5 Molecular docking studies of the isolated compound are described in this chapter and the possibility of the isolated compound to bind to the RT enzyme. The possible poses of the ligands and the interactions of the isolated bioactive compound with the active sites of RT are explored to determine their efficiency as anti-HIV agents by using SiteMap.
- Chapter 6 The general discussion and conclusions of the study are presented to interpret and explain the results of the study, with future recommendations and considerations made.
- Chapter 7 The appendix includes all the additional ^1H NMR spectra obtained in this study.

1.5 References

- Africa, S. S. (2017). Mid-year population estimates. Pretoria: Statistics South Africa.
- Akinyemi, O., Oyewole, S. O. & Jimoh, K. A. (2018). Medicinal plants and sustainable human health: a review. *Horticulture International Journal*, 2, 194–195.
- Anulika, N. P., Ignatius, E. O., Raymond, E. S., Osasere, O.-I. & Hilda, A. (2016). The chemistry of natural product: Plant secondary metabolites. *International Journal of Technology Enhancements and Emerging Engineering Research*, 4(8), 1–8.
- Cihlar, T. & Fordyce, M. (2016). Current status and prospects of HIV treatment. *Current Opinion in Virology*, 18, 50–56.
- Cohen, M. S., Hellmann, N., Levy, J. A., DeCock, K. & Lange, J. (2008). The spread, treatment, and prevention of HIV-1: evolution of a global pandemic. *The Journal of Clinical Investigation*, 118(4), 1244–1254.
- Dar, A. M. & Mir, S. (2017). Molecular docking: approaches, types, applications and basic challenges. *Journal of Analytical & Bioanalytical Techniques*, 8, 2.
- Lin, L.-T., Hsu, W.-C. & Lin, C.-C. (2014). Antiviral natural products and herbal medicines. *Journal of Traditional and Complementary Medicine*, 4(1), 24–35.
- Lourens, A. C. U., Viljoen, A. M., & Van Heerden, F. R. (2008). South African *Helichrysum* species: a review of the traditional uses, biological activity and phytochemistry. *Journal of Ethnopharmacology*, 119(3), 630–652.
- Meng, X.-Y., Zhang, H.-X., Mezei, M. & Cui, M. (2011). Molecular docking: a powerful approach for structure-based drug discovery. *Current Computer-Aided Drug Design*, 7(2), 146–157.
- Mundinger, T. A. & Efferth, T. (2008). Herpes simplex virus: Drug resistance and new treatment options using natural products. *Molecular Medicine Reports*, 1(5), 611–616.
- Pan, S. -Y., Zhou, S. -F., Gao, S. -H., Yu, Z. -L., Zhang, S. -F., Tang, M. -K., Sun, J. -N., Ma, D. -L., Han, Y. -F., Fong, W. -F. & Ko, K. -M. (2013). New perspectives on how to discover

- drugs from herbal medicines: CAM's outstanding contribution to modern therapeutics. *Evidence-Based Complementary and Alternative Medicine*, 2013, 1–25.
- Richman, D. D., Margolis, D. M., Delaney, M., Greene, W. C., Hazuda, D. & Pomerantz, R. J. (2009). The challenge of finding a cure for HIV infection. *Science*, 323(5919), 1304–1307.
- Salehi, B., Kumar, N.V.A., Şener, B., Sharifi-Rad, M., Kiliç, M., Mahady, G., Vlaisavljevic, S., Iriti, M., Kobarfard, F., Setzer, W., Ayatollahi, S.A., Ahtar, A. & Sharifi-Rad, J. (2018). Medicinal plants used in the treatment of human immunodeficiency virus. *International Journal of Molecular Sciences*, 19(5), 1459.
- WHO, (2018). <https://www.who.int/gho/hiv/en/> (Accessed 02/09/2019).
- Veeresham, C. (2012). Natural products derived from plants as a source of drugs. *Journal of Advanced Pharmaceutical Technology & Research*, 3(4), 200–201.
- Wink, M. (2003). Evolution of secondary metabolites from an ecological and molecular phylogenetic perspective. *Phytochemistry*, 64(1), 3–19.
- Zhang, A., Sun, H., Yan, G., Wang, P. & Wang, X. (2015). Metabolomics for biomarker discovery: moving to the clinic. *BioMed Research International*, 2015, 1–7.

Chapter 2



*“Look deep into nature, & you
will understand everything better.”*

Albert Einstein

Literature review

2.1 Introduction

The history of medicinal plants dates back to the origins of the oldest human civilizations known to man (Jamshidi-Kia *et al.*, 2018). The knowledge associated with traditional complementary or alternative herbal medicine has promoted advanced research and investigations of medicinal plants as potential medicines and has led to the isolation of many natural products that have become well-known pharmaceuticals (Dias *et al.*, 2012; Jamshidi-Kia *et al.*, 2018).

The rapid replication of HIV-1 and the errors made during viral replication cause the virus to develop rapidly in patients, leading to problems in vaccine development and drug therapy. In the absence of an effective vaccine, drugs are the only useful treatment. Unfortunately, HIV-1 develops resistance to all the available drugs. Although a number of useful anti-HIV drugs have been approved for use in patients, the problems associated with drug toxicity and the development of resistance shows that the search for new drugs is an ongoing process (Sarafianos *et al.*, 2009).

The reasons for an increasing interest in alternative therapies and the therapeutic use of plant secondary metabolites are mainly that conventional medicine has not yet provided an effective anti-HIV treatment and has several side effects. Their abusive and/or their incorrect use also result in side effects and other problems (Rates, 2001; Wangkheirakpam, 2018). A large percentage of the world's population does not have access to conventional pharmacological treatments, and folk medicine and ecological awareness suggest that "natural" products are usually safe to use (Wangkheirakpam, 2018).

The natural chemical constituents are often classified into two major groups: primary and secondary metabolites. There is an enormous source of natural chemical entities (NCE) in the plant kingdom with potential as novel drugs. The NCE are secondary metabolites, synthesized by plants as defense mechanisms against herbivores and pathogens or attraction of pollinators etc., and are grouped in three main chemical families: alkaloids, terpenoids and phenolic compounds (Brusotti *et al.*, 2014).

2.2 Primary metabolites

Sugars, fatty acids, amino acids and the polymers obtained from them such as polysaccharides, proteins, lipids, ribonucleic acid (RNA) and deoxyribonucleic acid (DNA) which are essential for growth, survival and security of the living organisms are known as primary metabolites. These compounds are responsible for the primary life processes of respiration, photosynthesis, growth, development, and other essential functions (Croteau *et al.*, 2000; Dias *et al.*, 2012).

2.3 Secondary metabolites

Some natural products are not essential for the growth, development or reproduction of organisms. They are produced as a result of the organism adapting to its environment or are formed to act as a defence mechanism against predators to assist in the survival of the organism. These natural organic products call secondary metabolites (Pagare *et al.*, 2015). Plants have evolved and adapted over millions of years to be able to resist infection of bacteria, fungi and even viruses and they have produced unique structurally diverse secondary metabolites. The ethnopharmacological properties of plant secondary metabolites have been used as a primary source of leads for the early stages of drug discovery (Dias *et al.*, 2012). The biosynthesis of secondary metabolites is derived from the fundamental processes of photosynthesis, glycolysis and the Krebs cycle to afford biosynthetic intermediates, which, ultimately, result in the formation of secondary metabolites (Dias *et al.*, 2012; Kabera *et al.*, 2014).

During the past decade, there have been increasing public interest and acceptance of natural therapies in both developing and developed countries. Due to poverty and limited access to modern medicine, it is estimated that up to four billion people (representing 80% of the world's population), especially living in the developing world, rely on herbal medicine as their source of primary healthcare, and 80% of 122 plant-derived drugs have ethnopharmacological origins (Kunle *et al.*, 2012). There are many examples of important drugs obtained from plants such as digoxin from *Digitalis* spp., paclitaxel (Taxol) from *Taxus brevifolia*, quinine and quinidine from *Chinchona* spp., vinblastine from *Catharanthus roseus*, atropine from *Atropa belladonna* and morphine and codeine from *Papaver somniferum*. In addition, compounds such as muscarine,

physostigmine, cannabinoids, forskolin, colchicine and phorbol esters, have all been obtained from plants (Rates, 2001; Veeresham, 2012).

Over 60 000 extracts of secondary metabolites isolated from the plants, marine, mushrooms and fungi organisms have already been tested against HIV-1 (Dias *et al.*, 2012). The most motivating result is probably the class of compounds known as the calanolides. Calanolide A and calanolide B isolated from *Calonphyllum* species, along with prostratin from *Homalanthus nutans*, have progressed into clinical and preclinical development (Dias *et al.*, 2012). A new farnesyl hydroquinone, ganomycin I, was isolated along with ganomycin B from the fruiting bodies of the Vietnamese mushroom *Ganoderma colossum*. These compounds inhibited HIV-1 protease with IC₅₀ values of 7.5 and 1.0 µg/mL, respectively (El Dine *et al.*, 2009).

2.4 Natural product chemistry and metabolomic analyses

The objective of metabolomics is to create unbiased observations using highly reproducible analytical tools followed by data analysis to discover links between all available data (Dias *et al.*, 2012). In the field of metabolomics, there is not a single analytical technique capable of profiling all low molecular weight metabolites of a given organism. Since plant extracts are extremely complex, given the huge chemical diversity of metabolites they represent, there is no one single analytical platform and methodology, which can analyze all metabolites simultaneously. Multiple separation chemical techniques must be employed to achieve a comprehensive analysis. Nuclear magnetic resonance (NMR) based metabolomics has many applications in science and a combination of metabolomics technologies together with other natural products discovery processes, will be beneficial in drug discovery on multiple levels (Cox *et al.*, 2014).

2.5 A summary of HIV-1 infection

After more than two decades since first recognizing AIDS, HIV-1 still requires continued global focus and investment (Cohen *et al.*, 2008). The cumulative total of individuals infected with HIV-1 and death due to AIDS since the pandemic began exceeds 60 million and 25 million people, respectively. Based on the latest UNAIDS data, the number of people living with HIV on

antiretroviral therapy has increased (UNAIDS, 2018). In the world's most affected region, eastern and southern Africa, the number of people on treatment has more than doubled since 2010, reaching nearly 10.3 million people. In 2015, there were 2.1 million new HIV infections worldwide, adding up to a total of 36.7 million people living with HIV (UNAIDS, 2018). The global estimate for people living with HIV is 37.9 million. About 5 000 new HIV infections (adults and children) per day have been reported according to the UNAIDS 2017 report (UNAIDS, 2018).

South Africa has the biggest and highest profile of HIV infection in the world, with an estimated 7.1 million people living with HIV in 2016. In the same year, there were 270 000 new infections while 110 000 South Africans died from AIDS-related illnesses (UNAIDS, 2018).

Beside all the impacts of HIV/AIDS on many angles of human life such as agriculture, healthcare and economics, the current program and treatments of HIV/AIDS have cost billions annually. South Africa has the largest antiretroviral treatment (ART) program globally and these efforts have been largely financed from its own domestic resources. The country now invests more than \$1.5 billion annually to run its HIV and AIDS programs (South African National AIDS Council, 2016). Therefore, huge challenges lie ahead.

There are two different types of HIV, HIV-1 and HIV-2, which cause infection and diseases in humans. HIV-1 has emerged from cross-species transmission of a chimpanzee virus to humans and HIV-2 from cross-species transmission of a Sooty mangabey virus (De Groot & Bontrop, 2013; Post *et al.*, 2016). HIV-1 has been grouped, based on different genomes in three groups, labeled M, N, and O. Group M viruses cause most HIV-1 infections, and these are divided into 9 subtypes known as clades (A-D, F-H, J and K). The most common clade in the Americas, Europe, and Australia is clade B, whereas clade C predominates in the most heavily affected part of the world, southern Africa. It is known that, different clades might be transmitted with different levels of efficiency and might differ in their pathogenic potential (Cohen *et al.*, 2008).

2.5.1 The HIV life cycle

HIV is a member of the genus *Lentivirus* in the *Retroviridae* family that infects the vital organs and cells of the human immune system. Retroviruses are small envelope viruses that contain a

diploid, single-stranded RNA genome. The virus particle contains an inner core that contains the viral nucleic acids, as well as enzymes required for early replication events. The inner core is surrounded by two layers, a capsid protein and a lipid membrane. A virus matrix protein is inserted into the inner surface of the membrane. An integral membrane protein, the envelope glycoprotein, protrudes through the membrane and forms the outer surface of the virus particle (Nisole & Saïb, 2004). Retroviruses are so called because their RNA genome is transcribed into DNA within the cell using the viral enzyme reverse transcriptase (RT). HIV infection usually progresses and, eventually, will develop into AIDS in the vast majority of cases. Once HIV is in the body, it targets and infects a certain type of white blood cell called a CD4 cell. The steps HIV goes through to complete this process are as follows (Figure 2.1) (Hosseini & Mac Gabhann, 2013):

- a) **Binding and Fusion:** HIV begins its life cycle when it binds to a CD4 receptor and one of two co-receptors on the surface of a CD4+ T-lymphocyte. The virus then fuses with the host cell. After fusion, the virus releases RNA, its genetic material, into the host cell.
- b) **Reverse transcription:** An HIV enzyme called reverse transcriptase converts the single-stranded HIV RNA to double-stranded HIV DNA.
- c) **Integration:** The newly formed HIV DNA enters the host cell's nucleus, where an HIV enzyme called integrase "hides" the HIV DNA within the host cell's own DNA. The integrated HIV DNA is called a provirus. The provirus may remain inactive for several years, producing few or no new copies of HIV.
- d) **Transcription:** When the host cell receives a signal to become active, the provirus uses a host enzyme called RNA polymerase to create copies of the HIV genomic material, as well as shorter strands of RNA called messenger RNA (mRNA). The mRNA is used as a blueprint to make long chains of HIV proteins.
- e) **Assembly:** An HIV enzyme called protease cuts the long chains of HIV proteins into smaller individual proteins. As the smaller HIV proteins come together with copies of HIV's RNA genetic material, a new virus particle is assembled.

- f) Budding: The newly assembled virus pushes out ("buds") from the host cell. During budding, the new virus steals part of the cell's outer envelope. This envelope, which acts as a covering, is studded with protein/sugar combinations called HIV glycoproteins. These HIV glycoproteins are necessary for the virus to bind CD4 and co-receptors. The new copies of HIV can now move on to infect other cells (Figure 2.1).

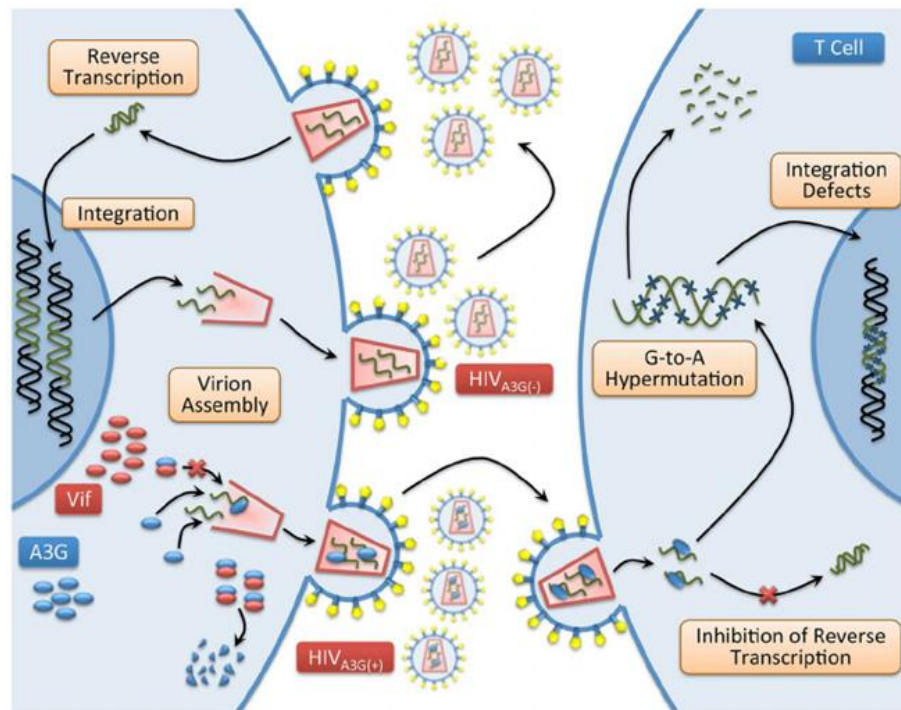


Figure 2.1. HIV life cycle and potential antiviral targets (Hosseini & Mac Gabhann, 2013).

2.6 Role of reverse transcriptase in viral replication

Viral enzymes play a key role in HIV infection. If viral enzymes could be neutralized, viral replication would not take place. The proteolytic processing of viral polyprotein precursors by a viral proteinase is essential for maturation of the virus. Designing specific inhibitors for each viral protease is thus a desirable objective (Jassim and Naji, 2003). Several viral proteins required for the early phases of infection are incorporated with the virion. These include protease (PR), which is essential for viral assembly, reverse transcriptase (RT) and integrase (IN), which are needed

after entry for viral DNA synthesis and integration (Bennett *et al.*, 2014). The fact that RT plays a very important role in controlling the replication of HIV makes it one of the most attractive targets in the development of anti-AIDS drugs. Recent efforts have often been focusing on the anti-HIV activity of medicinal plants at molecular level. Several studies compared various plants and their individual parts (stem, leaves, roots, etc.) in inhibiting viral RT and IN, the two essential enzymes in HIV infections. Reverse transcriptase inhibitors are already used in some of the anti-HIV agents (Mukhtar *et al.*, 2008; Malolo *et al.*, 2014).

There are presently two classes of inhibitors of RT: nucleoside analogues and non-nucleoside compounds, which are distinguished by their different inhibitory mechanisms. The analogues 3'-azido-2',3'-dideoxythymidine (AZT), 2',3'- dideoxycytidine (DDC), 4'-ethynyl-2-fluoro-2'-deoxyadenosine triphosphate and 2',3'-didexyinosine (DDI) belong to the nucleoside analogues which act by chain termination and inhibit competitively the deoxynucleoside triphosphate substrates.

The non-nucleoside inhibitors include compounds such as nevirapine, calanolide, coumarin derivatives, benzodiazepine derivatives and psychotrine. They have an effect at sites other than the substrate binding sites of the polymerase. The rapid drug cross-resistance of these compounds is the major problem of using them in treatment of HIV patients (Min *et al.*, 2000; Sluis-Cremer & Tachedjian, 2008; Michailidis *et al.*, 2009).

2.7 Antiviral potential of medicinal plants

Unlike bacterial, fungal and parasitic infections, viruses are not autonomous organisms. These pathogens require living cells in which to replicate. Consequently, most of the steps in their replication involve normal cellular metabolic pathways, and this makes it difficult to design a treatment to attack the virion directly, or its replication, without accompanying adverse effects on the infected cells (Jassim & Naji, 2003). Medicinal plants have been widely considered as treatments in a variety of infectious and non-infectious diseases (Table 2.1).

Table 2.1. Some plant-derived products possessing inhibitory effects on various viruses (Babar *et al.*, 2013).

| Mechanism of Action | Principal Ingredient | Botanical Source | Activity against |
|---|-----------------------------------|---|---|
| Immune stimulants | Polyphenol complex | <i>Geranium sanguineum</i> | Influenza viruses |
| | β -sitosterol | <i>Nigella sativa</i> , <i>Serenoa repens</i> | Multiple viruses |
| | Essential oils, extracts | Family Asteraceae | Respiratory viruses, HSV ¹ |
| Entry inhibitors | Mannose-specific lectins | <i>Galanthus</i> spp., <i>Narcissus</i> spp. | HIV ² , Influenza, CMV ³ , FIPV ⁴ |
| | Elenoic acid | <i>Olive</i> spp. | Influenza, HSV |
| | Galactofucan | <i>Achyrocline flaccida</i> | HSV |
| | Polysaccharides | <i>Stevia rebaudiana</i> | Rotavirus |
| Replication and Translation inhibitors | Glycyrrhizin | <i>Glycyrrhiza</i> spp. | HIV, SARS-coV, Hepatitis A |
| | Phytolacca American Protein (PAP) | <i>Phytolacca americana</i> <i>Phytolacca farmosus</i> | HSV, HIV, HBV ⁵ |
| | Emetine | <i>Psychotria ipecacuanha</i> | Influenza, Dengue Virus, Animal viruses |
| | Quercetin | <i>Quercus</i> spp. | Influenza, HCV ⁶ , JEV ⁷ |
| | Fisetin | <i>Acacia</i> spp., <i>Gleditsia</i> spp. | Dengue, HCV |
| Viral assembly and release inhibitors | Hesperidin | <i>Citrus</i> spp. | Influenza |
| | Naringenin | <i>Citrus</i> spp. | HCV |

¹HSV: Herpes simplex virus, ²HIV: Human immunodeficiency virus, ³CMV: Cytomegalovirus, ⁴FIPV: Feline Infectious Peritonitis Virus, ⁵HBV: Hepatitis B virus, ⁶HCV: Hepatitis C virus, ⁷JEV: Japanese encephalitis virus.

Among several ailments, viral infections, particularly infections associated with HIV-1 and HIV-2, and newly emerging infectious viruses have challenged human survival. The limitation of the isolation of active antiviral components from plants in the past were the highly infectious nature of viruses and the lack of suitable separation techniques for the identification of antiviral compounds from natural resources (Mukhtar *et al.*, 2008; Pushpa *et al.*, 2013).

Even though using medicinal plants to treat viral infections has a long history, the first recognized interest and efforts in their development as antiviral agents were done by the Boots drug company (Nottingham, England) in the mid-1900's. Later on researchers reported the inhibitory effects of medicinal plant extracts on the replication of several viruses, such as Herpes simplex virus type 2 (HSV-2), HIV, Hepatitis B virus (HVB) and severe acute respiratory syndrome (SARS) (Mukhtar *et al.*, 2008).

2.7.1 Anti-HIV activity of medicinal plants

According to De Clercq (2009), there are several different inhibitors in anti-HIV drug discovery: nucleoside reverse transcriptase inhibitors (NRTIs), nucleotide reverse transcriptase inhibitors (NtRTIs), non-nucleoside reverse transcriptase inhibitors (NNRTIs), protease inhibitors (PIs), fusion inhibitors (FIs), co-receptor inhibitors (CRIs) and integrase inhibitors (INIs). The importance of anti-HIV drug combination regimens called HAART (highly active antiretroviral therapy) has become widely accepted which is the combination of three (or more) anti-HIV compounds (De Clercq, 2009).

The major accomplishment of HIV/AIDS medicine, which is widely used to treat patients, is the highly active antiretroviral therapy (HAART) for chronic suppression of HIV replication (Richman *et al.*, 2009). The toxicity rate of the newer HAART drugs is low but many of these drugs modulate lipid and glucose metabolism. There is already concern about increased rates of heart disease, diabetes, liver disease, and many forms of cancer in aging HIV-infected patients who are receiving treatment. Whether these are because of long-term HIV infection, therapeutic drug treatment, or both, is uncertain. Additionally, the cost of HAART may be too high to sustain treatments on a global scale, as millions are affected (Richman *et al.*, 2009).

Polyphenols and the proanthocyanidins isolated from the bark of *Hamamelis virginiana* and two hydrolysable tannins, shephagenins A and B, and hippophaenin A and strictinin isolated from the leaf extract of *Shepherdia argentea*, showed a remarkable inhibitory activity against HIV-1 reverse transcriptase (RT). The inhibitory effect of the ethanol leaf extract of *S. argentea* extract on HIV-1 RT was related to the isolated tannins. Interestingly, their activities were stronger than epigallocatechin gallate used as a positive control (Yoshida *et al.*, 1996). A flavonoid compound isolated from *Scutellaria baicalensis*, baicalein, has illustrated anti-inflammatory and anti-HIV-1 activities. Baicalein may interfere with the interaction of HIV-1 envelope proteins with chemokine co-receptors and block HIV-1 entry of target CD4 cells and baicalein could be used as a basis for developing novel anti-HIV-1 agents (Li *et al.*, 2000).

According to Dai *et al.* (1998), the oligostilbenes isolated from the leaves of *Hopea malibato* extract was tested against HIV and found that a new oligostilbene dibalanocarpol, together with one known oligostilbene balanocarpol exhibited partial HIV-inhibitory activity.

According to a review by Jassim and Naji (2003), *Calophyllum* species have strong anti-HIV activity potential. Species of the *Calophyllum* tree have been tested to identify novel inhibitors of HIV-1-RT by screening, isolation and identification of natural compounds. The most extensive screening was conducted on inophyllum, calanolide A and coumarins isolated from *C. inophyllum*, *C. lanigerum*, *C. teysmannii* latex and *C. cerasiferum*. It was found that both inophyllum and calanolide A represented a subclass of non-nucleoside RT inhibitors and merited consideration for anti-HIV drug development (Jassim & Naji, 2003).

2.7.2 *Helichrysum* species and their therapeutic potential

The genus name *Helichrysum* Mill. derives from two Greek words *helio* (sun) and *chrysos* (gold) which refers to the attractive yellow flowers exhibited by several species (Lourens *et al.*, 2008). *Helichrysum*, which is in the Asteraceae family, has been used in Europe and Africa for the treatment of several medical conditions. It is a very large genus consisting of approximately 500–600 species of which 245 are indigenous to southern Africa including Namibia (Lourens *et al.*, 2004; Lourens *et al.*, 2008). These species exhibit tremendous morphological diversity, which

resulted in their subdivision into 30 morphological groups, using the shape and size of the flower heads as differentiating characteristics. The flower heads are either solitary or occur in compact or spreading inflorescences. The aerial parts are usually hairy or woolly and plants occur as herbs or shrublets that are sometimes dwarfed, and cushion-shaped. They are often aromatic (Lourens *et al.*, 2008).

Helichrysum species are widely used in southern African traditional medicine. The first written record of the medicinal use of this genus dates back to 1727 when Boerhaave noted that a *Helichrysum* species was used to treat nervousness and hysteria (Lourens *et al.*, 2008; Van Vuuren, 2008). *Helichrysum* species are traditionally used in the treatment of wounds, infections and respiratory conditions. The extracts and the essential oils from this species have exhibited promising biological activities in several *in vitro* assays, which include anti-oxidant, antimicrobial and anti-inflammatory activity. This genus has been the source of many interesting and bioactive compounds (Lourens *et al.*, 2004).

The antioxidant and anti-inflammatory activities of extracts and isolated compounds from plants belonging to the large *Helichrysum* genus have been well documented. Arzanol (a phloroglucinyl α -pyrone) is a constituent of *H. italicum* that has been reported to inhibit the NF- κ B transcription factor, cyclooxygenase and lipoxygenase, as well as the release of pro-inflammatory cytokines (Appendino *et al.*, 2007; Bauer *et al.*, 2011). Based on the Bauer and co-researchers' investigation, arzanol at a concentration of 50 μ M significantly suppressed the survival of human lung carcinoma A549 cells (Bauer *et al.*, 2011). In the study of Kucukoglu and co-workers, methanolic extracts prepared from different *Helichrysum* species were found to inhibit DNA topoisomerase (Kucukoglu *et al.*, 2006).

2.8 Selected *Helichrysum* species for the current study

Even though this large genus has been extensively investigated, its biological activity, especially anti-HIV activity, and/or chemical composition for many species remain unrecorded.

This study investigated 32 *Helichrysum* species based on their availability from different geographical regions in South Africa that were not previously investigated by Heyman (2013).

Their morphological characteristics, grouped according to Hilliard, and their uses are described below (Hilliard, 1983).

2.8.1 *Helichrysum acutatum* DC.

Helichrysum acutatum DC. (synonym *Helichrysum schlechteri* Bolus) belongs to the morphological group 21. This perennial, woody herb has a stout rootstock and crown, sometimes woolly and often with remnants of burnt stems. Leaves are mostly basal. Flowering stems are solitary or several together and upright up to 450 to 600 mm high, simple and cobwebby to woolly-tomentose. The diagnostic characters of this species are the presence of large leaves (sessile or petiolate) with prominent nerves, occurrence of large compact, often branched inflorescences and with bright turmeric-yellow bracts. Heads are homogamous, oblong to bell-shaped, $5-7 \times 3$ mm, many in dense corymbose clusters and open or tightly corymbosely arranged (Hilliard, 1983).

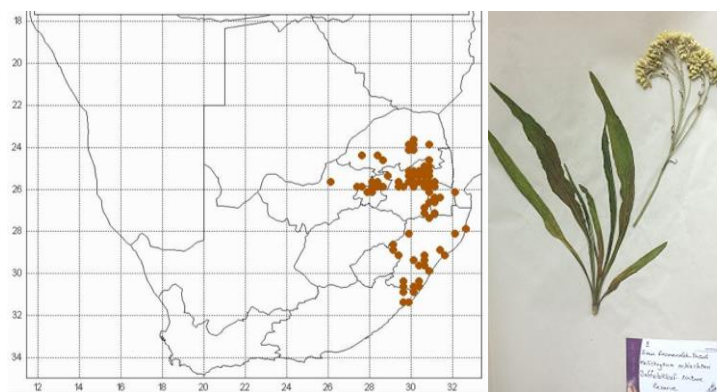


Figure 2.2. *Helichrysum acutatum* collected from Buffelskloof Nature Reserve, Mpumalanga, South Africa.

Involucral bracts are in 4 series, closely imbricate. Its outermost bracts are webbed together with wool. The inner part is slightly shorter than or equaling the flowers. Flowers are found between September and January. It grows in exposed grassland with rocky outcrops from sea level to 1 950 m elevation. Its biomes are grassland, savanna and thicket (Figure 2.2) (Hilliard, 1983). *H. acutatum* contains flavonoid derivatives (flavanone and chalcone), diterpenes and terpenes. The

extract of *H. acutatum* exhibited antimicrobial and antibacterial activity (Bohlmann & Abraham, 1979).

2.8.2 *Helichrysum adenocarpum* DC.

Helichrysum adenocarpum DC. belongs to the morphological group 28. Its common name is pink everlasting. The diagnostic characters of this species are perennial woolly plants with basal leaf rosettes, large solitary heads, and shiny white bracts and mostly with red tips. The radical leaves are sub-orbicular to elliptic-oblong and prostrate (Figure 2.3). Flowering season is mainly between January and April. This beautiful species is found in open grassland, often on moist slopes or in moist depressions from sea level to 3 000 m. It is found in savanna, grassland and thicket biomes (Hilliard, 1983).

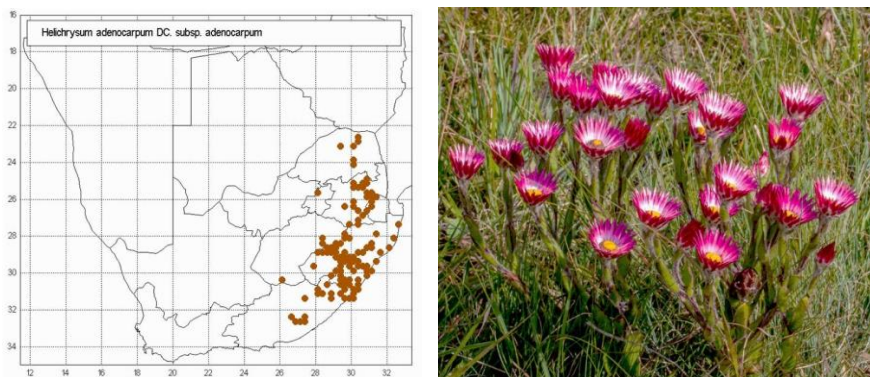


Figure 2.3. *Helichrysum adenocarpum* collected from Amsterdam in Mpumalanga, South Africa.

A decoction of the plant is used to treat diarrhoea and vomiting in children in traditional medicine (Lourens *et al.*, 2008). No biological activity has been reported for this species, but acetylene derivatives have been isolated (Lourens *et al.*, 2008).

2.8.3 *Helichrysum albilanatum* Hilliard

Helichrysum albilanatum Hilliard belongs to the morphological group 30. The height of this subshrub is up to 1 m. It has many stems from the base, smoothly curved, without abrupt angles. It is woody, brittle and forking above into the compound inflorescence, with thin silvery-grey woolly hairs, and long red patent glandular hairs. Leaves of this species are mostly on the inflorescence branches. They are smaller near the heads, lanceolate, acute and sharply pointed. The leaf margins near the tip are almost straight and form an angle of less than 90 degrees. The lower surface of leaves is thick and woolly silvery-grey and they fit closely to each other. The diagnostic characters of this species are bright yellow bracts with large solitary heads (Figure 2.4) (Hilliard, 1983). It flowers between January and June. It is found in savanna, grassland and thicket biomes (Hilliard, 1983). No biological activity and no isolated chemical compounds have been reported for this species.



Figure 2.4. *Helichrysum albilanatum* collected from Buffelskloof Nature Reserve, Mpumalanga, South Africa.

2.8.4 *Helichrysum argyrophyllum* DC.

Helichrysum argyrophyllum DC. belongs to the morphological group 29. It is a hardy, evergreen, small compact shrub, dwarf shrub with beautiful, small, grey leaves with silvery, white hairs. The clusters of papery, canary-yellow flowers are carried well above the plant between December and March. Each flower stays fresh on the plant for about two months. It grows in sun or semi-shade

in well-drained soil, in rockeries or retaining walls where it will cascade (Figure 2.5). It is found in grassland and savanna biomes. The root infusion of *H. argyrophyllum* is used to treat intestinal troubles (Hilliard, 1983). Diagnostic characters of *H. argyrophyllum* are large heads in branched inflorescences with turmeric-yellow bracts. Lourens *et al.* (2008) reported flavonoid derivatives (dihydrochalcone), as well as diterpenes and terpenes from *H. argyrophyllum*.

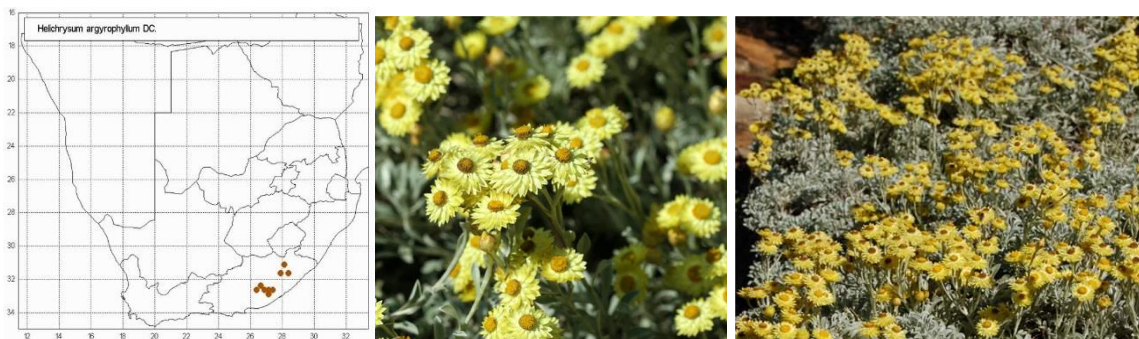


Figure 2.5. *Helichrysum argyrophyllum* collected from Kirstenbosch Botanical Garden, Cape Town, Western Cape, South Africa.

2.8.5 *Helichrysum athrxiifolium* (Kuntze) Moeser

Helichrysum athrxiifolium (Kuntze) Moeser belongs to morphological group 9. The height of the species is up to 450 mm with woody stems. The young parts are thinly appressed greyish white and woolly-hairy. Leaves of this bushy perennial herb are in 'groups' or clusters, margins rolled inwards. The dwarf shoots sometimes smaller and usually very narrow, linear or linear-lanceolate. The upper surface is thinly cobwebby and soon glabrescent, with the lower surface thinly white-tomentose.

Flowers are in small, compact to open inflorescences with many small heads with off-white/cream-coloured bracts. Primary leaves are often subtending very dwarf lateral shoots, making the leaves look fascicled. Flowering time is recorded in all months (Figure 2.6).

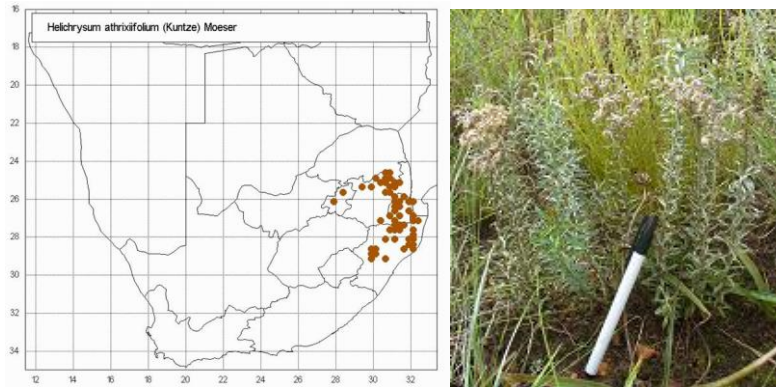


Figure 2.6. *Helichrysum athrixiifolium* collected from Voortrekker Monument Nature Reserve, Gauteng, South Africa.

The diagnostic characters of this species are: leaves in 'groups' or clusters, margins rolled inward, small compact to open inflorescences with many small heads and off-white/cream-coloured bracts. This species grows in grassland or open woodland on sandy soils (Hilliard, 1983). 8-Prenylnaringenin has been isolated from *H. athrixiifolium* that has been recently reported for ethnomedicinal use as a potent phytoestrogen (Bohlmann & Ates, 1984; Štulíková *et al.*, 2018).

2.8.6 *Helichrysum aureum* (Houtt.) Merr. var. *aureum*

Helichrysum aureum (Houtt.) Merr. var. *aureum* belongs to morphological group 30. The perennial herb *H. aureum* is very variable in stature, leaf-size, indumentum and head size. The rootstock becoming very stout and woody with the crown up to 25 mm in diameter. This species produces several leaf rosettes, with several flowering stems lateral to the rosettes. It is simple or sparingly branched towards the top and glandular-setose, often cobwebby or loosely white-woolly. The leaves of this species are narrowly or broadly elliptic spatulate. Lower or both surfaces of leaves are sometimes woolly, with wool sometimes confined to margins and midline. Flowers are yellow and flowering occurs mainly between July and November (Figure 2.7). The biomes of this species are savanna, grassland, fynbos and thicket. The leaves with woolly margins, large solitary heads and sunny-yellow bracts are the diagnostic characters of this species (Hilliard, 1983).

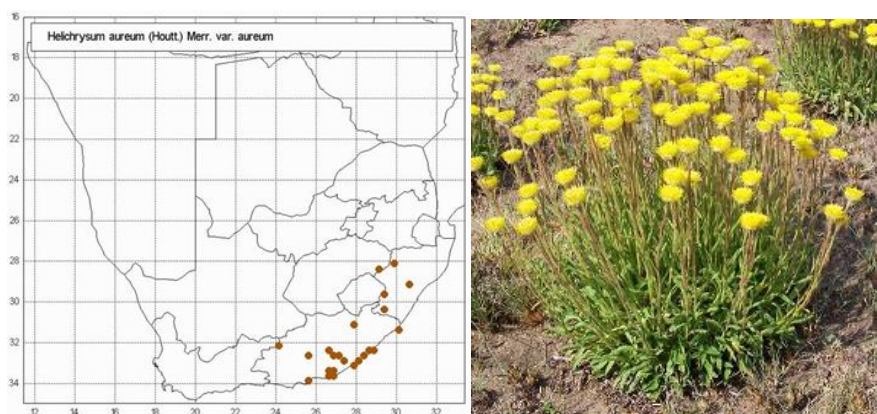


Figure 2.7. *Helichrysum aureum* collected from Buffelskloof Nature Reserve, Mpumalanga, South Africa.

A decoction of *H. aureum* is used for washing sore eyes in traditional medicine. Compounds isolated from this species belong to diterpenes and terpenes (Lourens *et al.*, 2008).

2.8.7 *Helichrysum aureum* (Houtt) Merr. var. *monocephalum* (DC.) Hilliard

Helichrysum aureum (Houtt) Merr. var. *monocephalum* (DC.) Hilliard, belonging to the morphological group 30, is a perennial herb, which is very variable in stature, leaf-size, indumentum and head size. The roots are very stout and woody. Flowering stems are 5 to 300 mm high, which are simple, glandular-setose and often thinly woolly or cobwebby as well, particularly above. The colour of the radical leaves is greyish white-woolly or wool confined to margins. Flowering time is between July and November.

The diagnostic characters of this species are leaves in a rosette and large solitary heads, with a flimsy (thin) herbaceous stem with bright yellow bracts. This species grows in grassland, savanna and thicket biomes (Figure 2.8) (Hilliard, 1983).

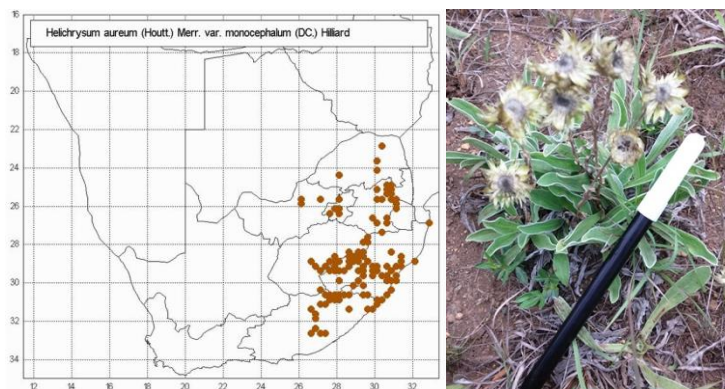


Figure 2.8. *Helichrysum aureum* var. *monocephalum* collected from Buffelskloof Nature Reserve, Mpumalanga, South Africa.

2.8.8 *Helichrysum caespititium* (DC.) Harv.

Helichrysum caespititium (DC.) Harv. is grouped in morphological category 12. It is a prostrate perennial mat-forming herb, profusely branched and densely tufted. Branchlets are only 10 mm tall and closely leafy. Leaves are almost patent, linear, subacute or obtuse, base broad and clasping and its margins are revolute. Both surfaces are enveloped in silvery ‘tissue-paper-like’ indumentum breaking down to wool. Mat-forming, prostrate, densely branched, reduced needle-like leaves and numerous heads are diagnostic characters of this species. Flower heads are white or pink. Flowering time starts from August to December. It is found in grassland and savanna biomes. (Figure 2.9) (Hilliard, 1983). It is traditionally used to treat colds and cure nausea (Pooley, 2005). The crushed, burnt and inhaled smoke of this species is used to treat head and chest colds. Anti-inflammatory, antibacterial and antifungal activity of this species have been reported. It is also used to treat gastrointestinal conditions that include mainly colic, nausea, diarrhoea, stomach pain and also used to dress wounds (Lourens *et al.*, 2008). Meyer and co-researchers (2002) have reported that *H. caespititium* acetone extract was successful to inhibit a drug sensitive-strain of *Mycobacterium tuberculosis* at a concentration of 0.5 mg/mL in the agar plate method. They reported an observed MIC of 0.1 mg/mL using the rapid radiometric method (Meyer *et al.*, 2002). Phloroglucinols have been isolated from the whole plant (Mathekga *et al.*, 2000).

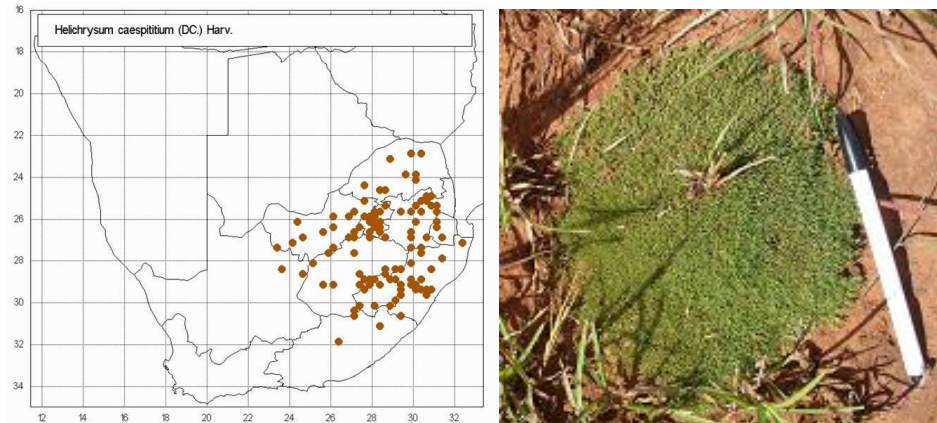


Figure 2.9. *Helichrysum caespitium* collected from Voortrekker Monument Nature Reserve, Gauteng, South Africa.

2.8.9 *Helichrysum callicomum* Harv.

Helichrysum callicomum Harv. belonging to the morphological group 2, is a tufted perennial herb up to 400 mm high. Stems are woody at base, mostly branching from there and above into the compound inflorescence. It is closely greyish white-felted and compactly leafy. The size of the leaves is up to 25×6 mm, smaller and more distant upwards, passing into inflorescence bracts, spatulate and oblong-spatulate or oblong upwards. Upper leaves sometimes are acute and base half-clasping. Both surfaces are closely greyish-felted. Heads are heterogamous. The colour of the flower is yellow. The flowering season is from March to May. Diagnostic characters of this species are yellow bracts, small heads and in large terminal clusters, spatulate grey-green hairy leaves and capitula are in terminal branched clusters. It often forms large stands in overgrazed grassland in the grassland and savanna biomes (Figure 2.10) (Hilliard, 1983).

Antibacterial and antifungal activity of *H. callicomum* extract has been reported. The most phytochemicals isolated from *H. callicomum* are flavonoid derivatives, phloroglucinols, pyrones, diterpens and terpenes (Lourens *et al.*, 2008).

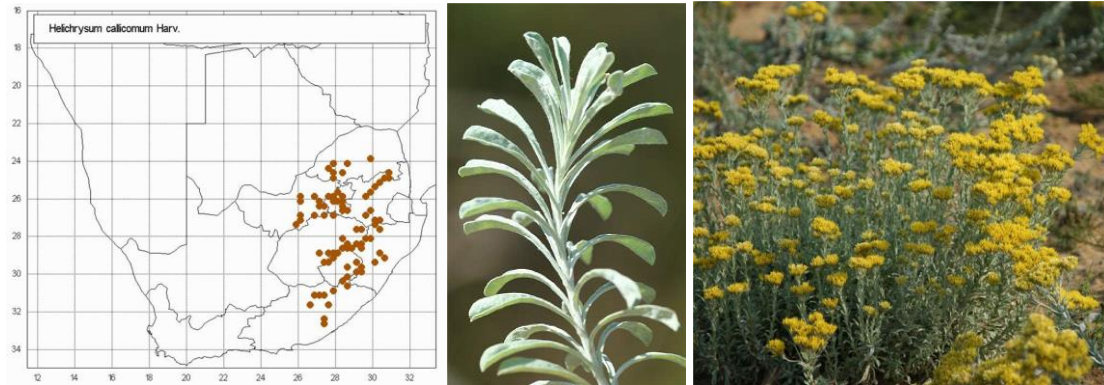


Figure 2.10. *Helichrysum callicomum* collected from Buffelskloof Nature Reserve, Mpumalanga, South Africa.

2.8.10 *Helichrysum cephaloideum* DC.

Helichrysum cephaloideum DC. (synonym: *Helichrysum infusum* Burtt Davy) belongs to morphological group 24. This species is a dwarf shrublet forming mats or cushions up to 200 mm high, of which the old branches are woody, decumbent and nude, rooting, branchlets closely grey-woolly, densely leafy, becoming nude and remotely leafy upwards (Hilliard, 1983).

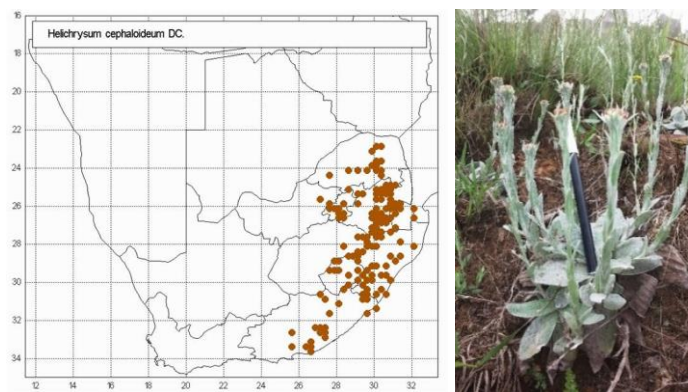


Figure 2.11. *Helichrysum cephaloideum* collected from Buffelskloof Nature Reserve, Mpumalanga, South Africa.

Leaves of this species are up to 12×1.5 mm and smaller and more distant upwards and linear. Upper surface of the leaf is thinly grey-woolly and the lower surface is densely white-woolly. Heads are homogamous, cylindric and many are in compact clusters at the branch tips. Outer tips

of the head are pale brown and the inner are bright canary-yellow. Diagnostic characters of this species are yellow bracts, compact inflorescences on short stalks, bi-coloured leaves (white below), inrolled leaf margins and needle-like leaves (Figure 2.11). Flowering time is from January to April. Distribution of this species is in the grassland biome (Hilliard, 1983).

2.8.11 *Helichrysum chrysargyrum* Moeser

Helichrysum chrysargyrum Moeser belongs to morphological group 22. It is a bushy perennial herb up to 400 mm high. Old stems are bare and woody below, otherwise leafy throughout. Stems, leaves and base of each head enveloped in silvery, silky, skin-like indumentum. Leaves are up to 75×5 mm, narrowly lanceolate, base slightly narrowed, half-clasping. The head of this species is heterogamous and broadly campanulate. Its involucre bracts are closely imbricate, glossy, outer palest golden-brown or straw-coloured. Flowering season is from February to April. Its diagnostic characters are bright yellow bracts, large heads, and branched inflorescences with long and linear grey leaves. The biomes of *H. chrysargyrum* are grassland and savanna (Figure 2.12) (Hilliard, 1983).

According to Bohlmann and Abraham (1979), flavonols, phloroglucinols and terpenes have been isolated from *H. chrysargyrum*. There is no traditional usage or biological activity report for this species.

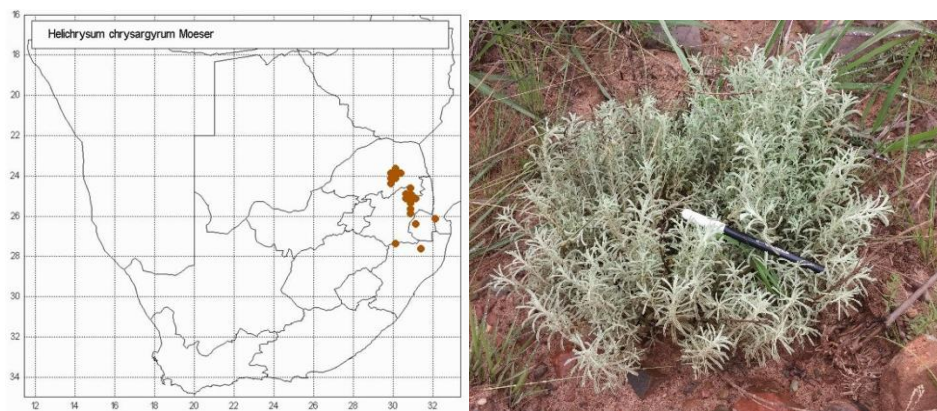


Figure 2.12. *Helichrysum chrysargyrum* collected from Buffelskloof Nature Reserve, Mpumalanga, South Africa.

2.8.12 *Helichrysum dasyanthum* (Willd.) Sweet

Helichrysum dasyanthum (Willd.) Sweet is categorised in the morphological group 10. This shrub or subshrub has long, thin and greyish white-woolly branches. It has long spreading hairs as well. Leaves are smaller below the heads, elliptic, sometimes recurved and margins subrevolute. Leaves are often undulate, thinly greyish white and woolly. Heads are heterogamous campanulate and mostly compact and terminal. Flowering time is mainly in September, October and November. Diagnostic characters of this species are leaves and stems covered in spreading hairs, overhead dark green leaves and yellowish in lower parts, inflorescence a compact branch, with medium-sized heads, woolly-hairy outer bracts and dark-coloured tips of outer bracts. It grows in the fynbos biome (Figure 2.13) (Hilliard, 1983).

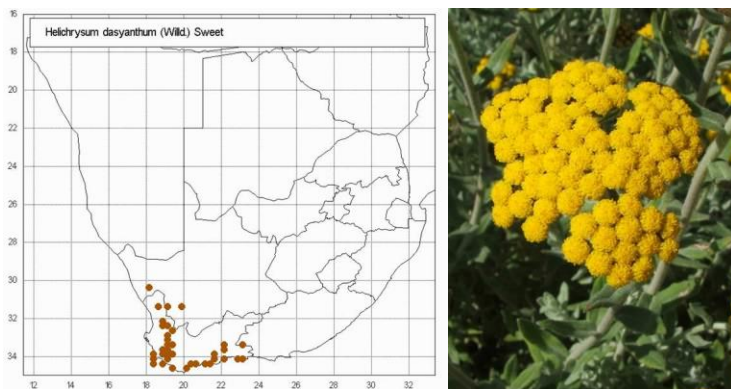


Figure 2.13. *Helichrysum dasyanthum* collected from Kirstenbosch National Botanical Gardens, Western Cape, South Africa.

Helichrysum dasyanthum contains mainly sesquiterpenes of the guaianolide type (which is absent in the other species). According to Lourens and co-authors (2008), flavonoids (flavonol), diterpenes (kaurenoic acid derivatives) and terpenes (cadinenes and guaianolides) have been isolated from *H. dasyanthum*. It showed the best activity against *Bacillus cereus* (MIC = 16 mg/mL) and was the only extract that exhibited activity against three fungal strains tested (*Cryptococcus neoformans*, 1 mm; *Candida albicans*, 3 mm; and *Alternaria alternata*, 2 mm), (Lourens *et al.*, 2004; Reddy, 2008).

2.8.13 *Helichrysum gerberifolium* A.Rich.

Helichrysum gerberifolium A.Rich. (following Hilliard, 1983) (current accepted name is *Helichrysum nudifolium* (L.) Less. var. *nudifolium*) belongs to morphological group 23. This species is a perennial herb, its roots are narrowly fusiform with a woody rootstock and crowned with old fibrous leaf bases, with some brown wool hidden in the axils. Flowering stem is solitary, white-woolly felted. Leaves are mostly radical, roughly half the length of the petiole, blade elliptic. Heads are homogamous campanulate, congested in a globose terminal cluster. Leaves are initially silky grey-woolly on both surfaces. This species is found in savanna, grassland, thicket, fynbos, Nama Karoo and Succulent Karoo biomes (Figure 2.14) (Hilliard, 1983). The infusion of *H. gerberifolium* is used to treat colds traditionally (Lourens *et al.*, 2008). Phytochemical composition and biological activity of *H. gerberifolium* have not been studied extensively.

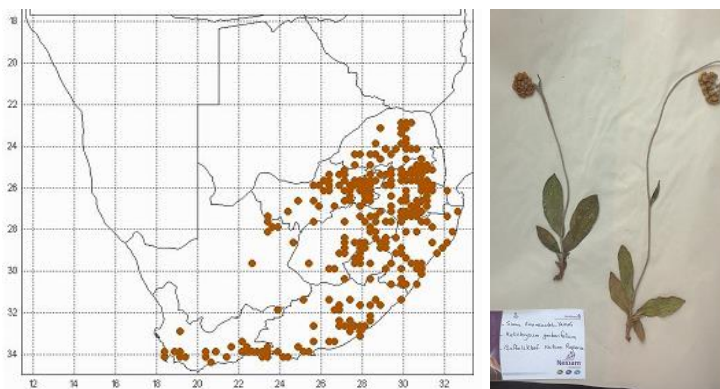


Figure 2.14. *Helichrysum gerberifolium* collected from Buffelskloof Nature Reserve, Mpumalanga, South Africa.

2.8.14 *Helichrysum harveyanum* Wild

Helichrysum harveyanum Wild belongs to morphological group 23. It is a perennial herb with slender roots and flowering stems are solitary. The radical leaves are often deficient, with a wiry petiole, blade linear-lanceolate and triplinerved with weakly revolute margins. Both surfaces are

scabrid and hairs are often only near the margins and above veins. Cauline leaves mostly 40–170 × 1–5 mm, smaller and more distant upwards and passing into bracts, linear-lanceolate or linear.

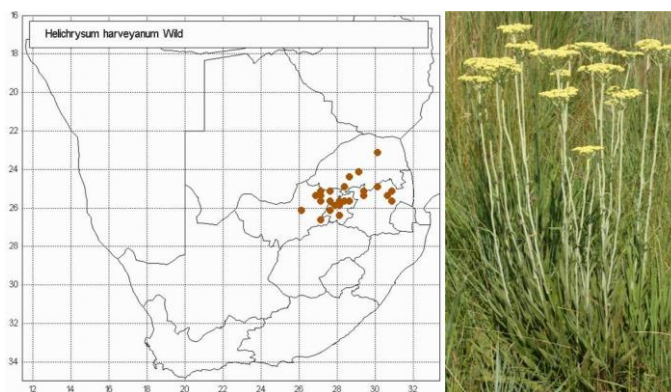


Figure 2.15. *Helichrysum harveyanum* collected from Buffelskloof Nature Reserve, Mpumalanga, South Africa.

Margins of leaves are strongly revolute and the upper surface and midrib below are scabrid with some woolly hairs as well. Flowers mainly appear from October to January. Diagnostic characters of this species are large heads, branched open inflorescences and long lanceolate to linear leaves (Figure 2.15). Distribution of *H. harveyanum* is in grassland and savanna biomes (Hilliard, 1983). No biological activity and no identified chemical composition have been reported.

2.8.15 *Helichrysum kraussii* Sch.Bip.

Helichrysum kraussii Sch.Bip. is categorized in morphological group 8. It is a bushy aromatic shrublet up to 1 m tall. Branches are stiff and thinly greyish white-felted and closely leafy. Leaves are spreading or reflexed up to 20 × 2 mm. The sharply pointed leaves are long and narrow without stalk and attached directly. The lower surface is sometimes nearly obscuring and upper surface is cobwebby and glabrescent. Heads are heterogamous or homogamous, sometimes on one plant and cylindric. Flowers are not radiating, glossy and pale lemon-yellow or straw-coloured. Diagnostic characters are glandular leaves and stems, linear leaves are bicoloured (green & white), whitish bracts, compact to open inflorescences and branched (Figure 2.16). This species is found in savanna and grassland biomes (Hilliard, 1983).

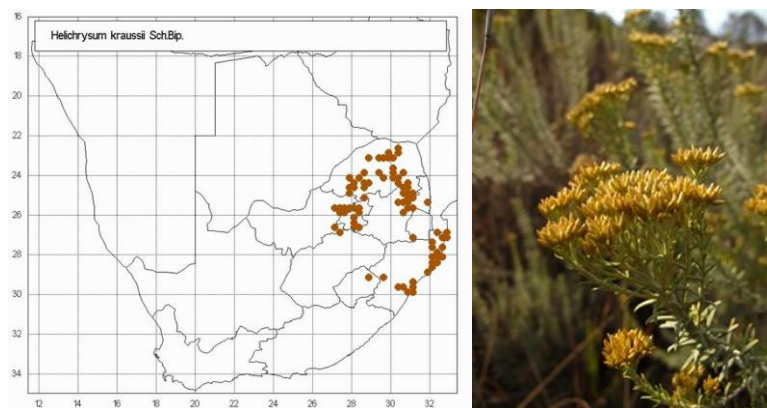


Figure 2.16. *Helichrysum kraussii* collected from Pretoria Botanical Garden, Gauteng, South Africa.

A decoction of *H. kraussii* leaf is used to wash keloid scars in traditional medicine. It is used to treat respiratory complaints such as coughs and colds (Lourens *et al.*, 2008). Flavonoid derivatives, phloroglucinols, pyrones, terpenes and diterpenes have been isolated from *H. kraussii* (Bremner & Meyer, 2000; Bougatsos *et al.*, 2003; Prinsloo & Meyer, 2006; Lourens *et al.*, 2008).

2.8.16 *Helichrysum lepidissimum* S.Moore

Helichrysum lepidissimum S.Moore belongs to the morphological group 19. It is a dense twiggy shrublet, 100–600 mm high. Its lower branches are often decumbent, rooting, all closely leafy, the younger parts loosely greyish white-woolly. The leaves are diminishing slightly upwards and usually broadly elliptic. Leaf margins are more or less crisped, lightly and loosely greyish white-woolly-felted below. The heads of *H. lepidissimum* are homogamous and campanulate. The involucre bracts are in 5 series, graded, imbricate and inner about equalling flowers. This species is always found in rocky places, particularly rocky mountains and cliff edges in grassland and savanna biomes (Figure 2.17) (Hilliard, 1983).

According to Lourens *et al.* (2008), the powder and ointment prepared from this species are used as a body ointment in traditional usage. The phytochemicals isolated from *H. lepidissimum* are diterpenes, phloroglucinols and flavonoid derivatives (flavanone) (Lourens *et al.*, 2008).



Figure 2.17. *Helichrysum lepidissimum* collected from Buffelskloof Nature Reserve, Mpumalanga, South Africa.

2.8.17 *Helichrysum mariepsopicum* Hilliard

Helichrysum mariepsopicum Hilliard belongs to the morphological group 29. This species is named after Mariepskop in the Drakensberg of Mpumalanga where this plant was first collected. White bracts with maroon brown tips and large solitary heads are two diagnostic characters of this beautiful species. It is a tufted perennial herb or shrublet about 150–300 mm tall. Its stems are glandular and covered with fine short soft hairs. The leaves are mostly $10\text{--}30 \times 2\text{--}5$ mm, becoming smaller and more distant upwards and passing into scale-tipped bracts. The heads are heterogamous, campanulate, ± 12 mm long, double that across the radiating bracts, solitary at branchlet tips. The beautiful flowers are acute and glossy white but innermost tipped brown, sometimes with a rosy cast. The flowering season is between September and April, with its peak between October and January (Figure 2.18) (Hilliard, 1983).

It grows in damp mountain grassland particularly among rock outcrops. It grows in grassland and savanna biomes (Hilliard, 1983). No biological activity and no identified chemical composition have been reported.

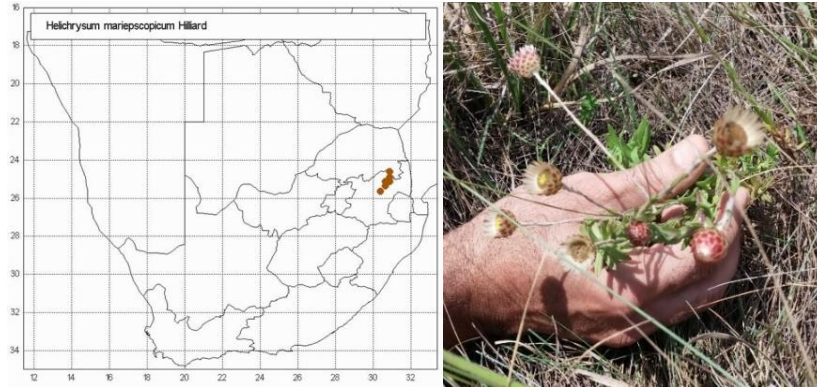


Figure 2.18. *Helichrysum mariepsopicum* collected from Buffelskloof Nature Reserve, Mpumalanga, South Africa.

2.8.18 *Helichrysum milleri* Hilliard

Helichrysum milleri Hilliard belongs to the morphological group 30. The occurrence of large solitary heads and brown bracts are two remarkable diagnostic characters of this species. It is a shrub up to 1 m tall with brittle branches. Its leaves are mostly $20\text{--}25 \times 6\text{--}12$ mm and with the sides parallel or nearly so, for most of their length. The leaves also are obtuse to acute. Both surfaces of the leaf are greyish white-woolly, wool persistent on sterile twigs, shed on flowering twigs to reveal the glandular-setose surface. The heads are heterogamous, ± 15 mm long and ± 32 mm across the radiating bracts and depressed-globose. The flowering season is in October and November (Figure 2.19) (Hilliard, 1983).



Figure 2.19. *Helichrysum milleri* collected from Buffelskloof Nature Reserve, Mpumalanga, South Africa.

It is distributed mostly in coarse herbage on the margins of forest patches. It appears in grassland and savanna biomes (Hilliard, 1983). No biological activity and no chemical studies have been found.

2.8.19 *Helichrysum mimetes* S.Moore

Helichrysum mimetes S.Moore belongs to the morphological group 19. Its diagnostic characters are leaves with distinct petioles, open branched inflorescences, medium-sized heads and cream bracts. This species is a shrublet up to 600 mm high, branches thinly greyish white-tomentose and leafy. Its leaves are on coppice shoots and sappy growth ovate to subrotund, which is nearly circular or round with the two-dimensional shape between oblong and rounded in outline. The heads are homogamous, bell-shaped; with a tube about as long as wide and a spreading upper part, many in corymbose clusters arranged in corymbose panicles. It is flowering mainly between May and September. Its distribution is mostly in rocky outcrops and broken rocky cliffs. It grows in grassland and savanna biomes (Figure 2.20) (Hilliard, 1983).

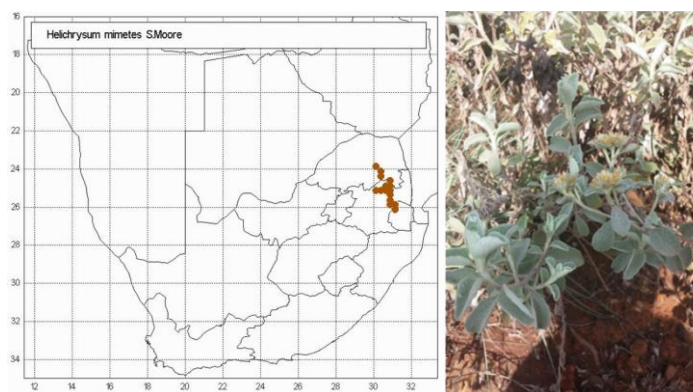


Figure 2.20. *Helichrysum mimetes* collected from Buffelskloof Nature Reserve, Mpumalanga, South Africa.

Flavones, pyrones, diterpenes, terpenes (sesquiterpens) and phloroglucinols are some of the classes of compounds isolated from *H. mimetes* (Jakupovic *et al.*, 1986; Lourens *et al.*, 2008). No traditional uses, biological activity and medicinal properties have been reported.

2.8.20 *Helichrysum mundtii* Harv.

Helichrysum mundtii Harv. belongs to the morphological group 23. Its diagnostic characters are bi-coloured leaves, white-woolly below, medium-sized heads, and open-branched inflorescences. This species is a robust perennial herb up to 1.5 m tall, stock stout, woody, creeping, with slender leafy runners as well. Its flowering stem is simple, woody and up to 8 mm in diameter at base, herbaceous, upper part thinly white-felted and leafy throughout. The leaves are radical, up to 600 mm long, half of this petiolar and blade elliptic which is up to 60 mm broad. Heads are homogamous, campanulate (bell-shaped; with a tube about as long as wide and a spreading upper part.), 4×3.5 mm. Involucral bracts of flowers are in 5 to 6 series, graded, closely imbricate and inner about equalling flowers. Flowers appear between February and April. This species grows in marshy places, often along stream sides or in seepage, forming dense stands because of its creeping rootstock. Its biomes are savanna and grasslands (Figure 2.21) (Hilliard, 1983).

A decoction of *H. mundtii* is used to treat chest complaints. Flavonoid derivatives (dihydrochalcone and flavone), diterpenes and terpenes are some classes of compounds isolated from *H. mundtii* (Bohlmann *et al.*, 1978; Lourens *et al.*, 2008). There is no report of the medicinal properties and biological activity of *H. mundtii*.



Figure 2.21. *Helichrysum mundtii* collected from Buffelskloof Nature Reserve, Mpumalanga, South Africa.

2.8.21 *Helichrysum mutabile* Hilliard

Helichrysum mutabile Hilliard belongs to morphological group 30. Large heads in compact branched inflorescences, bright yellow (brownish) bracts and leaves woolly to glabrous are the diagnostic characters of this species. *H. mutabile* is a perennial herb up to 1 m tall. This plant has one or several stems from the stock, simple below and branching above into the compound inflorescence (Hilliard, 1983).

The sizes of the leaves are mostly $25\text{--}75 \times 4\text{--}12$ mm, sometimes larger (up to 90×24 mm) on the lower part of the stem, and often smaller on the inflorescence branches and further reduced near the heads and mostly oblong. Involucral bracts are in 9 series, graded, imbricate, inner much exceeding the flowers, bright yellow and outer light brown outside. It favours rocky sites and is distributed in woodland, or in grassland near forest patches, or rarely marshy places near rocks. Savanna and grassland are the main biomes of this species (Figure 2.22) (Hilliard, 1983). There is no information about the chemical composition and biological activity of this species.

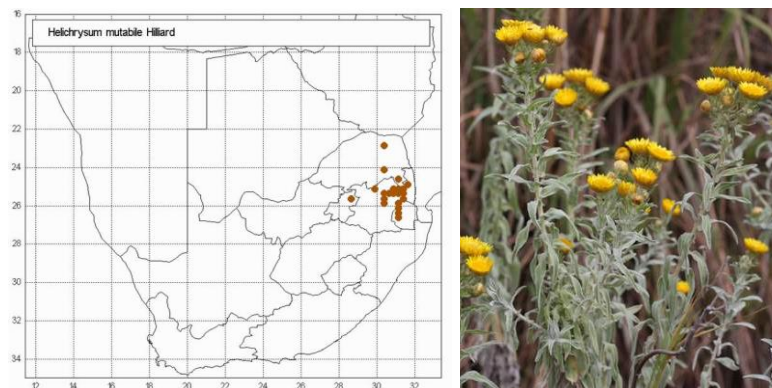


Figure 2.22. *Helichrysum mutabile* collected from Buffelskloof Nature Reserve, Mpumalanga, South Africa.

2.8.22 *Helichrysum nudifolium* (L.) Less. var. *nudifolium*

Helichrysum nudifolium (L.) Less. var. *nudifolium* [synonym *Helichrysum quinquenerve* (Thunb.) Less.] belongs to the morphological group 23. *H. nudifolium* var. *nudifolium* is a fast-growing perennial herb. The leaves are rough and shiny above, white-woolly beneath. The diagnostic

characters of this species are bright green leaves with long petioles and medium-sized heads, compact branched inflorescences and bright yellow/greenish yellow bracts. They have 3 to 7 prominent veins and are aromatic when dry. The flowers are blunt-tipped and pale yellow in a crowded, flattish inflorescence at the tip of a long stalk (Figure 2.23). The flowering stalks can reach a height of 1.5 m. It flowers during summer and autumn between October and May (Hilliard, 1983).

This species is a sun-loving herb with a pale-yellow inflorescence and shiny, light green leaves. There are many species very similar to *H. nudifolium* var. *nudifolium*, which can cause confusion. Culturally, medicinally, and historically, this species is one of the most important in South Africa. Although it has not enjoyed horticultural exposure; however, it is easy to grow in the garden and makes a good border plant. *H. nudifolium* var. *nudifolium* occurs naturally in rocky grasslands. It is frost and drought tolerant as it grows at high altitudes. This species is found in savanna, grassland, thicket, fynbos, Nama Karoo and Succulent Karoo biomes (Hilliard, 1983). Infusions of *H. nudifolium* var. *nudifolium* are used as demulcent and to treat catarrh, phthisis and other pulmonary affections in traditional medicine (Lourens *et al.*, 2008). The reported chemical entities isolated from *H. nudifolium* var. *nudifolium* are quinones, sesquiterpenes and diterpenes (Jakupovic *et al.*, 1986; Lourens *et al.*, 2008).

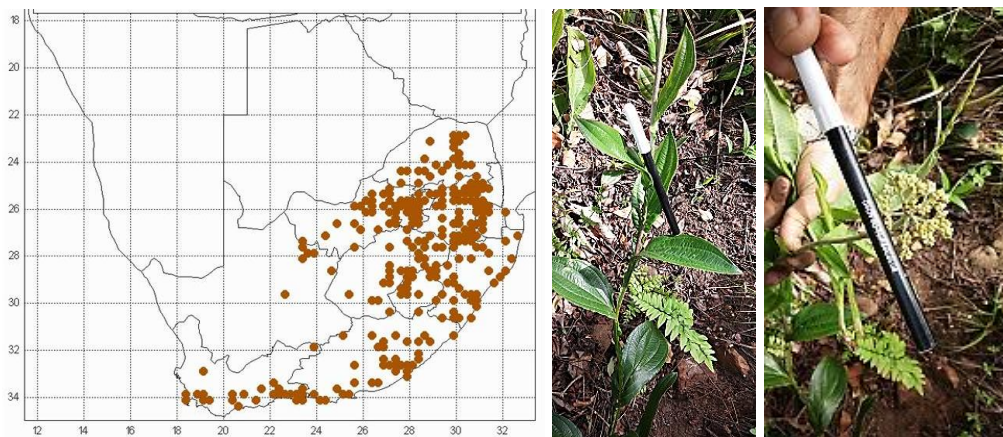


Figure 2.23. *Helichrysum nudifolium* var. *nudifolium* collected from Buffelskloof Nature Reserve, Mpumalanga, South Africa.

2.8.23 *Helichrysum opacum* Klatt

Helichrysum opacum Klatt belonging to the morphological group 24, is a perennial herb. Its roots are fusiform and crown clad in loose brown wool. The flowering stem reaches up to 400 mm high, nearly always solitary, thinly greyish white-felted and remotely leafy. Leaves are mostly radical and lanceolate up to 150×12 mm. They are only slightly narrowed to the broad clasping base, markedly discolourous, green and often drying blackish. Heads of the plant are homogamous, campanulate, ± 5 mm long, double that across the fully radiating involucral bracts and many in a corymbose panicle. Involucral bracts appear in ± 8 series, inner subequal (Hilliard, 1983). They are loosely imbricate with many exceeding flowers, very acute and snow-white. The head has 23–28 yellow flowers. The diagnostic characters of *H. opacum* are white bracts, large heads and compact branched inflorescences (Hilliard, 1983). Flowering season is in December and January. This species is found on grassy mountain slopes, in the grassland biome (Figure 2.24) (Hilliard, 1983). No chemical composition information or biological activity of *H. opacum* has been found.

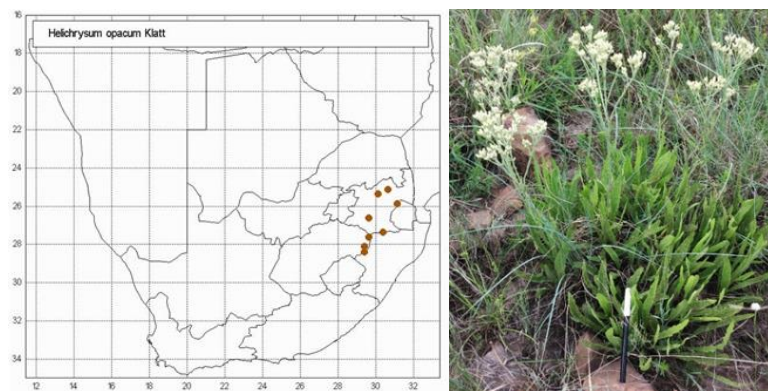


Figure 2.24. *Helichrysum opacum* collected from Buffelskloof Nature Reserve, Mpumalanga, South Africa.

2.8.24 *Helichrysum patulum* (L.) D.Don

Helichrysum patulum (L.) D.Don belongs to the morphological group 18. It has medium-sized heads, compact inflorescences, cream-coloured bracts and small hairy leaves as diagnostic characters. *H. patulum* is a straggling well-branched subshrub up to 1 m tall. The branches are

virgate, white-woolly and closely leafy becoming nude and pedunculoid below the inflorescence. Leaves are mostly $6\text{--}20 \times 2\text{--}12$ mm with a fiddle-shape. Upper parts of the leaves are broadly elliptic to suborbicular, abruptly contracted about the middle, apex very rounded, base is broad and ear-shaped with base of a leaf partly or wholly surrounding the stem. Margins of the leaves are crisped-undulate. Both surfaces are greyish white-woolly. The upper part is less densely so. Involucral bracts are in 5 series, graded, loosely imbricate and inner same as flowers. Flowers appear between September and February, mainly in December and January. This species grows in shrub communities on coastal dunes and inland on south-facing mountain slopes up to 600 m high. Its biome is Fynbos (Figure 2.25) (Hilliard, 1983).

The infusion of *H. patulum* has been used to treat heart problems and weakness, backache and kidney disease. It helps to control stress and fatigue and is a treatment for coronary thrombosis, bladder conditions or infections, asthma, influenza and gynaecological disorders (Lourens *et al.*, 2008). Scott *et al.* (2004) revealed that *H. patulum* had antimicrobial activity against *Staphylococcus aureus* in the disc diffusion assay that was comparable to that of the ciprofloxacin control. Phloroglucinols and terpenes have been isolated from *H. patulum* (Scott *et al.*, 2004).

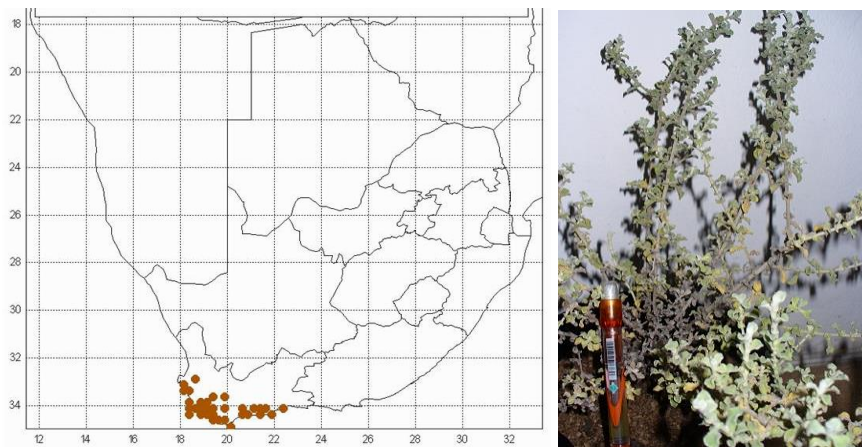


Figure 2.25. *Helichrysum patulum* collected from Stellenbosch University Botanical Garden, Western Cape, South Africa.

2.8.25 *Helichrysum petiolare* Hilliard & B.L.Burt

Helichrysum petiolare Hilliard & B.L.Burt belonging to the morphological group 18, is a loosely branched and soft-wooded shrub. Tangled masses cover several meters across when supported by other vegetation. Leaves with petiole, covered in hairs, large heads, large compact branched inflorescences and light yellow/greenish bracts are the diagnostic characteristics of *H. petiolare*. Branches are long, slender and thinly grey-woolly. Leafy branches become pedunculoid and distantly bracteates below the inflorescences. Leaf blades mostly $10\text{--}35 \times 10\text{--}30$ mm, subrotund to broadly ovate or elliptic-rhomboid. Both surfaces of the leaf are grey-woolly-felted, upper sometimes only cobwebby, flat and sometimes winged. Heads are homogamous and nearly or almost round and bell-shaped. This plant has 18 to 30 yellow flowers with a sweet fragrance. Flowering season is in December and January. It grows in shrubby places in damp Fynbos, thicket, savanna and grassland biome, in sheltered kloofs and on forest margins (Figure 2.26) (Hilliard, 1983).

According to Lourens *et al.* (2008), a tea of the leaves of *H. petiolare* is used traditionally as an antiseptic, and to treat stomach ailments. It is applied to wounds and used for infections of the respiratory tract. This tea is used to treat coughs, colds, catarrh, headaches, fever, menstrual disorders and urinary tract infections as ethnomedicine (Arnold *et al.*, 2002; Lourens *et al.*, 2008).

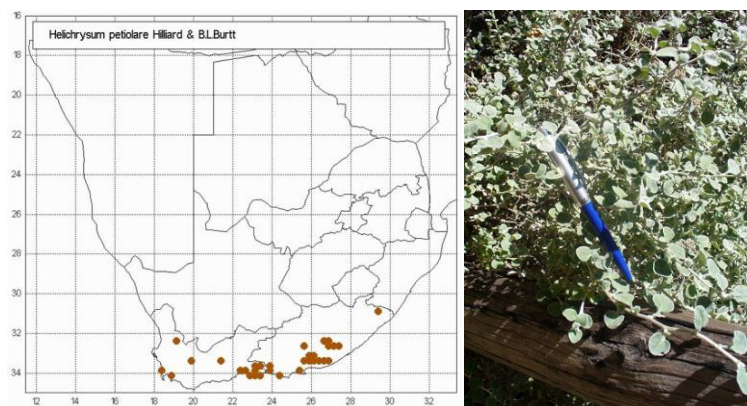


Figure 2.26. *Helichrysum petiolare* collected from Stellenbosch University Botanical Garden, Western Cape, South Africa.

Based on a study conducted by Lourens *et al.* (2004), the antioxidant activity (as indicated with the DPPH assay) of acetone and methanol extracts of *H. petiolare* was comparable to that of vitamin C, as is expected for species rich in phenolic compounds (Lourens *et al.*, 2004). *H. petiolare* displayed activity against *Staphylococcus aureus* and *Bacillus cereus* (Lourens *et al.*, 2008). A fraction from a dichloromethane/methanol extract of *H. petiolare* determined that administration of 300 mg/kg of extract to mice reduced mean blood pressure by 21% and caused a 6% reduction in heart rate (Swanepoel, 1997). Flavonoids, phloroglucinol, terpenes (sesquiterpenes) and diterpenes are some of the chemical compounds that have been isolated from *H. petiolare* (Lourens *et al.*, 2008).

2.8.26 *Helichrysum platypterum* DC.

Helichrysum platypterum DC. belongs to the morphological group 20. Its diagnostic characters are large lanceolate leaves without hairs/wool, large heads and branched open compact inflorescences. It is a perennial herb with a woody tuber up to 60 mm in diameter. The stems are solitary or several together, erect up to 1 m high, simple, thinly white cottony, leafy particularly below, bracteates above. Leaves are up to 250 × 80 mm. Lower ones are broadly elliptic, contracted to the broadly winged base and upper ones are narrower and elliptic (Hilliard, 1983).



Figure 2.27. *Helichrysum platypterum* collected from Buffelskloof Nature Reserve, Mpumalanga, South Africa.

Heads are homogamous, campanulate and 5×5 mm. Involucral bracts are in 5 or 6 series, graded, closely imbricate. Its base is woolly, inner about equalling the flowers and tips are rounded. It is found in the rank growth on forest margins or on damp grassy mountain slopes, in savanna, grassland and thicket biomes (Figure 2.27) (Hilliard, 1983).

The root decoction of *H. platypterum* has been used to renew virility in men. Different classes of chemical compounds such as flavonoids (benzopyrones), phloroglucinols, diterpenes and miscellaneous other compounds have been isolated from *H. platypterum* (Jakupovic *et al.*, 1986; Jakupovic *et al.*, 1987; Lourens *et al.*, 2008). No specific biological activity has been reported for these compounds.

2.8.27 *Helichrysum polycladum* Klatt

Helichrysum polycladum Klatt belonging to the morphological group 8, is a bushy herb forming thick rounded clumps up to 1 m tall and as much across. The name of this species originated from two words, *poly* (many, numerous) and *cladus* (branch, shoots). The diagnostic characters of *H. polycladum* are cream-coloured bracts, small compact inflorescences, and long fine needle-like leaves that are sharply pointed. The stems of this species are long, delicate, thin, sometimes tangled, brittle and thinly greyish white-woolly.

Leaves are mostly $7\text{--}22 \times 1\text{--}2$ mm or less, diminishing slightly upwards and linear-lanceolate. Margins of leaves are rolled backwards. Upper surface is more or less loosely white-woolly and often glabrescent. The lower surface is persistently loosely white-woolly and gland-dotted. The heterogamous heads of this species are $\pm 3 \times 1.5$ mm and cylindric.

There are some woolly hairs at base and many in the compact corymbose panicles. Its involucral bracts are in 5 series, imbricate, graded and inner about equalling dirty white flowers. Flowering season is in March, April and May (Hilliard, 1983). It favours rocky sites and is distributed in grassland and savanna biomes (Figure 2.28) (Hilliard, 1983). Flavonoids and phloroglucinol have been isolated from this species (Lourens *et al.*, 2008). No biological activity of this species has been reported.



Figure 2.28. *Helichrysum polycladum* collected from Buffelskloof Nature Reserve, Mpumalanga, South Africa.

2.8.28 *Helichrysum reflexum* N.E.Br.

Helichrysum reflexum N.E.Br. belonging to the morphological group 29, is a twiggy shrublet 300–600 mm high. Cream bracts, white-tipped, large solitary heads, small needle-like leaves that are bent downwards are the diagnostic characters of this species. Its young stems are thinly white-woolly, glandular-pubescent and closely leafy throughout. Leaves spreading later appearing reflexed, which means it is abruptly recurved at a sharp angle or bent downward or backwards. Its size is $5\text{--}11 \times 0.75\text{--}1.50$ mm, linear or linear-lanceolate and very acute. Margins of leaves are strongly revolute, sometimes thinly greyish white-woolly as well and densely white-woolly below. Heads are heterogamous or rarely homogamous and campanulate (Hilliard, 1983).

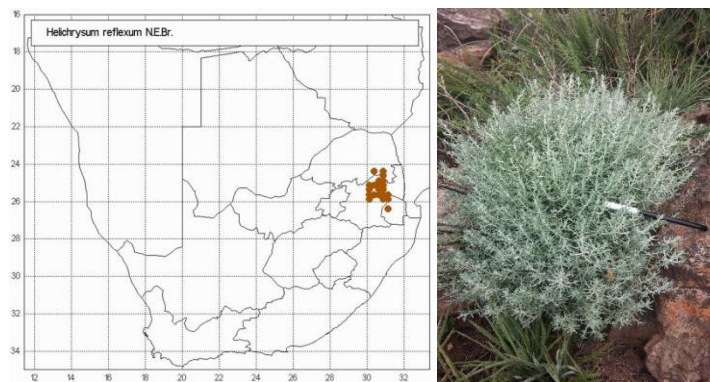


Figure 2.29. *Helichrysum reflexum* collected from Buffelskloof Nature Reserve, Mpumalanga, South Africa.

Involucral bracts are in 10 series, graded, imbricate, and inner much exceeding flowers, acute, glossy white and outer is tinged light brown often with a rosy cast. Flowering season is mainly between February and April. The species distribution is common among rock outcrops. It grows in grassland and savanna biomes (Figure 2.29) (Hilliard, 1983). Diterpenes and terpenes have been isolated from aerial parts of *H. reflexum* (Lourens *et al.*, 2008). No biological activity of this species has been reported.

2.8.29 *Helichrysum setosum* Harv.

Helichrysum setosum Harv. belongs to the morphological group 30. This beautiful species has bright yellow bracts and large solitary heads. It is an herbaceous perennial or subshrub. It is branched from the base and stock with vegetative buds or small leaf tufts. Stems are up to 1 m tall, but often only 500 mm, woody and brittle. Uppermost parts are sometimes white-cobwebby and closely leafy. Leaves are mostly 20–50 × 10–20 mm, slightly smaller on the inflorescence branches, mostly ovate and longer than broad and with the sides parallel or nearly so for most of their length. Both surfaces and margins of leaves are glandular-setose. Heads are heterogamous with 10–14 mm long, about double that across the radiating bracts, depressed-globose and solitary at the tips of long leafy branchlets corymbosely arranged. (Figure 2.30) (Hilliard, 1983).

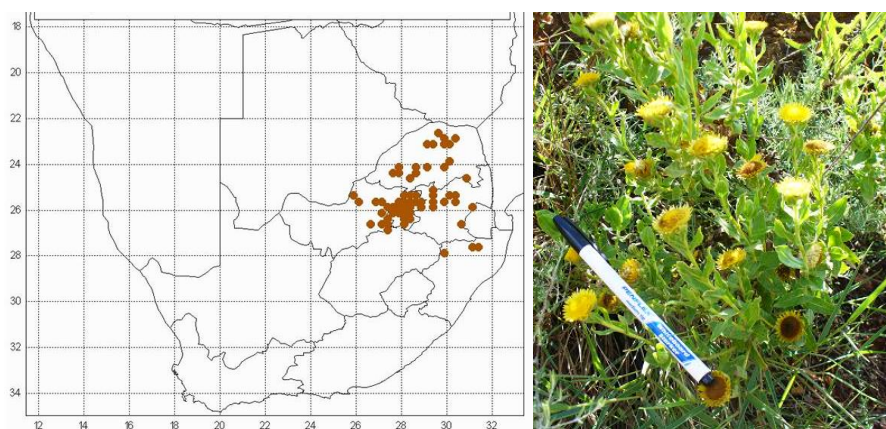


Figure 2.30. *Helichrysum setosum* collected from Buffelskloof Nature Reserve, Mpumalanga, South Africa.

Involucral bracts are in 9 series, graded and imbricate. The inner part is much exceeding the flowers, glossy yellow and often overlaid pale brown outside. Its flowering season is May to August. It grows in grassland and savanna biomes (Hilliard, 1983).

A leaf decoction of *H. setosum* is traditionally used to treat epilepsy and root powder is rubbed on snakebite (Lourens *et al.*, 2008). Jakupovic *et al.* (1986) have isolated diterpenes from this species.

2.8.30 *Helichrysum truncatum* Burt Davy

Helichrysum truncatum Burt Davy belonging to the morphological group 13, is a mat-forming perennial herb. It is decumbent and lying on the ground, but with distal part often rooting at the base. It is simple or branching from the base and leafy. Leaves are rosetted initially, oblanceolate, uppermost lanceolate, up to $50 \times 5(-7)$ mm, becoming shorter and narrower upwards and passing into bracts with brown scarious tips. The diagnostic characters of *H. truncatum* are rosetted leaves, numerous flowering stems from a creeping base, grey leaves with brown tips, brown bracts (also on stalk) and compact flower heads (Figure 2.31). This species grows in marshy grassland or sedge mats over rock flushes and it flowers between January and April (Hilliard, 1983). There is no report of biological properties and/or chemical composition of *H. truncatum*.

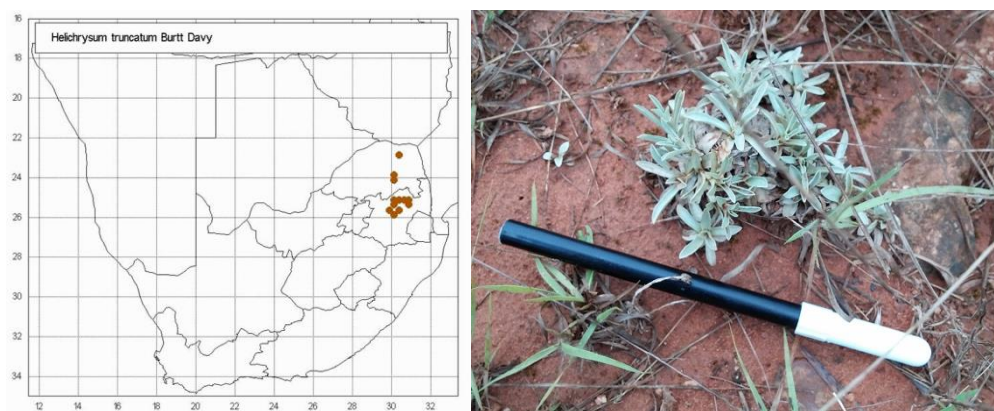


Figure 2.31. *Helichrysum truncatum* collected from Buffelskloof Nature Reserve, Mpumalanga, South Africa.

2.8.31 *Helichrysum wilmsii* Moeser

Helichrysum wilmsii Moeser belongs to the morphological group 29. It is a soft-wooded subshrub. The diagnostic characters of this species are large solitary heads, brown or white bracts and bicoloured leaves. Branches are long, loose and straggling or sprawling. It has glandular leaves that it is covered with fine short soft hairs. Leaves are mostly $12\text{--}30 \times 3\text{--}9$ mm, small and more distant upwards. The flowering season is recorded between November and July, at its peak in April and May. This species forms straggling tangled clumps in rough rocky grassland and forest margin herbage. It is found in savanna and grassland biomes (Figure 2.32) (Hilliard, 1983).

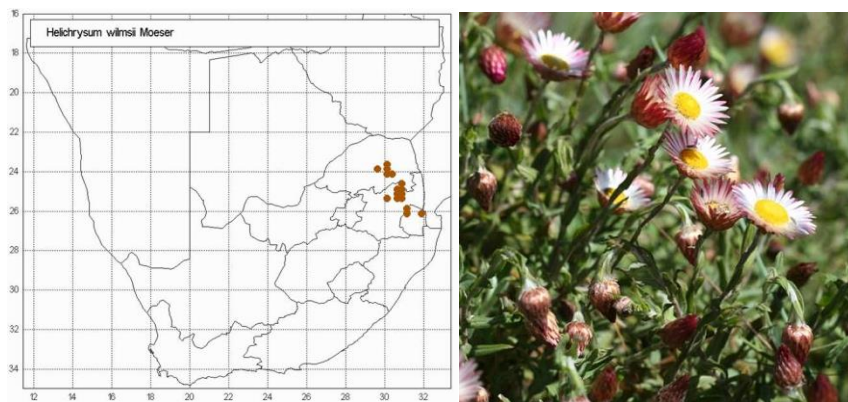


Figure 2.32. *Helichrysum wilmsii* collected from Buffelskloof Nature Reserve, Mpumalanga, South Africa.

There is no report of biological properties and/or chemical composition of *H. wilmsii*.

2.8.32 *Helichrysum zeyheri* Less.

Helichrysum zeyheri Less. belonging to the morphological group 1, is a dense or open shrublet 150–1 000 mm high. Branches are virgate, greyish white-woolly and leafy. Leaves are mostly $6\text{--}23 \times 2\text{--}9$ mm, diminishing upwards, linear-oblong and oblong or obovate. The base is sometimes petiole-like in the larger obovate leaves. It is usually broad and often subcordate-clasping. Margins of leaves are often undulate or crisped, both surfaces closely greyish white-woolly. Heads are homogamous, cylindric, 4×2 mm and many in terminal compact corymbose panicles. Involucral

bracts are in 4 or 5 series, graded, inner about equalling the flowers. They are not radiating. The tips are dense white or inner sometimes rosy. There are nearly always 5 flowers in a head (Hilliard, 1983).



Figure 2.33. *Helichrysum zeyheri* collected from Kalahari Thornveld, North West, South Africa.

Flowering is mainly between November and May. This species is found on sandy and stony soils in savanna, grassland, Nama Karoo, Succulent Karoo, fynbos and thicket biomes (Figure 2.33) (Hilliard, 1983). Coumarin was isolated from *H. zeyheri* (Jakupovic *et al.*, 1986). No biological activity and phytomedicinal properties of this species have been found.

2.9 Metabolomic analysis as a diagnostic aid

Metabolomics has become a well-known technique for the study of all types of organisms. It was developed from metabolic profiling and is the most recent of the ‘-omics’ techniques that has emerged and very different in relation to the other ‘-omics’ technologies. Genomics deals with the DNA, which is a specific chemical entity consisting of only four basic units, nucleotides. In proteomics one deals with proteins, which consists of 20 amino acids mostly and in transcriptomics with messenger RNA (mRNA), also built with the same basic four nucleotides. But to analyse the complete metabolome, multiple analyses are required. At the moment about 200 000 natural compounds are known, but certainly many more await discovery. The enormous diversity of chemical structure, especially within the huge secondary metabolites group makes plant metabolomics much more complex than metabolomics of humans and animals. Interestingly every

species exhibits a specific set of metabolites (Schripsema, 2010). Metabolomics is generally defined as a holistic qualitative and quantitative analysis of all metabolites present within a biological system under specific conditions. To provide a high degree of sensitivity, selectivity and reproducibility, advanced analytical tools are required. This newly emerged ‘omics’ has become a valuable tool for advancing our understanding of primary and secondary metabolites in plants (Tugizimana *et al.*, 2013).

The definition of metabolomics according to Dettmer *et al.* (2007) is “identification and qualification of all metabolites in a biological system” and the term metabolite profiling stands for “quantitative analysis of a particular set of metabolites in a biochemical pathway or a specific class of compounds”. It includes target analysis, the analysis of a very limited number of metabolites, such as single analytes as precursors or products of biochemical reactions (Dettmer *et al.*, 2007).

Metabolic analysis is divided into four main areas: 1) Targeted compound analysis to quantify specific metabolites, 2) Metabolic profiling to determine quantification and qualification of a group of related compounds or of specific metabolic pathway, 3) Metabolic fingerprinting to classify samples by rapid global analysis, and 4) Metabolomic analysis to quantify and qualify analysis of all metabolites (Heyman & Meyer, 2012; Kumar *et al.*, 2016).

To conduct a metabolomic analysis three main critical experimental steps must be done (Figure 2.34) (Tugizimana *et al.*, 2013):

- 1) Preparation of the sample is a critical step in transforming the sample into a solution that can be analysed to define the range of metabolite classes present.
- 2) Data acquisition using advanced analytical methods makes it possible to technologically separate, quantify and identify most metabolites within a biological sample.
- 3) Data mining chemometric methods followed by compound identification.

The choice of analytical platform depends mainly on the type of study, the class of compounds, their chemical and physical properties, and their concentration levels. Nuclear magnetic resonance spectroscopy (NMR) and mass spectrometry (MS) are the two techniques most often used.

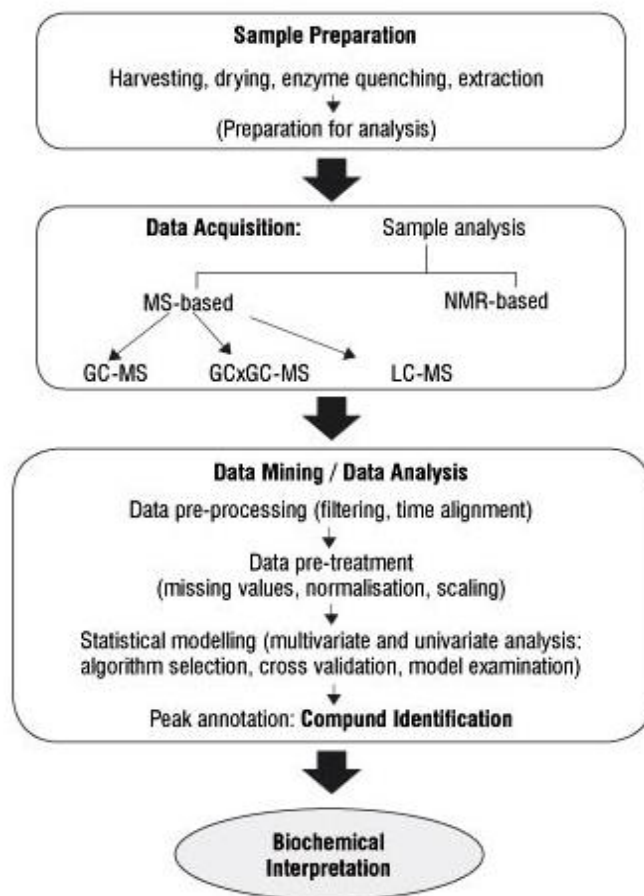


Figure 2.34. Flowchart for plant metabolomic studies (Tugizimana *et al.*, 2013). (MS: mass spectroscopy, NMR: nuclear magnetic resonance, GC: gas chromatography, LC: liquid chromatography)

As mentioned above, plant metabolites are structurally diverse, forming a high complex spectrum of compounds of different size, solubility, volatility, polarity, quantity and stability. Any extraction method would certainly produce a characteristically multidimensional sample arising from the chemical and physical differences of constituents. There are several methods of extraction of metabolites and the choice of method depends on a variety of factors, such as the phytochemical properties of the target metabolites, the biochemical composition of the system under investigation and the properties of the solvent to be used. However, there is no comprehensive extraction method for the recovery of all classes of compounds that exists in plants (Kim *et al.*, 2011; Rai *et al.*, 2013).

Metabolites identified by using ^1H NMR can be linked to a particular bioactivity by using artificial networks and this helps to predict their mode of action (Schauer & Fernie, 2006; Hong *et al.*, 2016).

Metabolic fingerprinting is an unbiased ‘global’ screening approach to classify samples based on metabolite patterns or ‘fingerprints’ that change in response to disease, environmental or genetic perturbations with the ultimate goal to identify discriminating metabolites (Schipsema, 2010). Many metabolomic studies do not go further than the metabolite fingerprinting stage: producing metabolite patterns by high-throughput analytical methods (MS or NMR) and searching for discriminating factors by chemometric methods (Schipsema, 2010; Sheridan *et al.*, 2012; Markley *et al.*, 2017).

As an example of secondary metabolome diversity in intra-species a metabolomic analysis was applied to characterize the intra-species diversity of the secondary metabolome of 98 *Myxococcus xanthus* bacterial strains. The compounds which were expected to be present in *M. xanthus* were found in all or large subsets of the analysed strains. Remarkably, 37 new candidate compounds were also detected in individual strains or subgroups of the species (Krug *et al.*, 2008). This result shows the benefit of the capacities of metabolomic analysis compared to genome-based approaches. Genomic analyses will also pose a major problem if the observed diversity is not due to differential absence/presence of gene clusters, but the result of differential regulation of clusters that are shared throughout the species (Krug *et al.*, 2008; Breitling *et al.*, 2013).

A general strategy for using metabolomics to prioritize microbial strains was established for more detailed drug discovery efforts based on their metabolomics profiles. Based on the obtained results, the phylogenetically close strains were not necessarily producing the same secondary metabolites. They clustered strains according to similarities in metabolite profiles using principal component analysis and identified compounds that were unique to individual strains based on the loading plots (Hou *et al.*, 2012; Wu *et al.*, 2016).

2.10 NMR-based metabolomics

With the development of NMR techniques and multivariate data analysis, metabolomics is increasingly playing an important role in every aspect of biomedical and phytochemical research fields, including biomarker screening, quality control, activity and toxicity prediction, clinical chemistry, chemotaxonomy and environmental metabolism (Liu *et al.*, 2010; Clish, 2015). More than 200 000 metabolites are estimated to be present in the plant kingdom and despite the positive progress and improved coverage of metabolite studies; this interesting field of study still remains a crucial component of the future development of science (Schauer & Fernie, 2006; De Souza *et al.*, 2017). It is apparent that there is still a long way to detecting the full complement of small molecules in plants. In metabolomics research, NMR and mass spectrometry are the principle detection techniques to be used and play important roles to identify and quantify metabolites (Schripsema, 2010).

The use of NMR-based fingerprinting marked the beginning of metabolomics as a tool in biochemistry and phytochemical analysis. In NMR the sensitivity is less, but the structural information content, reproducibility and quantitative aspects are superior to MS. The preparation of the samples is simpler and the analysis swifter as there is no analytical separation process involved. NMR can provide selectivity without separation and is independent of analyte polarity. The magnetic properties of tested nuclei (^1H , ^{13}C , etc.) allow for a powerful tool for observing the environments of such nuclei bonded all over a molecular skeleton. This makes NMR the ideal tool for broad-range profiling of abundant metabolites and for metabolite fingerprinting of extensive sample collections (Dixon *et al.*, 2006; Bingol, 2018). In ^1H NMR each signal corresponds to a specific hydrogen atom within a molecule and within a spectrum for every hydrogen atom of a molecule a signal is found. Isomeric signals of a compound should be considered. In NMR spectra, frequently secondary metabolites are directly observed from plant tissues. Even in cell cultures, secondary metabolites can be observed in crude extracts that generally have lower levels (Schripsema, 2010) .

Proton NMR is fast and simple and has been used as a major analytical tool for many applications in plant metabolomics such as quality control, chemotaxonomy and characterization and analysis

of the equivalence. Therefore, this technique has been the predominant profiling method for metabolomic analysis (Kim *et al.*, 2011; Emwas, 2015).

In general, NMR analysis has a great advantage over other techniques because it facilitates high-throughput analysis, has usually simple sample preparation and can be performed quite rapidly. The ease of quantification of the NMR data is one of the major advantages of this method. The signal intensity is only determined by molar concentration. Therefore, NMR can provide information on the absolute quantity of metabolites and thus the ratio and number of components in a mixture can be determined. Nuclear magnetic resonance spectroscopy is a very useful analytical method to provide the most comprehensive structural information (Kruk *et al.*, 2017).

Although NMR spectroscopy can yield detailed information on the quantities and identities present in extracts, the chemical elucidation of NMR-detected compounds can be complex because of overlapping signals and shielding effects by neighboring electrons. By using higher strength superconducting magnets and 2D-NMR that spreads the spectral content over a two-dimensional plane, the identification of compounds can be facilitated and minor compounds can be better observed, even allowing for structural elucidation in crude extracts (Kim *et al.*, 2011).

2.10.1 Data mining and data processing

The extremely large volume of data generated by high performance instruments such as NMR is handled and comprehended using automated software that can identify peaks from raw data, align the peaks among different samples and replicates, and identify and quantify each metabolite (Liland, 2011).

The procedures of data pre-processing and data pre-treatment help in cleaning the data to focus on the biologically relevant information in the data-mining step using various software packages (Allwood *et al.*, 2008). Centering, scaling and transformation are the different methods of pre-treatment. The centering procedure by calculating the average of each variable and subtracting it from each observation can adjust the conversion of all concentrations to fluctuate around the zero value. Centering the data simplifies the high and low levels of compounds in samples. By scaling

the data, each variable is divided by a function related to its standard deviation to adjust for the variation in fold differences between detected metabolites. Pre-treatment of raw data and mathematical transformation are performed because of the possibility of non-linearity in variables from a biological system. These methods transform the data into data matrices suitable for linear modelling techniques by converting multiplicative relations into additive relations, and correcting for random variables with different variability (heteroscedasticity) (Liland, 2011; Zacharias *et al.*, 2018). To provide model-based descriptions of the biological variation in the system under study, the treated data are then subjected to statistical analysis.

2.10.2 Multivariate data analysis

Multivariate data analysis (MVDA) is a mathematical modelling approach that can extract meaningful information from the large observed data sets. The metabolomic data analysis is chemometrically analysed in two methods, unsupervised and supervised.

Unsupervised data modelling is focused on the basic structure, relations and linkage of the data and is sometimes referred to as descriptive models. Supervised modelling, on the other hand, seeks to transform the multivariate data from metabolite profiles into a representation of biological interest under the guidance of a ‘supervisor’. These models are often called predictive models. The basis of supervised modelling is that there is some pattern such as metabolic fingerprints, in data that have predefined responses such as effect of treatment or condition, and the goal of supervised methods is to find a model or mapping that will correctly associate the inputs with the responses. The collected data is algebraically represented in two types of matrices: the descriptor matrix X which are the observed variables, and response matrix Y which are the pre-defined traits (Worley & Powers, 2013).

The multivariate model is commonly interpreted and validated in two ways, by means of the R^2 and Q^2 cumulative values after cross validation. The R^2 parameter informs the amount of Y variables explained by the model after cross validation and gives an overview on the fitness of the model, while Q^2 gives information about the prediction quality of the model. The values close to 1 display a good model. Nuclear magnetic resonance spectroscopy bucketed data is analysed using

the Principal Component Analysis (PCA) multivariate statistical method or other statistical methods. The PCA score plots shows the similarities and differences in the metabolite profiling obtained from the samples e.g. medicinal herbs (Eriksson *et al.*, 2013; Wu & Wang, 2015).

Orthogonal projections to latent structure-discriminant analysis (OPLS-DA), is a type of supervised classification and regression method that correlates spectroscopic data to a certain property. OPLS-DA is a linear regression method, which has been successfully used for prediction modelling in metabolomics and biochemical applications. It is a supervised classification model that differs from PCA by the addition of grouping variables that indicate in which class the samples belong. Where PCA modelling is a descriptive method, OPLS-DA method is an explicative or predictive analysis. The latter facilitates the identification of the metabolite ions responsible for the discrimination between groups (Roux *et al.*, 2011).

2.11 Molecular docking study

Molecular docking is a kind of bioinformatic modelling which involves the interaction of two or more molecules to give a stable adduct. It has become an increasingly important computational tool for the study of molecular recognition and drug discovery. Since the 1980s, it has been widely used to design structure-based drugs (Huang & Zou, 2010; Guedes *et al.*, 2014; Dar & Mir, 2017). The aims of the computational tool is to predict the binding mode and binding affinity of a complex formed by constituent molecules with standard structures (Huang & Zou, 2010). It is valuable to understand and reveal drug-biomolecular interactions for rational drug discovery and design by studying the binding of molecules or ligands into the best binding site of the specific region of a receptor in a non-covalent fashion to make a stable complex of potential efficacy and more specificity (Guedes *et al.*, 2014; Agarwal & Mehrotra, 2016).

The specific interaction between two or more molecules through non-covalent binding such as hydrogen bonding, metal coordination, hydrophobic forces, Van der Waals forces and/or electromagnetic effects refers to molecular recognitions which includes enzyme-substrate, drug-protein, drug-nucleic acid, protein-nucleic acid, and protein-protein interactions. Molecular recognitions play important roles in many biological processes such as signal transduction, cell

regulation and other macromolecular assemblies. Therefore, in molecular docking, discovery of the binding mode and affinity between the protein-ligand molecules is key to understanding the interaction mechanisms and to designing therapeutic structure-based drugs (Huang & Zou, 2010).

The development of high-throughput protein purification, crystallography and NMR techniques help to identify many structural details of proteins and protein-ligand complexes. These advanced techniques lead to the computational strategies to pervade all aspects of drug discovery such as virtual screening techniques for identification and methods for principal optimization (Meng *et al.*, 2011). The main aim of molecular docking is to give a prediction of the ligand-receptor complex structure using the computation method. There are two correlated steps which can be achieved by docking: first by sampling conformations of the ligand in the active site of the protein; then ranking these conformations via a scoring function (Meng *et al.*, 2011). The molecular docking model can be used to describe the interaction between a small molecule and protein at the atomic level, which can characterize the behavior of small molecules in the binding site of target proteins, as well as to explain fundamental biochemical processes. There are two steps in the process of molecular docking: prediction of the ligand conformation, as well as its position and orientation within these sites, which is referred to as pose, and assessment of the binding affinity. These two steps are related to sampling methods and schemes, respectively (Ferreira *et al.*, 2015). The pose with the lowest energy score is recognized as the best match or the binding mode (Kuntz *et al.*, 1982). Recognizing the location of the binding site before docking processes will help to increase the efficiency of the analysis. To obtain the information about the sites, the target protein can be compared with a family of proteins sharing a similar function or with proteins co-crystallized with other ligands. If there is no knowledge about the binding sites, cavity detection programs or online servers such as GRID, POCKET, SurfNet, PASS and MMC can be utilized to identify putative active sites within proteins (Meng *et al.*, 2011; Pagadala *et al.*, 2017). There are various kinds of molecular docking procedures. In rigid docking, the possible binding conformations of a ligand in a specific area of the receptor are evaluated by rotating its bonds and translating the molecule. Flexible docking is like rigid docking in the sense that the search area is specific but on this type of docking, several bonds can rotate. Blind docking is the analysis of a ligand and receptor without any assumption about the binding site (Meng *et al.*, 2011; Dar *et al.*, 2017).

Very careful preparatory work must be done before an attempt to do a docking analysis. This includes determining the stable 3D structure using energy minimization for ligand and protein. The preparatory work has been illustrated in a flow chart in Figure 2.35.

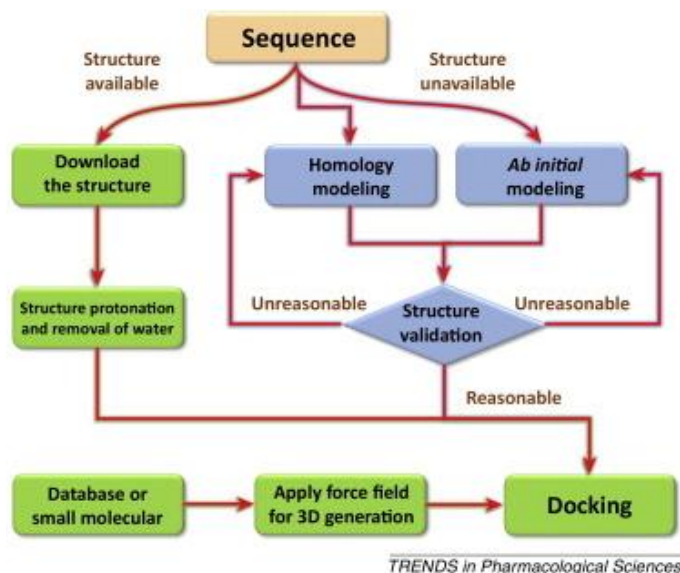


Figure 2.35. Flow chart of the docking procedure (Chen, 2015).

Protein conformational changes are induced by ligand binding, which range from local rearrangements of side-chains to large domain motions. The most challenging issue can be the protein flexibility, due to the large size and many degrees of freedom of proteins in molecular docking. There are four categories for current methods to account for protein flexibility: soft docking, side-chain flexibility, molecular relaxation, and protein ensemble docking (Totrov & Abagyan, 2008; Huang & Zou, 2010; Iglesias *et al.*, 2018).

The most basic factor in protein-ligand docking is ligand sampling. Given a protein target, the sampling algorithm generates putative ligand orientations/conformations around the chosen binding site of the protein. The binding site can be the experimentally determined active site, a dimer interface or other site of interest. Ligand sampling is the most successful area being developed in protein-ligand docking. There are three types of ligand sampling algorithms: shape matching, systematic search, and stochastic algorithms (Huang & Zou, 2010).

The original concept of docking is based on the concept of ‘lock and key’ of rational drug design, and the precise algorithms used to fit the ‘key’ (the ligand) into the ‘lock’ (the receptor protein) are varied across programs. The number of new algorithms has been increasing in recent years (Figure 2.36) (Chen, 2015; Tripathi & Bankaitis, 2017).

The scoring function is a key element of a protein-ligand docking algorithm, because it directly determines the accuracy of the algorithm. Speed and accuracy are the two important aspects of a scoring function. An ideal scoring function would be both computationally efficient and reliable. Numerous scoring functions have been developed in the past decades and can be grouped into three basic categories according to their methods of derivation: force field, empirical and knowledge-based scoring functions (Huang & Zou, 2010).

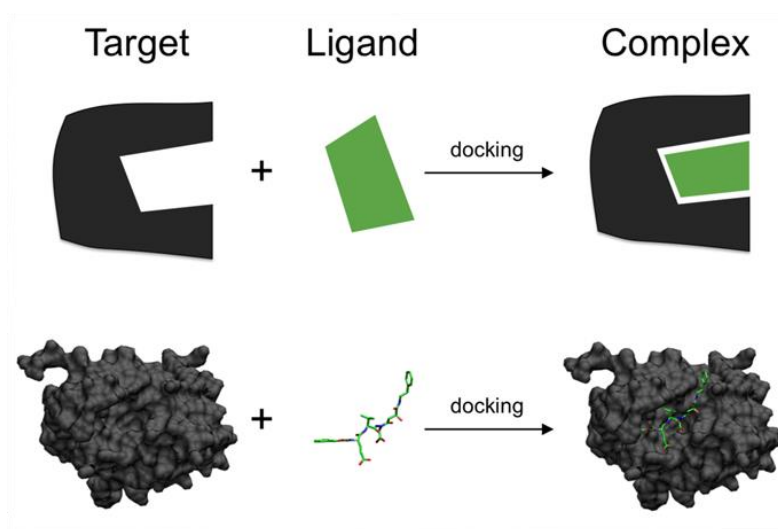


Figure 2.36. Schematic design of docking: a small molecule ligand (green) to a protein target (black) producing a stable complex.

The docking mode divides into four models (Figure 2.37): lock and key, conformation isomerism, induced fit and conformation selection. Only the shape of the binding pocket in induced fit mode is transformed to the new shape. However, the entry into the binding pocket will sometimes change the shape of the binding site, according to simulation from molecular docking experiments.

Computational methods play an important role in modern anti-HIV drug development. Gu *et al.* (2014) explained advances in the application of computational methods to anti-HIV drug development applied to five key targets as follows: reverse transcriptase, protease, integrase, C-C chemokine receptor type 5 (CCR5), and C-X-C chemokine receptor type 4 (CXCR4).

Molecular docking techniques are very important scientific advances for the understanding of potential of compounds against HIV-1. An example of one of these studies was on the anti-HIV activity of β -carboline derivatives. The highly active compound 1-formyl-beta-carboline-3-carboxylic acid methyl ester with anti-HIV activity ($IC_{50} = 2.9 \mu M$) was docked into the active sites of HIV-1-RT, integrase and protease. The binding energy score and binding interactions were good with RT compared to PR and IN. Based on the obtained result there are two H bonding interactions with the Lys103 residue and a good binding free energy score of -8.63 kcal/mol at temperature 298.15 K for the HIV-1-RT protein (Kumar & Garg, 2010).

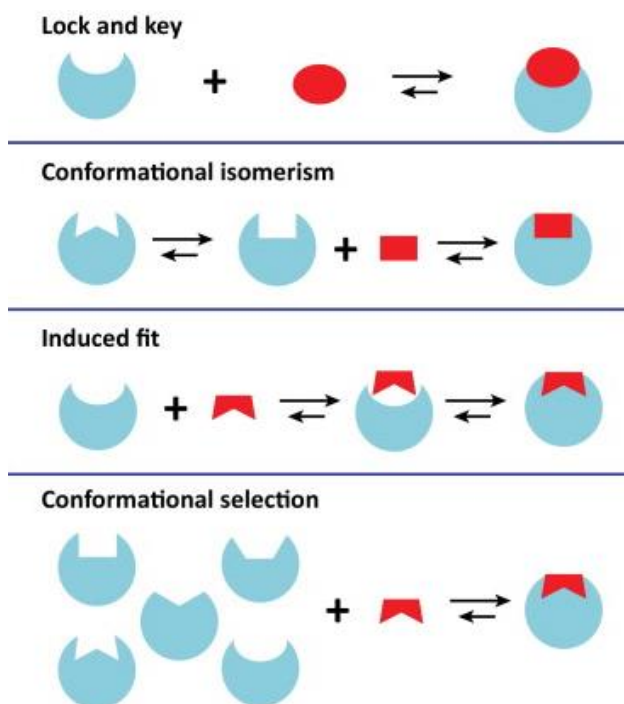


Figure 2.37. The docking mode divided into four types of docking mode (Chen, 2015).

Balakrishnan (2012) also studied the molecular docking of a series of diphenyl imidazolidin diones against HIV-1-RT. They conducted the docking studies using Auto dock. 31-(2,5-Dioxo-4,4-diphenyl imidazolidin-1-yl) benzamide derivatives were designed with variation in the aromatic ring of the benzamide portion of the molecule. Out of all the designed compounds four exhibited the top scoring with respect to the calculated free energy of binding (kcal/mol). These four compounds were 2-phenyl (2,5-dioxo-4,4-diphenyl imidazolidin-1-yl) benzamide (-12.21 kcal/mol), 4-phenyl (2,5-dioxo-4,4-diphenyl imidazolidin-1-yl) benzamide (-11.23 kcal/mol), 3-nitro (2,5-dioxo-4,4-diphenyl imidazolidin-1-yl) benzamide (-11.81 kcal/mol) and 3-ethoxy (2,5-dioxo-4,4-diphenyl imidazolidin-1-yl) benzamide (-11.57 kcal/mol) (Balakrishnan, 2012).

2.12 Conclusion

Viruses are obligate intracellular parasites, which contain little more than bundles of gene strands of either RNA or DNA and may be surrounded by a lipid-containing envelope (Wagner & Hewlett, 1999). Unlike bacterial cells, which are free-living entities, viruses utilize the host cell environment to propagate new viruses. They use the reproductive machinery of cells they invade to cause ailments. Using medicinal plant extracts of various species that can act therapeutically in various viral infections, and the recent successful achievements mentioned above, have raised hopes about the future of phyto-antiviral agents.

Plants produce an amazing variety of metabolites that are gaining importance for their therapeutic and biological applications. Due to the difficulties and economic cost of the experimental methods for determining the structures of complexes, computational methods such as metabolomic analysis and molecular docking are ideal for identifying and predicting putative binding modes and affinities of active phytochemical components of medicinal plants. Metabolomics is a tool for improving the understanding of the metabolism and biochemistry of organisms and isolated natural products from plants. It provides a deeper biological and chemical meaning of a studied metabolome. Nuclear magnetic resonance spectroscopy-based metabolomics is an important tool for studying biological systems and obtaining chemical structural data. Applying NMR-based

metabolomics combined with PCA and OPLS-DA multivariate analyses can probably be an efficient tool for discriminating and predicting biological activity of secondary metabolites.

2.13 References

- Agarwal, S. & Mehrotra, R. (2016). An overview of molecular docking. *JSM Chemistry*, 4(2), 1024.
- Allwood, J. W., Ellis, D. I. & Goodacre, R. (2008). Metabolomic technologies and their application to the study of plants and plant-host interactions. *Physiologia Plantarum*, 132(2), 117–135.
- Appendino, G., Ottino, M., Marquez, N., Bianchi, F., Giana, A., Ballero, M., Sterner, O., Fiebich, B. L. & Munoz, E. (2007). Arzanol, an anti-inflammatory and anti-HIV-1 phloroglucinol α -pyrone from *Helichrysum italicum* ssp. *microphyllum*. *Journal of Natural Products*, 70(4), 608–612.
- Arnold, T. H., Prentice, C. A., Hawker, L. C., Snyman, E. E., Tomalin, M., Crouch, N. R. & Pottas-Bircher, C. (2002). Medicinal and magical plants of southern Africa: an annotated checklist. *Strelitzia* 13. National Botanical Institute, Pretoria.
- Babar, M., Najam-us-Sahar, S.Z., Ashraf, M. & Kazi, A.G. (2013). Antiviral drug therapy-exploiting medicinal plants. *Journal of Antivirals and Antiretrovirals*, 5(2), 2–36.
- Balakrishnan, V. (2012). Molecular docking studies of diphenyl imidazolidin diones with HIV reverse transcriptase. *Journal of Pharmacy Research*, 5(3), 1371–1373.
- Bauer, J., Koeberle, A., Dehm, F., Pollastro, F., Appendino, G., Northoff, H., Rossi, A., Sautebin, L. & Werz, O. (2011). Arzanol, a prenylated heterodimeric phloroglucinyl pyrone, inhibits eicosanoid biosynthesis and exhibits anti-inflammatory efficacy *in vivo*. *Biochemical Pharmacology*, 81(2), 259–268.
- Bennett, J. E., Dolin, R. & Blaser, M. J. (2014). Mandell, Douglas, and Bennett's Principles and Practice of Infectious Diseases E-Book. Elsevier Health Sciences, London, United Kingdom.
- Bingol, K. (2018). Recent advances in targeted and untargeted metabolomics by NMR and MS/NMR methods. *High-Throughput*, 7(2), 9.
- Bohlmann, F. & Ates, N. (1984). Three prenylated flavanoids from *Helichrysum athrixifolium*. *Phytochemistry*, 23, 1338–1339.

- Bohlmann, F. & Abraham, W.-R. (1979). Neue diterpene aus *Helichrysum acutatum*. *Phytochemistry*, 18(10), 1754–1756.
- Bohlmann, F., Mahanta, P. K. & Zdero, C. (1978). Neue chalkon-derivate aus südafrikanischen *Helichrysum*-arten. *Phytochemistry*, 17(11), 1935–1937.
- Bougatsos, C., Meyer, J. J. M., Magiatis, P., Vagias, C. & Chinou, I. B. (2003). Composition and antimicrobial activity of the essential oils of *Helichrysum kraussii* Sch.Bip. and *H. rugulosum* Less. from South Africa. *Flavour and Fragrance Journal*, 18(1), 48–51.
- Breitling, R., Cenicerros, A., Jankevics, A. & Takano, E. (2013). Metabolomics for secondary metabolite research. *Metabolites*, 3(4), 1076–1083.
- Bremner, P. D. & Meyer, J. J. M. (2000). Prenyl-butyrylphloroglucinol and kaurenoic acid: two antibacterial compounds from *Helichrysum kraussii*. *South African Journal of Botany*, 66(2), 115–117.
- Brusotti, G., Cesari, I., Dentamaro, A., Caccialanza, G. & Massolini, G. (2014). Isolation and characterization of bioactive compounds from plant resources: the role of analysis in the ethnopharmacological approach. *Journal of Pharmaceutical and Biomedical Analysis*, 87, 218–228.
- Chen, Y.-C. (2015). Beware of docking! *Trends in Pharmacological Sciences*, 36(2), 78–95.
- Clish, C. B. (2015). Metabolomics: an emerging but powerful tool for precision medicine. *Molecular Case Studies*, 1(1), a000588.
- Cohen, M. S., Hellmann, N., Levy, J. A., DeCock, K. & Lange, J. (2008). The spread, treatment, and prevention of HIV-1: evolution of a global pandemic. *The Journal of Clinical Investigation*, 118(4), 1244–1254.
- Cox, D. G., Oh, J., Keasling, A., Colson, K. L. & Hamann, M. T. (2014). The utility of metabolomics in natural product and biomarker characterization. *Biochimica et Biophysica Acta (BBA)-General Subjects*, 1840(12), 3460–3474.

- Croteau, R., Kutchan, T. M., Lewis, N. G. & others. (2000). Natural products (secondary metabolites). *Biochemistry and Molecular Biology of Plants*, 24, 1250–1319.
- Dai, J. -R., Hallock, Y. F., Cardellina, J. H. & Boyd, M. R. (1998). HIV-inhibitory and cytotoxic oligostilbenes from the leaves of *Hopea malibato*. *Journal of Natural Products*, 61(3), 351–353.
- Dar, A. M. & Mir, S. (2017). Molecular docking: approaches, types, applications and basic challenges. *Journal of Analytical & Bioanalytical Techniques*, 8, 2.
- Dar, R. A., Shah Nawaz, M., Rasool, S. & Qazi, P. H. (2017). Natural product medicines: A literature update, *The Journal of Phytopharmacology*, 6(6): 340–342.
- De Clercq, E. (2009). Anti-HIV drugs: 25 compounds approved within 25 years after the discovery of HIV. *International Journal of Antimicrobial Agents*, 33(4), 307–320.
- De Groot, N. G. & Bontrop, R. E. (2013). The HIV-1 pandemic: does the selective sweep in chimpanzees mirror humankind's future? *Retrovirology*, 10:53, 1–15.
- De Souza, L. P., Naake, T., Tohge, T. & Fernie, A. R. (2017). From chromatogram to analyte to metabolite. How to pick horses for courses from the massive web-resources for mass spectral plant metabolomics. *Giga Science*, 6, 1–20.
- Dettmer, K., Aronov, P. A. & Hammock, B. D. (2007). Mass spectrometry-based metabolomics. *Mass Spectrometry Review*, 26, 51–78.
- Dias, D. A., Urban, S. & Roessner, U. (2012). A historical overview of natural products in drug discovery. *Metabolites*, 2(2), 303–336.
- Dixon, R. A., Gang, D. R., Charlton, A. J., Fiehn, O., Kuiper, H. A., Reynolds, T. L., Tjeerdema, R.S., Jeffery, E.H., German, J.B., Ridley, W. & Seiber, J.N. (2006). Applications of metabolomics in agriculture. *Journal of Agricultural and Food Chemistry*, 54(24), 8984–8994.

- El Dine, R. S., El Halawany, A. M., Ma, C. M. & Hattori, M. (2009). Inhibition of the dimerization and active site of HIV-1 protease by secondary metabolites from the Vietnamese mushroom *Ganoderma colossum*. *Journal of Natural Products*, 72(11), 2019–2023.
- Emwas, A. H. M. (2015). The strengths and weaknesses of NMR spectroscopy and mass spectrometry with particular focus on metabolomics research. In Walker, J. M. (ed.) *Methods in Molecular Biology*. Clifton, New Jersey, United States. pp. 161–193.
- Eriksson, L., Byrne, T., Johansson, E., Trygg, J. & Vikström, C. (2013). Multi-and megavariate data analysis basic principles and applications (Vol. 1). Umetrics Academy.
- Ferreira, L., Dos Santos, R., Oliva, G. & Andricopulo, A. (2015). Molecular docking and structure-based drug design strategies. *Molecules*, 20(7), 13384–13421.
- Gu, W. -G., Zhang, X. & Yuan, J. -F. (2014). Anti-HIV drug development through computational methods. *American Association of Pharmaceutical Scientists*, 16(4), 674–680.
- Guedes, I. A., de Magalhães, C. S. & Dardenne, L. E. (2014). Receptor-ligand molecular docking. *Biophysical Reviews*, 6(1), 75–87.
- Heyman, H. M. & Meyer, J. J. M. (2012). NMR-based metabolomics as a quality control tool for herbal products. *South African Journal of Botany*, 82, 21–32.
- Heyman, H. M. (2013). Identification of anti-HIV compounds in *Helichrysum* species (Asteraceae) by means of NMR-based metabolomic guided fractionation. University of Pretoria (Ph.D. thesis).
- Hilliard, O. M. (1983). Flora of Southern Africa, Asteraceae, Part 7 Inuleae Fascicle 2 Gnaphaliinae (First Part). (O. A. Leistner, Ed.) (Volume 33). Pretoria, South Africa: Botanical Research Institute, Department of Agriculture. (Vol. 33, pp. 61–310)
- Hong, J., Yang, L., Zhang, D. & Shi, J. (2016). Plant metabolomics: an indispensable system biology tool for plant science. *International Journal of Molecular Sciences*, 17(6), 767.
- Hosseini, I. & Mac Gabhann, F. (2013). APOBEC3G-augmented stem cell therapy to modulate HIV replication: a computational study. *PloS One*, 8(5), e63984.

- Hou, Y., Braun, D. R., Michel, C. R., Klassen, J. L., Adnani, N., Wyche, T. P. & Bugni, T. S. (2012). Microbial strain prioritization using metabolomics tools for the discovery of natural products. *Analytical Chemistry*, 84(10), 4277–4283.
- Huang, S. Y. & Zou, X. (2010). Advances and challenges in protein-ligand docking. *International Journal of Molecular Sciences*, 11(8), 3016–3034.
- Iglesias, J., Saen-oon, S., Soliva, R. & Guallar, V. (2018). Computational structure-based drug design: Predicting target flexibility. *Wiley Interdisciplinary Reviews: Computational Molecular Science*, 8(5), e1367.
- Jakupovic, J., Kuhnke, J., Schuster, A., Metwally, M. A. & Bohlmann, F. (1986). Phloroglucinol derivatives and other constituents from South African *Helichrysum* species. *Phytochemistry*, 25(5), 1133–1142.
- Jakupovic, J., Schuster, A., Sun, H., Bohlmann, F. & Bhakuni, D. S. (1987). Prenylated phthalides from *Anaphalis araneosa* and *Helichrysum platypterum*. *Phytochemistry*, 26(2), 580–581.
- Jamshidi-Kia, F., Lorigooini, Z. & Amini-Khoei, H. (2018). Medicinal plants: Past history and future perspective. *Journal of Herbmed Pharmacology*, 7(1), 1–7.
- Jassim, S. A. A. & Naji, M. A. (2003). Novel antiviral agents: a medicinal plant perspective. *Journal of Applied Microbiology*, 95(3), 412–427.
- Kabera, J. N., Semana, E., Mussa, A. R. & He, X. (2014). Plant secondary metabolites: biosynthesis, classification, function and pharmacological properties. *Journal of Pharmacy and Pharmacology*, 2, 377–392.
- Kim, H. K., Choi, Y. H. & Verpoorte, R. (2011). NMR-based plant metabolomics: where do we stand, where do we go? *Trends in Biotechnology*, 29(6), 267–275.
- Krug, D., Zurek, G., Revermann, O., Vos, M., Velicer, G. J. & Müller, R. (2008). Discovering the hidden secondary metabolome of *Myxococcus xanthus*: a study of intraspecific diversity. *Applied and Environmental Microbiology*, 74(10), 3058–3068.

- Kruk, J., Doskocz, M., Jodłowska, E., Zacharzewska, A., Łakomiec, J., Czaja, K. & Kujawski, J. (2017). NMR techniques in metabolomic studies: A quick overview on examples of utilization. *Applied Magnetic Resonance*, 48(1), 1–21.
- Kucukoglu, O., Ozturk, B., Kamataki, T. & Topcu, Z. (2006). Inhibitory Activities of *Helichrysum*. Taxa on Mammalian Type I DNA Topoisomerase. *Pharmaceutical Biology*, 44(3), 189–193.
- Kumar, D., Rawat, A., Dubey, D., Kumar, U., Keshari, A. K., Saha, S. & Guleria, A. (2016). NMR based metabolomics: an emerging tool for therapeutic evaluation of traditional herbal medicines. SM-EBOOK: Nuclear Magnetic Resonance Spectroscopy, pp. 1–18.
- Kumar, R. & Garg, P. (2010). Active site binding interactions of β -carboline derivative for HIV reverse transcriptase, protease and integrase. *International Journal of Drug Discovery*, 2(2), 51–55.
- Kunle, O. F., Egharevba, H. O. & Ahmadu, P. O. (2012). Standardization of herbal medicines - A review. *International Journal of Biodiversity and Conservation*, 4(3), 101–112.
- Kuntz, I. D., Blaney, J. M., Oatley, S. J., Langridge, R. & Ferrin, T. E. (1982). A geometric approach to macromolecule-ligand interactions. *Journal of Molecular Biology*, 161(2), 269–288.
- Li, B. Q., Fu, T., Dongyan, Y., Mikovits, J. A., Ruscetti, F. W. & Wang, J. M. (2000). Flavonoid baicalin inhibits HIV-1 infection at the level of viral entry. *Biochemical and Biophysical Research Communications*, 276(2), 534–538.
- Liland, K. H. (2011). Multivariate methods in metabolomics--from pre-processing to dimension reduction and statistical analysis. *Trends in Analytical Chemistry*, 30(6), 827–841.
- Liu, N. Q., Cao, M., Frédérick, M., Choi, Y. H., Verpoorte, R. & Van der Kooy, F. (2010). Metabolomic investigation of the ethnopharmacological use of *Artemisia afra* with NMR spectroscopy and multivariate data analysis. *Journal of Ethnopharmacology*, 128(1), 230–235.

- Lourens, A. C. U., Reddy, D., Başer, K. H. C., Viljoen, A. M. & Van Vuuren, S. F. (2004). In vitro biological activity and essential oil composition of four indigenous South African *Helichrysum* species. *Journal of Ethnopharmacology*, 95(2–3), 253–258.
- Lourens, A. C. U., Viljoen, A. M. & Van Heerden, F. R. (2008). South African *Helichrysum* species: a review of the traditional uses, biological activity and phytochemistry. *Journal of Ethnopharmacology*, 119(3), 630–652.
- Malolo, F. -A. E., Nougä, A. B., Kakam, A., Franke, K., Ngah, L., Flausino, O. & Mpondo, E. M. (2015). Protease-inhibiting, molecular modeling and antimicrobial activities of extracts and constituents from *Helichrysum foetidum* and *Helichrysum mechowianum* (Compositae). *Chemistry Central Journal*, 9(1), 32.
- Markley, J. L., Brüschweiler, R., Edison, A. S., Eghbaltia, H. R., Powers, R., Raftery, D. & Wishart, D. S. (2017). The future of NMR-based metabolomics. *Current Opinion in Biotechnology*, 43, 34–40.
- Mathekga, A. D. M., Meyer, J. J. M., Horn, M. M. & Drewes, S. E. (2000). An acylated phloroglucinol with antimicrobial properties from *Helichrysum caespititium*. *Phytochemistry*, 53(1), 93–96.
- Meng, X. -Y., Zhang, H. -X., Mezei, M. & Cui, M. (2011). Molecular docking: a powerful approach for structure-based drug discovery. *Current Computer-Aided Drug Design*, 7(2), 146–157.
- Meyer, J. J. M., Lall, N., Mathekga, A. D. M. & Jäger, A. K. (2002). In vitro inhibition of drug-resistant and drug-sensitive strains of *Mycobacterium tuberculosis* by *Helichrysum caespititium*. *South African Journal of Botany*, 68(1), 90–93.
- Michailidis, E., Marchand, B., Kodama, E. N., Singh, K., Matsuoka, M., Kirby, K. A., Ryan, E. M., Sawani, A. M., Nagy, E., Ashida, N., Mitsuya, H., Parniak, M. A. & Sarafianos, S. G. (2009). Mechanism of inhibition of HIV-1 reverse transcriptase by 4'-ethynyl-2-fluoro-2'-deoxyadenosine triphosphate, a translocation-defective reverse transcriptase inhibitor. *Journal of Biological Chemistry*, 284(51), 35681–35691.

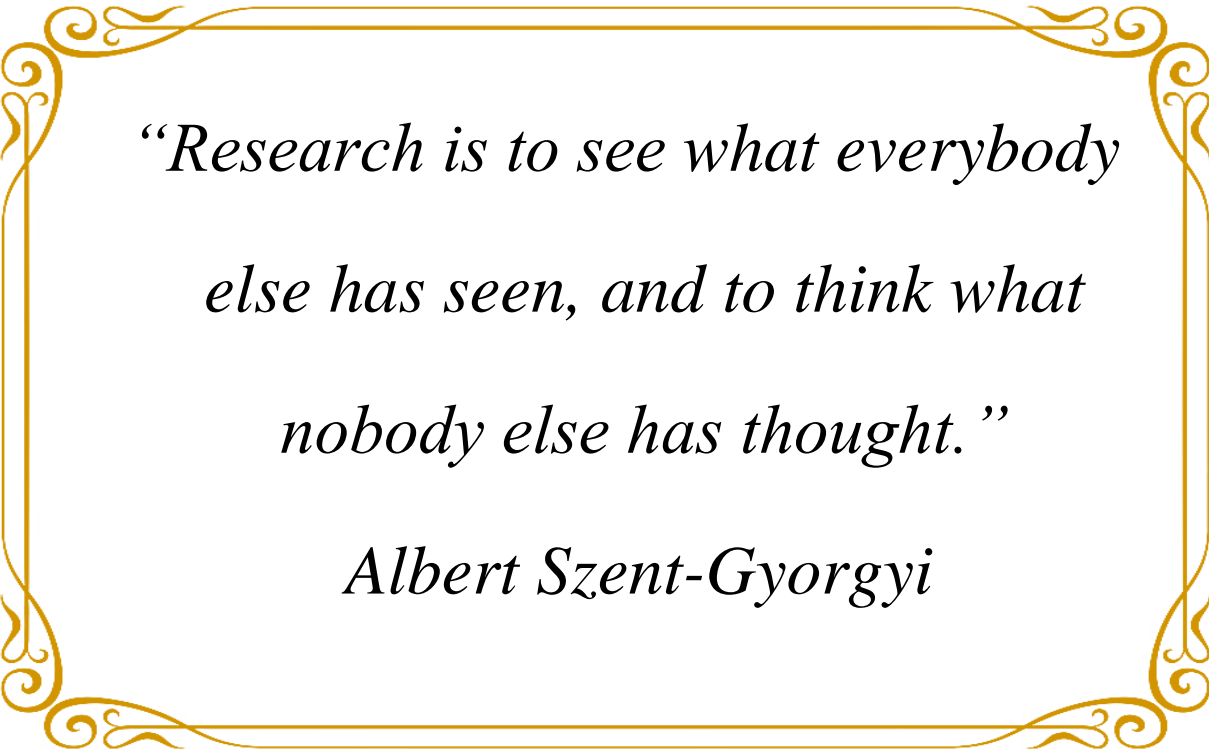
- Min, B. -S., Nakamura, N., Miyashiro, H., Kim, Y. -H. & Hattori, M. (2000). Inhibition of human immunodeficiency virus type 1 reverse transcriptase and ribonuclease H activities by constituents of *Juglans mandshurica*. *Chemical and Pharmaceutical Bulletin*, 48(2), 194–200.
- Mukhtar, M., Arshad, M., Ahmad, M., Pomerantz, R. J., Wigdahl, B. & Parveen, Z. (2008). Antiviral potentials of medicinal plants. *Virus Research*, 131(2), 111–120.
- Nisole, S. & Saïb, A. (2004). Early steps of retrovirus replicative cycle. *Retrovirology*, 1(1), 9.
- Pagadala, N. S., Syed, K. & Tuszynski, J. (2017). Software for molecular docking: a review. *Biophysical Reviews*, 9(2), 91–102.
- Pagare, S., Bhatia, M., Tripathi, N., Pagare, S. & Bansal, Y. K. (2015). Secondary metabolites of plants and their role: Overview. *Current Trends in Biotechnology and Pharmacy*, 9(3), 293–304.
- Pooley, E. (2005). A field guide to wildflowers: KwaZulu-Natal and the eastern region (Second edition). Natal Flora Publications Trust, Durban.
- Post, K., Olson, E. D., Naufer, M. N., Gorelick, R. J., Rouzina, I., Williams, M. C., Forsyth, K. M. & Levin, J. G. (2016). Mechanistic differences between HIV-1 and SIV nucleocapsid proteins and cross-species HIV-1 genomic RNA recognition. *Retrovirology*, 13:89, 1–18.
- Prinsloo, G., & Meyer, J.J.M. (2006). In vitro production of phytoalexins by *Helichrysum kraussii*. *South African Journal of Botany*, 72(3), 482–483.
- Pushpa, R., Nishant, R., Navin, K. & Pankaj, G. (2013). Antiviral potential of medicinal plants: An overview. *International Research Journal of Pharmacy*, 4(6), 8–16.
- Rai, A., Umashankar, S. & Swarup, S. (2013). Plant metabolomics: from experimental design to knowledge extraction. *Methods in Molecular Biology*, 1069, 279–312.
- Rates, S. M. K. (2001). Plants as source of drugs. *Toxicon*, 39(5), 603–613.
- Reddy, D. (2008). The phytochemistry and microbial activity of selected indigenous *Helichrysum* species. University of the Witwatersrand. South Africa. (Ph.D. thesis).

- Richman, D. D., Margolis, D. M., Delaney, M., Greene, W. C., Hazuda, D. & Pomerantz, R. J. (2009). The challenge of finding a cure for HIV infection. *Science*, 323(5919), 1304–1307.
- Roux, A., Lison, D., Junot, C. & Heilier, J. -F. (2011). Applications of liquid chromatography coupled to mass spectrometry-based metabolomics in clinical chemistry and toxicology: A review. *Clinical Biochemistry*, 44(1), 119–135.
- Sarafianos, S. G., Marchand, B., Das, K., Himmel, D. M., Parniak, M. A., Hughes, S. H. & Arnold, E. (2009). Structure and function of HIV-1 reverse transcriptase: molecular mechanisms of polymerization and inhibition. *Journal of Molecular Biology*, 385(3), 693–713.
- Schauer, N. & Fernie, A. R. (2006). Plant metabolomics: towards biological function and mechanism. *Trends in Plant Science*, 11(10), 508–516.
- Schripsema, J. (2010). Application of NMR in plant metabolomics: techniques, problems and prospects. *Phytochemical Analysis: An International Journal of Plant Chemical and Biochemical Techniques*, 21(1), 14–21.
- Scott, G., Springfield, E. P. & Coldrey, N. (2004). A pharmacognostical study of 26 South African plant species used as traditional medicines. *Pharmaceutical Biology*, 42(3), 186–213.
- Sheridan, H., Krenn, L., Jiang, R., Sutherland, I., Ignatova, S., Marmann, A., Liang, X. & Sendker, J. (2012). The potential of metabolic fingerprinting as a tool for the modernisation of TCM preparations. *Journal of Ethnopharmacology*, 140(3), 482–491.
- Sluis-Cremer, N. & Tachedjian, G. (2008). Mechanisms of inhibition of HIV replication by non-nucleoside reverse transcriptase inhibitors. *Virus Research*, 134(1–2), 147–156.
- South African National AIDS Council, (2016). Republic of South Africa 2016 Global AIDS response progress report (quantitative report). Retrieved from https://sanac.org.za/wp-content/uploads/2017/06/MandE-SANAC-Global-AIDS-Response-Progress-Report_2016.pdf
- Štulíková, K., Karabín, M., Nešpor, J. & Dostálek, P. (2018). Therapeutic perspectives of 8-prenylnaringenin, a potent phytoestrogen from Hops. *Molecules*, 23(3), 1–13.

- Swanepoel, D.P. (1997). The medicinal value of the Southern African Asteraceae. University of Pretoria, South Africa. (Master dissertation).
- Totrov, M. & Abagyan, R. (2008). Flexible ligand docking to multiple receptor conformations: a practical alternative. *Current Opinion in Structural Biology*, 18(2), 178–184.
- Tripathi, A. & Bankaitis, V. A. (2017). Molecular docking: from lock and key to combination lock. *Journal of Molecular Medicine and Clinical Applications*, 2(1), 1-19.
- Tugizimana, F., Piater, L. & Dubery, I. (2013). Plant metabolomics: A new frontier in phytochemical analysis. *South African Journal of Science*, 109(5–6), 1–11.
- UNAIDS DATA, (2018). Report on the Global HIV/AIDS Epidemic 2018. https://www.unaids.org/sites/default/files/media_asset/unaids-data-2018_en.pdf (Accessed 17/09/2018).
- Van Vuuren, S. F. (2008). Antimicrobial activity of South African medicinal plants. *Journal of Ethnopharmacology*, 119(3), 462–472.
- Veeresham, C. (2012). Natural products derived from plants as a source of drugs. *Journal of Advanced Pharmaceutical Technology and Research*, 3(4), 200-201.
- Wagner, E.K. & Hewlett, M.J. (1999). Basic Virology. Malden, MA, USA: Blackwell Science.
- Wangkheirakpam, S. (2018). Traditional and Folk Medicine as a Target for Drug Discovery. In Mandal, S.C., Mandal, V. & Konishi, T. (ed.) *Natural Products and Drug Discovery*. Elsevier, Amsterdam, Netherland. pp. 29–56.
- Worley, B. & Powers, R. (2013). Multivariate analysis in metabolomics. *Current Metabolomics*, 1(1), 92–107.
- Wu, C., Choi, Y. H. & Van Wezel, G. P. (2016). Metabolic profiling as a tool for prioritizing antimicrobial compounds. *Journal of Industrial Microbiology & Biotechnology*, 43(2–3), 299–312.

- Wu, J. -F. & Wang, Y. (2015). 'Multivariate Analysis of Metabolomics Data.' 'in' Qi, X., Chen, X. & Wang, Y. (ed.) *Plant Metabolomics*. Springer. Berlin, Germany. pp. 105–122.
- Yoshida, T., Ito, H., Hatano, T., Kurata, M., Nakanishi, T., Inada, A., Murata, H., Inatomi, Y., Matsuura, N., Ono, K., Nakane, H., Noda, M., Lang, F. A. & Murata, J. (1996). New hydrolyzable tannins, shephagenins A and B, from *Shepherdia argentea* as HIV-1 reverse transcriptase inhibitors. *Chemical and Pharmaceutical Bulletin*, 44(8), 1436–1439.
- Zacharias, H., Altenbuchinger, M. & Gronwald, W. (2018). Statistical analysis of NMR metabolic fingerprints: established methods and recent advances. *Metabolites*, 8(3), 47.

Chapter 3



*“Research is to see what everybody
else has seen, and to think what
nobody else has thought.”*

Albert Szent-Gyorgyi

NMR-based metabolomic analysis and anti-HIV activity of selected *Helichrysum* species

3.1 Introduction

Since the first discovery of HIV/AIDS in 1981, more than 25 million people have been killed worldwide and it is one of the major threats to human health today. The AIDS syndrome is responsible for the dysfunction of the immune system, which leads to the immune system being targeted by opportunistic infections of bacteria, fungal, protozoan or viral aetiology. Based on the long history of the usage of herbal extracts against the wide variety of ailments, medicinal plant extracts/compounds may play an enormous role and can probably be beneficial in the treatment of HIV/AIDS. Some of these species could be effective due to the inhibition of HIV replication, or by boosting the immune system or even inhibiting several other opportunistic infections. However, there is still limited data available on the potential of therapeutic effects of South African medicinal plants against HIV infections (Bessong *et al.*, 2005; Mukhtar *et al.*, 2008; Salehi *et al.*, 2018). Medicinal plants with promising anti-HIV properties and low toxicity were reported by Kurapati *et al.* (2016). Most of the currently licensed antiviral drugs are of synthetic origin or synthetic analogues of natural products (Kapoor *et al.*, 2017). Medicinal plants have shown inhibitory effects on viral proteases, enzymes essential for proteolytic processing of the polyprotein precursor into proteins for the assembly of viral particles (Jassim & Naji, 2003; Kapoor *et al.*, 2017).

Nuclear magnetic resonance spectroscopy (NMR), one of the major analytical platforms utilized in the metabolomic field, has contributed very significantly to show the potential of this technique. Numerous characteristics of NMR make it an ideal chemical analysis tool, including its excellent reproducibility, highly quantitative nature and ability to identify unknown metabolites using intact bio-specimens compensating for its relatively low sensitivity. In addition, NMR offers some unique capabilities to reliably identify active metabolic pathways, measure metabolic fluxes and enzyme activity through tracing the flow of nuclei such as ^1H , ^{13}C and ^{15}N from labeled substrates as they are transformed into downstream metabolites (Gowda & Raftery, 2016).

Metabolomics is the comprehensive analysis of the biochemical content of cells, tissues or biofluids, usually from analysis of extracts. Typically, metabolomic experiments have utilised NMR and/or MS-based analytical techniques to explore the metabolite content of samples. Nuclear magnetic resonance spectroscopy-based metabolomic applications have exploited the unique strengths of NMR that are largely complementary to MS (Gowda & Raftery, 2016). Metabolomic interactions between phytochemical and biological activity systems play an important role in determining the efficacy and toxicity of chemo-preventive phytochemicals. NMR is a suitable tool to detect a broad range of extracted metabolites. An advanced data analysis tool to extract information from the high dimensional data set resulting from these analyses, is required (Heyman and Meyer, 2012). This method should be able to link the chemical profile of the plant extract to its bioactivity data using metabolomics combined with projection-based multivariate data analysis (Bailey *et al.*, 2002; Taketa *et al.*, 2008; Shang *et al.*, 2015).

The aim of the work described in this chapter was isolation and identification of the anti-HIV and anti-RT compounds from the *H. mimetes* extract using NMR-based metabolomic analysis.

3.2 Materials and methods

3.2.1 Plant collection and extraction

The aerial parts of 32 different *Helichrysum* species were collected from different geographical regions during spring and summer of 2014 and 2015. The samples of *Helichrysum* species were obtained from Kirstenbosch Botanical Garden (Cape Town, Western Cape), the Kalahari Thornveld (North West Province), Voortrekker Monument Nature Reserve (Pretoria, Gauteng), Pretoria Botanical Garden (Pretoria, Gauteng) and Buffelskloof Private Nature Reserve (Mpumalanga). Herbarium specimens were identified by Dr M. Koekemoer and Ms J.A. Reddy from the South African National Biodiversity Institute (SANBI) together with the personnel at the H.G.W.J. Schweickerdt Herbarium. A representative of each plant was collected, and herbarium voucher specimens were deposited in the H.G.W.J. Schweickerdt Herbarium (PRU) of the University of Pretoria, South Africa (Table 3.1). All plants were dried in the dark at room temperature in the basement of the Plant Sciences Complex at room temperature.

Table 3.1. Collected *Helichrysum* species, voucher numbers, GPS of locality, morphological groups (Hilliard, 1983) and the percentage yield (g extract/ g dry mass x 100) after extraction.

| Selected plants | PRU ^a Voucher no. | Locality GPS | Morphological Group | % Yield extraction | |
|--|------------------------------------|----------------------|------------------------|--------------------|-------|
| | | | | Non- polar | Polar |
| <i>H. acutatum</i> DC. | 121012 | 33°00'S, 18°00'E | 21 | 14.88 | 23.00 |
| <i>H. adenocarpum</i> DC. | 120986 | 26°00'S, 30°00'E | 28 | 8.85 | 19.25 |
| <i>H. albilanatum</i> Hilliard | 121022 | 25°00'S, 30°00'E | 30 | 3.67 | 17.63 |
| <i>H. argyrophyllum</i> DC. | 120814 | 25°00'S, 28°00'E | 29 | 6.91 | 19.80 |
| <i>H. athrixifolium</i> (Kuntze) Moeser | 121537 | 25°00'S, 30°00'E | 9 | 6.34 | 22.93 |
| <i>H. aureum</i> (Houtt.) Merr. | 121002 | 25°00'S, 30°00'E | 30 | 2.44 | 15.03 |
| <i>H. aureum</i> var. <i>monocephalum</i> (DC.) Hilliard | 121008 | 25°00'S, 28°00'E | 30 | 33.73 | 26.80 |
| <i>H. caespititium</i> (DC.) Harv. | 121538 | 25°00'S, 30°00'E | 12 | 18.17 | 8.11 |
| <i>H. callicomum</i> Harv. | 121005 | 25°00'S, 30°00'E | 2 | 12.60 | 16.95 |
| <i>H. cephaloideum</i> DC. | 121018 | 33°00'S, 18°00' E | 24 | 3.73 | 17.93 |
| <i>H. chrysargyrum</i> Moeser | 121004 | 25°00'S, 30°00'E | 22 | 7.08 | 14.51 |
| <i>H. dasyanthum</i> (Willd.) Sweet | 120813 | 23°56'S, 29°56'E | 10 | 5.35 | 21.54 |
| <i>H. gerberifolium</i> A.Rich. | 121003 | 25°00'S, 30°00'E | 23 | 3.24 | 19.51 |
| <i>H. harveyanum</i> Wild | 121547 | 25°00'S, 28°00'E | 23 | 2.72 | 8.93 |
| <i>H. kraussii</i> Sch.Bip | 121025 | 25°00'S, 30°00'E | 8 | 7.62 | 16.90 |
| <i>H. lepidissimum</i> S.Moore | 121009 | 25°00'S, 30°00'E | 19 | 6.62 | 21.72 |
| <i>H. mariepsopicum</i> Hilliard | 121013 | 25°00'S, 30°00'E | 29 | 3.62 | 15.67 |
| <i>H. milleri</i> Hilliard | 121015 | 25°00'S, 30°00'E | 30 | 8.90 | 27.58 |
| <i>H. mimetes</i> S.Moore | 121017 | 25°00'S, 30°00'E | 19 | 10.97 | 22.03 |

| Selected plants | PRU ^a Voucher no. | Locality GPS | Morphological Group | % Yield extraction | |
|--|------------------------------------|---------------------|------------------------|--------------------|-------|
| | | | | Non- polar | Polar |
| <i>H. mundtii</i> Harv. | 121014 | 25°00'S, 30°00'E | 23 | 6.47 | 27.80 |
| <i>H. mutabile</i> Hilliard | 121021 | 25°00'S, 30°00'E | 30 | 9.06 | 30.27 |
| <i>H. nudifolium</i> (L.) Less.var. <i>nudifolium</i> | 121010 | 33°55'S, 18°51'E | 23 | 4.38 | 22.10 |
| <i>H. opacum</i> Klatt | 121019 | 33°55'S, 18°51'E | 24 | 2.38 | 22.71 |
| <i>H. patulum</i> (L.) D.Don | 121536 | 25°00'S, 30°00'E | 18 | 2.64 | 18.92 |
| <i>H. petiolare</i> Hilliard & B.L.Burt | 121535 | 25°00'S, 30°00'E | 18 | 6.10 | 17.00 |
| <i>H. platypterum</i> DC. | 121011 | 25°00'S, 30°00'E | 20 | 3.05 | 32.76 |
| <i>H. polycladum</i> Klatt | 121016 | 25°00'S, 30°00'E | 8 | 12.90 | 20.23 |
| <i>H. reflexum</i> N.E.Br. | 121006 | 25°00'S, 30°00'E | 29 | 4.80 | 16.69 |
| <i>H. setosum</i> Harv. | 121539 | 25°00'S, 28°00'E | 30 | 8.82 | 17.50 |
| <i>H. truncatum</i> Burt Davy | 121020 | 25°00'S, 30°00'E | 13 | 2.38 | 9.36 |
| <i>H. wilmsii</i> Moeser | 121007 | 25°00'S, 30°00'E | 29 | 7.02 | 23.63 |
| <i>H. zeyheri</i> Less. | 121534 | 27°00'S, 23°00'E | 1 | 3.04 | 15.50 |

^a H.G.W.J. Schweikerdt Herbarium of the University of Pretoria

Dried material of all 32 species (5 g) were ground to small pieces but not to a fine powder. Different solvent systems with increasing polarity [hexane, dichloromethane (DCM), acetone (Ace), and methanol (MeOH): water (50:50)] were used for extractions (Table 3.2, Figure 3.1). Extraction of the collected plant material was done on a SpeedExtractor E-914/E-916 (Buchi, Switzerland) in 40 mL steel pressure vessels. Thereafter, the filtrate was concentrated under vacuum to dryness using a Genevac (EZ-2 Plus, GeneVac, UK). The hexane, dichloromethane and acetone extractions were combined and is referred to as the non-polar extract, while the methanol: water (50:50) extract was kept separately as the polar extract. The samples were stored at 4°C and used for the anti-HIV bioassays, RT inhibition and NMR analysis.

Table 3.2. Extraction parameters on Buchi SpeedExtractor for samples.

| Parameter | Value/Solvent |
|--------------------|---|
| Temperature | 50°C |
| Pressure | 100 bar |
| Solvents | Hexane, dichloromethane, acetone, [methanol: water (50:50)] |
| Cycles | 2 |
| Heat-up | 1 min |
| Hold | 15 min |
| Discharge | 5 min |
| Flush with solvent | 5 min |
| Flush with gas | 8 min |

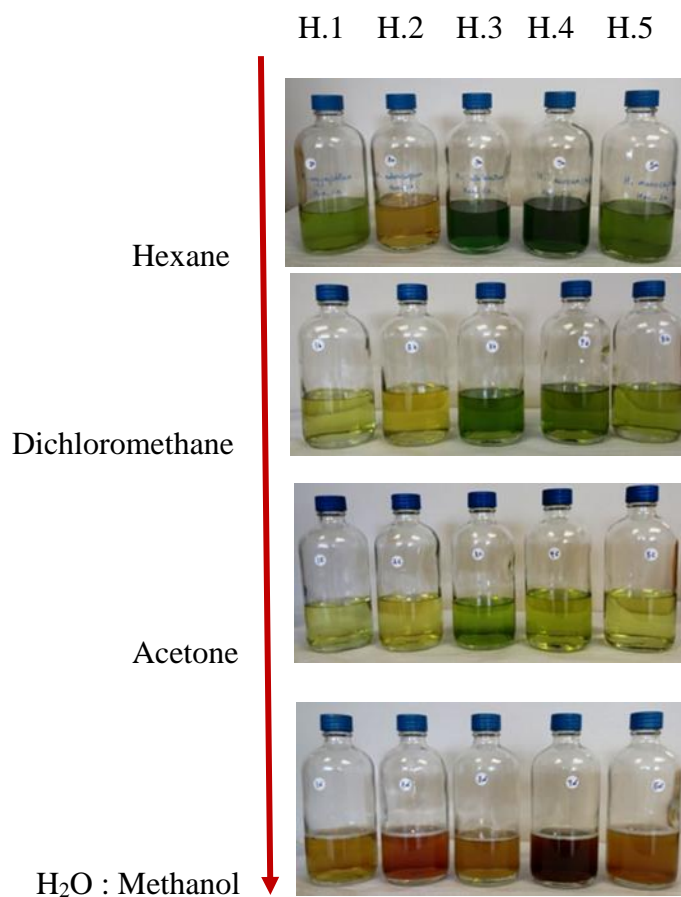


Figure 3.1. Examples of the five extracts of different *Helichrysum* (H) species using increasing polarities.

3.3 Antiviral bioassays

3.3.1 Anti-HIV screening bioassay and cytotoxicity

All non-polar and polar extracts (64 in total) were screened in duplicate for anti-HIV activity using a colorimetric cell-based (HeLa-SXR5) assay at 2.5 µg/mL and 25 µm/mL concentrations as described previously (Heyman *et al.*, 2015). Extracts were prepared in cell culture medium with a final DMSO concentration of 5%. A positive drug control, Efavirens (a non-nucleotidic RT inhibitor, Sigma-Aldrich, St. Louis, USA) (5% DMSO, 1 – 300 nM) and negative control (PBS 5% DMSO) were included in the assay. The analysed inhibitory range in patients is comparable with the *in vitro* activity in this replicative system (Heyman *et al.*, 2015). The bioassay produces replication in a time window of 4 days with the Dual-Enhancement of Cell-Infection to Phenotype Resistance (deCIPhR) method as previously described (Vidal *et al.*, 2011). To investigate the toxicity of the plant extracts, cytotoxicity and cell morphology of the culture were investigated microscopically after 4 days. The screening bioassay was conducted by Mr Vincent Vidal at InPheno AG, Department of Biomedicine, University of Basel, Switzerland.

3.3.2 Anti-HIV deCIPhR assay

To determine the anti-viral properties of the selected *Helichrysum* extracts, they were screened in the deCIPhR system that is designed to detect any inhibitors of viral replication. The principle of the deCIPhR test is a proprietary assay system of InPheno AG, Switzerland. Two HIV laboratory strains differing by their tropism of co-receptor utilization for viral entry: pNL4-3 for CXCR4-usage and pNL-AD87 for CCR5-usage were used during the assessment. This system avoids the pitfalls of target-based research that is very narrow and often misses the most interesting activities. The system uses a fully replicative virus and hence can assess the activity of any antiretroviral substance acting at a specific step/target of the HIV life cycle and on a wide variety of cellular factors. The pro-viral DNA pNL4-3 was obtained from the AIDS reagent center (Genbank accession number #AF324493). After transfection, pNL4-3 produces a full-length infectious virus often used as reference for a B-Subtype, CXCR4-tropic strain. The unique test format allows 3 to 5 rounds of viral replication and permits a dynamic parallel read-out of viral fitness and resistance

to the respective drugs under investigation. Diluted natural substances were tested in a 96 well format. After 4 days of culture, plates were fixed with formaldehyde 5%, glutaraldehyde 0.1% for 5 minutes at room temperature, rinsed twice with saline phosphate buffer and LacZ gene activity was measured via conversion of ortho-nitro-phenyl-galactopyranoside to ortho-nitro-phenol yielding a yellow color that was quantified by reading optical density at 405 nm. To investigate the toxicity of the plant extracts, cytotoxicity and cell morphology of the culture were investigated microscopically after 4 days.

3.3.3 HIV-1 reverse transcriptase colorimetric assay

Enzymatic RT inhibition of the active extracts was evaluated using a non-radioactive HIV-RT colorimetric ELISA kit (Roche, Germany) according to the method described by Fonteh's research group (Fonteh *et al.*, 2009). The extracts were tested at 50 µg/mL and 25 µg/mL. The recombinant HIV-1 RT (0.2 U) and extract were incubated for 1 h at 37°C. Subsequently, an antibody conjugated to peroxidase was added that binds to the digoxigenin-labeled DNA. In the final step, the 2,2'-azino-bis-(3-ethylbenzothiazoline-6-sulfonic acid) (ABTS substrate solution) is cleaved by the peroxidase enzyme, producing a colored reaction product. Doxorubicin, an anticancer drug and an inhibitor of viral RT was employed as a positive drug control at 50 µg/mL and 25 µg/mL. The experiment was conducted in duplicate. The plate was then incubated at room temperature (15–25°C) for a further 10–30 minutes. The absorbance of the samples was measured at 405 nm (reference wavelength: 492 nm) using a microtiter plate reader (Multiskan Ascent; Thermo Labsystems; USA) (Figure 3.2).

$$\% \text{ RT inhibition} = \frac{100 - A_{405\text{nm}} - A_{492\text{nm}} (\text{extract})}{A_{405\text{nm}} - A_{492\text{nm}} (\text{positive control})} \times 100$$

The active extracts were further tested using the above-mentioned method, at three different concentrations (200 µg/mL, 100 µg/mL and 50 µg/mL) to calculate the IC₅₀ value of selected extracts.

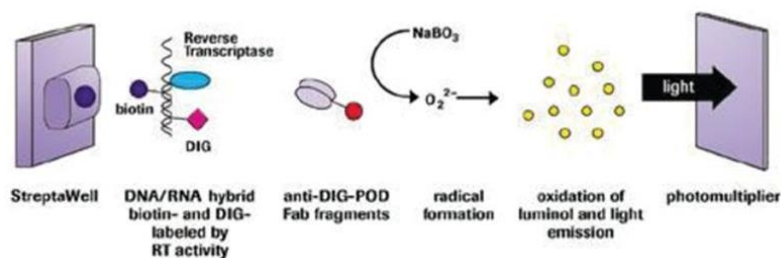


Figure 3.2. HIV-1 reverse transcriptase colorimetric assay principle.

(www.sigmaaldrich.com/catalog/product/roche/11468120910?lang=en®ion=ZA)

3.3.4 ^1H NMR analysis

A Varian 600 MHz spectrometer (Council for Scientific and Industrial Research, CSIR) was used for the NMR analysis of the samples (Figure 3.3).



Figure 3.3. Nuclear magnetic resonance Bruker 600 MHz spectrometer (Council for Scientific and Industrial Research, CSIR).

The non-polar fractions were re-dissolved to 15 mg/mL in CDCl_3 with 0.1% tetramethylsilane (TMS) as internal standard (0.00 ppm). The polar fractions were re-dissolved to 15 mg/mL in a

buffered mixture of CD₃OD and KH₂PO₄-D₂O solution, with the pH adjusted to pH 6.0 with NaOD (1M). The internal standard trimethylsilyl propionic acid-D₄ sodium salt (0.1% TSP- 0.00 ppm) was used for spectral referencing of the 50% methanolic samples. The samples (800 µl) were transferred to 5 mm NMR tubes and queued for analyses. For each spectrum, 64 scans were recorded with a spectral width of 14 ppm. Temperature was kept at 25°C constantly.

3.3.5 Multivariate data analysis

All ¹H NMR spectra were referenced, baseline corrected (Whittaker smoother) and normalised using MestReNova 12.0.1 (Mestrelab Research). Normalisation was done by scaling the spectral intensities to 0.1% of TMS (non-polar extracts) and 0.1% TSP (polar extract) and the region of 0.00–10.00 ppm was reduced to bins of 0.04 ppm in width. The region ranging from 3.28–3.36 ppm (residual MeOH) and 4.60–5.00 ppm (residual water) were removed prior to statistical analyses for the methanolic samples. The ¹H NMR spectra were reduced to ASCII files. The ASCII files generated were then imported into Microsoft Excel for secondary variable labelling after which the files were imported into SIMCA-P 13.0.0 (Umetrics, Umeå, Sweden). The data was Pareto scaled before being subjected to Principal Component Analysis (PCA) and Orthogonal Projections to Latent Structures-Discriminant Analysis (OPLS-DA).

3.4 Results and discussion

3.4.1 Anti-HIV screening bioassay and cytotoxicity

Anti-HIV screening of the 64 extracts of selected *Helichrysum* species showed that 15 (8 polar & 7 non-polar) of the extracts inhibited HIV in the cell-based assay to more than 80% at 25 µg/mL. The screening test of polar extracts at 2.5 µg/mL demonstrated that 17 polar extracts showed more than 80% inhibition against HIV (Table 3.3). There is a contradiction in comparing the activity of polar extracts at high and low concentrations. It is usually assumed that more extracts would be active at a high concentration than a low concentration. But the obtained results indicated that the cytotoxic effect strengthened with increasing concentrations of some of polar extracts. On the other

hand, if the plant extract, compound or drug was not active enough, then cell growth increased in the 12 hours to give values of more than 100% viability.

The non-polar extracts at 2.5 µg/mL had no activity against HIV. Between all active extracts, the extracts of *H. chrysargyrum*, *H. infusum*, *H. kraussii*, *H. mimetes*, *H. platypterum*, *H. setosum* and *H. zeyheri* either had activity at both 2.5 µg/mL and 25 µg/mL concentrations or they illustrated activity in both polar and non-polar extracts with no cytotoxicity, determined by microscopic observation.

Table 3.3. Anti-HIV screening result (% inhibition) of *Helichrysum* species. No activity against HIV was observed for any of the non-polar extracts at 2.5 µg/mL.

| Plant species | % Inhibition | | |
|---|--------------|-----------|-----------|
| | 25 µg/mL | 2.5 µg/mL | 25 µg/mL |
| | Polar | Polar | Non-polar |
| <i>H. acutatum</i> | CA | CA | CA |
| <i>H. adenocarpum</i> | 122 | NO | NO |
| <i>H. albilanatum</i> | CA | 85 | CA |
| <i>H. argyrophyllum</i> | CA | NO | CA |
| <i>H. athrixifolium</i> | CA | NA | CA |
| <i>H. aureum</i> var. <i>aureum</i> | CA | 95 | CA |
| <i>H. aureum</i> var. <i>monocephalum</i> | 126 | NO | CA |
| <i>H. caespitium</i> | 124 | NO | CA |
| <i>H. callicomum</i> | CA | NO | 108 |
| <i>H. cephalodeum</i> | 115 | NO | 108 |
| <i>H. chrysargyrum</i> | 120 | 103 | CA |
| <i>H. dasyanthum</i> | CA | 110 | CA |
| <i>H. gerberifolium</i> A.Rich. | CA | 92 | NO |
| <i>H. harveyanum</i> | CA | 107 | CA |

| Plant species | % Inhibition | | |
|---|--------------|-----------|-----------|
| | 25 µg/mL | 2.5 µg/mL | 25 µg/mL |
| | Polar | Polar | Non-polar |
| <i>H. kraussii</i> | CA | 97 | 125 |
| <i>H. lepidissimum</i> | CA | 108 | CA |
| <i>H. mariepsopicum</i> | 121 | NO | CA |
| <i>H. millerii</i> | 133 | NO | 129 |
| <i>H. mimetes</i> | 132 | 121 | CA |
| <i>H. mundti</i> | CA | NO | CA |
| <i>H. mutabile</i> | CA | 111 | CA |
| <i>H. nudifolium</i> var. <i>nudifolium</i> | 120 | NO | CA |
| <i>H. opacum</i> | CA | 100 | CA |
| <i>H. patulum</i> | CA | 114 | CA |
| <i>H. petiolare</i> | CA | NO | CA |
| <i>H. platypterum</i> | CA | 118 | 100 |
| <i>H. polycladum</i> | CA | NO | 95 |
| <i>H. reflexum</i> | CA | NO | CA |
| <i>H. setosum</i> | CA | 81 | 103 |
| <i>H. truncatum</i> | CA | 98 | CA |
| <i>H. wilmssii</i> | CA | 118 | CA |
| <i>H. zeyheri</i> | CA | 105 | 85 |

CA: Cytotoxic Activity observed, NA: No Activity, NO: Not Observable.

Positive control: Efavirenz 5% DMSO, testing range 1 – 300 nM - 100% inhibition.

Negative control: PBS/5% DMSO - 0% inhibition.

Previous studies have shown that *Helichrysum* species contain a large amount of phloroglucinol derivatives, which have shown promising antimicrobial activity for this type of compound. According to Viegas *et al.* (2014), flavonoids and phloroglucinols isolated from *H. italicum* has

inhibition activity against HSV and HIV, respectively. Most interesting though are the findings by Appendino *et al.* (2007) that arzanol (a phloroglucinol α -pyrone) inhibits HIV-1 replication in T-cells and inhibited NF- κ B ($IC_{50} = 5\mu\text{g/mL}$) indicating that this group of compounds may exhibit both antiviral and anti-inflammatory properties.

Aqueous extracts isolated from *H. aureonitens* exhibited antiviral activity against the Herpes simplex virus type I *in vitro* at a concentration of 1.35 mg/mL (Meyer *et al.*, 1996). The flavone, galangin, isolated from this plant also exhibited antiviral activity against Herpes simplex virus type I and the Cocksackie virus at concentrations of 6 $\mu\text{g/mL}$ (Meyer *et al.*, 1997).

The HSV-1 and genotoxic activities of the diethyl ether extract from flowering tops of *H. italicum* were previously investigated. The extract showed significant antiviral activity at concentrations ranging from 400 to 100 $\mu\text{g/mL}$. This activity was not due to the cytotoxic effect of the extract since Vero cells exhibited altered morphology or growth characteristics indicative of cytotoxic effects only at higher concentrations of 800 $\mu\text{g/mL}$. Furthermore, *H. italicum* extract showed no DNA-damaging activity at concentrations up to 2000 $\mu\text{g/disk}$ (Nostro *et al.*, 2003).

Both Herpes simplex (HSV) (DNA) and para-influenza-3 (PI-3) viruses (RNA) were used for the determination of antiviral activity of the water and ethanol extracts of *Helichrysum* species by using MDBK and Vero cell lines. Ethanoic extracts of *H. arenarium* and *H. armenium* ssp. *armenium* showed antiviral action against both HSV and PI-3 (Aslana *et al.*, 2006).

Heyman *et al.* (2015) reported that five of the 30 *Helichrysum* species selected for their study had significant anti-HIV activity ranging between 12 and 21 $\mu\text{g/mL}$ (IC_{50}) by using the same in-house developed DeCIPhR method on a full virus model. The most active extracts were the polar extracts of *H. populifolium* (12 $\mu\text{g/mL}$), *H. appendiculatum* (17 $\mu\text{g/mL}$), *H. cymosum* ssp. *clavum* (19 $\mu\text{g/mL}$), *H. oxyphyllum* (19 $\mu\text{g/mL}$) and *H. cymosum* ssp. *cymosum* (21 $\mu\text{g/mL}$). Little or no toxicity was also revealed for these active extracts (Heyman *et al.*, 2015).

No reports have been found of any antimicrobial activity of *H. chrysargyrum*, *H. infusum*, *H. platypterum*, *H. mimetes*, *H. setosum* and *H. zeyheri*.

Two lipophilic phytoalexins: α -amyrin and β -amyrin that have anti-tuberculosis- and generally antibacterial activity have been isolated from *H. kraussii* (Prinsloo & Meyer, 2006). According to Twilley *et al.* (2017), *H. kraussii* showed 100% viral inhibition for all the concentrations tested when the viral dose was 10TCID₅₀ (50% tissue culture infective dose) and therefore was also comparable to the positive control, acyclovir. At a viral dose of 100TCID₅₀, *H. kraussii* inhibited 100% of the virus at the highest concentrations tested (100 μ g/mL). The screening assay was conducted to determine the range of anti-HIV activity value of samples for further testing.

3.4.2 Anti-RT activity

Reverse transcriptase of HIV-1 has an important role for viral replication. The crucial role of RT in the early stages of the HIV-1 life cycle has made it one of the most reliable targets for potential anti-AIDS chemotherapy (Min *et al.*, 2000). The numbers of *Helichrysum* species that have previously been tested against the HIV-1 virus and reverse transcriptase enzyme are small (Appendino *et al.*, 2007). Of all the active polar extracts with $\geq 80\%$ inhibition against the live virus, *H. platypterum*, *H. mariepsopicum*, *H. cephaloideum*, *H. mimetes* and *H. caespititium* exhibited $> 50\%$ inhibition at 100 μ g/mL (Table 3.4). None of the non-polar extracts exhibited anti-RT activity. The positive control, doxorubicin, exhibited an IC₅₀ < 25 μ g/mL. The value of doxorubicin is comparable to the values obtained in a study of Kapewangolo and co-researchers (2013).

Table 3.4. Anti-HIV-RT inhibition of selected *Helichrysum* species polar extracts at 100 μ g/mL.

| <i>Helichrysum</i> species | RT % Inhibition \pm SD |
|-----------------------------|--------------------------|
| <i>H. platypterum</i> | 61.01 (\pm 7.4) |
| <i>H. mariepsopicum</i> | 59.55 (\pm 7.7) |
| <i>H. mimetes</i> | 55.93 (\pm 2.1) |
| <i>H. cephaloideum</i> | 55.32 (\pm 3.3) |
| <i>H. caespititium</i> | 52.79 (\pm 4.8) |
| Doxorubicin (50 μ g/mL) | 94.31 (\pm 2.6) |

Doxorubicin was isolated from the fungus *Streptomyces peucetius*. Doxorubicin is used to treat acute leukaemia, soft tissue and bone sarcomas, lung cancer, thyroid cancer and both Hodgkins and non-Hodgkins lymphomas (Dias *et al.*, 2012). There are very limited reports of anti-RT activity in the *Helichrysum* species. The results of this study demonstrate the potential for the inhibition of HIV-RT by some *Helichrysum* species. A study by Heyman (2009) revealed that *H. populifolium* has a significant cytopathic effect against HIV-RT at 200 µg/mL.

3.4.3 ¹H NMR analysis and metabolomic investigation

Proton NMR stacked spectra of the promising *Helichrysum* species extracts (*H. cephaloideum*, *H. chrysargyrum*, *H. kraussii*, *H. mimetes*, *H. platypterum*, *H. setosum* and *H. zeyheri*) showed significant similarities with the presence of aromatic compounds (6.00–8.00 ppm) and carbohydrate moieties (3.00–6.00 ppm) (Figure 3.4), characteristic signals of phenylpropanoids or chlorogenic acids. These compounds are a diverse family of organic compounds that are synthesized by plants from the amino acids, phenylalanine and tyrosine. Various bio-activities have been reported for these phytochemicals such as antiviral, anti-cancer and other biological effects (Miyamae *et al.*, 2011).

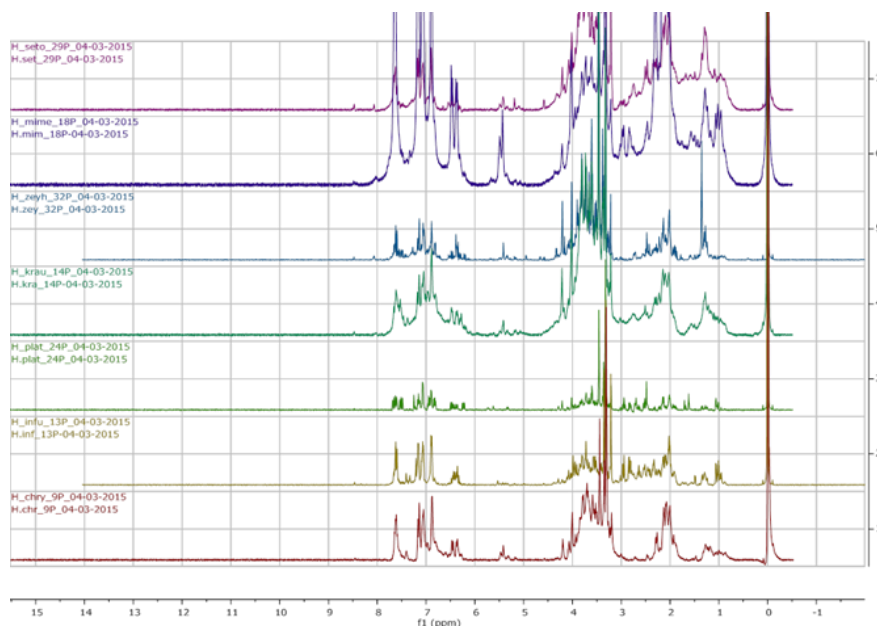


Figure 3.4. ¹H NMR stacked spectra of the most active polar *Helichrysum* species extracts.

All polar extracts were subjected to metabolomic analysis. To fast-track the selection of the best extract for active compound purification, metabolomic tools were used to aid it by investigating differences in the chemical profiles of the extracts of the 32 *Helichrysum* species using ^1H NMR spectroscopy. PCA was used to determine if the *Helichrysum* species with anti-HIV activity had similar compounds, which are not present in the non-active species. Since all samples belonged to the *Helichrysum* genus, it was predicted that not many different groups would be obtained in the PCA. The datasets used for the PCA score plots did not show distinct grouping correlating with the activity of the extracts but PC5, PC4 and PC2 demonstrated a separation of *H. mimetes* and *H. lepidissimum* from the rest of the species. The PC5 result was similar to PC2 and PC4 but *H. opacum* was observed as an outlier. This indicates that there is a marked phytochemical difference between this group and the rest of the samples. The PCA model with $R^2X= 0.80$ and $Q^2= 0.61$ values for component 5 indicated good predictability and reliability of the model (Figure 3.5).

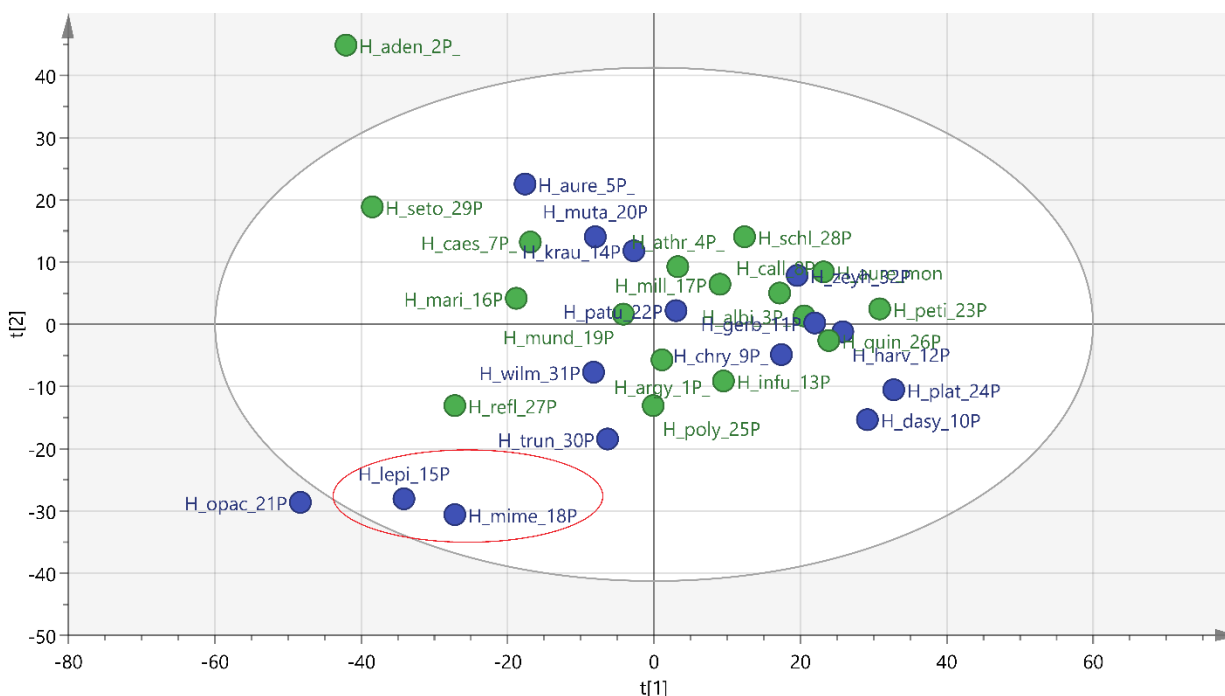


Figure 3.5. PCA score plot did not exhibit significant correlation between active and non-active *Helichrysum* polar extracts. R^2X : 0.80 and Q^2 (cum): 0.61. ● Active extracts, ● Extracts with no activity. The anti-HIV active extracts of *H. mimetes* and *H. lepidissimum* clustered closely together in all PC's.

In the OPLS-DA analysis, anti-HIV activity data was included as a secondary observation, which assisted in the correlation of the phytochemical composition and biological activity of the samples. The extent of grouping on similarity in chemical composition and bioactivity was good in this analysis (Figure 3.6). It explained the differences between the two groups on HIV activity quite well as indicated by the good $R^2Y=1.00$ value. The active *H. mimetes* and *H. lepidissimum* polar extracts clustered closely together and are well separated from the rest of the polar extracts (Figure 3.6). It indicates that, based on biological activity; there is a distinct phytochemical difference between these two extracts and the rest of the samples. The variation in X explains as much of the variation with the R^2X (cumulative) being 75%.

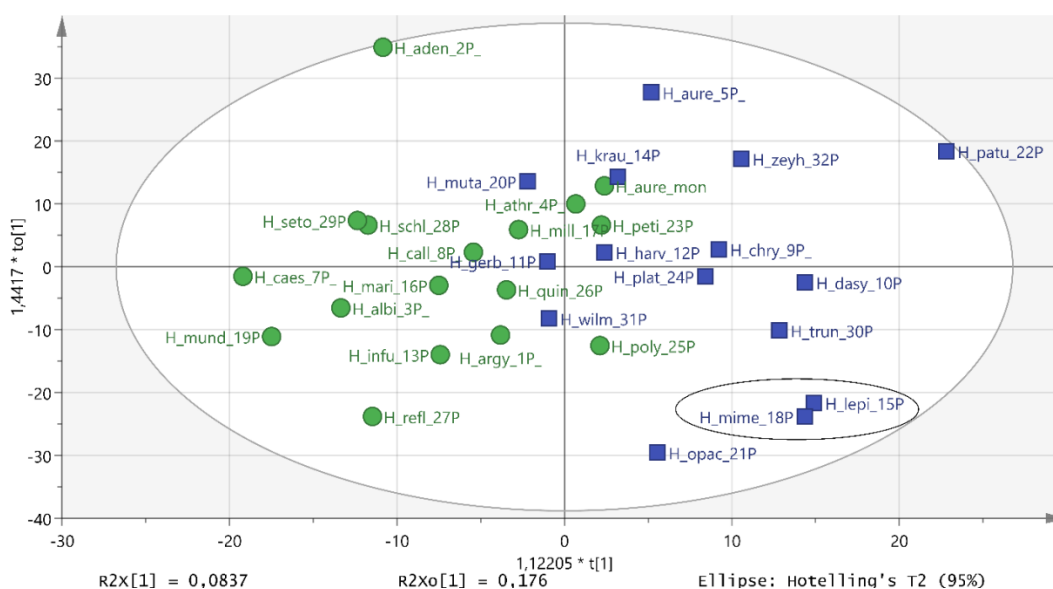


Figure 3.6. The OPLS-DA score plot exhibits separation of the active vs non-active *Helichrysum* polar extracts with some overlap in the center. ■ Active extracts, ● Non-active extracts. *H. mimetes* and *H. lepidissimum* polar extracts clustered closely together.

The predictive component (P1) only explained 4.6% of the variation in X related to the separation of the samples based on the activity. Based on the Q^2 of approximately 0.25, the predictability of the model was not significant. The obtained result was comparable to that of a study on other

Helichrysum species where they reported a Q^2 value of 0.3 (Heyman, 2013). However, the achieved R^2 value of the current study showed better fitness of the model.

A contribution plot (Figure 3.7) was generated based on the OPLS score plot of the loading plots of active and non-active groups of selected *Helichrysum* species. The generated profile could analyse the specific regions that may be related to the activity of the extract(s). The generated profile highlighted the phytochemical differences of the active extracts compared to the extracts that did not exhibit activity against HIV-1. The contribution plot indicated that the areas 2.00–2.32, 5.20–5.88, 6.2–7.16 and 7.68–7.80 ppm (bars above the line) may be responsible for the activity of the active *Helichrysum* species. It seemed that other types of compounds like sugar or amino acids did not play a major role in the activity of the *Helichrysum* species. However, it must be considered that the differences of the chemical shifts of the bars above the line (active extracts) and bars below the line (non-active extracts) could be related to the concentration of the compounds in the two groups of extracts and not a presence or absence of compounds.

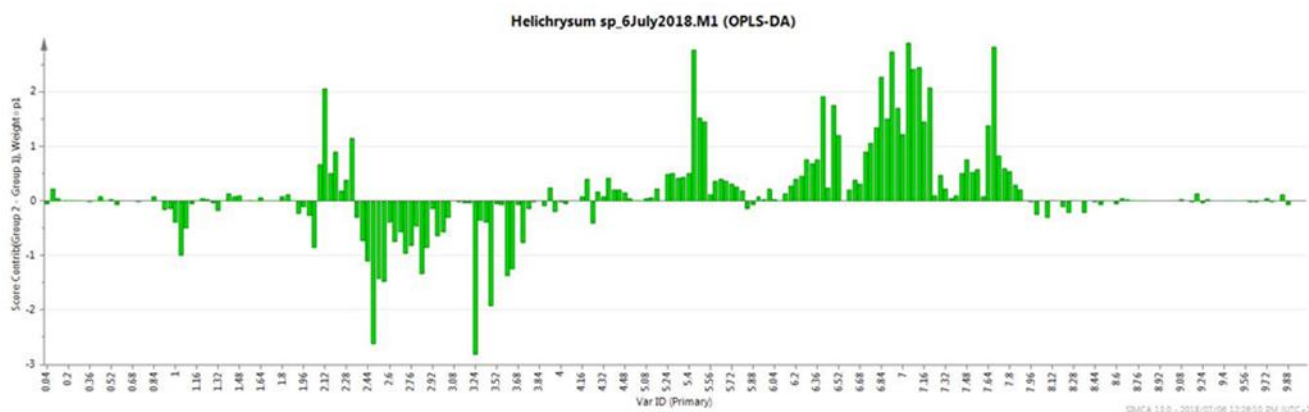


Figure 3.7. The contribution plot generated by comparing the active and non-active *Helichrysum* extracts. Bars above the line indicated the NMR regions that are positively associated with the activity of the active extracts.

Since all the tested plant extracts belong to the same genus and as the stacked ^1H NMR exhibited a similarity between all the active and non-active extracts, a concentration difference was more probable than a difference in chemical composition. All the NMR profiles of *H. cephaloideum*, *H.*

chrysargyrum, *H. kraussii*, *H. mimetes*, *H. platypterum*, *H. setosum* and *H. zeyheri* illustrated the characteristic signals of phenylpropanoids (chlorogenic acids).

3.5 Conclusion

Very little data is available on the HIV activity of *Helichrysum* species. The need for development of an effective and selective inhibitor of HIV-1 with a new mechanism of action remains. Comparing the present study with the previous research, there was better anti-RT activity of the *Helichrysum* species in this study. This can be attributed to various reasons such as the use of different solvent and extraction methods and maybe seasonal variation and geographical distribution.

In this study of the activity of *Helichrysum* species against the HI live virus, the polar extracts of *H. mimetes* and *H. chrysargyrum* (2.5 µg/mL), polar and non-polar extracts of *H. cephaloideum* (25 µg/mL) and polar and non-polar extracts of *H. zeyheri*, *H. setosum*, *H. platypterum* and *H. kraussii* at (2.5 µg/mL), had greater than 90% inhibitory activity.

The active polar and non-polar extracts were further tested on the HIV1-RT screening assay. *Helichrysum caespititium*, *H. cephaloideum*, *H. mariepsopicum*, *H. mimetes* and *H. platypterum* were the most active extracts against HIV1-RT enzyme with > 52% inhibition at 100 µg/mL. None of the active non-polar extracts showed inhibition against the RT enzyme.

The bioactivity data and the NMR data of all the *Helichrysum* species from the study was analysed using the SIMCA-P software to discriminate between the different species based on their bioactivity and chemical composition. The samples did not group well on the PCA, but had better separation using the OPLS-DA based on their activity and NMR spectral data. The contribution plot indicated regions which may be responsible for the difference between the species. Therefore, these regions can be investigated further as leads to identify the bioactive constituents.

Even though the PCA and OPLS analysis of the selected *Helichrysum* species did not show an ideal separation, it was still possible to use metabolomics to discriminate between samples based on their activity. In both the PCA and OPLS-DA score plots, *H. mimetes* and *H. lepidissimum* with

high activity against HIV-1 grouped together. This investigation shows that the metabolomic analysis could probably be used in future as a tool to identify active ingredients in medicinal plants and accelerate drug discovery. According to a literature review of biological activity of the tested *Helichrysum* species of this study, including their anti-HIV-1 and anti-RT, activity, *H. mimetes* had no report of its biological activity, and was thus selected for the purification of anti-HIV compound(s).

3.6 References

- Appendino, G., Ottino, M., Marquez, N., Bianchi, F., Giana, A., Ballero, M., Sterner, O., Fiebich, B. L. & Munoz, E. (2007). Arzanol, an anti-inflammatory and anti-HIV-1 phloroglucinol α -pyrone from *Helichrysum italicum* ssp. *microphyllum*. *Journal of Natural Products*, 70(4), 608–612.
- Aslana, M., Özçelik, B., Orhana, I., Karaoglu, T. & Sezika, E. (2006). Screening of antibacterial, antifungal and antiviral properties of the selected Turkish *Helichrysum* species. *Planta Medica*, 72(11), P_045.
- Bailey, N. J. C., Sampson, J., Hylands, P. J., Nicholson, J. K. & Holmes, E. (2002). Multi-component metabolic classification of commercial feverfew preparations via high-field ^1H -NMR spectroscopy and chemometrics. *Planta Medica*, 68(08), 734–738.
- Bessong, P. O., Obi, C. L., Andréola, M. -L., Rojas, L. B., Pouységu, L., Igumbor, E., Meyer, J. J. M., Quideau, S. & Litvak, S. (2005). Evaluation of selected South African medicinal plants for inhibitory properties against human immunodeficiency virus type 1 reverse transcriptase and integrase. *Journal of Ethnopharmacology*, 99(1), 83–91.
- Dias, D. A., Urban, S. & Roessner, U. (2012). A historical overview of natural products in drug discovery. *Metabolites*, 2(2), 303–336.
- Fonteh, P. N., Keter, F. K., Meyer, D., Guzei, I. A., & Darkwa, J. (2009). Tetra-chloro-(bis-(3, 5-dimethylpyrazolyl) methane) gold (III) chloride: An HIV-1 reverse transcriptase and protease inhibitor. *Journal of Inorganic Biochemistry*, 103(2), 190–194.
- Gowda, N. G. A. & Raftery, D. (2016). Recent advances in NMR-based metabolomics. *Analytical Chemistry*, 89(1), 490–510.
- Heyman, H. M. (2009). Metabolomic comparison of selected *Helichrysum* species to predict their antiviral properties. University of Pretoria (Master dissertation).
- Heyman, H. M. (2013). Identification of anti-HIV compounds in *Helichrysum* species (Asteraceae) by means of NMR-based metabolomic guided fractionation. University of Pretoria (Ph.D. thesis).

- Heyman, H. M. & Meyer, J. J. M. (2012). NMR-based metabolomics as a quality control tool for herbal products. *South African Journal of Botany*, 82, 21–32.
- Heyman, H. M., Senejoux, F., Seibert, I., Klimkait, T., Maharaj, V. J. & Meyer, J. J. M. (2015). Identification of anti-HIV active dicaffeoylquinic-and tricaffeoylquinic acids in *Helichrysum populifolium* by NMR-based metabolomic guided fractionation. *Fitoterapia*, 103, 155–164.
- Jassim, S. A. A. & Naji, M. A. (2003). Novel antiviral agents: a medicinal plant perspective. *Journal of Applied Microbiology*, 95(3), 412–427.
- Kapewangolo, P., Hussein, A. A. & Meyer, D. (2013). Inhibition of HIV-1 enzymes, antioxidant and anti-inflammatory activities of *Plectranthus barbatus*. *Journal of Ethnopharmacology*, 149(1), 184–190.
- Kapoor, R., Sharma, B. & Kanwar, S. S. (2017). Antiviral phytochemicals: an overview. *Biochemistry & Physiology*, 6(2), 7.
- Kurapati, K. R. V., Atluri, V. S., Samikkannu, T., Garcia, G. & Nair, M. P. N. (2016). Natural products as anti-HIV agents and role in HIV-associated neurocognitive disorders (HAND): a brief overview. *Frontiers in Microbiology*, 6, 1444.
- Meyer, J. J. M., Afolayan, A. J., Taylor, M. B. & Engelbrecht, L. (1996). Inhibition of herpes simplex virus type 1 by aqueous extracts from shoots of *Helichrysum aureonitens* (Asteraceae). *Journal of Ethnopharmacology*, 52(1), 41–43.
- Meyer, J. J. M., Afolayan, A. J., Taylor, M. B. & Erasmus, D. (1997). Antiviral activity of galangin isolated from the aerial parts of *Helichrysum aureonitens*. *Journal of Ethnopharmacology*, 56(2), 165–169.
- Min, B.-S., Nakamura, N., Miyashiro, H., Kim, Y. -H. & Hattori, M. (2000). Inhibition of human immunodeficiency virus type 1 reverse transcriptase and ribonuclease H activities by constituents of *Juglans mandshurica*. *Chemical and Pharmaceutical Bulletin*, 48(2), 194–200.

- Miyamae, Y., Kurisu, M., Han, J., Isoda, H. & Shigemori, H. (2011). Structure-activity relationship of caffeoylquinic acids on the accelerating activity on ATP production. *Chemical and Pharmaceutical Bulletin*, 59(4), 502–507.
- Mukhtar, M., Arshad, M., Ahmad, M., Pomerantz, R. J., Wigdahl, B. & Parveen, Z. (2008). Antiviral potentials of medicinal plants. *Virus Research*, 131(2), 111–120.
- Nostro, A., Cannatelli, M. A., Marino, A., Picerno, I., Pizzimenti, F. C., Scoglio, M. E. & Spataro, P. (2003). Evaluation of antiherpes virus-1 and genotoxic activities of *Helichrysum italicum* extract. *The New Microbiologica*, 26(1), 125–128.
- Prinsloo, G. & Meyer, J. J. M. (2006). *In vitro* production of phytoalexins by *Helichrysum kraussii*. *South African Journal of Botany*, 72(3), 482–483.
- Salehi, B., Kumar, N. V., Şener, B., Sharifi-Rad, M., Kiliç, M., Mahady, G., Vlasisavljevic, S., Iriti, M., Kobarfard, F., Setzer, W., Ayatollahi, S. A., Setzer, W., Ahtar, A. & Sharifi-Rad, J. (2018). Medicinal plants used in the treatment of human immunodeficiency virus. *International Journal of Molecular Sciences*, 19(5), 1459.
- Shang, N., Saleem, A., Musallam, L., Walshe-Roussel, B., Badawi, A., Cuerrier, A., Arnason, J. T. & Haddad, P. S. (2015). Novel approach to identify potential bioactive plant metabolites: pharmacological and metabolomics analyses of ethanol and hot water extracts of several Canadian medicinal plants of the Cree of Eeyou Istchee. *PLoS One*, 10(8), e0135721.
- Taketa, A. T. C., Pereda-Miranda, R., Choi, Y. H., Verpoorte, R. & Villarreal, M. L. (2008). Metabolomic profiling of the Mexican anxiolytic and sedative plant *Galphimia glauca* using nuclear magnetic resonance spectroscopy and multivariate data analysis. *Planta Medica*, 74, 1295–1301.
- Twilley, D., Langhansová, L., Palaniswamy, D. & Lall, N. (2017). Evaluation of traditionally used medicinal plants for anticancer, antioxidant, anti-inflammatory and anti-viral (HPV-1) activity. *South African Journal of Botany*, 112, 494–500.
- Vidal, V., Potterat, O., Louvel, S., Hamy, F., Mojarab, M., Sanglier, J. -J., Klimkait, T. & Hamburger, M. (2011). Library-based discovery and characterization of daphnane

diterpenes as potent and selective HIV inhibitors in *Daphne gnidium*. *Journal of Natural Products*, 75(3), 414–419.

Viegas, D. A., Palmeira-de-Oliveira, A., Salgueiro, L., Martinez-de-Oliveira, J. & Palmeira-de-Oliveira, R. (2014). *Helichrysum italicum*: from traditional use to scientific data. *Journal of Ethnopharmacology*, 151, 54–65.

Chapter 4

“A scientist in his laboratory is not only a technician: he is also a child placed before a natural phenomena which impress him like a fairy tale.”

Marie Curie

Isolation and identification of compound(s) from *Helichrysum mimetes* polar extract

4.1 Introduction

Plants used for traditional medicine contain a wide range of substances that can be used to treat various diseases (Duraipandiyan *et al.*, 2006; Yuan *et al.*, 2016). Since plant extracts usually occur as a combination of various types of bioactive compounds or phytochemicals with different polarities, their separation still remains a big challenge to achieve the characterization of the bioactive compounds. The major steps to utilize biologically active compounds from plant resources are extraction, pharmacological screening, isolation and characterization of bioactive compound, toxicological evaluation and clinical evaluation. It is common practice in isolation of bioactive compounds that a number of different separation techniques such as TLC, column chromatography, flash chromatography, Sephadex chromatography and high performance liquid chromatography (HPLC), are used to obtain pure compounds (Boligon & Athayde, 2014; De Souza *et al.*, 2018).

High performance liquid chromatography (HPLC) is a multipurpose analytical technique which is widely used for fingerprinting studies for the quality control of herbal plants (Fan *et al.*, 2006; Hua-Bin *et al.*, 2012). Natural products are frequently isolated following the evaluation of a crude extract or isolated compound(s) in a biological (e.g. antimicrobial) assay to fully characterize the active entity. The biologically active entity is often present only as a minor component in the extract and the resolving power of HPLC is ideally suited to the rapid processing of such multicomponent samples on both an analytical and preparative scale (Sasidharan *et al.*, 2011).

Nuclear magnetic resonance spectroscopy and mass spectrometry (MS) are the most popular analytical methods in metabolomics. NMR analysis gives rapid, high-throughput and automated analysis of crude extracts, and the quantitative detection of many different groups of metabolites. It also provides structural information with stereochemical details, though it is less sensitive than MS-based approaches. NMR data is good to comparing 'the tip of the iceberg', high concentration

compounds, while LC-MS also provides details of compounds present in lower concentrations (Commisso *et al.*, 2013).

The selection of the solvent system largely depends on the specific nature of the bioactive compound(s) being targeted. Different solvent systems are available to extract a bioactive compound from natural products. Based on the results described in the previous chapter of the 32 *Helichrysum* species, *H. mimetes* was subjected to isolation and identification of the active compounds.

4.2 Material and methods

4.2.1 Collection and extraction of *H. mimetes*

Fresh *H. mimetes* aerial parts were collected from the Buffelskloof Private Nature Reserve during November 2015 (Figure 4.1). Whole aerial plant parts were dried in the basement of the Plant Sciences Complex at room temperature in the dark. For the isolation and purification process, 30 g of air-dried *H. mimetes* aerial parts were subjected to a SpeedExtractor (Buchi, Switzerland) for extraction.



Figure 4.1. *H. mimetes* collected from Buffelskloof Private Nature Reserve.

Extraction cycles with different solvent systems were used with increasing polarity from hexane to MeOH:H₂O (50:50) to get the best separation of the polar components from the non-polar components (Table 4.1). The extract was concentrated to dryness using a freeze-drying process.

Table 4.1. Extraction parameters for *H. mimetes* extraction.

| Parameter | Value/Solvent |
|--------------------|--|
| Temperature | 50°C |
| Pressure | 100 bar |
| Solvents | Hexane, dichloromethane, acetone, methanol:water (50:50) |
| Cycles | 2 |
| Heat-up | 1 min |
| Hold | 15 min |
| Discharge | 5 min |
| Flush with solvent | 5 min |
| Flush with gas | 8 min |

The polar (MeOH:H₂O) extraction yield of *H. mimetes* was 8.33 g, which was used for an HIV bioassay, anti-RT analysis and NMR-based metabolomic analysis. The collected non-polar (Hex, DCM and Ace) extracts was stored separately in a freezer at -17°C (Figure 4.2).

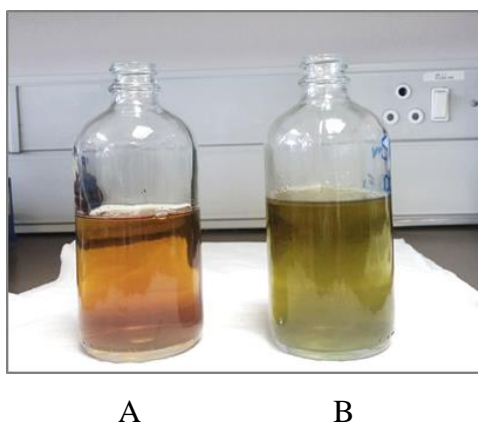


Figure 4.2. A) Polar *H. mimetes* extract, B) Non-polar *H. mimetes* extract.

4.2.2 Isolation and fractionation of *H. mimites*

Five grams of the total concentrated polar extract (8.33 g) was subjected to fractionation on a silica gel 60 column (500 mL, 6.5×10 cm) (Figure 4.3), using hexane: ethyl acetate mixtures of increasing polarity (0% to 100%) and ethyl acetate: MeOH mixtures also of increasing polarity to 100% MeOH. In total, 230 fractions were collected. The fractions with similar TLC profiles were combined to obtain 16 major fractions (Figure 4.3). TLC pre-coated plates with adsorbent silica gel 60, F254 of the 16 pooled fractions was developed with ethyl acetate (10): methanol (1.35): water (1) as eluent and then observed under UV-light (245 and 366 nm). After development, the TLC plates were also dipped in a vanillin solution (acidic vanillin: 0.34% vanillin in 3.5% sulphuric acid in ethanol) after which the plates were heated to detect compounds that did not absorb UV light and could therefore not be visualized. A 600 MHz NMR spectrometer (Council for Scientific and Industrial Research, CSIR, Pretoria) was used to elucidate the structure of the compounds in deuterated methanol solvent.



Figure 4.3. Silica gel column for separation of the concentrated *H. mimites* polar extract into fractions.

No compounds could be detected on the TLC plates sprayed with the vanillin solution. The presence of chlorogenic acid type compound(s) was however expected in the pooled fractions, and the TLC plates were subsequently sprayed with a natural products polyethylene glycol reagent (NP/PEG). To prepare the natural product polyethylene glycol reagent (NP/PEG), 2 g of diphenylborinic acid aminoethylester and 10 g of polyethylene glycol 400 were dissolved separately in 200 mL of ethyl acetate (Cretu *et al.*, 2013).

Based on the NMR spectral analyses and anti-HIV screening assay, fraction number 15 was identified for further investigation and subjected to a Sephadex LH-20 column chromatography using MeOH as eluent to isolate the active compound(s) (Figure 4.4).



Figure 4.4. Sephadex LH-20 column chromatography to purify fraction 15.

4.2.3 Anti-HIV screening and HIV-1 reverse transcriptase colorimetric assay of isolated fractions from *H. mimites*

The isolated fractions (1–16) were tested against the HI live virus and against RT enzyme to determine the active fraction(s) from which to purify the active compound(s). The procedures of both assays were described in Chapter 3, sections 3.3.2 and 3.3.3.

4.2.4 NMR-based metabolomics analysis of polar extracts

The NMR-based metabolomic analysis was conducted as described in Chapter 3, section 3.3.4. The ‘binned’ data of 16 fractions were exported to Excel and analysed using SIMCA-P 13.0.0 (Umetrics, Umeå, Sweden) statistical analysis software. The data was Pareto scaled before PCA and OPLS analysis.

4.2.5 Ultra performance liquid chromatography-tandem mass spectrometry (UPLC-MS/MS) analysis

LC-MS data was acquired on a Waters Acquity UPLC with a Waters Synapt G2 mass spectrometer. The UPLC was equipped with a Kinetex® 1.7 µm EVO C18, 2.1 mm × 100 mm column. The column temperature was set at 40°C. The flow rate was kept constant at 0.35 mL/min. The mobile phase consisted of: A) H₂O + 0.1% CH₂O₂ and B) MeOH + 0.1% CH₂O₂. A total run time of 10 min was used following a gradient elution method as follows: 0.0 min - 3% B; 4 min - 3% B; 6 min - 100% B; 8 min - 100% B; 9 min - 3% B; 10 min - 3% B. An injection volume of 5 µl was used. The mass spectrometer was operated in positive and negative ESI resolution mode. Nitrogen (N₂) gas was used as dissolution gas. MS data was acquired between 50 and 1200 m/z. The following parameters were used: capillary voltages were 2 600 V; sampling cone voltages as 30 V; extraction cone was 4 V; source temperature was 120°C; dissolution temperature was 300°C; dissolution gas 600 L/hr; Cone Gas flow 10.0 L/hr. Throughout all acquisitions, a 2 ng/µl solution of leucine enkephalin was used as the lock spray solution that was constantly infused at a rate of 3 µl/min through a separate orthogonal ESI probe so as to compensate for experimental drift in mass accuracy. The complete system was driven by Masslynx software.

4.2.6 Statistical analysis

All information and data were analysed statistically to quantify the value of the statistical analysis of both bioactivity and metabolomic analysis for a better understanding of the most active extract/compound. The IC_{50} of each extract was obtained using GraphPad Prism (GraphPad Software Inc. CA, USA). Data for RT inhibition were analysed for statistical significance and expressed as mean values \pm standard deviation (SD). $P < 0.05$ was considered statistically significant.

4.3 Results and discussion

4.3.1 Anti-HIV screening bioassay and cytotoxicity

All 16 isolated fractions and *H. mimetes* crude extract were screened against the HI live virus at two concentrations (2.5 μ g/mL and 25 μ g/mL). The obtained results are illustrated in Figure 4.5.

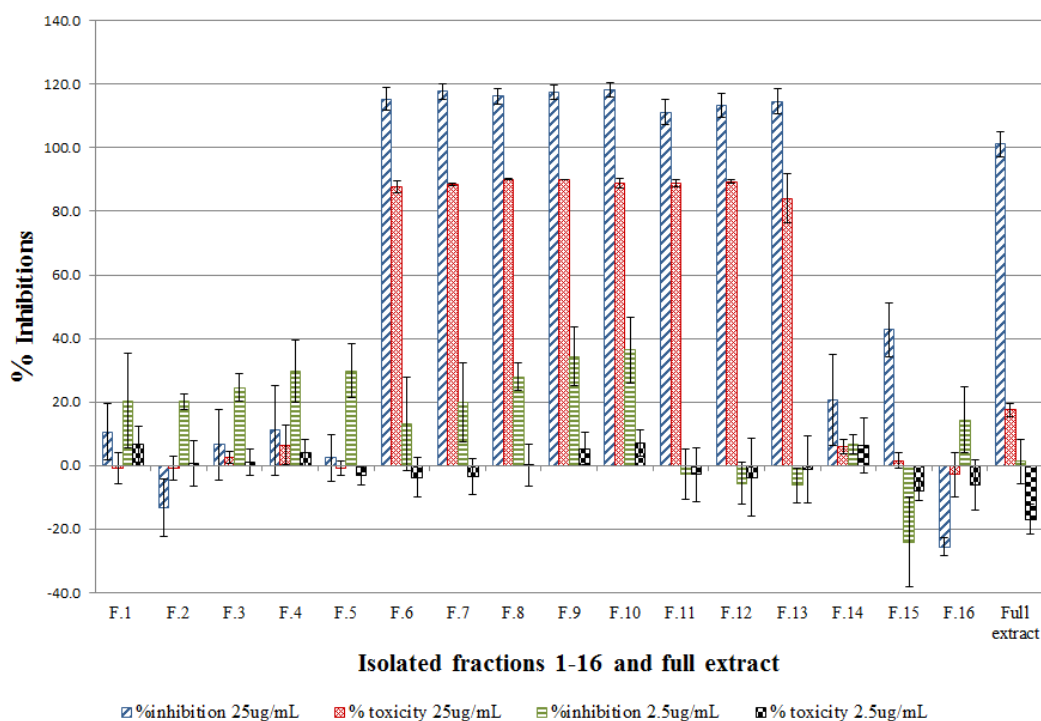


Figure 4.5. Activity and toxicity of 16 isolated fractions tested and *H. mimetes* crude extract against HI live virus at two concentrations (2.5 μ g/mL and 25 μ g/mL).

Fractions 1–5 had neither significant activity nor toxicity. Fractions 6–13 showed significant toxicity, which explained their “anti-HIV activity” at the same concentrations. Fractions 14 and 15 showed promising activity and relatively low toxicity. The crude extract illustrated significant inhibition with very low cytotoxicity at the highest concentration (25 $\mu\text{g/mL}$) which could represent synergistic interactions of the chemical entities of the extract. Little is known about the anti-HIV activity of the *Helichrysum* genus. There is no previous report on anti-HIV activity of *H. mimetes* extract.

4.3.2 HIV-1 reverse transcriptase colorimetric assay

Fractions (3–16) were subjected to a RT inhibition screening assay at two concentrations (25 $\mu\text{g/mL}$ and 50 $\mu\text{g/mL}$). This test was performed in duplicate. Fraction 14 had some activity and fraction 15 exhibited relatively good anti-RT activity especially at the higher concentration (50 $\mu\text{g/mL}$). Therefore, fractions 14 and 15 were re-tested against RT enzyme to calculate the IC_{50} values (Figure 4.6).

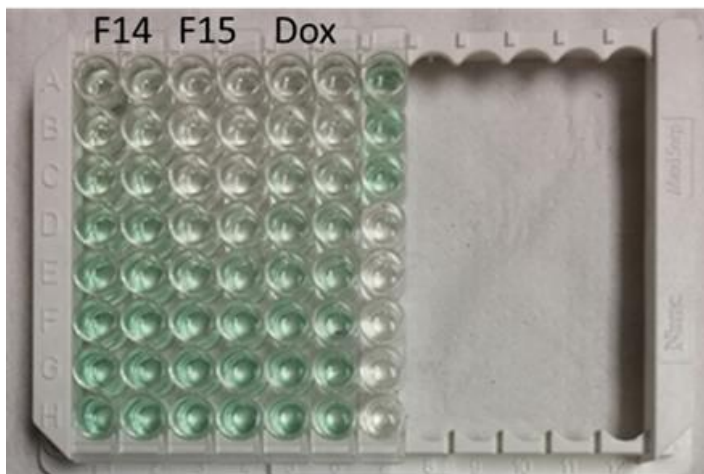


Figure 4.6. RT enzyme activity of fractions 14 and 15 to calculate the IC_{50} values.

Fraction 15 again exhibited good activity in the anti-RT assay with an IC_{50} value of 54.82 $\mu\text{g/mL}$, which is comparable to doxorubicin with an IC_{50} value of 40.31 $\mu\text{g/mL}$ (Table 4.2). The phases of the dose response curve of fraction 15 and doxorubicin are remarkably similar (Figure 4.7). Several studies illustrated general enzyme inhibition activity of *Helichrysum* species (Appendino *et al.*,

2007; Moll *et al.*, 2013; Malolo *et al.*, 2015). However, nothing was previously reported about anti-RT activity of *H. mimites* and the isolated components from this species.

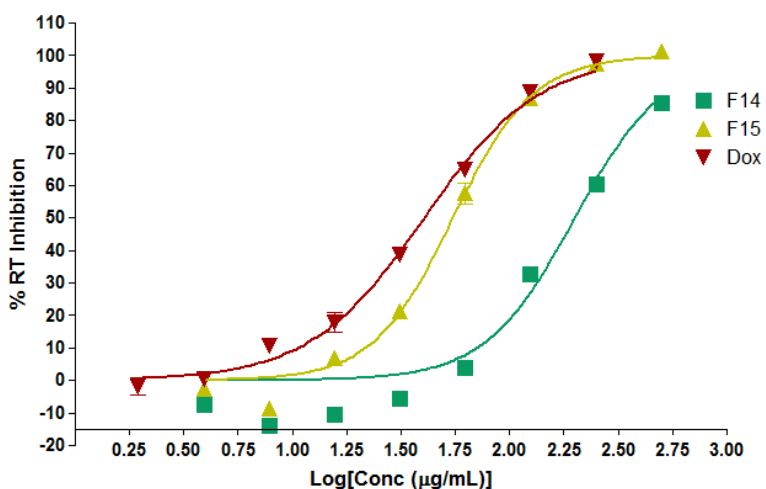


Figure 4.7. Inhibition of HIV-RT by F14 (green) & F15 (yellow) at different concentrations compared to the positive control doxorubicin (red).

Table 4.2. Screening assay result showing the IC₅₀ and % RT inhibition of the fractions and positive control doxorubicin.

| Sample | IC ₅₀ (µg/mL) ^a | % RT inhibition at 50 µg/mL |
|--------------------------|---------------------------------------|-----------------------------|
| F14 | 199.3 (± 8.4) | 23.89 (± 5.55) |
| F15 | 54.82 (± 4.2) | 65.62 (± 1.46) |
| Doxorubicin ^a | 40.31 (± 3.3) | 81.58 (± 11.6) |

^a Positive control

4.3.3 NMR-based metabolomic analysis and identification of most active fractions

One of the major types of compounds present in *Helichrysum* species are chlorogenic acids (Albayrak *et al.*, 2010). The ¹H NMR spectra of all fractions isolated in this study showed that the active compound(s) of fractions 6–13 could probably be caffeoylquinic acids. Comparing the

stacked NMR spectra of fractions 6–13 with a study conducted by Heyman *et al.* (2015) showed that all the chemical shifts linked to the caffeoylquinic acid type compounds existed in fractions 6 to 13 (Figure 4.8) (top 7 samples).

According to Heyman *et al.* (2015), NMR-based metabolomic analyses can reveal the specific chemical shift areas that could be linked to the presence of caffeoylquinic acids in samples. The NMR chemical shifts associated with caffeoylquinic acids were identified to be 2.56–3.08 ppm, 5.24–6.28 ppm, 6.44–7.04 ppm and 7.24–8.04 ppm.

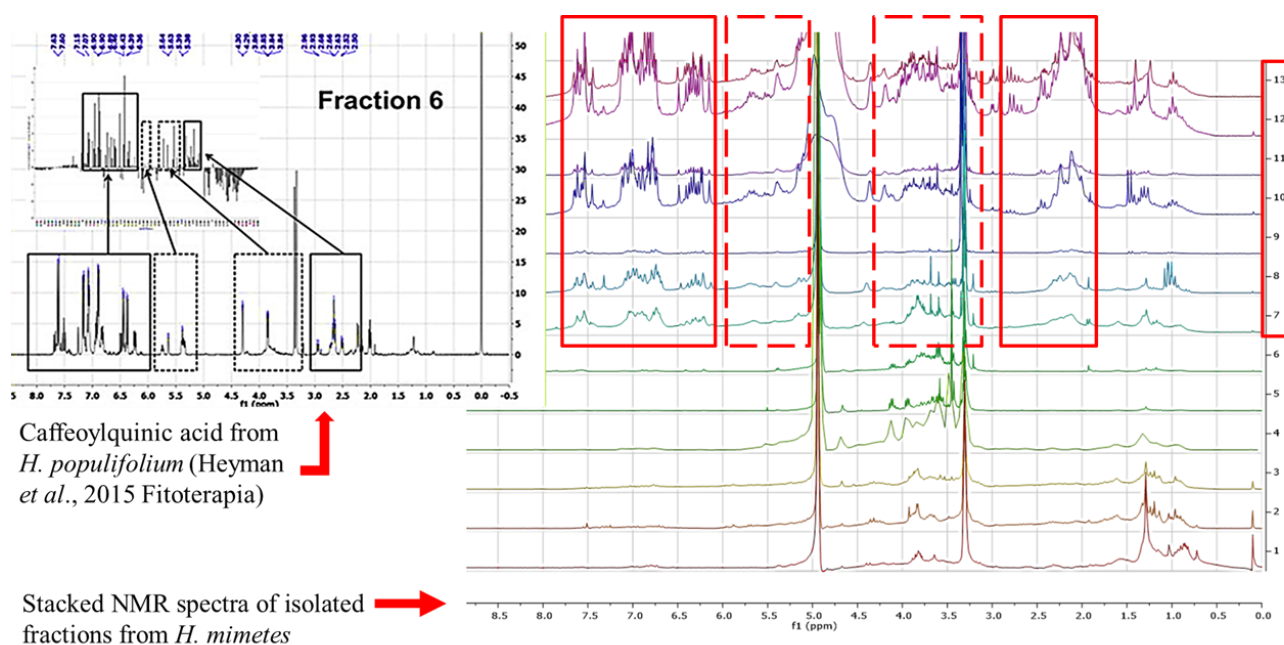


Figure 4.8. Comparison of the stacked NMR spectra of fractions (1-13) (right graph) with that of a study conducted by Heyman *et al.* (2015) (left graph). The chemical shifts linked to the caffeoylquinic acid type compounds were present in the isolated fractions (7-13 samples).

The ^1H NMR spectra of fractions 14 and 15 showed that the active component could not be caffeoylquinic acids due to the absence of the related chlorogenic acids chemical shifts (aromatic region) in these fractions. The anti-RT results therefore showed that the inhibition of fractions 14 and especially 15 was not because of the presence of chlorogenic acid types of compounds and that another type of compound(s) was probably responsible for their inhibitory effect.

PCA and OPLS-DA were employed to differentiate the isolated fractions based on their chemical profiles. The results of the PCA (Figure 4.9) showed good grouping based on the chemical shifts of the fractions with $R^2=0.953$ and $Q^2=0.778$. In the OPLS-DA the anti-RT activity data was included as a secondary observation. The active fraction 15 was separated from the rest of the fractions indicating a significant phytochemical difference with the others. Based on the Q^2 values in both PCA and OPLS-DA at 0.778 and 0.787, respectively, the predictability of the models was significant. It was therefore decided to purify fraction 15 by using a Sephadex LH-20 column.

The TLC analysis confirmed the presence/absence of caffeoylquinic acids in the fractions with the light blue/green fluorescent region in UV light at $\lambda=365$ nm of NP/PEG reagent on the TLC plates, indicating the presence of caffeoylquinic acids in fractions 6 to 13 and the *H. mimites* crude extract (Cretu *et al.*, 2013), however, there was no colour change in developed fractions 14 and 15 (Figure 4.10). None of the fractions also reacted with the vanillin reagent. A ^1H NMR analysis of the isolated sub-fractions showed that the chemical shifts of the purified compound present in fraction 15 and responsible for its anti-RT activity was quinic acid (QA). This was confirmed with comparison to an authentic standard sample of quinic acid (1,3,4,5-tetrahydroxycyclohexane carboxylic acid) (Figures 4.11, 4.12, 4.14 and 4.15).

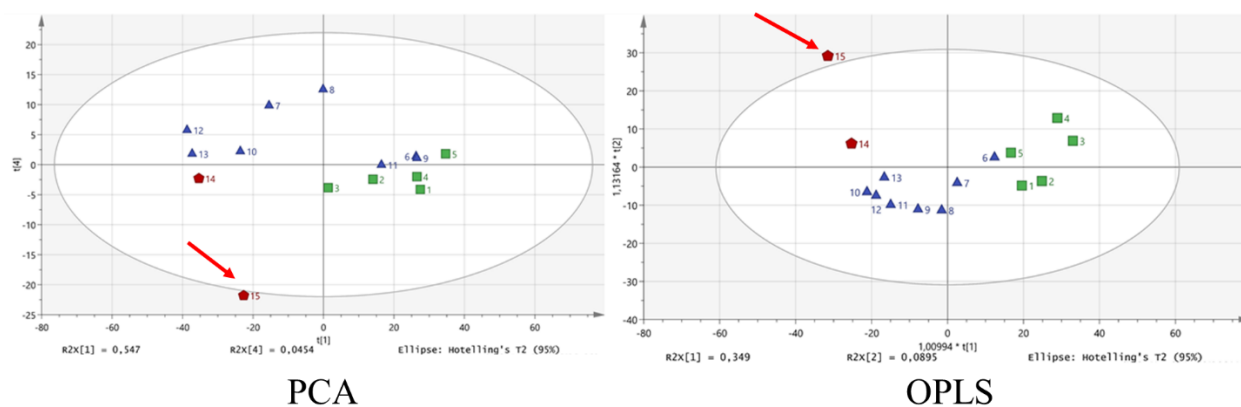


Figure 4.9. PCA ($R^2 = 0.953$ / $Q^2 = 0.778$) & OPLS-DA ($R^2 = 0.892$ / $Q^2 = 0.784$) score plots of isolated fractions. The active fraction 15 (red arrow) is separated from the rest of the fractions showing a phytochemical difference.

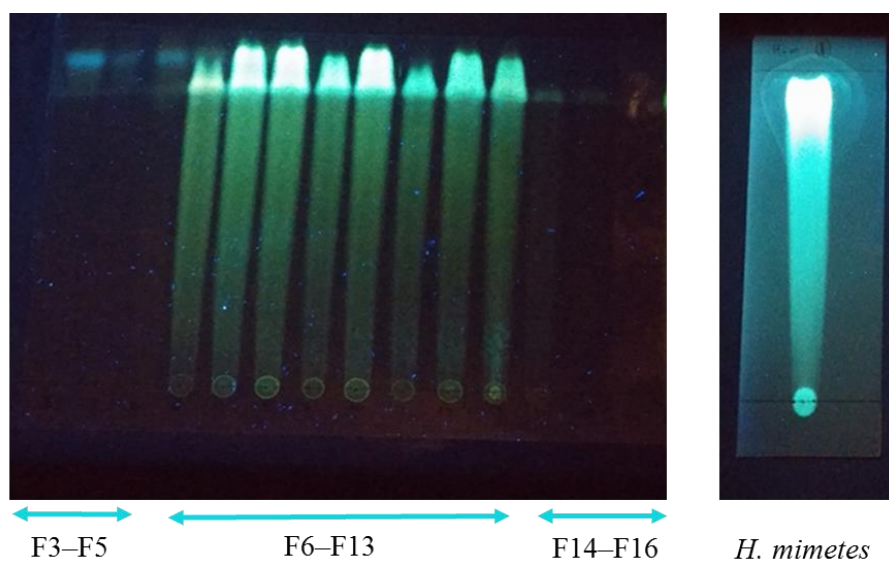


Figure 4.10. NP/PEG reagent showing the presence of caffeoylquinic acids in fractions 6–13 and the absence of chlorogenic acids in fractions 14–16 with the light blue/green fluorescent region in UV light at $\lambda = 365$ nm.

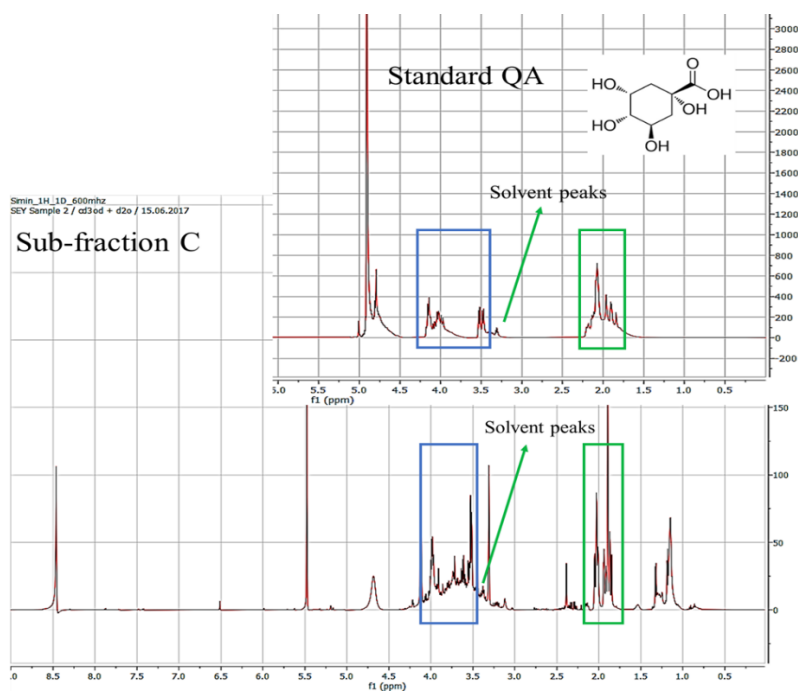


Figure 4.11. Comparison of the ¹H NMR spectrum of sub-fraction C (of fraction 15) with the ¹H NMR spectrum of standard quinic acid (QA) (Sigma-Aldrich). Coloured boxes indicate the relative chemical shifts of standard quinic acid and sub-fraction C peaks.

| ¹³ C | 1 | 2 | 3 | 4 | 5 | 6 | 7 |
|-----------------|--------|-------|-------|-------|-------|-------|------|
| Chemical shift | 184.16 | 79.75 | 77.95 | 73.13 | 69.73 | 43.43 | 40.1 |

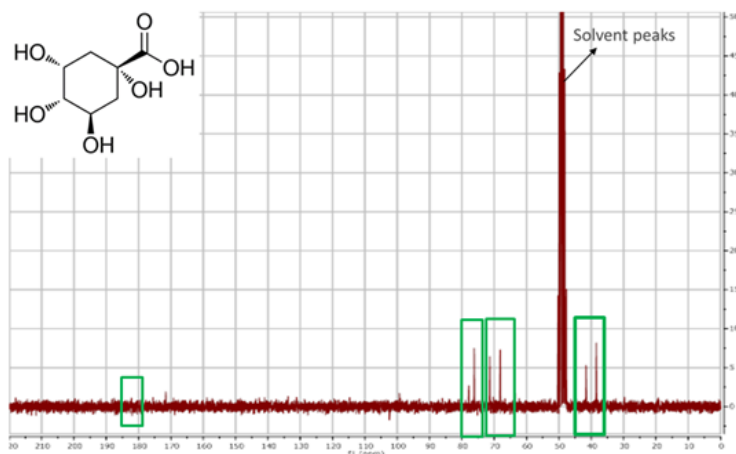


Figure 4.12. The ¹³C NMR spectrum of sub-fraction C. Green boxes indicate the chemical shifts of quinic acid carbons.

The phytochemical fingerprint of sub-fraction C isolated from the fraction 15 and standard quinic acid, were also compared using UPLC-MS to confirm the identity of the compound. The LC-MS chromatogram and mass spectrum in negative ionization mode is shown in Figures 4.14 and 4.16. A reverse phase C18 column was used with MeOH:H₂O as mobile phase and as expected, the sample eluted with 3% MeOH in less than 1 min because of the high polarity.

There was a polymeric contaminant that eluted with the quinic acid. It showed a loss of 68Da throughout in the positive and negative mode. Based on the chemical shifts and mass difference (68.2871) of the MS analysis, the polymeric contaminant was a sodium salt of formic acid (FA). Separation and collection of the quinic acid and the impurity component was not possible due to the close retention time (RT) of the two components and small quantity of the fraction.

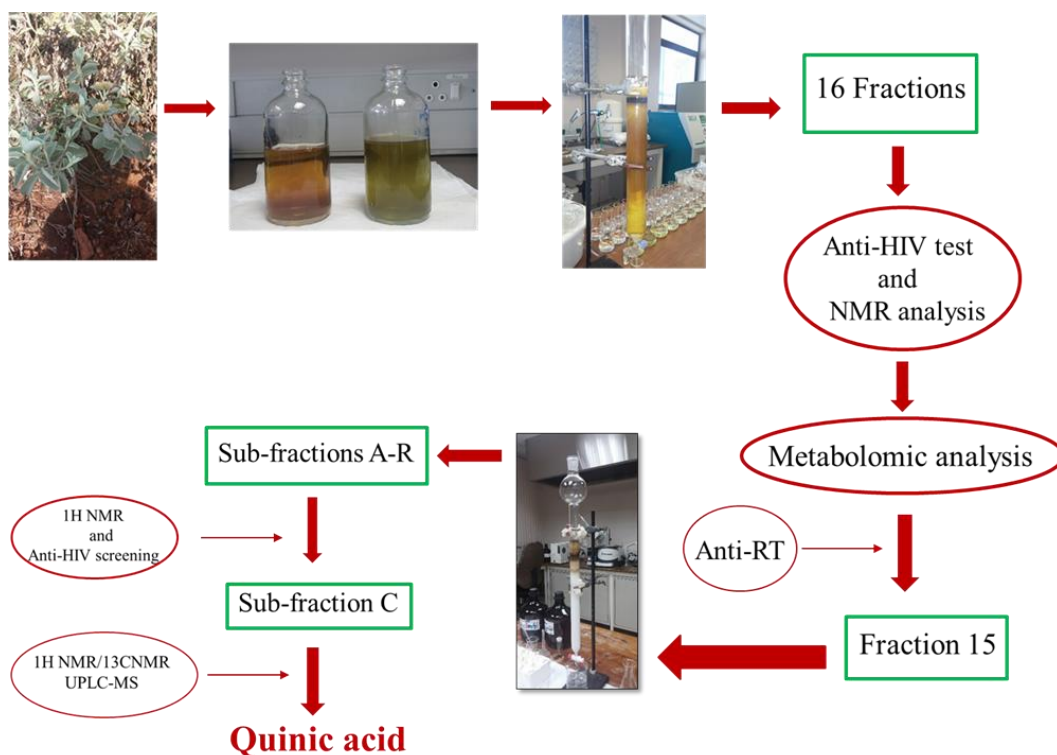


Figure 4.13. Diagram of quinic acid isolation from *H. mimetes*. First chromatography column: silica gel, eluent: hexane: ethyl acetate mixtures of increasing polarity (0% to 100%) and ethyl acetate: MeOH mixtures also of increasing polarity to 100% MeOH. Second chromatography column Sephadex LH-20, eluent: MeOH.

Figure 4.13 shows the process of isolation of quinic acid from *H. mimetes*. An elemental composition report of the ms analysis confirmed the presence of quinic acid in sub-fraction C with the mass of 191.0564 and molecular formula of $C_7H_{11}O_6$ (Figure 4.15 and 4.16). The mass spectrum of the contaminant was confirmed as a sodium salt of formic acid.

The presence of quinic acid identified by UPLC-MS/MS has been reported for the first time in *H. mimetes* and can explain the activity of *H. mimetes* against RT and HIV, although not at a significant level.

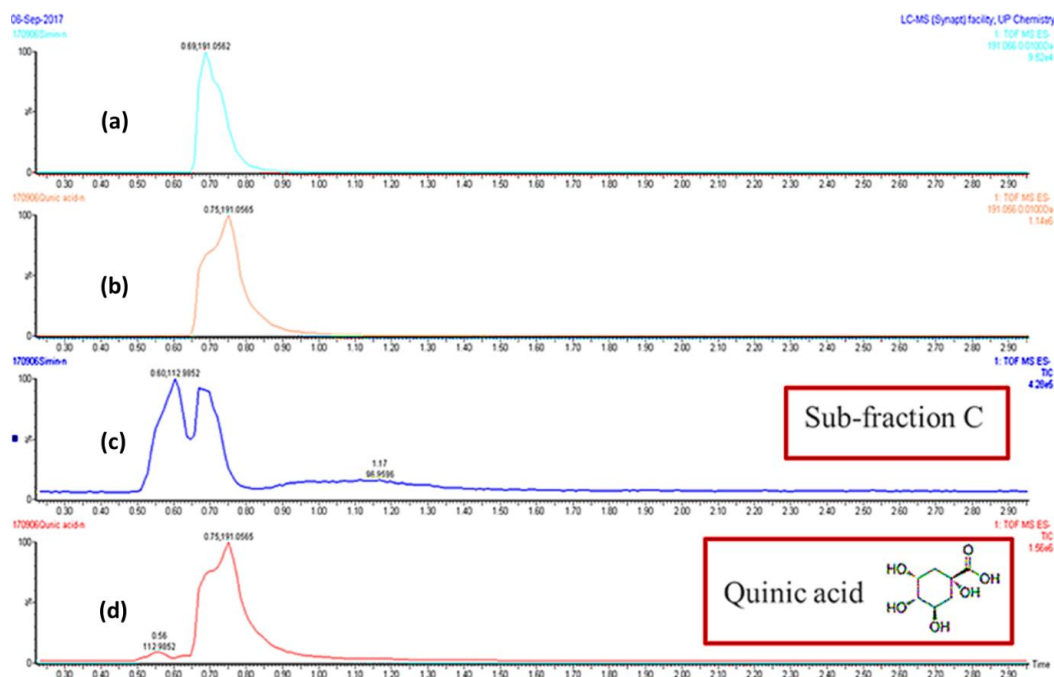


Figure 4.14. Chromatogram in negative mode of sub-fraction C and standard quinic acid (molecular weight: 192.167 g/mol). (a) 0.69; 191.0562, (b) 0.75; 112.9852, (c) 0.60; 112.9852/ 1.17; 96.9596 (d) 0.56; 112.9852/ 0.75; 191.0565

Single Mass Analysis

Tolerance = 3.0 mDa / DBE: min = -1.5, max = 50.0

Element prediction: Off

Number of isotope peaks used for i-FIT = 3

Monoisotopic Mass, Even Electron Ions

49 formula(e) evaluated with 1 results within limits (up to 50 best isotopic matches for each mass)

Elements Used:

C: 0-50 H: 0-100 O: 0-10 ²³Na: 0-1

Minimum: -1.5

Maximum: 3.0 5.0 50.0

| Mass | Calc. Mass | mDa | PPM | DBE | i-FIT | Norm | Conf(%) | Formula |
|----------|------------|-----|-----|-----|-------|------|---------|-----------|
| 191.0564 | 191.0556 | 0.8 | 4.2 | 2.5 | 67.4 | n/a | n/a | C7 H11 O6 |

Figure 4.15. Elemental composition report of isolated quinic acid.

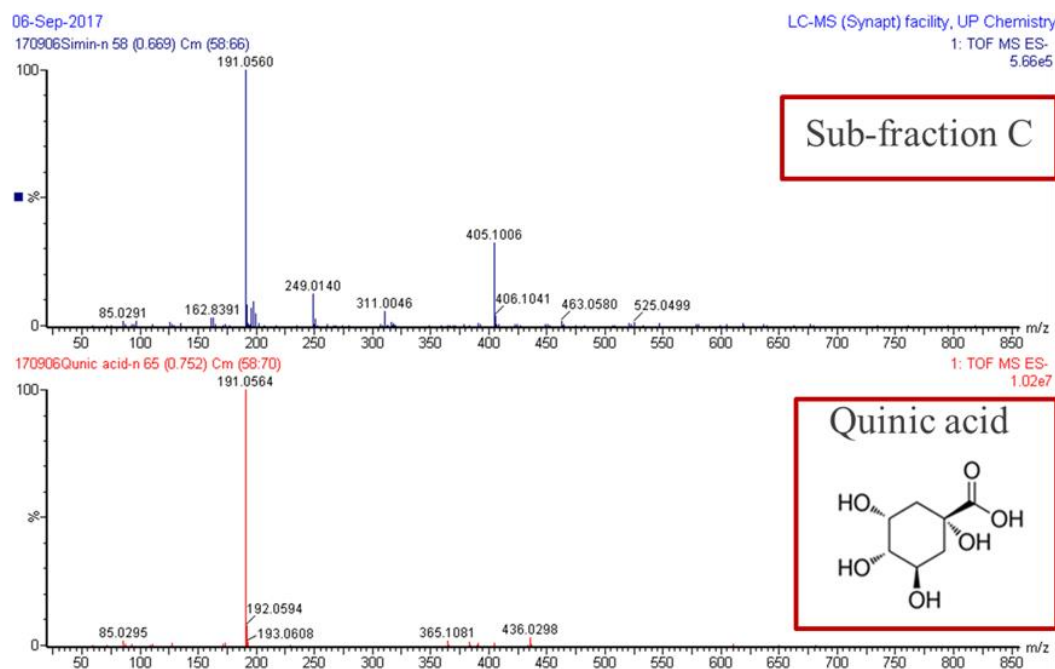


Figure 4.16. MS spectra in negative mode of sub-fraction C and standard quinic acid. The extra peak at 405.1006 is because two quinic acid molecules linked with a sodium molecule.

Isolated sub-fraction C, standard quinic acid, standard formic acid and mix of standard quinic acid and formic acid (50:50) were tested against HIV-1 to determine if the possible anti-HIV activity of the isolated sub-fraction C related to quinic acid or formic acid or both components. The anti-HIV-1 test showed that sub-fraction C had 40% inhibition at 200 $\mu\text{g/mL}$ and the standard of quinic acid also 40% at 200 $\mu\text{g/mL}$. The standard of FA did not exhibit any inhibition (Figure 4.17). Quinic acid did not show as much anti-HIV inhibition as the control, efavirens, but depending on how much quinic acid is present in an extract, significant inhibition might be observed. The antiviral activity of quinic acid derivatives (chlorogenic acids) was previously established but there is still a lack of information on the antiviral activity of quinic acid, especially on anti-HIV-1 activity.

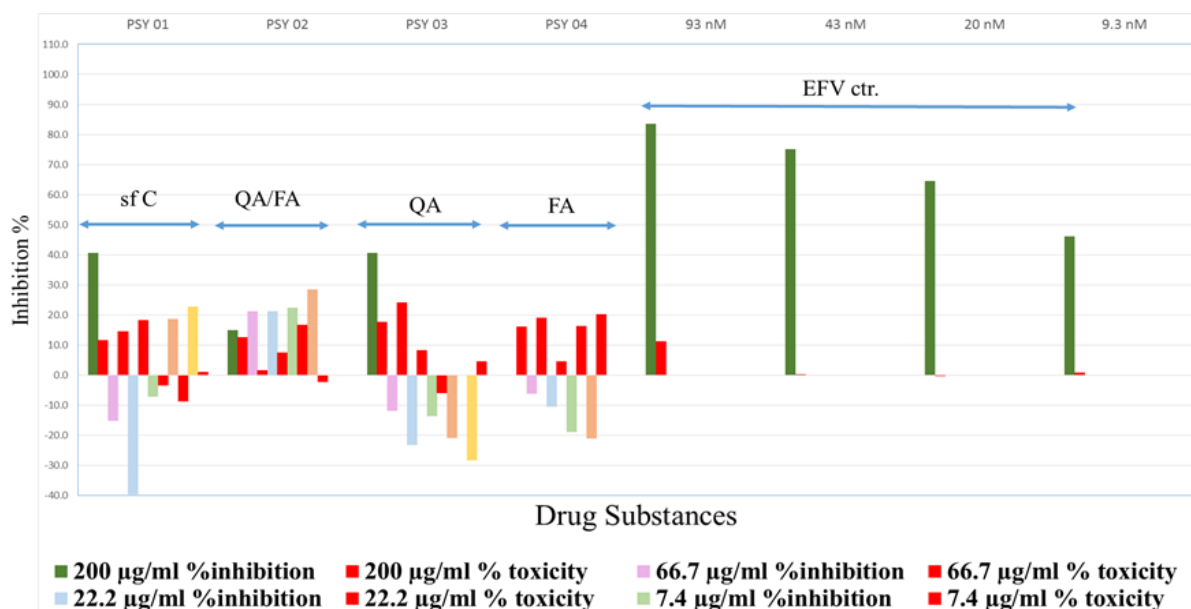


Figure 4.17. Screening isolated sub-fraction C and standards for HIV-1 (pNL-NF) inhibition in deCIPhR method. sf C: sub-fraction C, QA/FA: mixture of QA and FA, QA: quinic acid, FA: formic acid, EFV ctr.: Efavirens. Positive control: Efavirens (5% DMSO) 9.3 - 93 Nm 100% inhibition

Özçelik *et al.* (2011) tested the cytotoxicity, antiviral and antimicrobial activities of natural products consisting of alkaloids, flavonoids, and phenolic acids. Among the tested compounds, quinic acid had potent antiherpes type-1 activity in the therapeutic range of 0.05 to 0.80 µg/mL and also antiparainfluenza (type 3) activity with a therapeutic range of 0.4 to 1.6 µg/mL, without a cytotoxicity effect.

Wang *et al.* (2009) determined the antiviral activity of chlorogenic acid, caffeic acid and quinic acid against Hepatitis B Virus (HBV) using the HepG2.2.15 cell line and the DHBV-infected duckling model by using a crude coffee extract. In the cell model, all three compounds, chlorogenic acid, quinic acid and caffeic acid inhibited HBV-DNA replication as well as HBsAg production and therefore has anti-carcinogenic properties (Wang *et al.*, 2009).

An active ingredient of *Uncaria tomentosa* water extracts, called C-Med-100® inhibits cell growth without cell death thus providing enhanced opportunities for DNA repair, and therefore has a potential of immune stimulation, anti-inflammation and cancer prevention. The active ingredient

was determined to be quinic acid and shown to be bioactive also *in vivo*. C-Med 100® inhibits nuclear factor κ B (NF- κ B) activity and it was proposed that this activity leads at least partially, to the inhibition of proliferation (Åkesson *et al.*, 2003; Sheng *et al.*, 2005).

4.4 Conclusion

Since bioactive compounds occurring in plant material consist of multi-component mixtures, their separation and structure elucidation still creates problems. Practically most of them must be purified by the combination of several chromatographic techniques and various other purification methods to isolate bioactive compound(s) (Sasidharan *et al.*, 2011).

Although the antibacterial and antifungal activities of the *Helichrysum* species are well documented, their antiviral activity is still not well researched. Isolated compounds sometimes exhibit superior activity when compared to the crude extract, but often the crude extract has similar activity or less toxicity due to the synergistic effects (Lourens *et al.*, 2008).

In metabolomics, one of the objectives is often to identify differences in metabolite profiles between samples. Nuclear magnetic resonance-based metabolomics revealed that the correlation of the specific chemical shifts regions in some isolated active fractions against HIV-1 from *H. mimetes* were probably caffeoylquinic acids. However, the major activity was found in the samples without chlorogenic acid signals in this study. Interestingly fractions containing quinic acid isolated from *H. mimetes* showed promising anti-RT activity ($IC_{50}=53.82 \mu\text{g/mL}$) which is comparable to the positive drug control, doxorubicin ($IC_{50}=40.31 \mu\text{g/mL}$). The current study on *H. mimetes* is the first report on the activity of quinic acid isolated from it.

The antiviral activity of chlorogenic acid and its hydrolysates has been reported to be on a different target (HIV integrase) and little is mentioned about their activity against anti-RT. This study illustrated the potential of NMR-based metabolomics in discriminating classes of compounds that can be related to anti-HIV-1 and anti-RT activity. This study showed that with NMR-based metabolomics, it is possible to screen complex extracts to identify the active chemical's characteristics in such complex extracts. High-throughput methods such as UPLC-MS/MS

combined with metabolomic analysis for natural products chemistry can accelerate drug discovery from natural resources.

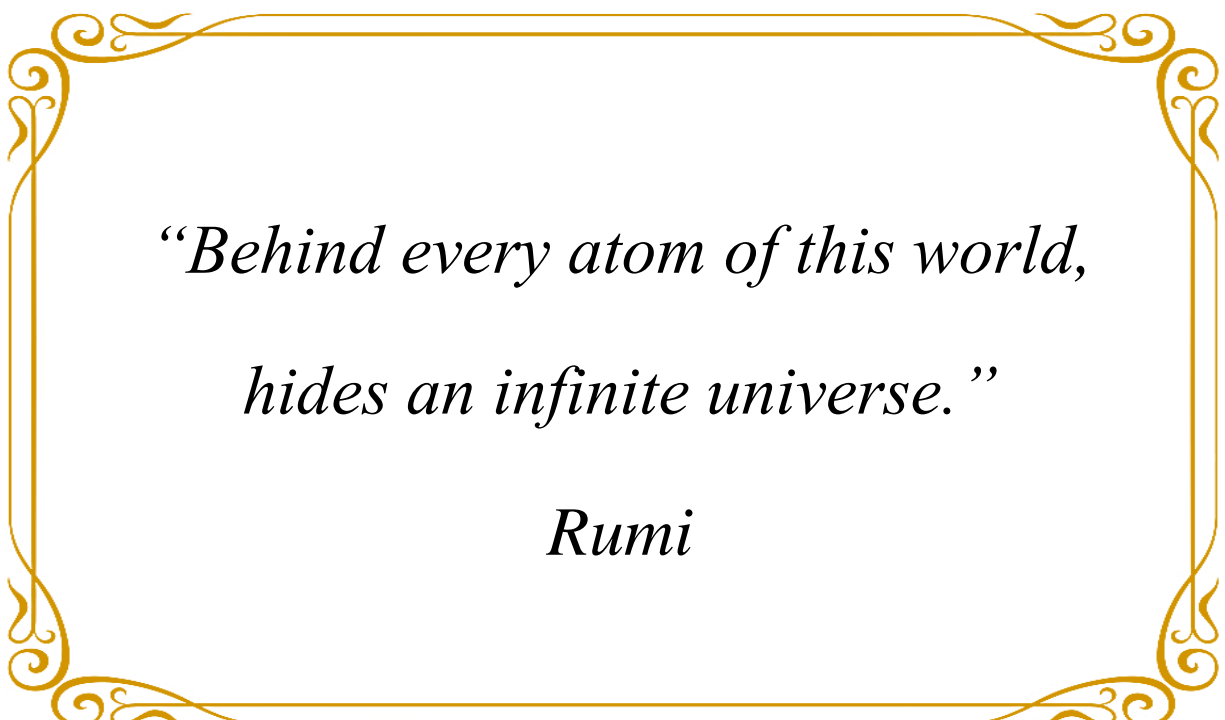
4.5 References

- Åkesson, C., Lindgren, H., Pero, R. W., Leanderson, T. & Ivars, F. (2003). An extract of *Uncaria tomentosa* inhibiting cell division and NF- κ B activity without inducing cell death. *International Immunopharmacology*, 3(13–14), 1889–1900.
- Albayrak, S., Aksoy, A., Sagdic, O. & Hamzaoglu, E. (2010). Compositions, antioxidant and antimicrobial activities of *Helichrysum* (Asteraceae) species collected from Turkey. *Food Chemistry*, 119(1), 114–122.
- Appendino, G., Ottino, M., Marquez, N., Bianchi, F., Giana, A., Ballero, M., Sterner, O., Fiebich, B. L. & Munoz, E. (2007). Arzanol, an anti-inflammatory and anti-HIV-1 phloroglucinol α -pyrone from *Helichrysum italicum* ssp. *microphyllum*. *Journal of Natural Products*, 70(4), 608–612.
- Boligon, A.A. & Athayde, M.L. (2014). Importance of HPLC in analysis of plants extracts. *Austin Chromatography*, 1(3), 2.
- Commisso, M., Strazzer, P., Toffali, K., Stocchero, M. & Guzzo, F. (2013). Untargeted metabolomics: an emerging approach to determine the composition of herbal products. *Computational and Structural Biotechnology Journal*, 4(5).
- Cretu, G., Morlock, G., Raluca, A. & Miron, A. C. N. (2013). A high-performance thin-layer chromatographic method for chlorogenic acid and hyperoside determination from berry extracts. *Romanian Biotechnological Letters*, 18(5), 8657.
- De Souza, J. A. L., Da Silva, W. A. V., Bezerra, I. C. F., Ferreira, M. R. A. & Soares, L. A. L. (2018). Chemical profiles by thin-layer chromatography and high-performance liquid chromatography of plant species from Northeast Brazil. *Pharmacognosy Magazine*, 14(56), 437.
- Duraipandiyan, V., Ayyanar, M. & Ignacimuthu, S. (2006). Antimicrobial activity of some ethnomedicinal plants used by Paliyar tribe from Tamil Nadu, India. *BMC Complementary and Alternative Medicine*, 6(1), 35.

- Fan, X. -H., Cheng, Y. -Y., Ye, Z. -L., Lin, R. -C. & Qian, Z. -Z. (2006). Multiple chromatographic fingerprinting and its application to the quality control of herbal medicines. *Analytica Chimica Acta*, 555(2), 217–224.
- Heyman, H. M., Senejoux, F., Seibert, I., Klimkait, T., Maharaj, V. J. & Meyer, J. J. M. (2015). Identification of anti-HIV active dicaffeoylquinic- and tricaffeoylquinic acids in *Helichrysum populifolium* by NMR-based metabolomic guided fractionation. *Fitoterapia*, 103, 155–164.
- Hua-Bin, Z., Ai-Qin, D., Xin-Ling, Z., Pei-Hai, W., Wei-Jie, L., Guo-Sheng, Y. & Aboul-Enein, H.Y. (2012). Quality control methodology and their application in analysis on HPLC fingerprint spectra of herbal medicines. *Chromatography Research International*, 2012, 1–13.
- Lourens, A. C. U., Viljoen, A. M. & Van Heerden, F. R. (2008). South African *Helichrysum* species: a review of the traditional uses, biological activity and phytochemistry. *Journal of Ethnopharmacology*, 119(3), 630–652.
- Malolo, F. -A. E., Nougä, A. B., Kakam, A., Franke, K., Ngah, L., Flausino, O. & Mpondo, E. M. (2015). Protease-inhibiting, molecular modeling and antimicrobial activities of extracts and constituents from *Helichrysum foetidum* and *Helichrysum mechowianum* (compositae). *Chemistry Central Journal*, 9(1), 32.
- Moll, A., Heyman, H. M. & Meyer, J. J. M. (2013). Plants with activity against the live HI virus and the enzyme, reverse transcriptase. *South African Journal of Botany*, 86, 148.
- Özçelik, B., Kartal, M. & Orhan, I. (2011). Cytotoxicity, antiviral and antimicrobial activities of alkaloids, flavonoids, and phenolic acids. *Pharmaceutical Biology*, 49(4), 396–402.
- Sasidharan, S., Chen, Y., Saravanan, D., Sundram, K. M. & Latha, L. Y. (2011). Extraction, isolation and characterization of bioactive compounds from plants' extracts. *African Journal of Traditional, Complementary and Alternative Medicines*, 8(1), 1-10.
- Sheng, Y., Åkesson, C., Holmgren, K., Bryngelsson, C., Giamapa, V. & Pero, R. W. (2005). An active ingredient of Cat's Claw water extracts: Identification and efficacy of quinic acid. *Journal of Ethnopharmacology*, 96(3), 577–584.

- Wang, G. -F., Shi, L. -P., Ren, Y. -D., Liu, Q. -F., Liu, H. -F., Zhang, R. -J., Li, Z., Zhu, F. H., He, P. L., Tang, W., Tao, P. Z., Li, C., Zhao, W. M. & Zuo, J. P. (2009). Anti-hepatitis B virus activity of chlorogenic acid, quinic acid and caffeic acid *in vivo* and *in vitro*. *Antiviral Research*, 83(2), 186–190.
- Yuan, H., Ma, Q., Ye, L. & Piao, G. (2016). The traditional medicine and modern medicine from natural products. *Molecules*, 21(5), 559.

Chapter 5



*“Behind every atom of this world,
hides an infinite universe.”*

Rumi

Molecular docking study of quinic acid isolated from *Helichrysum mimetes*

5.1 Introduction

Molecular docking could be described as a type of bioinformatics modelling used for structure-based drug design and discovery. In the 1980s the first algorithms of molecular docking were developed and became one of the essential tools in drug discovery (López-Vallejo *et al.*, 2011). It's an interesting platform that can explain drug-biomolecular interactions for drug design and discovery, as well as assist in mechanistic studies by placing a molecule (ligand) into the preferred binding site of the target specific region of the receptor (DNA/protein). It might show that it forms a stable complex of potential efficacy and more specificity. The results of a docking analysis predict the binding energy, free energy and stability of complexes (Dar & Mir, 2017).

The main aim of molecular docking is to evaluate the possible binding geometries of an identified ligand with a known target site. The binding geometries are often known as binding poses and include both the position of the ligand relative to the receptor and conformational state of the ligand and the receptor. The three basic tasks of any docking procedure are: (1) characterization of the binding site; (2) identifying of the position of the ligand into the binding site or orienting; and (3) evaluating the strength of interaction for a specific ligand-receptor complex that is called “scoring” (Seal *et al.*, 2011). The binding conformation for each ligand into identified cavities is determined, and the one having the lowest binding energy among the different conformations is generated. The lower energy scores represent better protein-ligand binding affinity as compared to higher energy values (Priya *et al.*, 2015).

In one of the first studies in the field, Debnath *et al.* (1999) conducted a systematic study to search for anti-HIV-1 lead compounds and targeted the HIV-1 envelope glycoprotein gp41 core structure. They used molecular docking techniques to screen a database of 20 000 organic molecules. They selected 16 compounds with the best fit for docking into a hydrophobic cavity within the gp41 core by searching for maximum possible interactions within the target site. These compounds were tested against HIV-1 by an enzyme-linked immunosorbent assay and two polysulfonic acid

compounds (ADS-J1 and ADS-J2) showed inhibitory activity at micromolar concentrations on the formation of the gp41 core structure and on HIV-1 infection. The best docked conformation energy of ADS-J1 was 13 kcal/mol higher than the CONCORD-generated docked conformation, confirming the validity of the conformer (a form of a compound having a particular molecular conformation) used for this study. The energy of the best-docked conformer from the systematic search of ADS-J2 was only 1.6 kcal/mol better than that corresponding to the docked conformer used in this study (Debnath *et al.*, 1999).

Seal *et al.* (2011) docked groups of phytochemicals such as curcumin, geraniin, gallotannin, tiliroside, kaempferol-3- *O*-glucoside and trachelogenin into five cavities of the HIV-RT (PDB ID: 1REV). All the potential active sites detected on HIV reverse transcriptase enzyme was subjected to the docking analysis. From the software's docking wizard, ligands were selected and the scoring function used was the MolDock score. These phytochemicals were found to be very effective according to their binding energy and ligand efficiency score and was considered as an effective anti-HIV-1 drug discovery tool by the authors. The best three scored phytochemicals belonged to geraniin (Cav.2, MolDock score: - 217.3), tiliroside (Cav.5, MolDock score: - 196.74) and tiliroside (Cav.1, MolDock score: - 183.39) (Seal *et al.*, 2011).

The molecular docking and molecular dynamics of 12 alkaloids from *Toddalia asiatica* against HIV were screened to find possible binding with the active site of the HIV-1-RT domain. The free energies of binding (ΔG) results suggested toddanol, toddanone and toddalenone to be potent inhibitors of HIV-1-RT. The molecular property prediction analysis revealed that toddanol and toddanone had the most rotatable bonds and a drug-likeness score of 0.23 and 0.11, respectively. This is comparable with the standard anti-HIV drug zidovudine, with a model score 0.28 (Priya *et al.*, 2015).

In a study conducted by Subbaih *et al.* (2017), antibacterial and molecular docking studies of a bioactive component, 3,4,4a,5,8,8a-hexahydro-6-methylisochromen-1-one (HMIC) from leaves of *Stachytarphete cayennensis* were examined to determine the orientation of inhibitors bound in the active site of GlcN-6-P synthase as target for antibacterial activity. The phytochemical constituent HMIC showed significant antibacterial activity against *Klebsiella pneumoniae* and *Pseudomonas aeruginosa* and it showed moderate activity on *Staphylococcus aureus*. It exhibited better

glucosamine-6-phosphate synthase inhibition in molecular docking studies with minimum docking and binding energy and better ligand efficiency when compared to the standard (Subbaiah *et al.*, 2017).

In this part of the current study the interactions of the isolated compound quinic acid (QA) from the *Helichrysum mimetes* polar extract with the active sites of HIV-RT, have been explored using SiteMap (Schrodinger LLC, New York, NY, 2018) to propose the efficiency of QA as an anti-HIV agent (Halgren, 2007; Halgren, 2009). The mechanism of action was determined by means of a HIV-1-RT reductase enzyme molecular docking experiment. This is the first report on an in-silico method to demonstrate the probable interactions of QA with HIV-1-RT.

5.2 Material and methods

5.2.1 Receptor and ligand preparation

The three-dimensional crystal structure of the target HIV-1 RT (PDB ID: 1RTH) was retrieved from the protein data bank and prepared using the protein preparation wizard in Maestro (Schrödinger suite v2017). Briefly, the structure was observed and preprocessed by the addition of hydrogens, bond order assignments and the removal of all crystallographic water molecules from the structure. H-bonds were optimized and the protonation states were predicted by using PROPKA at a pH of 7.0 and finally, the enzyme underwent a restraining minimization using the OPLS3 force field (Harder *et al.*, 2015).

The active phytochemical (QA) and the enzyme assay positive control (doxorubicin) was drawn on UCSF Chimera and imported into Maestro (Meng *et al.*, 2006). These two compounds together with U05 (co-crystal inhibition) (nevirapine derivative) were prepared and minimized using LigPrep (Figure 5.1). Epik was used to generate possible states at a pH of 7.0 and an OPLS3 force field was used for the minimization.



Figure 5.1. Three-dimensional structures of minimized ligands used in the docking study. From left to right quinic acid, doxorubicin and reference compound U05.

5.2.2 Active site prediction

A small region or cleft where the ligand can bind stably to the receptor protein is termed an active/catalytic site. Identification of this active site in the target protein structure has a great range of applications in molecular docking. Accurate identification of this catalytic binding site is difficult due to the constant conformational changes of the target protein (Jeffrey & Robert, 2007). The catalytic residue of protein 1RTH was examined with the help of a SiteMap (Schrödinger, LLC, New York, NY, 2018) which uses a simple Van der Waals probe and the interaction energy to locate energetically favorable binding sites (Halgren, 2007; Halgren, 2009). The five most favorable binding sites were identified (Figure 5.2).

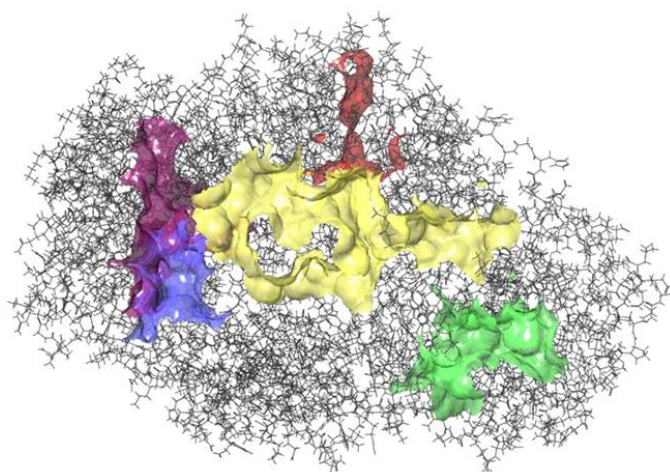


Figure 5.2. Structure of HIV reverse transcriptase (PDB: 1RTH) indicating the identified binding sites; cavity 1 (yellow), cavity 2 (purple), cavity 3 (green), cavity 4 (blue), cavity 5 (red).

5.2.3 Molecular docking using Glide XP

Docking was performed with the potential active sites detected on the HIV-1-RT enzyme using Glide software. Receptor grid files were prepared for each identified site using the receptor grid generation tool at a 6Å region around the center. Docking of the 3D structures of QA, doxorubicin and U05 in the active sites were performed using the XP function. All molecules were evaluated for possible molecular interactions with active site residues using the Pose viewer visualizer (Halgren *et al.*, 2004; Friesner *et al.*, 2006). The interaction of the protein-ligand complexes and their amino acid positions with bond distances were calculated and examined.

5.3 Results and discussion

A total of five cavities or receptor sites were detected in the RT enzyme by using SiteMap and were named cav1, cav2, cav3, cav4 and cav5 (Figure 5.2). The volume and surface area details are presented in Table 5.1. The 3D structure of HIV-1-RT was analysed, and QA was optimized to have minimal potential energy using Chimera. The catalytic site amino acid residues were identified for HIV-1-RT using SiteMap. Docking studies were performed on all sites. The catalytic site amino acids in domain A of HIV-1-RT are included in Table 5.1. These catalytic site residues were loaded as an input in Glide software, as a receptor grid file, to eliminate other amino acid residues and select only catalytic site amino acids of HIV-1-RT. Evaluation of binding mode and its stability of QA with HIV-1-RT were performed using Glide.

The binding conformation of QA into HIV-1-RT was determined, and the one having the lowest binding energy among the different conformations was generated. The result of this analysis has been compared to the protein reference (U05-nevirapine derivative) and doxorubicin. A lower energy or docking score represents a better prediction of protein-ligand binding affinity as opposed to higher energy values (Table 5.2).

The docking was performed successfully with all three ligands docking into the five sites, except for doxorubicin into site 2. Among the ligand-receptors, the co-crystalized reference ligand, U05 from the crystal structure, showed the lowest binding energy within cavity 4 (identical to the crystal structure), with a docking score of -9.55, this was followed by QA and doxorubicin with docking scores of -8.03 and -7.87, respectively in the same site (Figures 5.3, 5.4, 5.5).

Table 5.1. Possible binding site and cavity prediction of HIV-RT (PDB: 1RTH)

| Cavity | Volume (Å ³) | Size ^a | SiteScore ^b | Dscore ^c | Phobic ^d | Philic ^e | Residues ^f |
|--------------|-----------------------------|-------------------|------------------------|---------------------|---------------------|---------------------|--|
| Cav 1 | 1188.84 | 314 | 1.01 | 1.03 | 0.44 | 1.01 | Chain B: 29,30,33,36,37,40,41,62,63,64,65,6 6,67,68,70,71,72,73,74,75,107,108, 109,110,111,112,113,16,146,151,1 52,185,186,188,199,202,203,206,2 14,215,216,217,231,232,233,234,2 35,238,239,240,241,242,339,350,3 51,352,353,354,357,358,360,366,3 70,371,373,374,375,377,378,403,4 04,405,406,407,408,409,410,430,4 31,432,433 |
| Cav 2 | 607.45 | 280 | 1.06 | 1.07 | 0.71 | 1.05 | Chain A: 6,8,88,89,90,91,92,93,94,95,115,17 ,158,160,161,162,165,166,169,172, 173,175,176,178,179,180,181,182, 183,184; Chain B: 23,49,50,51,52,131,133,134,137, 138,139,140,141,142,143 |
| Cav 3 | 643.47 | 239 | 1.09 | 1.03 | 0.74 | 1.24 | Chain A: 363,364,365,400,401,403,404,405, 406,424,425,426,427,428,429,430, 431,503,506,507,508,509,511,532, 533,534,535; Chain B: 247,249,252,255,256,258,259,260, 262,263,330,331,332,333,334,392, 419,421,422,424,425,428,429 |
| Cav 4 | 394.45 | 194 | 1.15 | 1.20 | 2.13 | 0.73 | Chain A: 95,99,100,101,102,103,106,172, 179,180,181,182,188,189,190,227, 229,234,235,236,318,319,382,383; Chain B: 28,31,32,35,134,135,136,138,139, 140,142 |

| Cavity | Volume (Å) | Size ^a | SiteScore ^b | Dscore ^c | Phobic ^d | Philic ^e | Residues ^f |
|--------|---------------|-------------------|------------------------|---------------------|---------------------|---------------------|--|
| Cav 5 | 419.83 | 119 | 1.06 | 1.09 | 0.44 | 0.92 | Chain B: 74,75,76,77,78,81,82,86,87,93,94, 152,154,157,158,182,183,184,185, 324,325,385,386,387,388,409,410, 411,412,413 |

^aSize of the cavity given in number of site points, ^bSiteScore give an overall quality of the binding site ($\text{SiteScore} = 0.0733 \sqrt{n} + 0.6688 e^{-0.20 p}$), ^cdruggability score, ^dscore of hydrophobic characteristic, ^escore of hydrophilic characteristic, ^fresidue number involved in the cavity

Quinic acid had relatively low docking scores for two of the predicted binding sites, cavities 4 and 2, indicating a high affinity for these two sites. Figures 5.3 and 5.4 depict the binding prediction and conformation of QA and the reference ligand within cavity 4.

Table 5.2. Molecular docking results of quinic acid (QA), doxorubicin (Dox) and reference ligand U05 (Ref) within the five binding sites identified.

| Cav | Compounds | R bonds | XP GScore | glide evdw | glide ecoul | glide energy | glide einternal | glide emodel | XP HBond |
|-----|-----------|------------|--------------|---------------|----------------|-----------------|--------------------|-----------------|-------------|
| 1 | Dox | 7 | -8.62 | -54.35 | -4.71 | -59.06 | 5.61 | -79.34 | -1.46 |
| | QA | 6 | -7.87 | -21.94 | -9.65 | -31.59 | 1.20 | -36.50 | -4.59 |
| | Ref | 2 | -5.31 | -35.85 | -2.64 | -38.49 | 0.38 | -48.29 | -0.22 |
| 2 | QA | 6 | -8.69 | -27.48 | -7.93 | -35.41 | 3.24 | -42.85 | -4.67 |
| | Ref | 2 | -3.98 | -25.17 | 0.23 | -24.94 | 6.01 | -18.85 | -0.30 |
| | QA | 6 | -7.55 | -15.95 | -17.09 | -33.04 | 2.83 | -42.40 | -3.56 |
| 3 | Dox | 5 | -4.32 | -42.96 | -5.23 | -48.20 | 16.22 | -39.80 | -0.77 |
| | Ref | 2 | -2.18 | -29.49 | -3.6 | -33.11 | 1.10 | -42.32 | 0 |
| | Ref | 2 | -9.55 | -47.13 | -2.92 | -50.05 | 0.07 | -77.34 | 0 |
| 4 | QA | 6 | -8.03 | -22.50 | -12.92 | -35.42 | 2.29 | -42.7 | -3.97 |
| | Dox | 7 | -7.87 | -42.20 | -10.51 | -52.71 | 6.11 | -48.04 | -1.66 |
| | QA | 6 | -6.88 | -19.74 | -13.91 | -33.65 | 1.33 | -39.89 | -3.36 |
| 5 | Dox | 7 | -6.18 | -32.29 | -8.69 | -40.98 | 3.32 | -59.98 | -2.20 |
| | Ref | 2 | -2.93 | -28.14 | -3.38 | -31.52 | 0.94 | -40.84 | -0.91 |

Interestingly, the study revealed the probable binding site and conformation of doxorubicin within cavity 1, with a docking score of -8.62 and an emodel value of -79.34. The emodel value for the reference structure in cavity 4 was -77.34, indicating the high probability of doxorubicin binding in the identified site. The emodel value combines the docking score, the non-bonded interaction energy and the internal strain energy of the ligand conformation. Doxorubicin is structurally much larger than the other two ligands and it performed the best in cavity 1 with the largest volume of 1188.84 Å (Figure 5.5).

The binding affinity of QA with HIV-1-RT was investigated in detail. On analysis of the binding mode of QA into the catalytic site HIV-1-RT (cavity 4) it was found that the residues Lys 101 and Tyr 188 are involved in the H-bond interaction. Moreover, they contributed three hydrogen bonds between them (Figure 5.3).

Non-nucleoside reverse transcriptase inhibitors (NNRTI's), such as nevirapine, bind in a non-competitive manner to a specific pocket of HIV-1 RT and alter the viral replication mechanism by acting as a chain terminator. According to literature, despite the chemical diversity of the butterfly-like shaped compounds, this factor is important in the binding of the NNRTIs. The butterfly structure has a hydrophilic centre as a 'body' and two hydrophobic moieties representing the 'wings'. X-ray crystallographic studies revealed that the butterfly-like conformation of NNRTI play a role as pi electron donors surrounding the binding pocket. The NNRTIs are non-competitive inhibitors that bind allosterically to an asymmetric and hydrophobic cavity, about 10 Å away from the catalytic site of the HIV-1 RT. As a result of NNRTI binding, certain RT domains that actively participate in DNA synthesis are restricted in flexibility and mobility which, in turn, leads to a dramatic reduction in catalytic enzyme efficiency (Singh & Ganguly, 2017).

Molecular docking is based on algorithms and scoring functions, however inhibition concentration is calculated according to the results obtained from wet-lab experiments, so it is not possible to get an exact correlation between docking score and inhibitory activity. Docking gives the value with which the ligand binds to the protein and IC₅₀ gives the value responsible for inhibition. Therefore, docking scores cannot predict if the binding ligand is inhibiting enzyme function.

The purpose of molecular docking is to obtain reasonable models of protein-ligand interaction. In this study, the polar *H. mimites* extract showed anti-HIV activity on the live virus at 25 µg/mL

and at 2.5 $\mu\text{g/mL}$ ($> 98\%$) and its inhibition percentage activity against RT was 55.93 (± 3.3). Quinic acid isolated from this species exhibited good inhibition against RT with an IC_{50} value of 53.82 (± 4.2) $\mu\text{g/mL}$. Molecular docking confirmed that QA could bind well with RT and gave us a model of the protein-ligand complex.

Quinic acid is an organic acid involved in various fundamental pathways in plant metabolism and catabolism as intermediate or as end product. It is an intermediate of the biochemically important “shikimate pathway” (Pereira *et al.*, 2013). It is also one of the precursors of aromatic compounds in plants and micro-organisms. Quinic acid is a building block for the synthesis of several valuable secondary compounds, including coumaroyl- and caffeoylquinic acid derivatives with significant biological activity in several drug-target areas (Cheynier *et al.*, 2012). No previous reports were found on its HIV-RT activity.

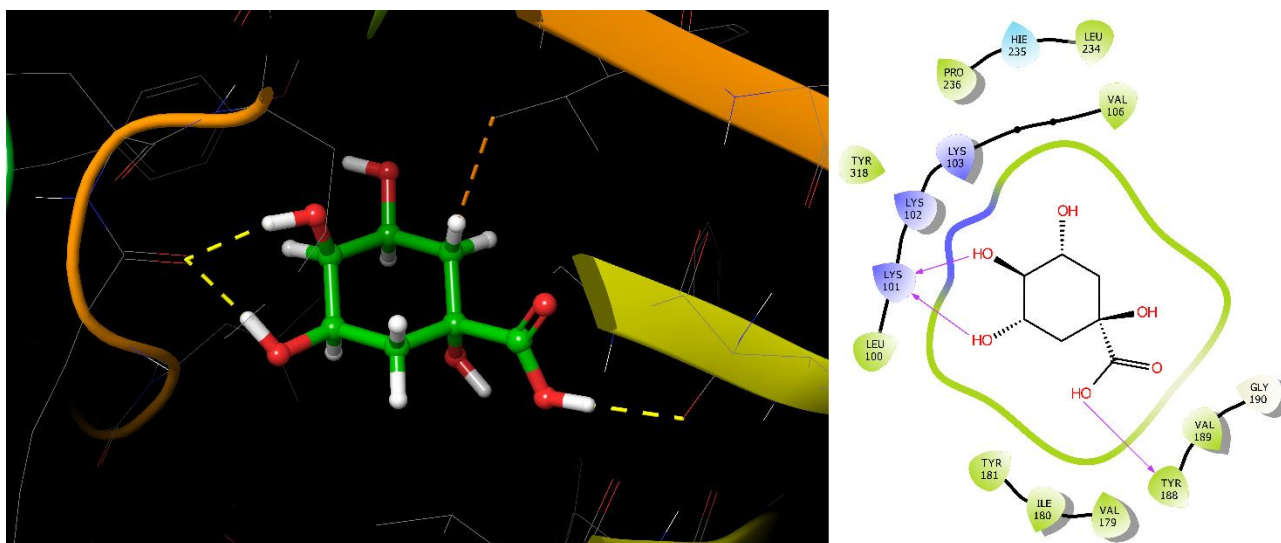


Figure 5.3. Quinic acid docked in cavity 4 with a docking score -8.03 (left), interaction diagram of QA indicating the hydrogen bonds between the ligand and binding site residues A: Tyr 188 and A: Lys 101 (right).

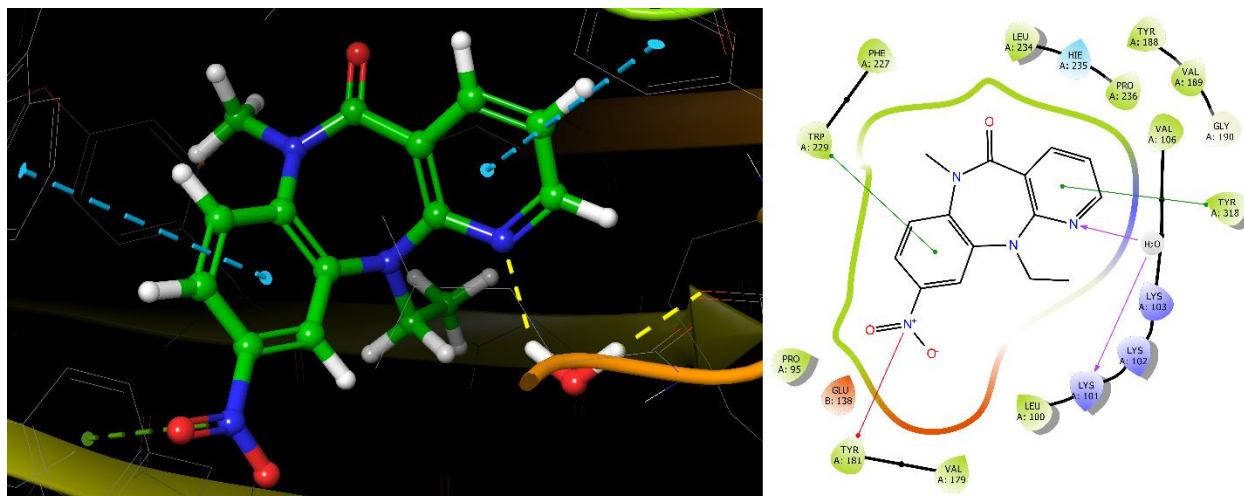


Figure 5.4. Reference compound U05 docked in cavity 4 with a docking score of -9.55 (left), interaction diagram of the Reference ligand indicating the salt bridges between ligand and residue A: Tyr 181 and pi-pi stacking with residues A: Trp 229 and A: Tyr 318.

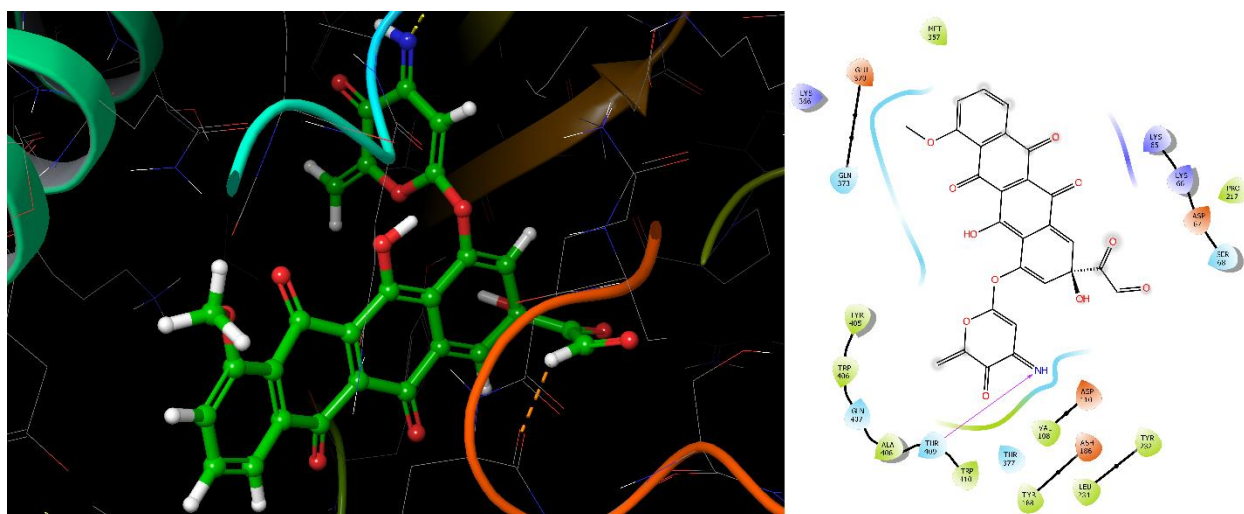


Figure 5.5. Doxorubicin docked in cavity 1 with a docking score of -7.87 (left), the interaction diagram of doxorubicin ligand indicating the salt bridges between ligand and residue as Thr 409.

5.4 Conclusion

Knowledge of the 3D structure of ligand-protein complexes provides a valuable understanding of the function of molecular systems. The main objective in the analyses of molecular docking is to obtain possible ligand-receptor complexes with optimized conformation with low binding energy (Dar & Mir, 2017). In this study, molecular docking was performed using Glide XP to explore the possible binding mode of HIV-1-RT with QA which was isolated and identified in *H. mimetes*. This investigation provided a possible mechanism of action of it against RT with a good IC₅₀ value of 53.82 (\pm 4.2) μ g/mL. The conclusion drawn from the docking analysis is that QA-Cav4 showed the highest binding affinity with HIV-1-RT. The QA-RT complex showed good stability and good H-bonding. Although the obtained IC₅₀ values of QA and doxorubicin in anti-RT test were very similar, their mode of action in terms of their active sites is probably different. Doxorubicin can attach to the receptor on the surface of the RT enzyme while the QA can bind to the cavities of the RT enzyme probably due to the size difference of the molecules. The combination of these two chemicals could possibly be used to reveal the synergistic effect of HIV treatment.

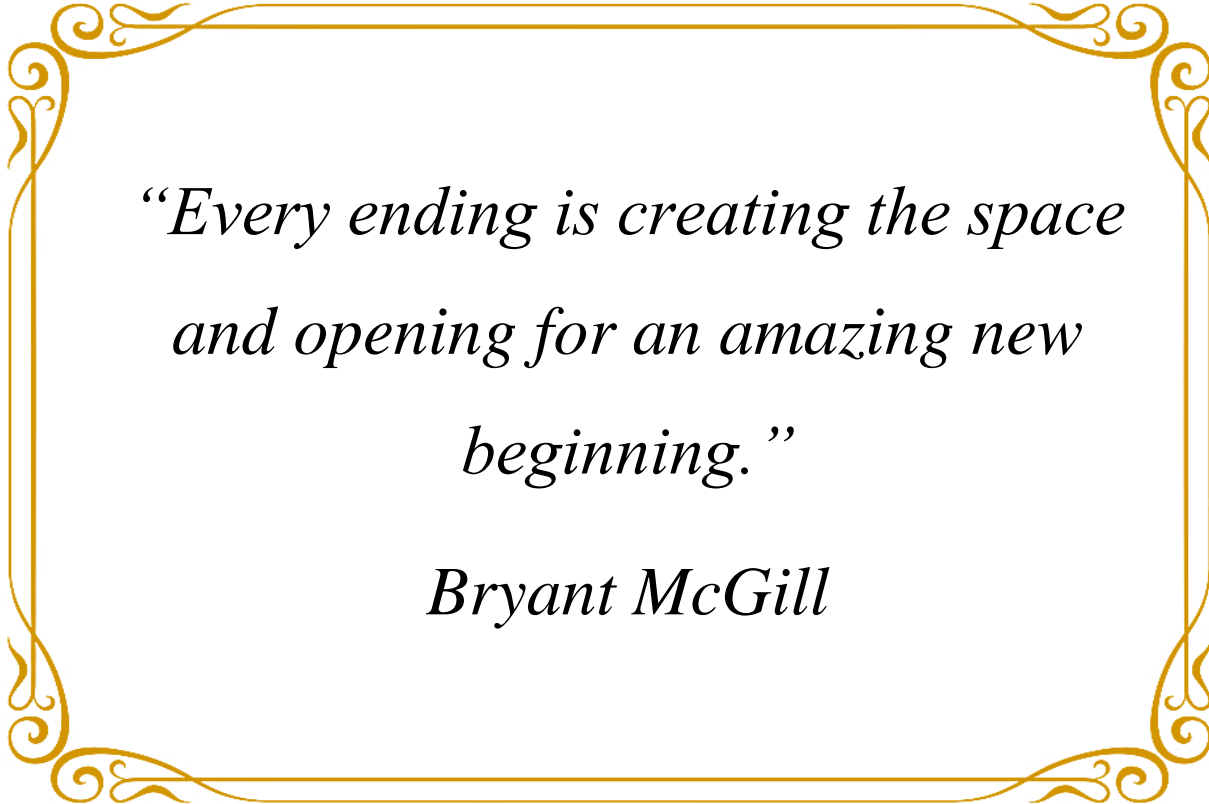
The present study provides a better understanding of the activity of QA against RT and can assist in designing more active compounds. Investigating the docking parameters for caffeoylquinic acids for their binding to HIV-RT and other enzymes might prove to be valuable. This study also provided interesting data on the mechanism of doxorubicin's RT activity.

5.5 References

- Cheynier, V., Sarni-Manchado, P. & Quideau, S. (2012). Recent advances in polyphenol research. John Wiley & Sons. West Sussex, UK.
- Dar, A. M. & Mir, S. (2017). Molecular docking: approaches, types, applications and basic challenges. *Journal of Analytical & Bioanalytical Techniques*, 8, 2.
- Debnath, A. K., Radigan, L. & Jiang, S. (1999). Structure-based identification of small molecule antiviral compounds targeted to the gp41 core structure of the human immunodeficiency virus type 1. *Journal of Medicinal Chemistry*, 42(17), 3203–3209.
- Friesner, R. A., Murphy, R. B., Repasky, M. P., Frye, L. L., Greenwood, J. R., Halgren, T. A., Sanschagrin, P. & Mainz, D. T. (2006). Extra precision glide: Docking and scoring incorporating a model of hydrophobic enclosure for protein-ligand complexes. *Journal of Medicinal Chemistry*, 49(21), 6177–6196.
- Halgren, T. (2007). New method for fast and accurate binding-site identification and analysis. *Chemical Biology & Drug Design*, 69(2), 146–148.
- Halgren, T. A. (2009). Identifying and characterizing binding sites and assessing druggability. *Journal of Chemical Information and Modeling*, 49(2), 377–389.
- Halgren, T. A., Murphy, R. B., Friesner, R. A., Beard, H. S., Frye, L. L., Pollard, W. T. & Banks, J. L. (2004). Glide: a new approach for rapid, accurate docking and scoring. 2. Enrichment factors in database screening. *Journal of Medicinal Chemistry*, 47(7), 1750–1759.
- Harder, E., Damm, W., Maple, J., Wu, C., Reboul, M., Xiang, J. Y., Wang, Lingle, L. D., Dahlgren, M. K. & Knight, J. L. (2015). OPLS3: a force field providing broad coverage of drug-like small molecules and proteins. *Journal of Chemical Theory and Computation*, 12(1), 281–296.
- Jeffrey, L. J. -L. & Robert, A. C. (2007). Targeting protein multiple conformations: a structure-based strategy for kinase drug design. *Current Topics in Medicinal Chemistry*, 7(14), 1394–1407.

- López-Vallejo, F., Caulfield, T., Martinez-Mayorga, K.A., Giulianotti, M., Nefzi, A. A., Houghten, R. & Medina-Franco, L. J. (2011). Integrating virtual screening and combinatorial chemistry for accelerated drug discovery. *Combinatorial Chemistry & High Throughput Screening*, 14(6), 475–487.
- Meng, E. C., Pettersen, E. F., Couch, G. S., Huang, C. C. & Ferrin, T. E. (2006). Tools for integrated sequence-structure analysis with UCSF Chimera. *BMC Bioinformatics*, 7(1), 339.
- Pereira, C., Barros, L., Carvalho, A. M. & Ferreira, I. C. F. R. (2013). Use of UFLC-PDA for the analysis of organic acids in thirty-five species of food and medicinal plants. *Food Analytical Methods*, 6(5), 1337–1344.
- Priya, R., Sumitha, R., Doss, C. G. P., Rajasekaran, C., Babu, S., Seenivasan, R. & Siva, R. (2015). Molecular docking and molecular dynamics to identify a novel human immunodeficiency virus inhibitor from alkaloids of *Toddalia asiatica*. *Pharmacognosy Magazine*, 11(3), 414–422.
- Seal, A., Aykkal, R., Babu, R. O. & Ghosh, M. (2011). Docking study of HIV-1 reverse transcriptase with phytochemicals. *Bioinformation*, 5(10), 430–439.
- Singh, R. & Ganguly, S. (2017). Molecular docking studies of novel imidazole analogs as HIV-1-RT inhibitors. *International Journal of Pharmaceutical Sciences and Research*, 8(9), 3751–3757.
- Subbaiah, S. G. P., Dakappa, S. S. & Lakshmikantha, R. Y. (2017). Antibacterial and molecular docking studies of bioactive component from leaves of *Stachytarpheta cayennensis* (Rich.) Vahl. *Research Journal of Phytochemistry*, 11, 28–34.

Chapter 6



*“Every ending is creating the space
and opening for an amazing new
beginning.”*

Bryant McGill

General discussion

6.1. Overview

Natural products with therapeutic properties play an enormous role in the life of humankind and for a long time mineral plant and animal products were the main sources of medicines (Newman & Cragg, 2016; Bernardini *et al.*, 2018). In South Africa nearly 27 million people still rely on traditional medicine and approximately 20 000 tons of indigenous South African plants are used each year from at least 771 plant species (Twilley *et al.*, 2017). *Helichrysum* (Asteraceae) belongs to a large genus consisting of approximately 500 species of which 245 are indigenous to South Africa. Species of *Helichrysum* have been widely used in South Africa by the indigenous population to treat various ailments, including coughs, colds, fever, infections, headache, menstrual pain and in wound dressings. This group of plants is extensively utilised throughout South Africa in traditional medicine and is commonly known as “imphepo” (Xhosa, Zulu), or “kooigoed” (Khoisan, Afrikaans). In traditional medicine, *Helichrysum* species are used to fumigate sick rooms. They are also used to repel insects and help bedding and insomnia (Lourens *et al.*, 2008).

Viruses have efficient means to survive and propagate in a wide variety of hosts and cell types. They are the most diverse group of microorganisms with respect to their host distribution, genomic organization and clinical presentations. They may possess a DNA or RNA genome and may follow diverse routes for replication, transcription and translation processes. Moreover, clinically, they may present themselves as self-resolving localized infections or may attain severe forms to affect the whole body (Babar *et al.*, 2013). Statistics show that HIV/AIDS is responsible for over 2 million deaths annually across the globe. HIV-1 is a pathogenic retrovirus belonging to the lentivirus family and causative agent of AIDS or AIDS-related disorders. The three viral enzymes: reverse transcriptase, protease and integrase of HIV play an important role in the virus replication cycle through host cells. Among them viral RT catalyzes the formation of proviral DNA from viral RNA, the key stage in viral replication (Vinod & Selvakumar, 2012)

Presented in this thesis is a metabolomic analysis on the anti-HIV and anti-RT activity of 32 selected *Helichrysum* species. *H. mimetes* was identified as a good candidate for further investigation based

on its anti-HIV activity. Principal component analysis of the polar extracts showed clustering related to the anti-HIV and RT activity of the extracts with good PCA predictability scores ($Q^2 > 0.5$). The results of this study are complimentary to another study on the anti-HIV activity of 30 other *Helichrysum* species (Heyman, 2013). He identified caffeoylquinic acids as the major anti-HIV metabolites in the *Helichrysum* species also by means of an NMR-based metabolomic investigation. In the current study, some fractions indeed showed the presence of chlorogenic acids. However, better activity was found in the fractions without chlorogenic acids present. Anti-HI virus bioassays showed that polar extracts of *H. chrysargyrum* (2.5 $\mu\text{g/mL}$), polar and non-polar extracts of *H. cephaloideum* (25 $\mu\text{g/mL}$), and polar and non-polar extracts of *H. zeyheri*, *H. setosum*, *H. platypterum* and *H. kraussii* (2.5 $\mu\text{g/mL}$), had higher than 90% inhibitory activity. The polar *H. mimetes* extract had anti-HIV-1 activity at 25 $\mu\text{g/mL}$ and 2.5 $\mu\text{g/mL}$ (> 98%) and its percentage inhibition activity against RT was 55.93 (± 3.3) at 100 $\mu\text{g/mL}$ and therefore is a possible indication of the mechanism of action. Quinic acid isolated from this species exhibited good inhibition against RT with an IC_{50} value of 53.82 (± 4.2) $\mu\text{g/mL}$. The obtained result was comparable to the positive drug control, doxorubicin ($\text{IC}_{50} = 40.31$ $\mu\text{g/mL}$). The presence of quinic acid in the active isolated fraction from *H. mimetes* was identified by NMR and UPLC-MS/MS and is reported for the first time in this species. The molecular docking investigation predicted the RT binding site and cavity and this compared well to the docking scores and emodel values of the reference compound (U05) and positive drug control (doxorubicin). Quinic acid and U05 docked in cavity 4 with a docking score of -8.03 and -9.55 respectively, while doxorubicin docked in cavity 1 with docking score of -7.87. This is the first report on the docking of doxorubicin and quinic acid on RT.

The quinic acid-RT complex showed good stability and good H-bonding. Although, the obtained IC_{50} values of quinic acid and doxorubicin in the anti-RT bioassay were comparable, their molecular mode of action in terms of their active sites was different. Doxorubicin was able to attach to the receptor on the surface of the RT enzyme while quinic acid could enter the cavities of the RT enzyme due to the size of the molecule. The present study will aid in a better understanding of the anti-HIV activity of quinic acid, as well as doxorubicin against RT.

Quinic acid is involved in various fundamental pathways in plant metabolism and catabolism as an intermediate or end product. It is an intermediate of the biochemically important “shikimate

pathway” (Pereira & Oakley, 2008) and one of the precursors of aromatic compounds in plants and microorganisms. This acid is often found in the free acid state or in bound forms with one or more of their hydroxyl groups esterified to phenolic carboxylic acids or often with dihydroxycinnamic or gallic acid, which are the so-called depsides and the chlorogenic acids found widely in the plant kingdom (Barco *et al.*, 1997).

Quinic acid is a building block for the synthesis of several valuable secondary compounds, including coumaroyl- and caffeoylquinic acid derivatives with significant biological activity in several drug-target areas (Cheynier *et al.*, 2012). There are some reports on biological activity of quinic acid. Quinic acid and its related compounds exhibited anti-inflammatory effects through mechanisms involving the inhibition of the pro-inflammatory transcription factor, nuclear factor kappa-B (NF- κ B) (Zeng *et al.*, 2009; Seung *et al.*, 2013). Another screening assay conducted by Mitra *et al.* (2016) showed the anti-inflammatory activity of quinic acid extracted from plant sources against LPS in RAW 264.7 macrophages. The transcription factor NF- κ B is one of the key regulators of genes involved in the immune/inflammatory response, as well as in HIV-1 gene regulation (Pereira & Oakley, 2008). Åkesson *et al.* reported that the quinic acid inhibits NF- κ B activity in cells grown in tissue culture *in vitro* (Åkesson *et al.*, 2005). Quinic acid was shown to inhibit TNF- α -stimulated phosphorylation of MAP kinase and NF- κ B activation. It inhibits the TNF- α -stimulated induction of VCAM-1 in VSMC by inhibiting the MAP kinase and NF- κ B signaling pathways and the adhesion capacity of VSMC, which may explain the ability of quinic acid to inhibit vascular inflammation such as atherosclerosis (Jang *et al.*, 2017).

There are very few reports on antiviral activity of quinic acid and it has never proved to be effective against RT enzyme. There is just a report by Wang *et al.* (2009) about substantial inhibitory activity of quinic acid against HBV-DNA replication in HepG2.2.15 cells.

With the above mentioned results of quinic acid's antiHIV activity, its bioavailability becomes an important factor. However, data on its bioavailability are scarce. The most reports on the bioavailability of phenolic compounds are on chlorogenic acids which are esters of caffeic acid and quinic acid and their bioavailability has not received as much attention as other types of compounds such as flavonoids (Lafay & Gil-Izquierdo, 2007).

A study conducted by Lee *et al.* (2016) reported that all three molecules, chlorogenic acid, caffeic acid and quinic acid are bioavailable after chlorogenic acid ingestion. It was reported that when chlorogenic acid reaches the colon, the gut microflora break the bonds in the molecule and releases caffeic acid and quinic acid. The results on antioxidant activity of chlorogenic acid should be similar after its breakdown into quinic acid and caffeic acid because quinic acid and caffeic acid both also have antioxidant activity (Lee *et al.*, 2016).

In another study of colonic availability of polyphenols and D-(–)-quinic acid after apple smoothie consumption, the most abundant substances found in the ileostomy bags were D-(–)-quinic acid (363.4 ± 235.5 mg) and 5-caffeoylquinic acid (76.7 ± 26.8 mg). In total, recovery of ingested polyphenols and D-(–)-quinic acid in the ileostomy process was $63.3 \pm 16.1\%$ from ingested 0.7 L of apple smoothie (Hagl *et al.*, 2010).

It is important to keep in mind that with a potent lead compound that has been computationally shown to have stable binding on the target enzyme and validated with bioassays, it is still a long road to develop this lead compound to a commercial drug.

The hypothesis “a metabolomic investigation of bioactivity and chemical variation in plant extracts can be statistically quantified and be used as a tool to predict anti-HIV activity in *Helichrysum* species”, was supported by the results presented in this thesis.

6.2 Recommendation for future research

Scientific studies and investigations are infinite and there are always new outcomes and solutions to develop future research and get the most satisfactory results. On the other hand, in the case of any scientific research project, there is always limitation and boundaries. Therefore, to develop the prospective work of this study, there are some recommendations and suggestions.

In the current study and the one by Heyman *et al.* (2015) on the anti-HIV activity of *Helichrysum* species, 62 species were investigated, leaving still more than 180 South African species and more than 400 species worldwide unexplored. In these two studies, the metabolomic investigation led to

the identification of chlorogenic acids and quinic acid as active compounds against HIV/RT. It would be interesting and valuable to analyse the rest of the *Helichrysum* species. Target-based drug discovery of small molecules by means of metabolomics enable faster and a more cost effective process. Investigation of other HIV targets as possible mechanisms of action of active compounds should also be considered.

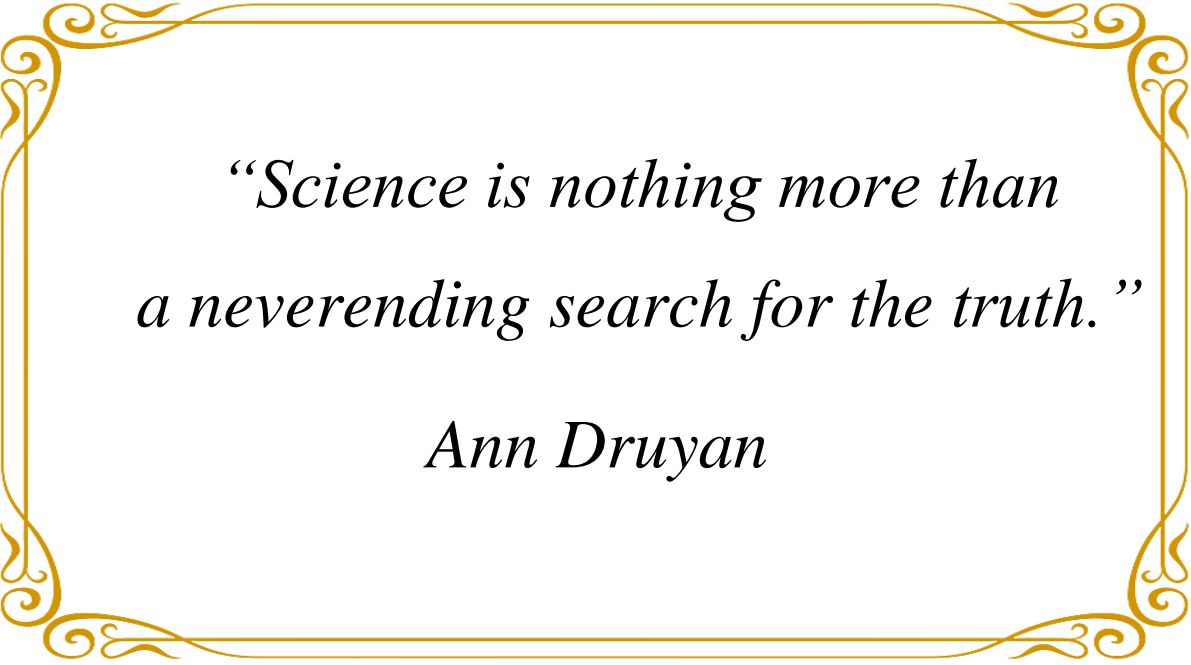
The results of the molecular docking experiment of this study showed that doxorubicin and quinic acid bind effectively on different sites of the RT enzyme, this suggests that a future study on the combination of these compounds could be valuable for an investigation on a possible synergistic interaction in a combination treatment. Alongside all the mentioned points for future investigations mentioned above, a study on the bioavailability of chlorogenic acids and quinic acid would also be valuable and interesting for drug discovery.

6.3 References

- Åkesson, C., Lindgren, H., Pero, R. W., Leanderson, T. & Ivars, F. (2005). Quinic acid is a biologically active component of the *Uncaria tomentosa* extract C-Med 100®. *International Immunopharmacology*, 5(1), 219–229.
- Babar, M., Najam-us-Sahar, S. Z., Ashraf, M. & Kazi, A. G. (2013). Antiviral drug therapy-exploiting medicinal plants. *Journal of Antivirals and Antiretrovirals*, 5(2), 28–36.
- Barco, A., Benetti, S., De Risi, C., Marchetti, P., Pollini, G. P. & Zanirato, V. (1997). D-(-)-Quinic acid: a chiron store for natural product synthesis. *Tetrahedron: Asymmetry*, 8(21), 3515–3545.
- Bernardini, S., Tiezzi, A., Laghezza Masci, V. & Ovidi, E. (2018). Natural products for human health: an historical overview of the drug discovery approaches. *Natural Product Research*, 32(16), 1926–1950.
- Cheynier, V., Sarni-Manchado, P. & Quideau, S. (2012). Recent advances in polyphenol research. John Wiley & Sons. West Sussex, UK.
- Hagl, S., Deusser, H., Soyalan, B., Janzowski, C., Will, F., Dietrich, H., Albert, F.W., Rohner, S. & Richling, E. (2011). Colonic availability of polyphenols and D-(-)-quinic acid after apple smoothie consumption. *Molecular Nutrition & Food Research*, 55(3), 368–377.
- Heyman, H. M. (2013). Identification of anti-HIV compounds in *Helichrysum* species (Asteraceae) by means of NMR-based metabolomic guided fractionation. University of Pretoria (Ph.D. thesis).
- Jang, S. -A., Park, D. W., Kwon, J. E., Song, H. S., Park, B., Jeon, H., Sohn, E. -H., Koo, H. J. & Kang, S. C. (2017). Quinic acid inhibits vascular inflammation in TNF- α -stimulated vascular smooth muscle cells. *Biomedicine & Pharmacotherapy*, 96, 563–571.
- Lafay, S. & Gil-Izquierdo, A. (2008). Bioavailability of phenolic acids. *Phytochemistry Reviews*, 7(2), 301.

- Lee, S.-J., Lee, S.-Y., Chung, M.-S. & Hur, S.-J. (2016). Development of novel *in vitro* human digestion systems for screening the bioavailability and digestibility of foods. *Journal of Functional Foods*, 22, 113–121.
- Lourens, A. C. U., Viljoen, A. M. & Van Heerden, F. R. (2008). South African *Helichrysum* species: a review of the traditional uses, biological activity and phytochemistry. *Journal of Ethnopharmacology*, 119(3), 630–652.
- Mitra, S., Kar, S., Surajlata, K. & Banerjee, E. R. (2016). Screening of novel natural product derived compounds for drug discovery in inflammation. *Journal of Plant Biochemistry & Physiology*, 3, 1–9.
- Newman, D. J. & Cragg, G. M. (2016). Natural products as sources of new drugs from 1981 to 2014. *Journal of Natural Products*, 79(3), 629–661.
- Pereira, S. G. & Oakley, F. (2008). Nuclear factor- κ B1: regulation and function. *The International Journal of Biochemistry & Cell Biology*, 40(8), 1425–1430.
- Seung, Y. L., Eunjung, M., Sun, Y. K. & Kang, R. L. (2013). Quinic acid derivatives from *Pimpinella brachycarpa* exert anti-neuroinflammatory activity in lipopolysaccharide-induced microglia. *Bioorganic and Medicinal Chemistry Letters*, 23, 2140–2144.
- Twilley, D., Langhansová, L., Palaniswamy, D. & Lall, N. (2017). Evaluation of traditionally used medicinal plants for anticancer, antioxidant, anti-inflammatory and anti-viral (HPV-1) activity. *South African Journal of Botany*, 112, 494–500.
- Vinod, B. & Selvakumar, D. (2012). Molecular docking studies of Diphenyl Imidazolidin Diones with HIV-1 Reverse Transcriptase. *Journal of Pharmacy Research*, 5(3), 1371–1373.
- Wang, G. -F., Shi, L. -P., Ren, Y. -D., Liu, Q. -F., Liu, H. -F., Zhang, R. -J., Li, Z., Zhu, F. H., He, P. L., Tang, W., Tao, P. Z., Li, C., Zhao, W. M. & Zuo, J. P. (2009). Anti-hepatitis B virus activity of chlorogenic acid, quinic acid and caffeic acid *in vivo* and *in vitro*. *Antiviral Research*, 83(2), 186–190.
- Zeng, K., Thompson, K. E., Yates, C. R. & Miller, D. D., (2009) Synthesis and biological evaluation of quinic acid derivatives as anti-inflammatory agents. *Bioorganic & Medicinal Chemistry Letters*, 19, 5458–5460.

Chapter 7



*“Science is nothing more than
a neverending search for the truth.”*

Ann Druyan

Appendix

7.1 NMR spectra of the polar extracts of *Helichrysum* species using nuclear magnetic resonance Bruker 600 MHz spectrometer (Council for Scientific and Industrial Research, CSIR). Solvent: CD₃OD and KH₂PO₄-D₂O solution.

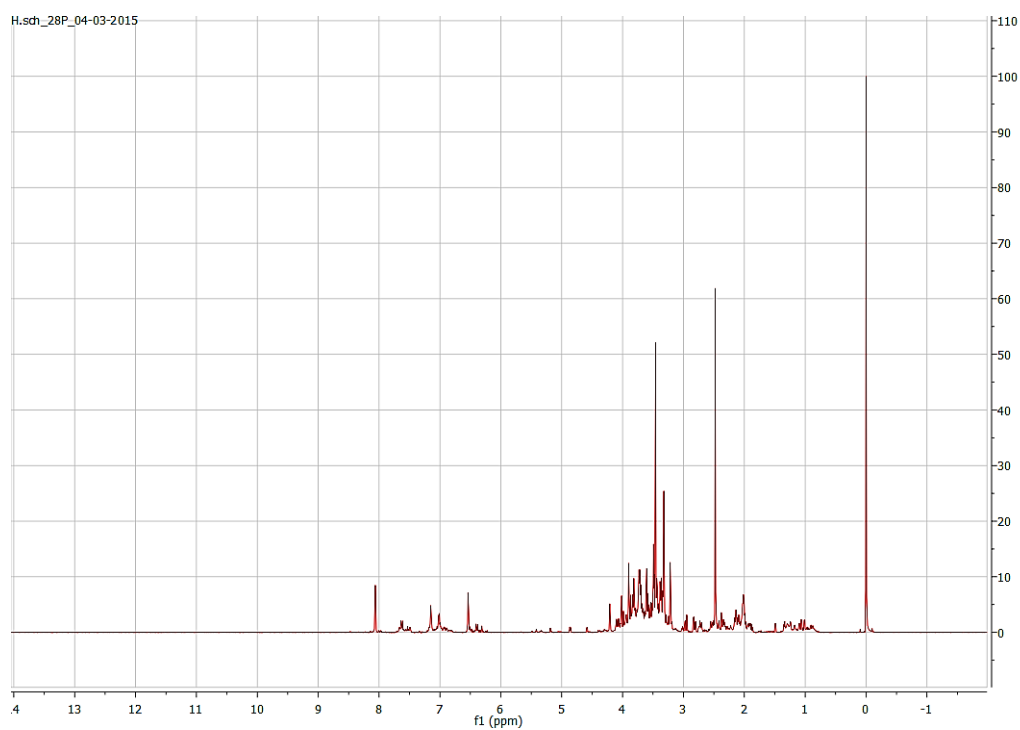


Figure 7.1. ¹H NMR spectrum of *H. acutatum* DC. [synonym *H. schlechteri*].

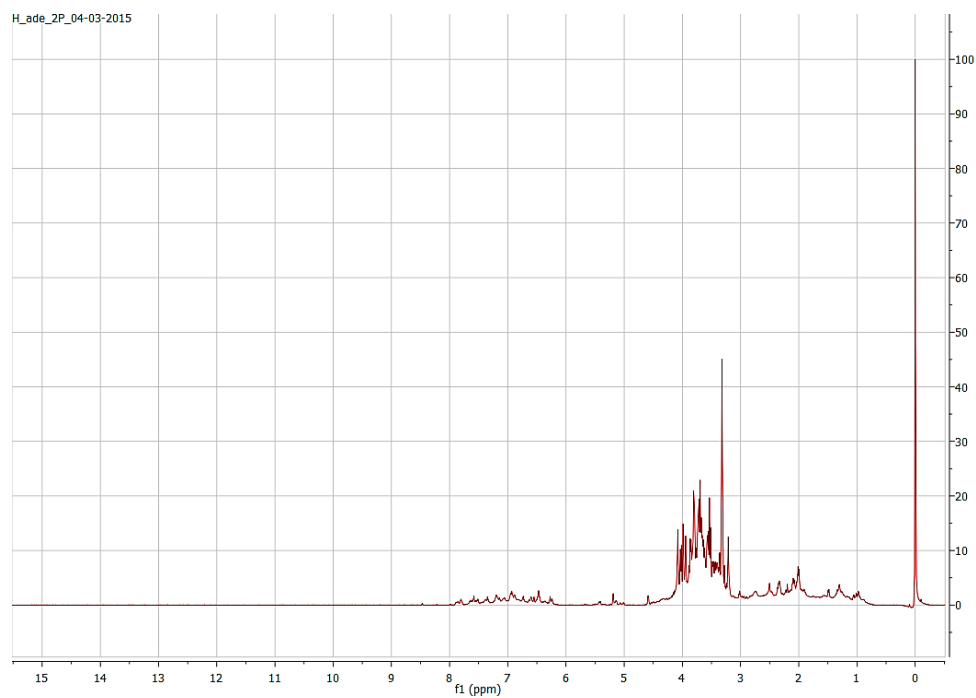


Figure 7.2. ^1H NMR spectrum of *H. adenocarpum* DC.

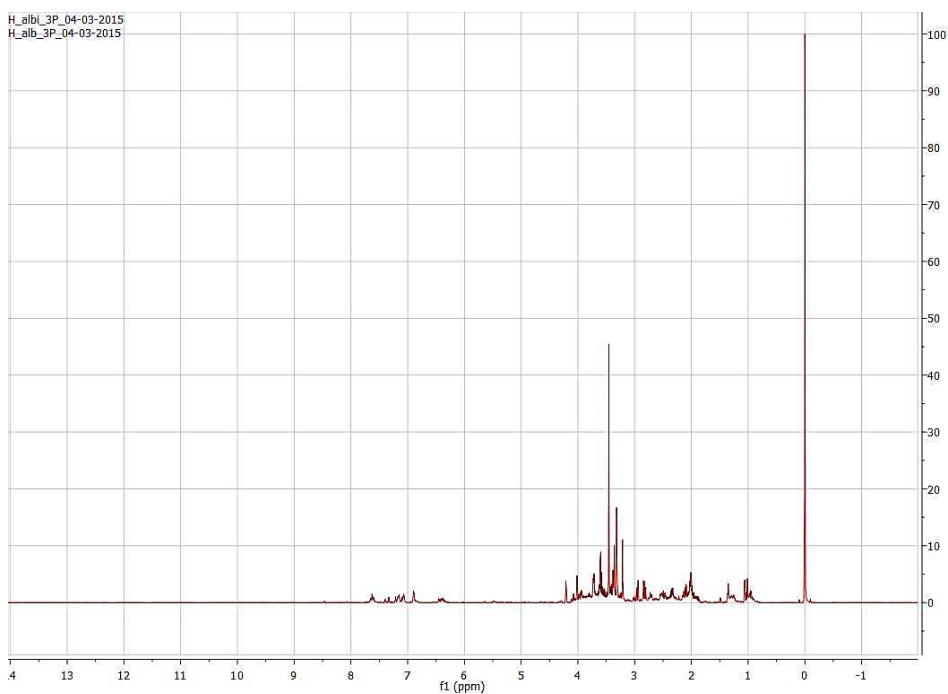


Figure 7.3. ^1H NMR spectrum of *H. albilanatum* Hilliard.

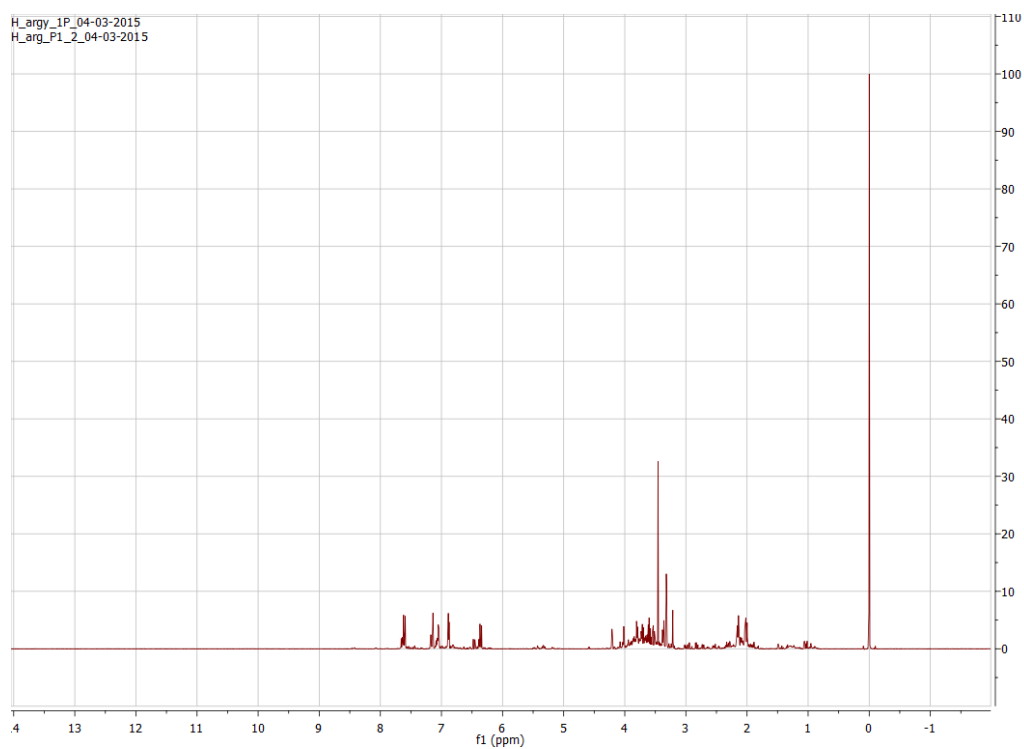


Figure 7.4. ^1H NMR spectrum of *H. argyrophyllum* DC.

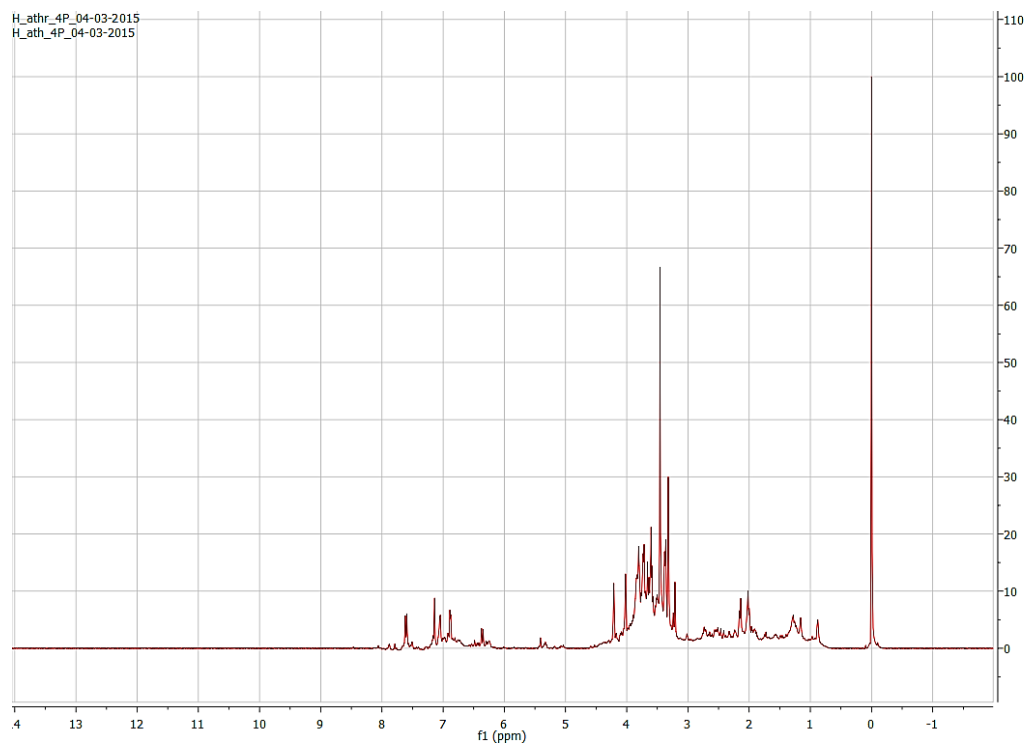


Figure 7.5. ^1H NMR spectrum of *H. athrixiifolium* (Kuntze) Moeser.

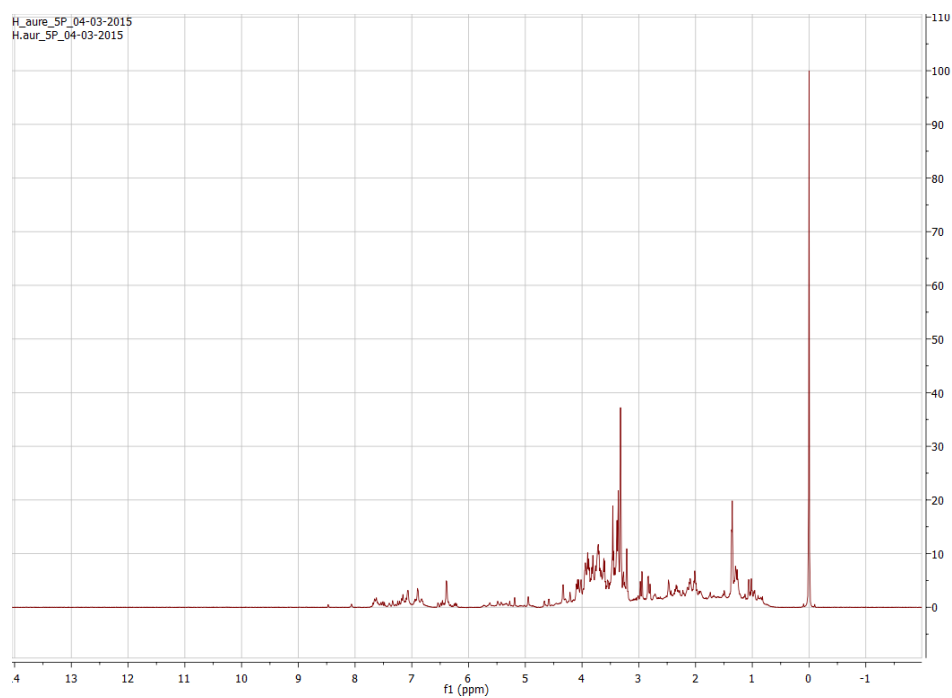


Figure 7.6. ^1H NMR spectrum of *H. aureum* (Houtt.) Merr.

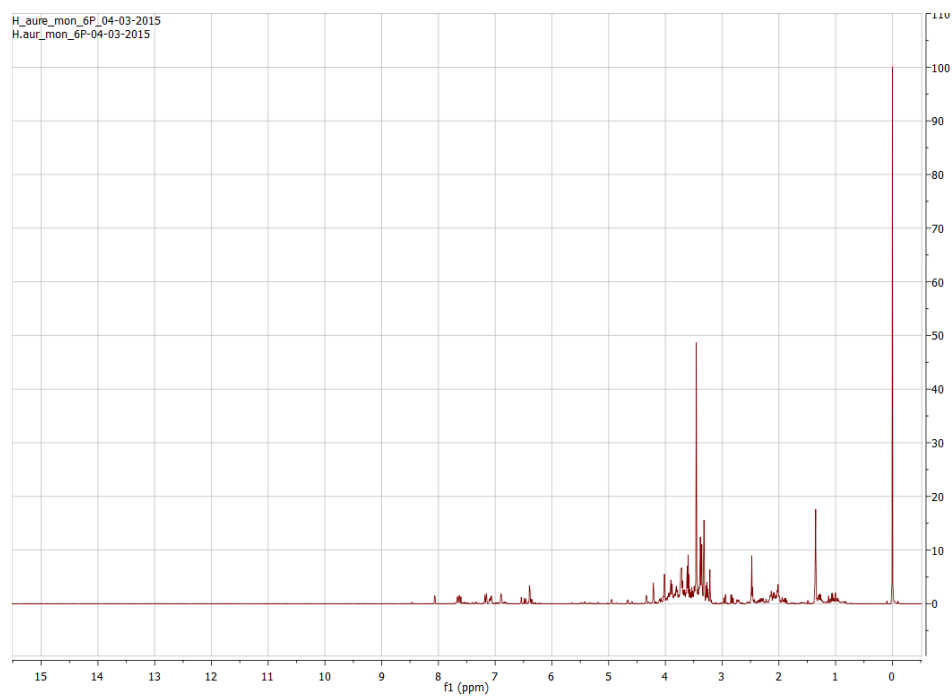


Figure 7.7. ^1H NMR spectrum of *H. aureum* (Houtt.) Merr. var. *monocephalum* (DC.) Hilliard.

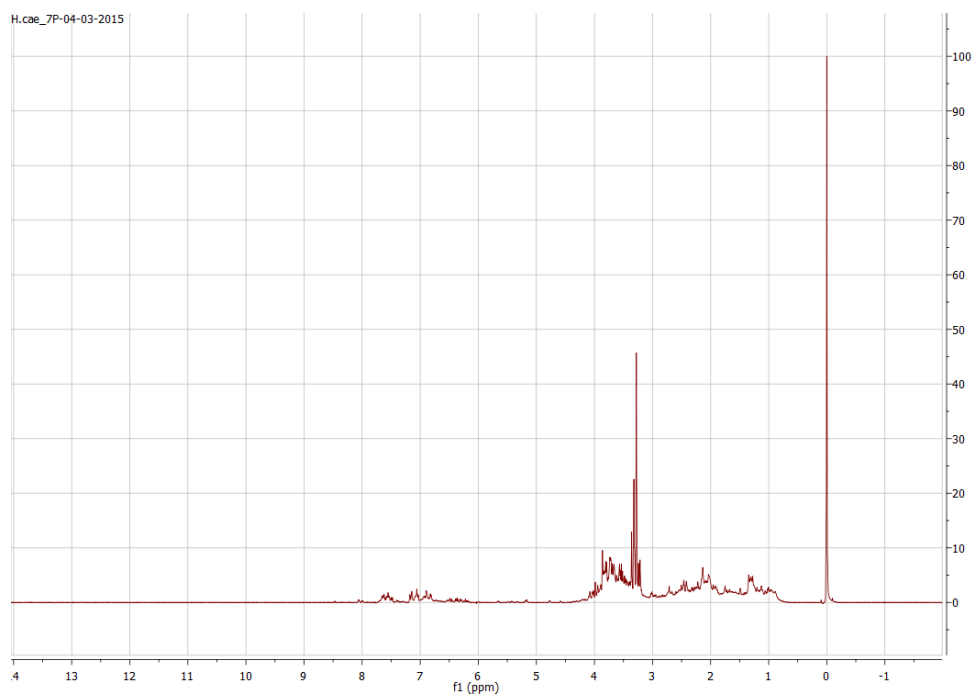


Figure 7.8. ^1H NMR spectrum of *H. caespitium* (DC.) Harv.

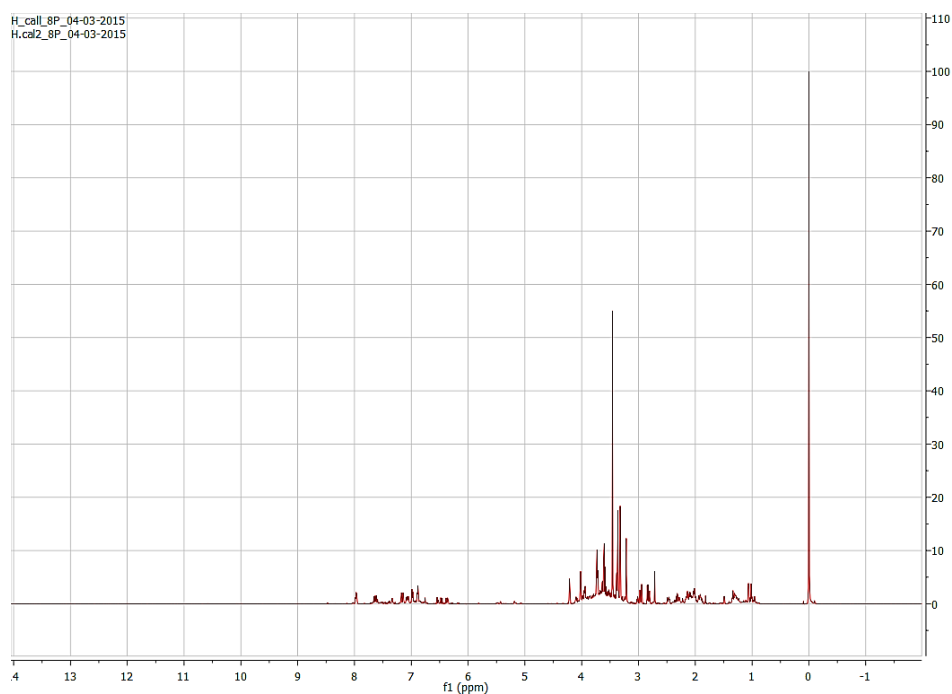


Figure 7.9. ^1H NMR spectrum of *H. callicomum* Harv.

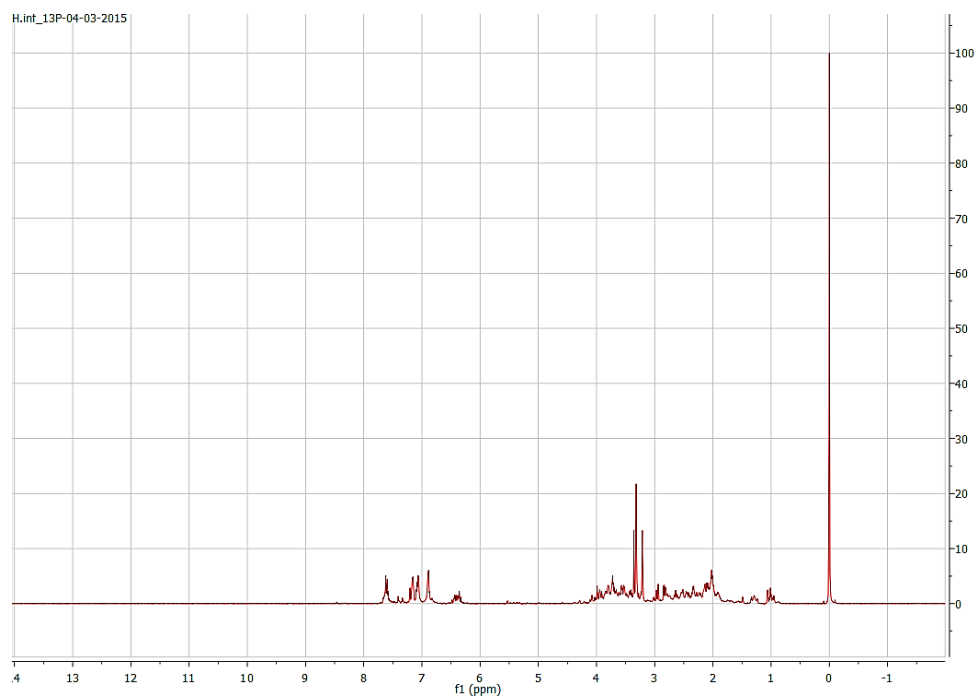


Figure 7.10. ¹H NMR spectrum of *H. cephaloideum* DC.

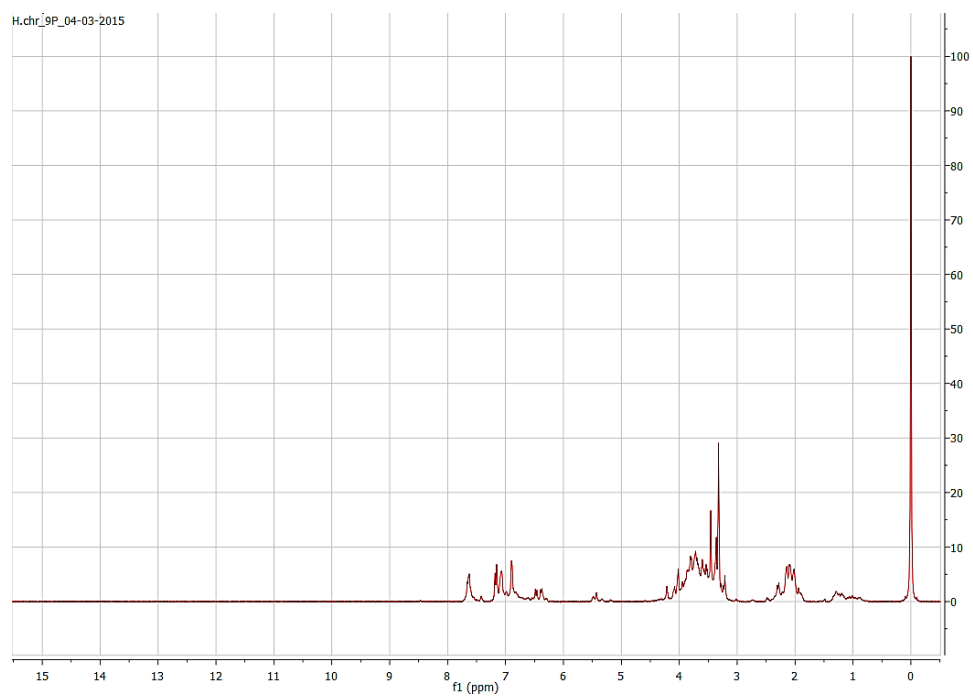


Figure 7.11. ¹H NMR spectrum of *H. chrysargyrum* Moeser.

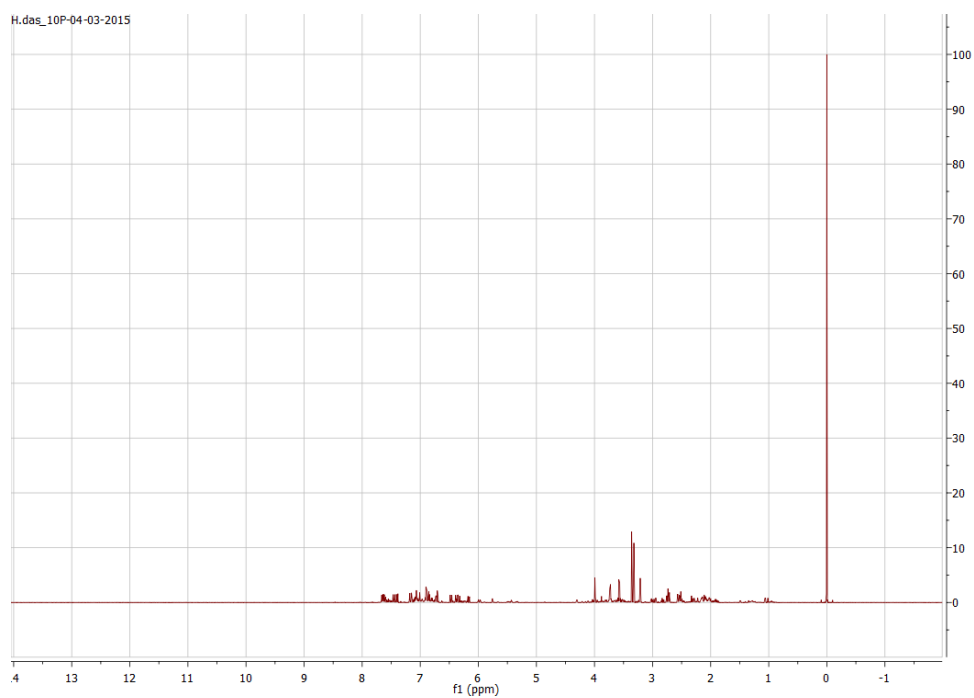


Figure 7.12. ^1H NMR spectrum of *H. dasyanthum* (Willd.) Sweet.

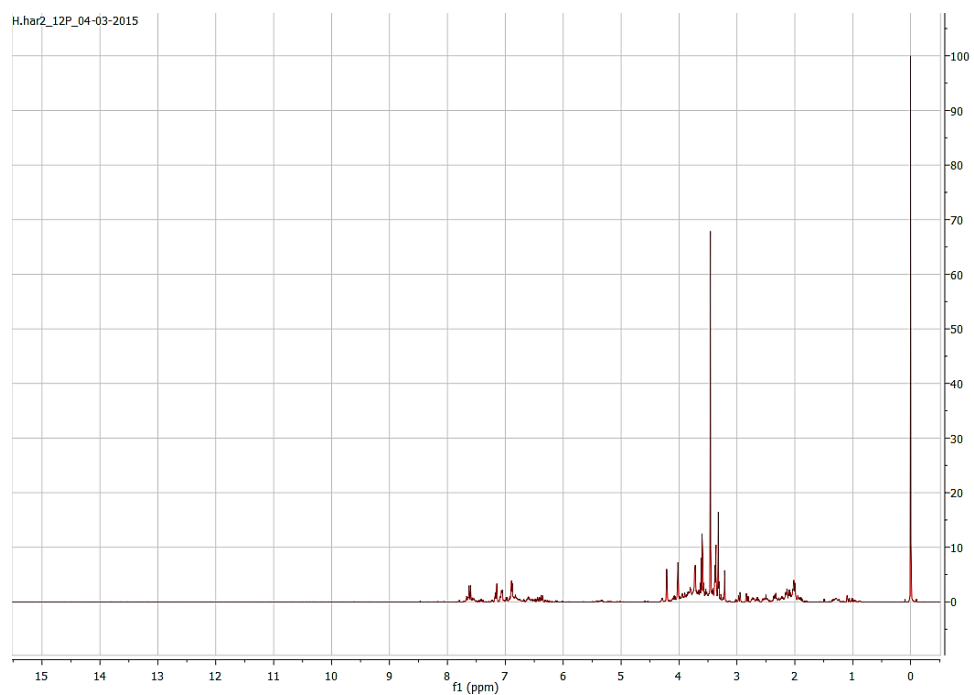


Figure 7.13. ^1H NMR spectrum of *H. harveyanum* Wild.

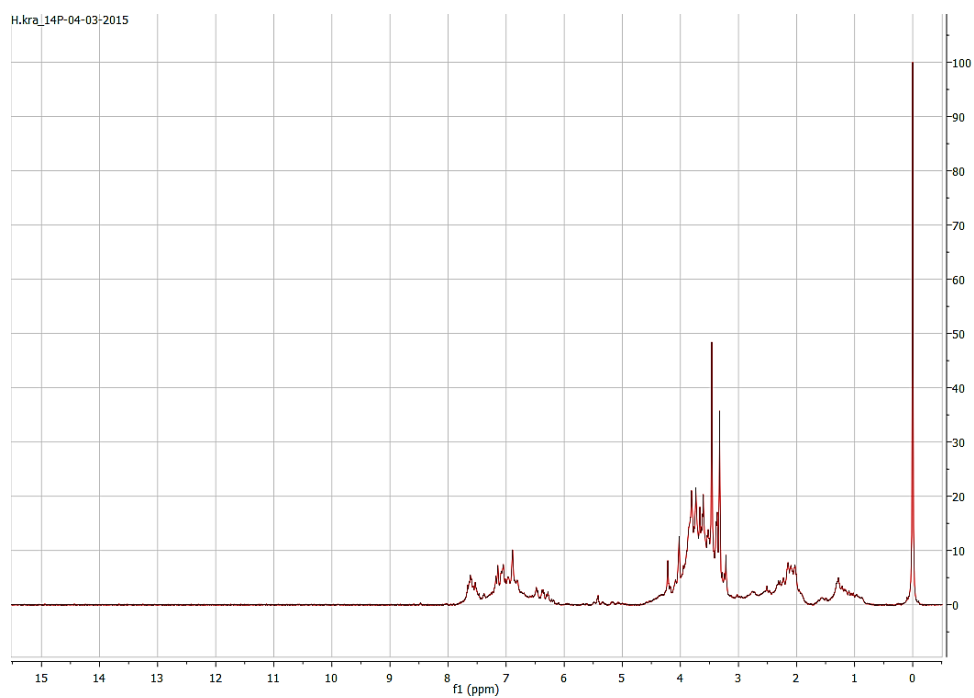


Figure 7.14. ¹H NMR spectrum of *H. kraussii* Sch.Bip.

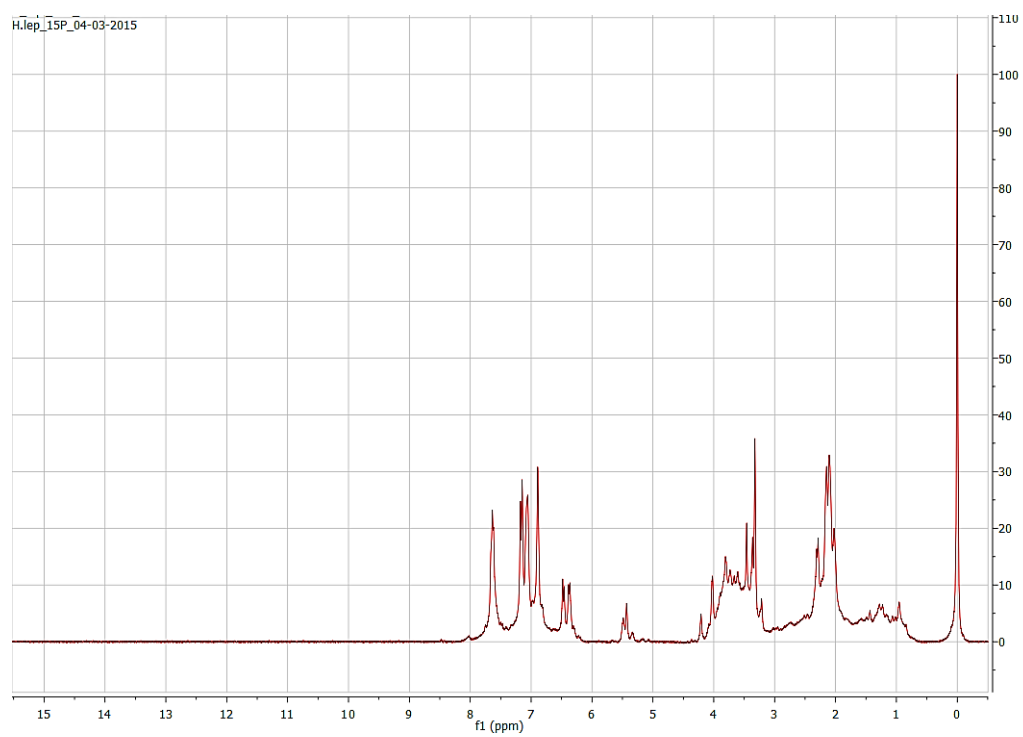


Figure 7. 15. ¹H NMR spectrum of *H. lepidissimum* S.Moore.

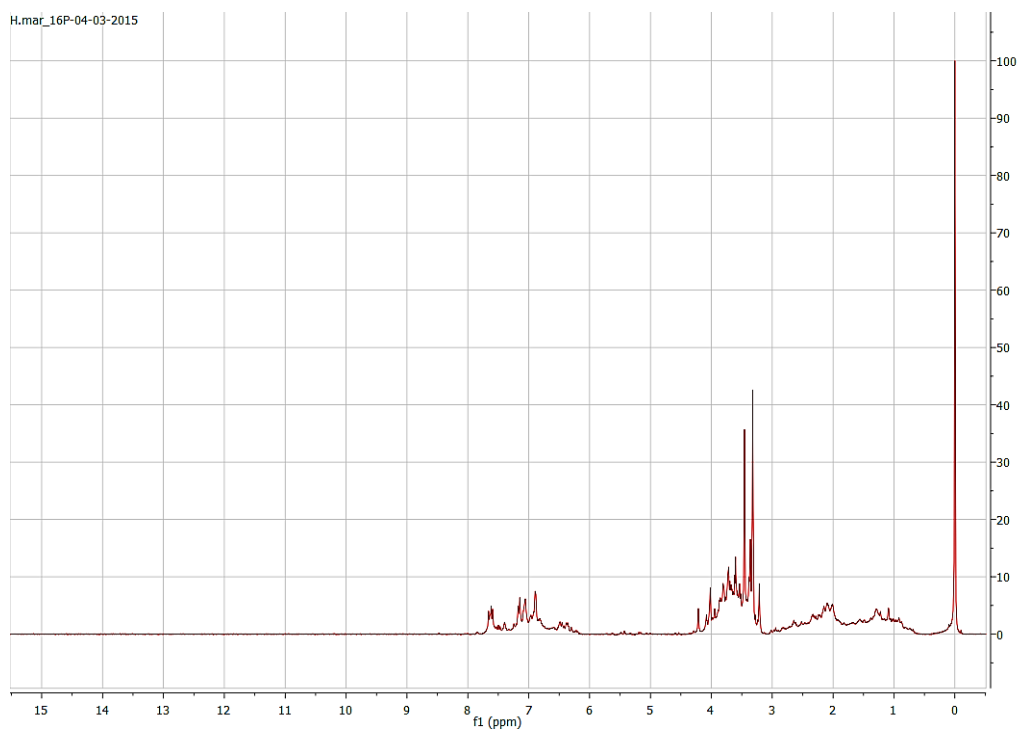


Figure 7.16. ¹H NMR spectrum of *H. mariepsopicum* Hilliard.

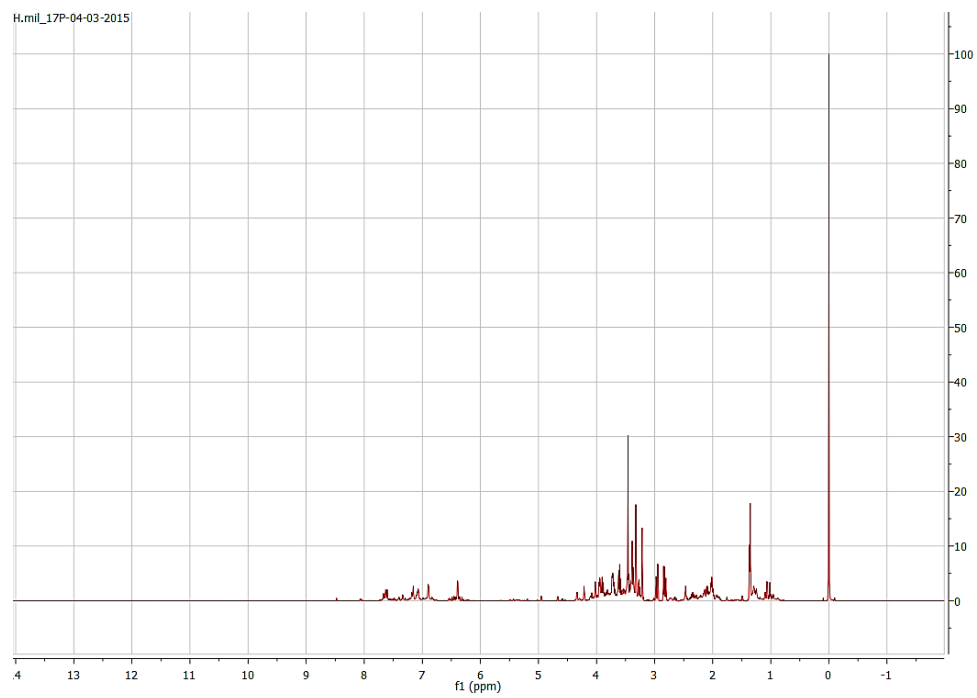


Figure 7.17. ¹H NMR spectrum of *H. milleri* Hilliard.

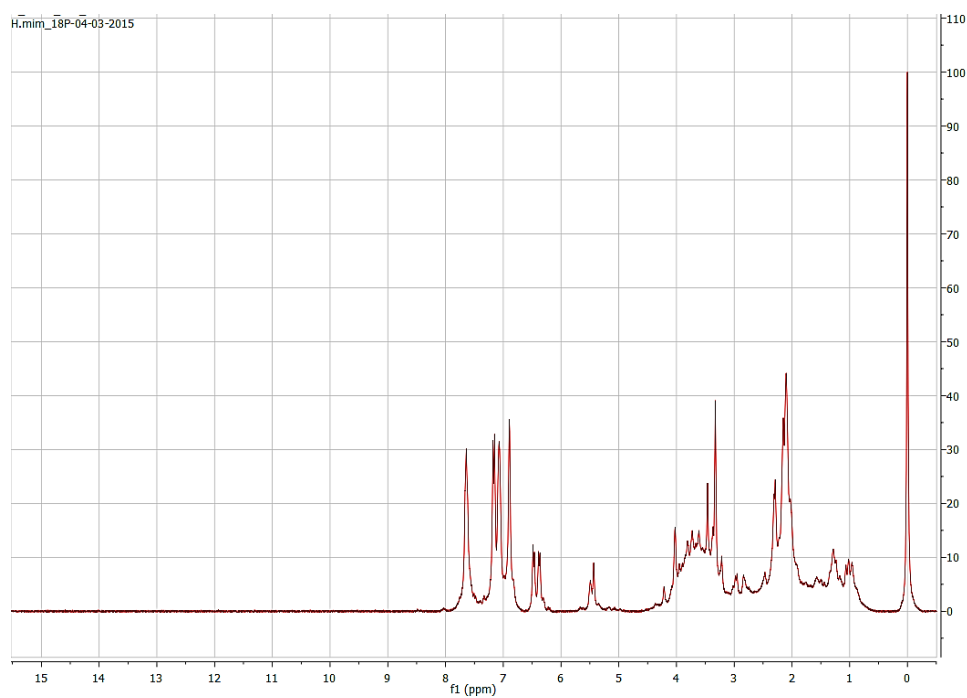


Figure 7.18. ^1H NMR spectrum of *H. mimetes* S.Moore.

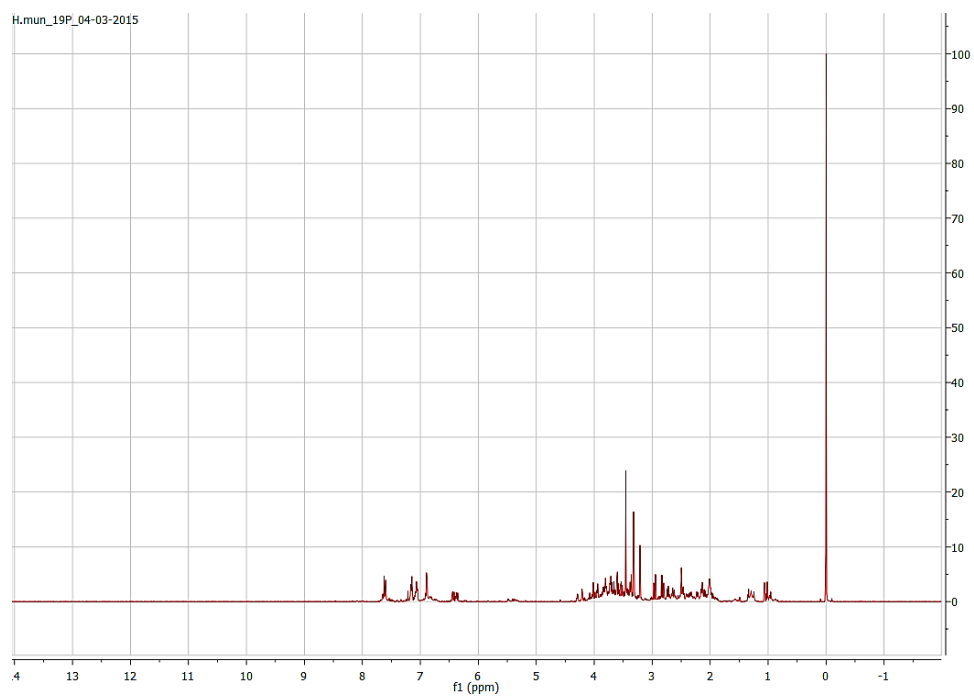


Figure 7.19. ^1H NMR spectrum of *H. mundti* Harv.

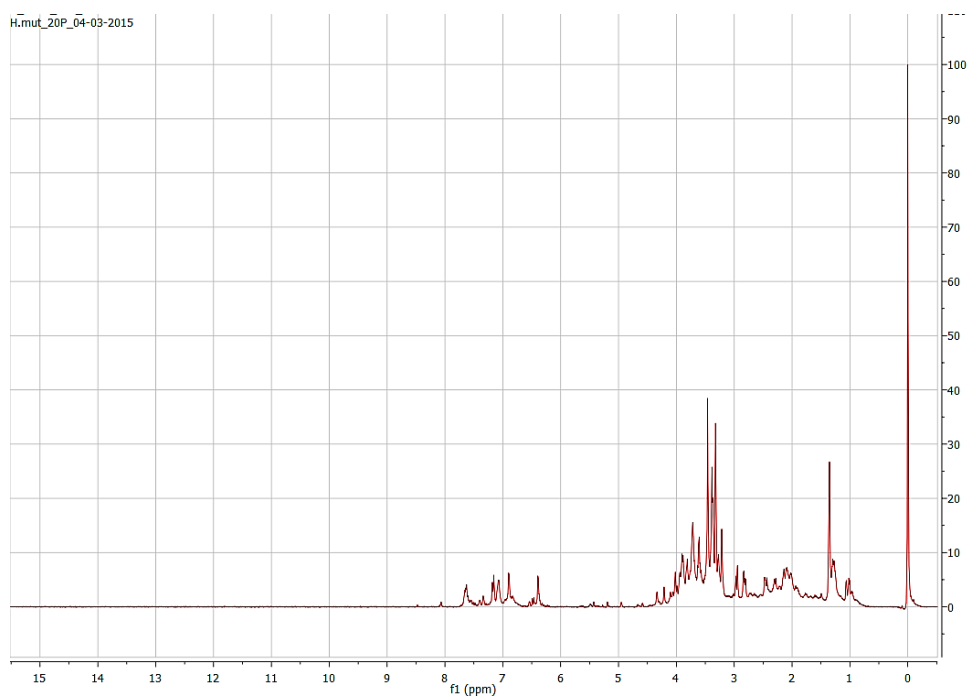


Figure 7.20. ¹H NMR spectrum of *H. mutabile* Hilliard.

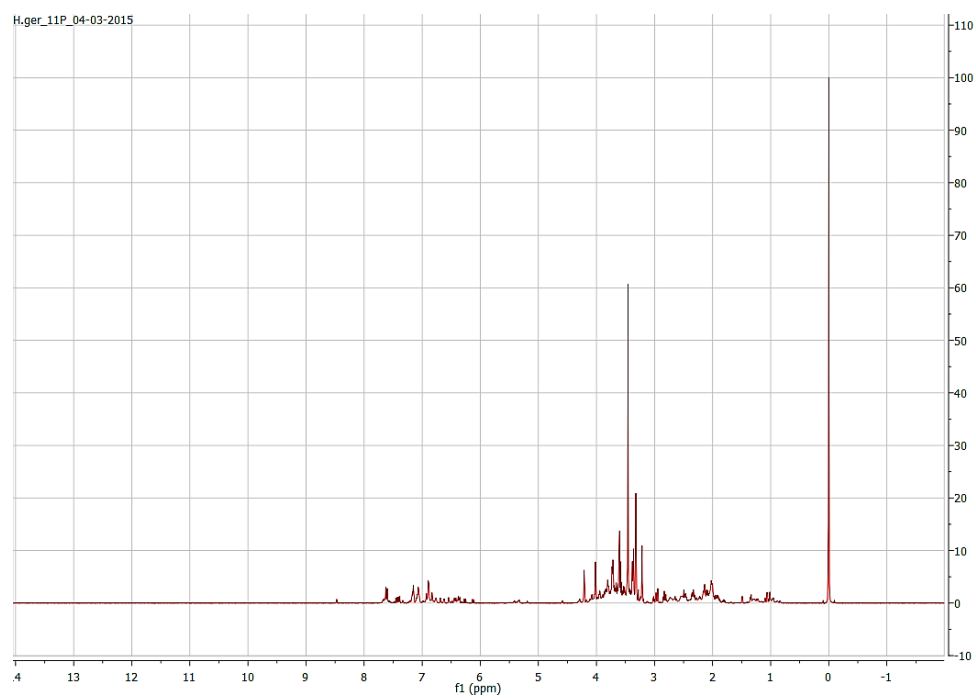


Figure 7.21. ¹H NMR spectrum of *H. gerberifolium* A.Rich.

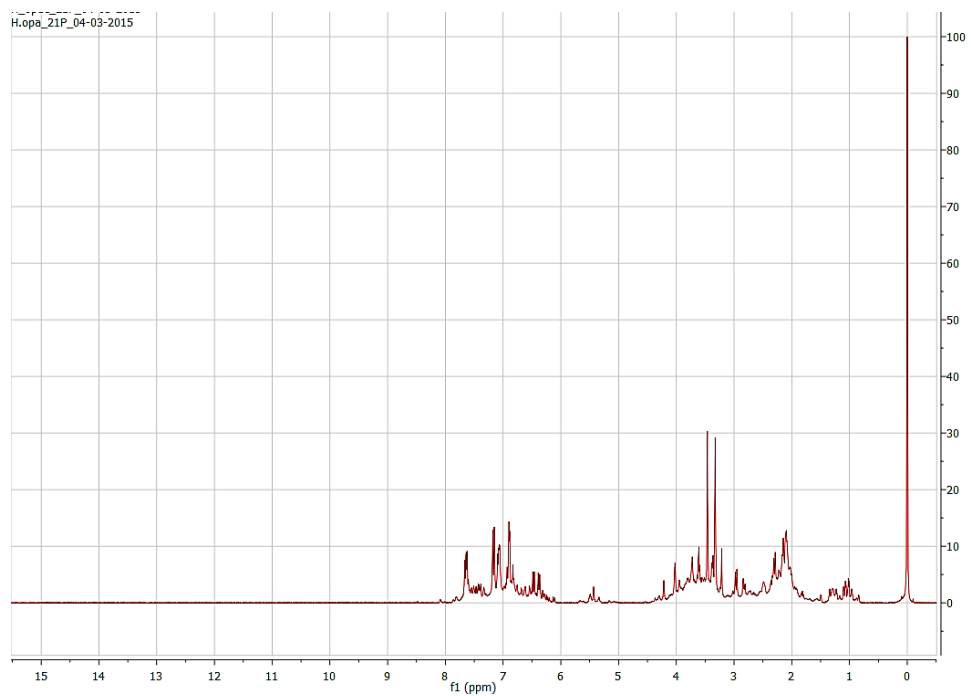


Figure 7.22. ¹H NMR spectrum of *H. opacum* Klatt.

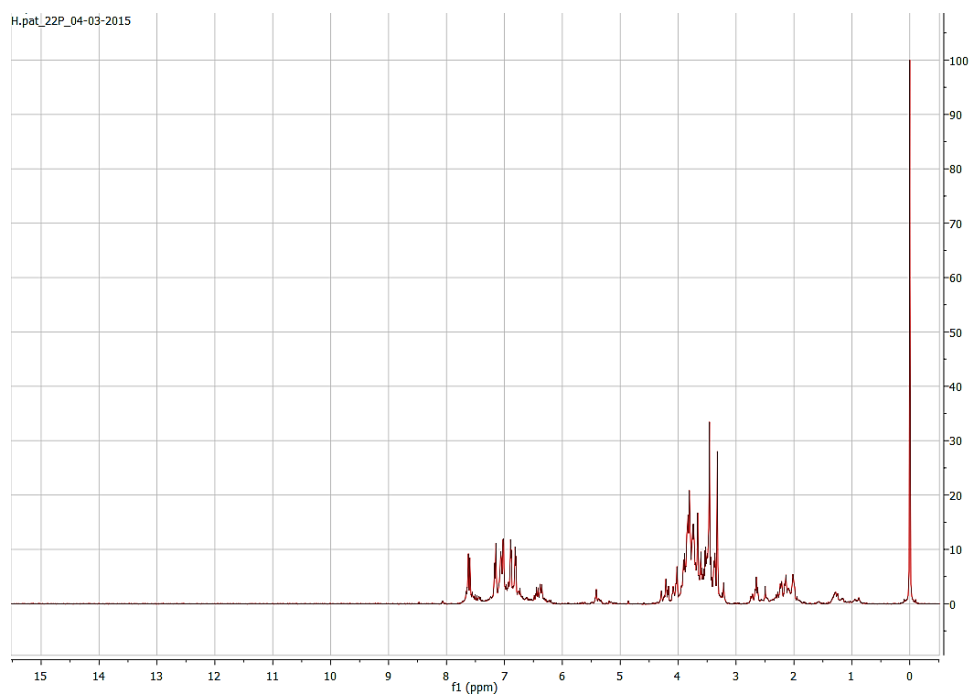


Figure 7.23. ¹H NMR spectrum of *H. patulum* (L.) D. Don.

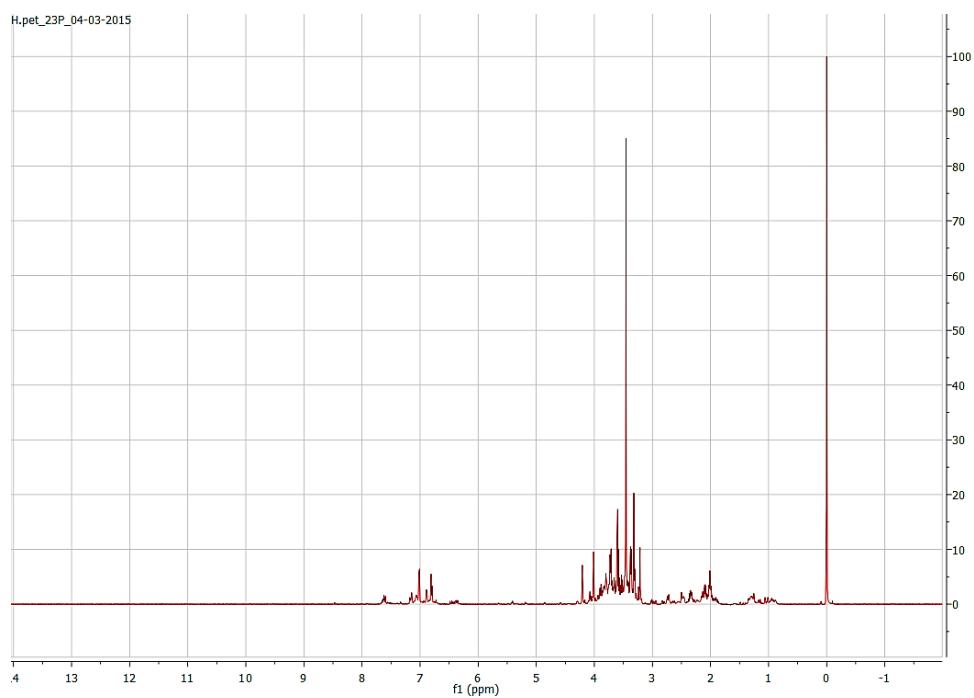


Figure 7.24. ^1H NMR spectrum of *H. petiolare* Hilliard & B.L.Burt.

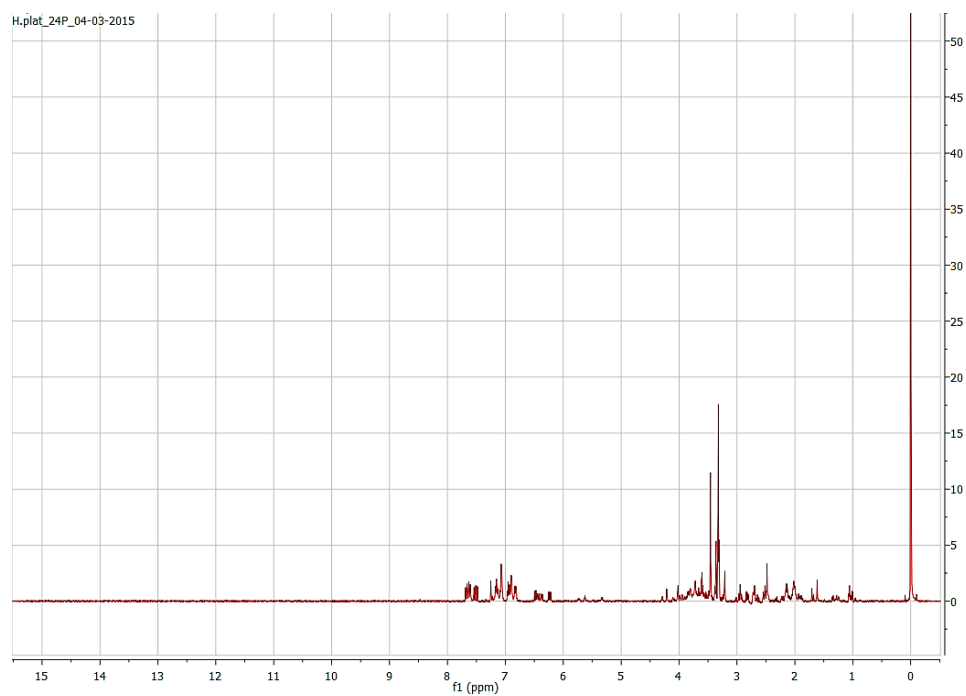


Figure 7.25. ^1H NMR spectrum of *H. platypterum* DC.

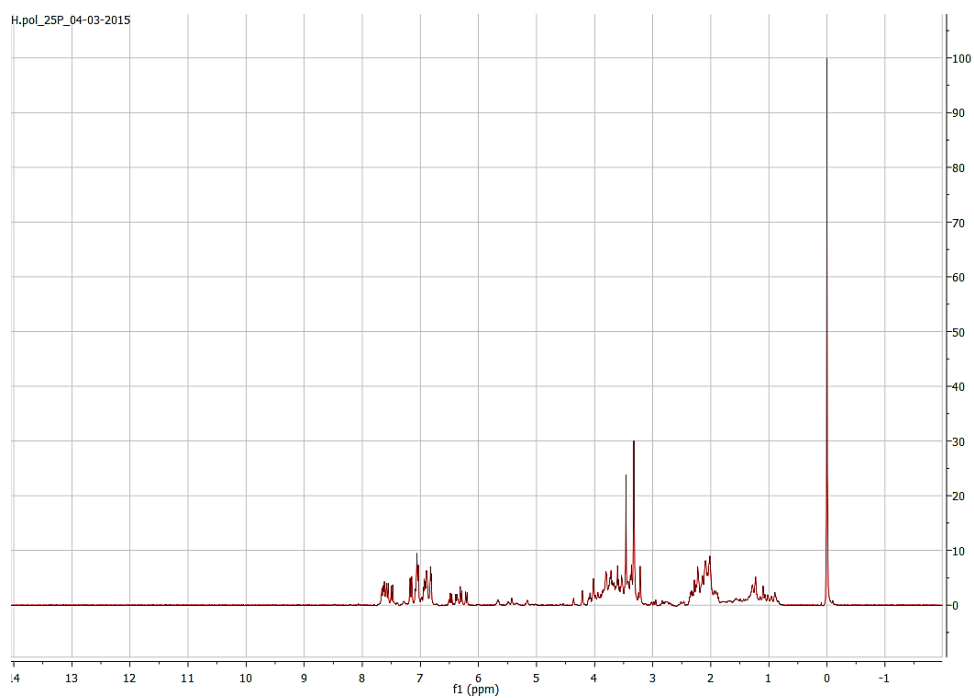


Figure 7.26. ^1H NMR spectrum of *H. polycladum* Klatt.

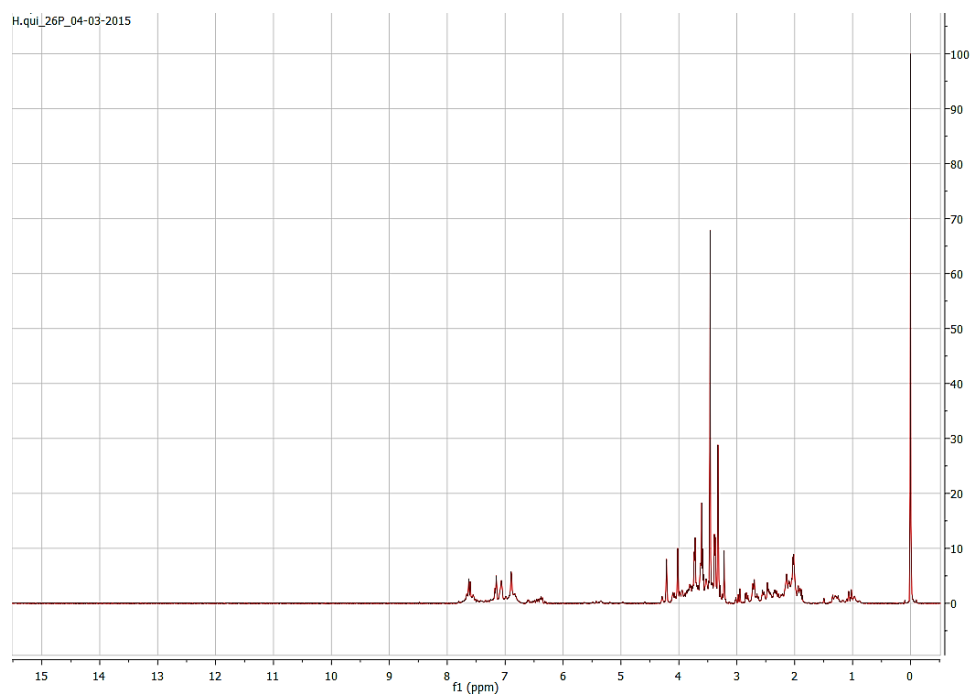


Figure 7.27. ^1H NMR spectrum of *H. nudifolium* (L.) Less. var. *nudifolium*

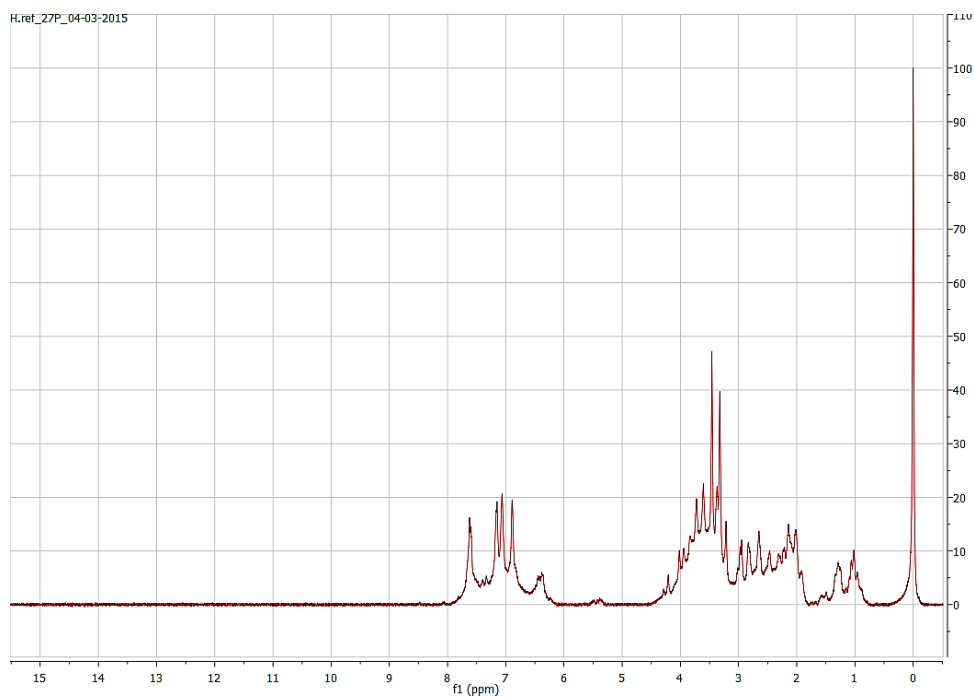


Figure 7.28. ¹H NMR spectrum of *H. reflexum* N.E.Br.

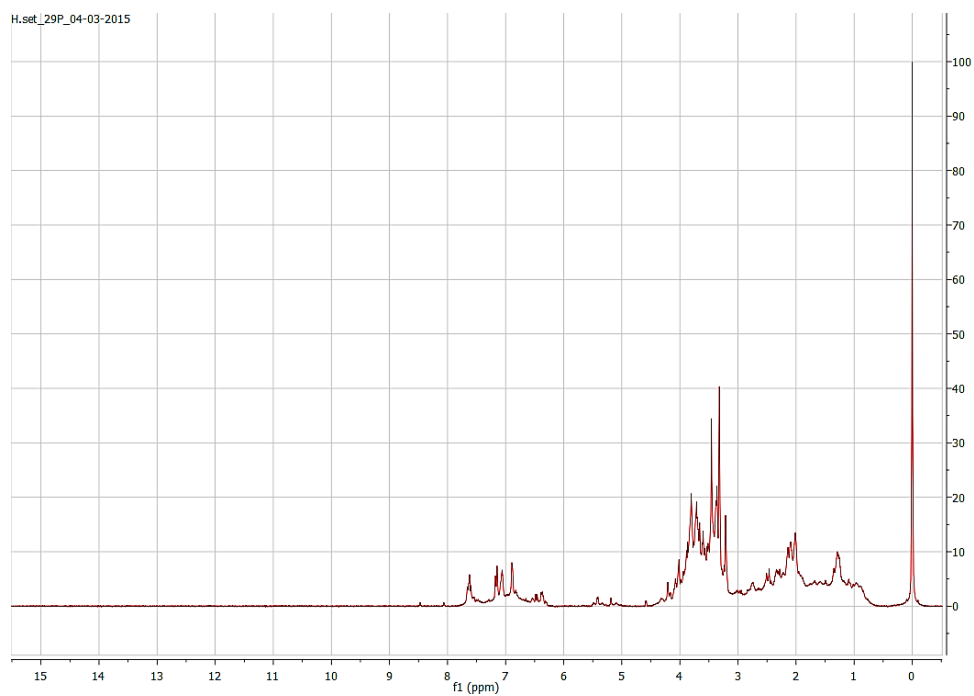


Figure 7.29. ¹H NMR spectrum of *H. setosum* Harv.

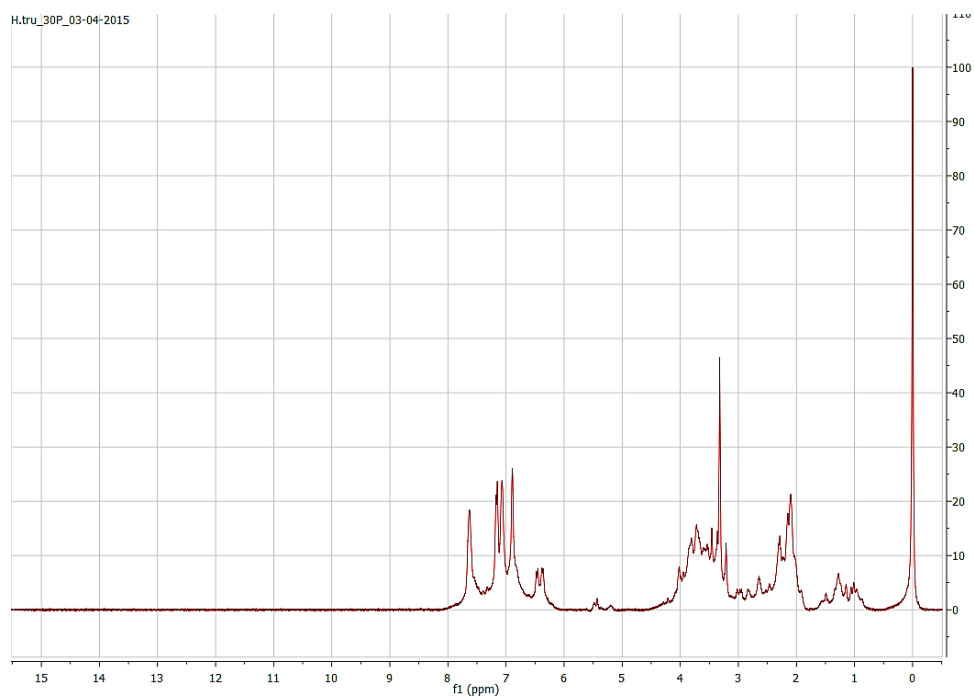


Figure 7.30. ^1H NMR spectrum of *H. truncatum* Burt Davy.

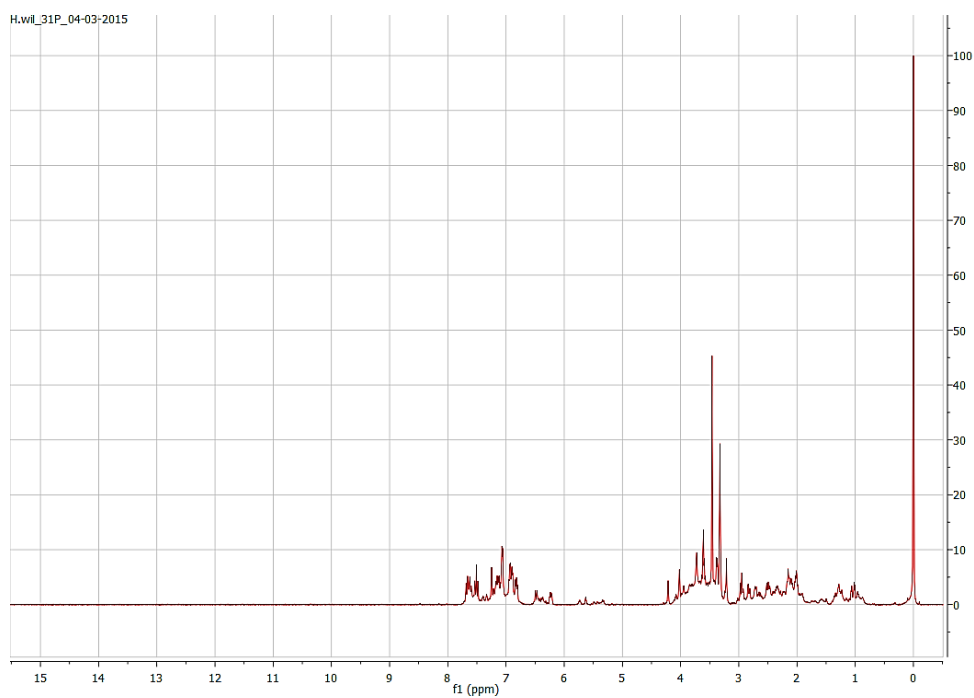


Figure 7.31. ^1H NMR spectrum of *H. wilmsii* Moeser.

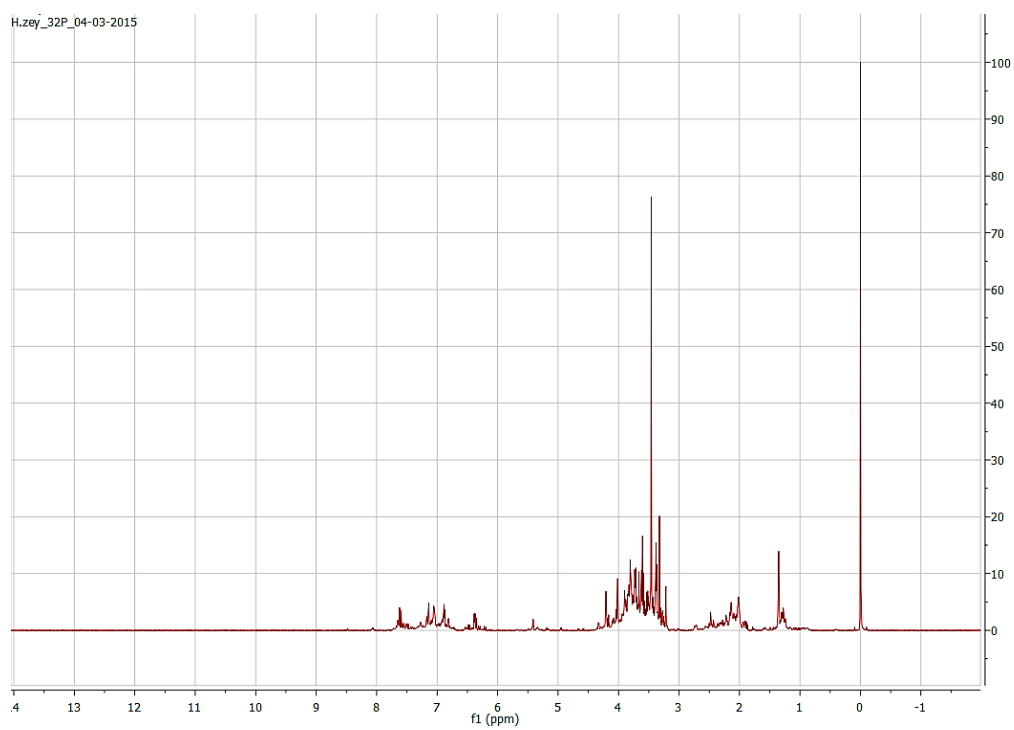


Figure 7.32. ^1H NMR spectrum of *H. zeyheri* Less.